Stem Cells International

Noncoding RNAs and Stem Cell Function and Therapy

Lead Guest Editor: Yaoliang Tang
Guest Editors: Wei Lei, Yanfang Chen, Xiaolong Wang, Mark W. Hamrick, and Mi Zhou

Noncoding RNAs and Stem Cell Function and Therapy

Stem Cells International

Noncoding RNAs and Stem Cell Function and Therapy

Lead Guest Editor: Yaoliang Tang
Guest Editors: Wei Lei, Yanfang Chen, Xiaolong Wang, Mark W. Hamrick, and Mi Zhou

Editorial Board

Contents

Hindawi
Stem Cells International
Volume 2018, Article ID 7306034, 2 pages
https://doi.org/10.1155/2018/7306034

Editorial

Noncoding RNAs and Stem Cell Function and Therapy

Yaoliang Tang[1], **Wei Lei**[2], **Yanfang Chen**[3], **Xiaolong Wang**[4], **Mark W. Hamrick**[1] and **Mi Zhou**[5]

[1]*Medical College of Georgia, Augusta University, Augusta, GA, USA*
[2]*Laboratory of Cardiovascular Diseases, Guangdong Medical University, Zhanjiang 524001, China*
[3]*Department of Pharmacology & Toxicology, Boonshoft School of Medicine, Wright State University, Dayton, OH 45435, USA*
[4]*Cardiovascular Department, Cardiovascular Research Institute of Traditional Chinese Medicine, Shuguang Hospital, Shanghai University of Traditional Chinese Medicine, Shanghai 201203, China*
[5]*Department of Cardiac Surgery, Ruijin Hospital, Shanghai Jiao Tong University, Shanghai, China*

Correspondence should be addressed to Yaoliang Tang; yaotang@augusta.edu

Received 5 March 2018; Accepted 6 March 2018; Published 5 June 2018

Noncoding RNAs (ncRNAs), including small microRNAs (miRNAs) and long noncoding RNAs (lncRNAs), are responsible for fine regulation of gene expression in stem cells [1]. This special issue focuses on the two main ncRNAs currently under investigation, miRNAs and lncRNAs, the latter of which are ill-understood compared to miRNAs.

miRNAs are a family of endogenous noncoding RNA molecular about 22 nucleotide in length [2, 3]. Mature miRNAs can mediate translational repression through miRNA-induced silencing complexes that bind to the 3′-untranslated region (3′UTR) of the target mRNA. During mouse embryonic stem cell (mESC) differentiation, many miRNAs are either upregulated or downregulated. Z.-Y. Chen et al. performed a miRNA array screen, and identified miR-142-3p significantly downregulated during mESC differentiation into the mesodermal and cardiac progenitor cells, they did miR-142-3p overexpression and inhibition experiments, and found that regulation of miR-142-3p level does not change the characteristics of undifferentiated mESCs; however, ectopic expression of miR-142-3p inhibits the expression of cardiac transcription factor Mef2c by targeting 3′-untranslated region of Mef2c, suggesting an important regulatory role of miR-142-3p in early cardiac differentiation.

Notch signaling pathway is evolutionarily conserved from invertebrates to vertebrates, Notch signaling is activated via juxtacrine binding of an adjacent cell's Jagged ligands (Jag1 and 2) or Delta-like ligands (Dll1, 3, and 4) with 4 Notch receptors (Notch 1, 2, 3, and 4), Notch signaling pathway directly controls stem cell survival, proliferation, and differentiation [1, 4]. C. Chen et al. investigated the role and mechanism of microRNA-1 (miR-1) in the differentiation of adipose-derived stem cells (ASCs) into cardiomyocyte-like cells. They found that miR-1 could promote the differentiation of ASCs in the myocardial microenvironment, and Notch/Hes1 signaling is involved in ASC differentiation into cardiomyocytes.

Adult cardiomyocytes (CM) have limited proliferative capacity; therefore, stimulating CM proliferation becomes a promising strategy for inducing cardiac regeneration. Noncoding RNAs were found differently expressed in CMs with different proliferation potential. Modulating noncoding RNAs might be a potential strategy to promote adult CM proliferation. S. Qu et al. reviewed the microRNAs which were proved to promote or suppress CM proliferation and the underlying mechanism of miRNA-mediated CM proliferation.

Recent studies proved that the beneficial effect of MSC in cardioprotection is contributed to paracrine effect. Y. Zhou et al. tried to explore the major factors which account for the beneficial effects of MSC; they identified that hepatoma-derived growth factor (HDGF) was one of

the important factor secreted by MSCs but not by cardiac fibroblast. Knockdown of HDGF can ablate the cellular protective effect of conditioned medium (CdM) from MSC. Furthermore, they found HDGF-mediated cellular protection is protein kinase C epsilon (PKCε) dependent.

Stem cells can secrete exosomes/microvesicles (30–150 nm), which shuttle miRNAs between cells, and play an important role in miRNA communication between donor stem cells and recipient tissues [5–7]. Exosomes containing biological active miRNAs mediate paracrine effect of mesenchymal stem cells (MSC), and exosome membrane protect miRNAs from RNase degradation. A. Luarte et al. reviewed the latest progress regarding the impact of stress in the biology of the neurogenic niche, especially how exosomes mediate communication between astrocytes and niche cells via exosomes. Tumor-derived exosomes can induce mesenchymal stem cell (MSC) transformation into cancer-associated fibroblast (CAF). Q. Cheng et al. investigated the effects of multiple myeloma- (MM-) derived exosomes on regulating the proliferation of MSC, CAF transformation of MSC, and IL-6 secretion of MSCs; they found that miR-21 and miR-146a from MM derived exosomes play an important role in regulating MSC transformation and cytokine secretion.

lncRNAs are noncoding RNAs that are longer than 200 nucleotides in length that cover the largest and most diverse group of ncRNAs. lncRNAs regulate stem cell potency and differentiation [8]. S. Lee et al. reviewed the major lncRNAs involved in the transcriptional and epigenetic regulation of stem cell differentiation and maintenance. The mechanisms of cytoplasmic lncRNAs and nucleus lncRNAs are different, particularly, cytoplasmic lncRNAs regulate turnover, translation, and silence of partially complementary mRNAs; they can also act as a miRNA sponge to reduce miRNA availability and can modulate signaling pathways via interaction with signaling molecular. Nuclear lncRNAs can be decoys for transcription factors, or serve as a scaffold for ribonucleoprotein (RNP) or serve as an epigenetic regulator by recruiting chromatin modification factors.

3,4-Benzopyrene (Bap) is an important component of cigarette smoke and automobile exhaust. Bap is one of the leading risk factor of abdominal aortic aneurysm (AAA). Macrophage activation plays a key role for Bap-induced AAA; however, the mechanism is unclear. Y. Zhou et al. used a mouse lncRNAs array to investigate the expression signatures of lncRNAs and mRNAs in Bap-activated macrophage. They found that 8 pathways associated with inflammation were upregulated, particularly, the AGE-RAGE pathway, which is involved in Bap-induced dysfunction of endothelial progenitor cell (EPC). This study provides potential targets for AAA caused by smoking.

Endothelial dysfunction is an early step in neointima formation, L. Lv et al. used RNA-sequencing (RNA-seq) to analyze the expression profiles of lncRNAs in human stenosed and nonstenotic uremic veins. They identified unannotated lncRNAs, uc001pwg.1, which was one of the most significantly downregulated lncRNAs. Further studies revealed that uc001pwg.1 overexpression could increase nitric oxide synthase (eNOS) phosphorylation and nitric oxide (NO) production in endothelial cells (ECs). Mechanistically, uc001pwg.1 improves endothelial function via mediating MCAM expression. This study represents the first effort of identifying a novel attractive target for improving arteriovenous fistula (AVF) function in uremic patients.

Yaoliang Tang
Wei Lei
Yanfang Chen
Xiaolong Wang
Mark W. Hamrick
Mi Zhou

References

[1] Y. Tang, Y. Wang, L. Chen, Y. Pan, and N. Weintraub, "Chapter 8 - cross talk between the Notch signaling and noncoding RNA on the fate of stem cells," *Progress in Molecular Biology and Translational Science*, vol. 111, pp. 175–193, 2012.

[2] M. Tatsuguchi, H. Y. Seok, T. E. Callis et al., "Expression of microRNAs is dynamically regulated during cardiomyocyte hypertrophy," *Journal of Molecular and Cellular Cardiology*, vol. 42, no. 6, pp. 1137–1141, 2007.

[3] L. Zhang, M. Zhou, Y. Wang et al., "miR-92a inhibits vascular smooth muscle cell apoptosis: role of the MKK4–JNK pathway," *Apoptosis*, vol. 19, no. 6, pp. 975–983, 2014.

[4] L. Chen, M. Ashraf, Y. Wang et al., "The role of *notch 1* activation in cardiosphere derived cell differentiation," *Stem Cells and Development*, vol. 21, no. 12, pp. 2122–2129, 2012.

[5] Y. Wang, L. Zhang, Y. Li et al., "Exosomes/microvesicles from induced pluripotent stem cells deliver cardioprotective miRNAs and prevent cardiomyocyte apoptosis in the ischemic myocardium," *International Journal of Cardiology*, vol. 192, pp. 61–69, 2015.

[6] W. Stoorvogel, "Functional transfer of microRNA by exosomes," *Blood*, vol. 119, no. 3, pp. 646–648, 2012.

[7] Z. Chen, Y. Li, H. Yu et al., "Isolation of extracellular vesicles from stem cells," in *Extracellular Vesicles*, W. Kuo and S. Jia, Eds., vol. 1660 of Methods in molecular biology, pp. 389–394, Humana Press, New York, NY, USA, 2017.

[8] M. Hagan, M. Zhou, M. Ashraf et al., "Long noncoding RNAs and their roles in skeletal muscle fate determination," *Noncoding RNA Investigation*, vol. 1, no. 5, 2017.

Hindawi
Stem Cells International
Volume 2018, Article ID 7494530, 13 pages
https://doi.org/10.1155/2018/7494530

Research Article

MicroRNA-1 Regulates the Differentiation of Adipose-Derived Stem Cells into Cardiomyocyte-Like Cells

Can Chen,[1,2,3] **Quanxiang Yan**,[2] **Yiguang Yan**,[1] **Mudi Ma**,[1] **Yuan He**,[2] **Xiaorong Shui**,[4,5] **Zhigang Yang**,[6,7] **Xiaozhong Lan**,[8] **Yaoliang Tang**,[5] **and Wei Lei**[1,2,3]

[1]*Laboratory of Cardiovascular Diseases, Guangdong Medical University, Zhanjiang 524001, China*
[2]*Cardiovascular Medicine Center, Affiliated Hospital of Guangdong Medical University, Zhanjiang 524001, China*
[3]*Precision Medicine Center, Affiliated Hospital of Guangdong Medical University, Zhanjiang 524001, China*
[4]*Laboratory of Vascular Surgery, Guangdong Medical University, Zhanjiang 524001, China*
[5]*Vascular Biology Center, Department of Medicine, Medical College of Georgia, Augusta University, Augusta, GA, USA*
[6]*Department of Hematology, Affiliated Hospital of Guangdong Medical University, Zhanjiang 524001, China*
[7]*Central People's Hospital of Zhanjiang, Zhanjiang 524045, China*
[8]*Medicinal Plants Research Centre, Tibet Agricultural and Animal Husbandry College, Nyingchi 860000, China*

Correspondence should be addressed to Wei Lei; leiwei2006@126.com

Received 30 June 2017; Revised 11 January 2018; Accepted 31 January 2018; Published 5 April 2018

Academic Editor: Heinrich Sauer

Stem cell transplantation is one of most valuable methods in the treatment of myocardial infarction, and adipose-derived stem cells (ASCs) are becoming a hot topic in medical research. Previous studies have shown that ASCs can be differentiated into cardiomyocyte-like cells, but the efficiency and survival rates are low. We investigated the role and mechanism of microRNA-1 (miR-1) in the differentiation of ASCs into cardiomyocyte-like cells. ASCs and cardiomyocytes were isolated from neonatal rats. We constructed lentivirus for overexpressing miR-1 and used DAPT, an antagonist of the Notch1 pathway, for *in vitro* analyses. We performed cocultures with ASCs and cardiomyocytes. The differentiation efficiency of ASCs was detected by cell-specific surface antigens. Our results showed that miR-1 can promote the expression of Notch1 and reduce the expression of Hes1, a Notch pathway factor, and overexpression of miR-1 can promote the differentiation of ASCs into cardiomyocyte-like cells, which may occur by regulating Notch1 and Hes1.

1. Introduction

Myocardial cells are nonregenerative cells that play significant roles in maintaining the function of tissue perfusion. However, after myocardial ischemic-anoxia, fiber scar repair could lead to reduced contractility, resulting in inadequate blood supply for important organs, reduced cardiac output, and even cardiac pump failure, which can greatly affect the cure of myocardial infarction. Currently, regular treatment measures for myocardial infarction, cardiac failure, and arrhythmia have been restricted in use because the myocardium does not completely regenerate. However, the use of stem cells and progenitor cells after myocardial infarction has been demonstrated to promote reconstruction and recovery of cardiac function. As a result, much of the recent research has been focused on searching for multifunction cells that could regenerate into myocardial cells, such as embryonic stem cells, cardiac progenitor cells, endothelial progenitor cells, and mesenchymal stem cells (MSCs).

Stem cells are a type of highly proliferative cells that can differentiate to somatic cells. These cells can also be induced and differentiate into many different kinds of functioning cells to repair diseased and aging tissues and organs. Based on the tissue source of the stem cells, the cells can be classified as adipose-derived stem cells (ASCs), MSCs, and neural stem cells, among others [1]. Myocardial cell transplantation methods involve direct injection of stem cells through the vein and infarcted myocardium. However, the deposition of

transplanted cells in the myocardium cannot be adequately controlled, and the nutrient supply can also be severely destroyed [2–4]. In addition, other factors, including the hypoxia environment and pH levels, can also make it difficult for the cardiac progenitor cells to penetrate and survive in the ischemic myocardial microenvironment [2].

ASCs were first isolated from human lipoplasty by Zuk et al. in 2001. These cells share the same phenotype as MSCs and have multidifferentiation functions [5]. ASCs are abundant and easy to obtain, and therefore, these cells have become a research focus in many laboratories [6]. Several studies showed that ASCs can differentiate into cardiomyocyte-like cells and can be transplanted into the damaged heart to improve heart function [6, 7]. Cai et al. used DAPI-labeled ASCs to coculture with cardiomyocyte-like cells for several days, and the ASCs showed spontaneous contractility [7]. These cells also expressed cTnI and GATA proteins in helping the repair of impaired myocardium and improving the heart failure condition in myocardial infarction rats; however, the differentiation rate and repair abilities of these cells after *in vivo* transplantation were low [7, 8]. Thus, it is critical to improve the differentiation efficiency and curative abilities of ASCs for myocardial infarction.

miRNA-1 (miR-1) is a muscle-specific miRNA that plays important roles in regulating heart development and muscle differentiation [9, 10]. miR-1 can promote the differentiation of embryonic stem cells and cardiac progenitor cells to cardiomyocyte-like cells and HeLa and C2C12 cells to skeletal myogenic cells [11–15]. Moreover, overexpression of miR-1 arrested development in mice, which further caused thinning of the wall of the left ventricle and resulted in heart failure [16]. Knockdown of either miR-1-1 or miR-1-2 led to aberrations in cardiac morphology, electrophysiological conduction, cell cycle regulation, and other heart functions [17]. Therefore, better understanding of the functions and related signal pathways of miR-1 may be of great importance for the use of stem cells and miR-1 to treat ischemic heart disease.

The Notch signal pathway, consisting of the Notch receptors, ligands, and target genes, plays key roles in cardiomyocyte differentiation and conduction cell lineage [18]. Notch1 plays multiple functions in regulating heart cell differentiation in chicken embryo formation; it not only affects the conduction system of the ventricle but also controls the differentiation of heart cells [19]. Furthermore, activated Notch1 could lead to aberrations in ventricular conduction [19]. A previous study reported that miR-34a prevented the proliferation and migration of vascular smooth muscle cells via regulating Notch1 gene expression [20]. Expression levels of miR-34a were lower in the injured artery than in the control. Furthermore, overexpression of miR-34a could significantly downregulate the expression of Notch1 and decrease the proliferation of vascular smooth muscle cells as well as inhibit the formation of neointima in the damaged femoral artery [20]. Another study also showed that miR-1 could promote the differentiation of MSCs into cardiac cells by decreasing the expression of Hes1, a Notch pathway target gene [21]. Despite these few studies, the relationship between miRNAs and Notch in heart development and myocardial cell proliferation and differentiation has been largely unknown. In this study, we investigated the role and potential mechanism of miR-1 in the differentiation of ASCs into cardiomyocyte-like cells.

2. Materials and Methods

2.1. Separation and Culture of ASCs. The inguinal fat pads from both sides of male SD mice (4–6 weeks old) were collected in D-Hanks solution with 1000 U/l penicillin-streptomycin (Solarbio, Beijing, China) and then washed by D-Hanks solution without antibiotics three times. The remaining vascular muscle tissues were removed and cut into 1 mm × 1 mm × 1 mm pieces. An equal volume of 0.25% of EDTA trypsin supplemented with 0.1% of type I collagenase solution was added, and the samples were gently vibrated in a 37°C incubator shaker for 45 min. An equal volume of DMEM containing 10% FBS was added to end the digestion. Cells were collected and centrifuged at 1000 rpm for 10 min; the supernatant was removed and the cells were resuspended with DMEM supplemented with 10% FBS. After filtering using a 200-mesh sieve, cells were transferred into a culture dish and incubated in 37°C with 5% CO_2 for 24 h. Medium was changed every 2 to 3 days. Cells were observed using a phase-contrast microscope daily. Cell morphology and proliferating rates were recorded, and when cells reached 80–90% confluence, cells were digested with 0.25% EDTA trypsin and subcultured into several culture dishes.

2.2. Identification of ASCs

2.2.1. Surface Antigen Analysis. The cell surface antigens CD29, CD31, and CD45 were detected by flow cytometry to identify the ASCs. The 3rd, 4th, and 5th generations of ASCs were collected and divided into two groups (5×10^5 cells in each group): the experimental group and the control group (each group in duplicate). Cells were washed and resuspended in 500 μl of PBS, and 5 μl of CD29, CD31 or CD45 antibody was added. Cells were incubated at 4°C in the dark for half an hour and then washed by PBS twice before analysis by flow cytometry.

2.2.2. Osteogenic Induction of ASCs and Identification. The 4th-generation cells were digested by 0.25% EDTA trypsin, collected, resuspended in DMEM/F12 medium containing 10% FBS, and seeded in 6-well plates. After 24 h of incubation, the medium was removed and an osteogenesis-inducing solution was added. The control cells received the medium only. The medium was exchanged after 3 days, and cells were induced for 21 days. Cells were then washed with PBS once and fixed in 4% formaldehyde for 30 min at room temperature. The formaldehyde was removed, and cells were washed in PBS once and then stained with Alizarin Red for 5 min. The staining solution was removed, and then cells were washed by PBS three times and observed and photographed using an inverted microscope.

2.2.3. Adipogenic Induction of ASCs and Identification. The 4th-generation cells were collected and seeded into 6-well plates. When the cells reached 100% confluence, adipogenic

inducing solution A was added; after 3 days of incubation, the medium was replaced with adipogenic inducing solution B for 24 h and then replaced with solution A. This was repeated for four more cycles. Solution B was added for another 7 d of incubation, and the culture medium was changed every 3 d. The control cells were cultured as normal. After 23 days of induction, cells were subjected to Oil Red O staining. The cells were washed with PBS and then observed and photographed using an inverted microscope.

2.3. Separation and Culture of Cardiomyocytes. A neonatal mouse (1–3 d old) was immersed in 75% of ethyl alcohol for 1–2 min. The heart was obtained by an infrasternal small incision and then immersed in D-Hanks solution with 1000 U/l penicillin-streptomycin for 10 min and then washed twice in D-Hanks solution without antibiotics. Blood clots and fibrous tissue around the heart were removed, and only the tip portion was kept. After three washes in cold PBS, the heart was cut into 1 mm^3 pieces; next, 0.25% trypsin was added and the mixture was gently shaken in a 37°C water bath for 10 min. After 3 min, the supernatant was removed, which mainly contained the red blood cells, dead cells, and cell debris. Trypsin (5–10 ml) was added, and the mixture was digested at 37°C for 10 min. Cells were washed down using straw, after precipitation. The supernatant containing digested cells was transferred into a new centrifuge tube containing complete medium. This process was repeated 5-6 times (each round taking approximately 10 min) until the tissues were completely digested. The cell suspension was centrifuged at 1000 rpm for 10 min, and the supernatant was removed. The cells were resuspended in medium and then seeded into a culture flask. After 1 h of culture in 37°C and 5% CO_2, the medium, which mainly contained purified cardiomyocytes (CMs), was gently transferred to another culture flask. After 24 h culture, the medium was changed and was exchanged every 2–3 days.

2.4. Vector Construction and Lentivirus Package. The miR-1 overexpression vector was constructed, and the lentivirus shuttle plasmid and carrier plasmid were prepared. High-purity endotoxin-free plasmid extraction was performed, and plasmids were used to transfect 293T cells. After 6 h of transfection, the medium was removed and exchanged with a regular medium. After 48 and 72 h of culture, the cellular supernatant, containing abundant lentivirus particles, was collected and ultracentrifugation of the supernatant was performed to concentrate the virus. The lentivirus vector contained the GFP reporter gene and puromycin resistance gene, and thus, the transfection rate could be estimated by observing GFP fluorescence and the multiplicity of infection (MOI) could be estimated. The puromycin resistance gene was used for puromycin screening. The 2nd-generation ASCs were divided into two transfection groups: lentivirus with miR-1 overexpression and control lentivirus (produced by empty vector alone).

2.5. Lentivirus Infection of ASCs. To determine the proper MOI, ASCs were seeded into 12-well plates, with 2×10^4 cells/cm^2 in each plate. Cells were infected once they reached 50–70% confluence. We performed preliminary tests to determine a nontoxic concentration for polybrene (infection reagent), from 2 μg/ml to 8 μg/ml in 24 h, and the concentration was set as 5 μg/ml. Each MOI value (10, 20, 40, 60, and 80) was evaluated in duplicate. The day after cells reached the appropriate confluence, polybrene was added to each well at the final concentration of 5 μg/ml, and then miR-1 lentivirus was added into each well. After 12 h, the medium was replaced with a fresh medium. After 2 days, GFP was observed under fluorescence microscope and the cell number was recorded under a light microscope. The transfection rate was estimated, and the transfection proportion of different MOI values was calculated via flow cytometry. The MOI of 60 was established for the following experiments.

For experimental analyses, ASCs were plated in 6-well plates. The medium was removed and 2 ml of polybrene mixture was added to each well. The lentivirus stock was taken out of the refrigerator and heated in a 37°C water bath and then added into plates and mixed with cells. After 12 h, the medium was replaced with fresh complete medium, and the cells were cultured at 37°C. At 48 h, GFP expression was monitored using a fluorescence microscope. Cells were selected by puromycin screening, and the 3rd and 4th generations of cells were collected. The miR-1 expression level was detected by qPCR, and the following experiments were performed.

2.6. DAPT Treatment. The 4th generation of infected ASCs was divided into six treatment groups: (1) Lv-miR-1-DA: DAPT-treated miR-1 overexpression group; (2) Lv-miR-1-DM: DMSO-treated miR-1 overexpression group; (3) Lv-miR-1: miR-1 overexpression group; (4) Lv-NC-DA: DAPT-treated control virus-infected group; (5) Lv-NC: control virus-infected group; and (6) untreated ASCs. The Notch antagonist DAPT was purchased from Sigma-Aldrich Co. and used at a concentration of 5 μg/ml in groups 1 and 4 [22], and the same dosage of DMSO was added to group 2. After 5 days, the RNA and total protein were collected.

2.7. Prescreening with Puromycin. To identify the proper concentration of puromycin for experimental use, myocardial cells and lentivirus-infected ASCs were treated with various concentrations for puromycin (1.3, 1.5, 1.7, and 1.9 μg/ml) and cultured for 7 d. Each concentration was examined in duplicate. The concentration in which all myocardial cells died was set as the experimental concentration (1.7 μg/ml).

2.8. Coculture of ASCs and CMs. The 3rd-generation ASCs were divided into three treatment groups: (1) Lv-miR-1-CMs: ASCs infected with miR-1 overexpression lentivirus cocultured with CMs for 7 days; 2) Lv-miR-1: ASCs infected with miR-1 overexpression lentivirus, no coculture; and (3) Lv-NC-CM: ASCs infected with control lentivirus and cocultured with CMs for 7 days. Two groups of CMs were added: one was for a puromycin screening control, and the other was for positive control of myocardium-specific protein expression in the experimental group. Puromycin screening was carried out, and the expression of puromycin resistance genes was identified; the whole process lasted for 7 d. Cells

were then cultured in standard conditions (DMEM/F12 medium with 10% of FBS in 37°C, 5% of CO_2) for two more generations, and the protein and total RNA were collected.

2.9. Reverse Transcription and qPCR Assay for miR-1. Total RNA was isolated following the TRIzol method. U6 was used as an internal reference. The forward primer used for miR-1 amplification was 5′-GGCGGTGGAATG TAAAGAAGT-3′; the U6 primers were forward 5′-CTC GCTTCGGCAGCACA-3′ and reverse 5′-AACGCTTCAC GAATTTGCGT-3′. Reverse transcription qPCR was carried out following the manufacturer's instructions; the reaction condition was 95°C for 10 s and 40 cycles of 95°C for 5 s and 60°C for 20 s. The $2^{-\Delta Ct}$ method was used to analyze the results, in which $\Delta Ct\,(\text{miR}-1\ \text{overexpression}) = Ct\,(\text{experimental group}) - Ct\,(U6)$ and $\Delta Ct\,(\text{virus control group}) = Ct\,(\text{control group}) - Ct\,(U6)$.

2.10. Reverse Transcription and qPCR Assay for GATA4, cTnI, Notch1, and Hes1 mRNAs. Total RNA was isolated using the TRIzol method. The AMV enzyme was used for reverse transcription. Specific primers for GATA4, cTnI, Notch1, and Hes1 mRNAs were designed and are listed in Table 1. The qPCR kit was used for detection of GATA4, cTnI, Notch1, and Hes1 mRNA expression, and the reaction was carried out on a Roche LightCycler® 480 II. Reactions were run in triplicate, and β-actin was used as the internal reference.

2.11. Immunofluorescent Assay. Cells plated on slides were washed with PBS three times, 3 min each, and then fixed in 4% paraformaldehyde for 15 min. Slides were then washed with PBS for three times, 3 min each time, and permeabilized in 0.5% Triton X-100 (dissolved in PBS) for 15 min at room temperature. Cells were washed with PBS three times, 3 min each time. A goat serum blocking reagent was added, and slides were incubated at room temperature for 30 min and then washed with PBS for 3 min. The primary antibodies (cTnI, connexin 43, Notch1, and Jagged1) were added, and samples were incubated at 4°C overnight. The slides were washed with PBS three times, 3 min each time, and then incubated with fluorescence secondary antibodies at 37°C for 1 h. Cells were then washed in PBS three times, 3 min each, in a dark environment. Samples were stained with DAPI for 15 min and then washed in PBS three times, 3 min each time. Filter paper was used to absorb the remaining liquid on the slides, and then an antifluorescence quenching agent was added to block the slides before slides were observed and photographed by laser confocal fluorescence microscopy using a Leica TCS SP5 II fluorescence microscope.

2.12. Statistical Analysis. The data were analyzed using GraphPad Prism 5.0, and the results are expressed as mean ± SEM. Student's *t*-test was performed when comparing 2 values, and an ANOVA test was used when comparing more than 2 samples. $P < 0.05$ and $P < 0.01$ were considered statistically significant and very significant, respectively.

Table 1: Primer sequences.

Name	Sequence
cTnI-F	5′-GCAATCCCATTCTCTACCTCTG-3′
cTnI-R	5′-CATCTCCTGCTTCGCAATCT-3′
Gata4-F	5′-GGGACTTTCTCCAGCACAGA-3′
Gata4-R	5′-CTTCCATCCATCACCCTTGT-3′
Hes1-F	5′-GTGGGTCCTAACGCAGTGTC-3′
Hes1-R	5′-TGATTAGCAGTGGCCTGAGC-3′
Notch1-F	5′-CACCCACATTCCAGAGGCAT-3′
Notch1-R	5′-GAGCACTGGAAAGGACTCCC-3′

3. Results

3.1. ASC Phenotype Observation. ASCs were isolated from inguinal fat pads from male SD mice as described in Materials and Methods. The cell morphology of the ASCs cultured *in vitro* showed rhomboid, polygon, or spindle shapes, and cells were connected in swirl-like patterns, as shown in Figure 1.

3.2. ASC Identification

3.2.1. Flow Cytometry Analysis of Various Generations of ASCs Using Cell Surface Antigens. We next identified ASCs via the detection of CD29, CD31, and CD45 markers using flow cytometry. We performed analyses on the 3rd-, 4th-, and 5th-generation ASCs (Figure 2(a)). The flow cytometry results showed that the $CD29^+$ rate was 98.8 ± 1.1%, the $CD31^+$ rate was 0.8 ± 0.5%, and the $CD45^+$ rate was 6.3 ± 3.1%. These findings are consistent with the cell surface antigen expression patterns of MSCs.

3.2.2. Osteoblast Induction and Observation. To evaluate the effects of osteoblastic induction on ASCs, cells were subjected to osteoblastic induction as described in Materials and Methods and then stained with Alizarin Red and observed under an optical microscope. In comparison with the noninduced cells stained with Alizarin Red, the induced cells showed the formation of red mineralized nodules after osteoblastic induction (Figure 2(b)), which confirmed that ASCs could differentiate into osteoblasts.

3.2.3. Adipogenic Induction and Observation. To evaluate the effects of adipogenic differentiation on ASCs, cells were subjected to adipogenic induction as described in Materials and Methods and stained with Oil Red staining. In comparison with noninduced cells, we clearly observed red lipid droplet formation in the induced cells (Figure 2(c)), which indicated that ASCs could differentiate into adipocytes. These results demonstrate that ASCs exhibit stem cell properties and can be induced to differentiate into other cell lines.

3.3. ASC Infection with Lentivirus. To examine the potential functions of miR-1 in ASCs, we first constructed a lentivirus expressing miR-1 and assessed the MOI concentrations. Cells infected with the miRNA-1 lentivirus (harboring a GFP

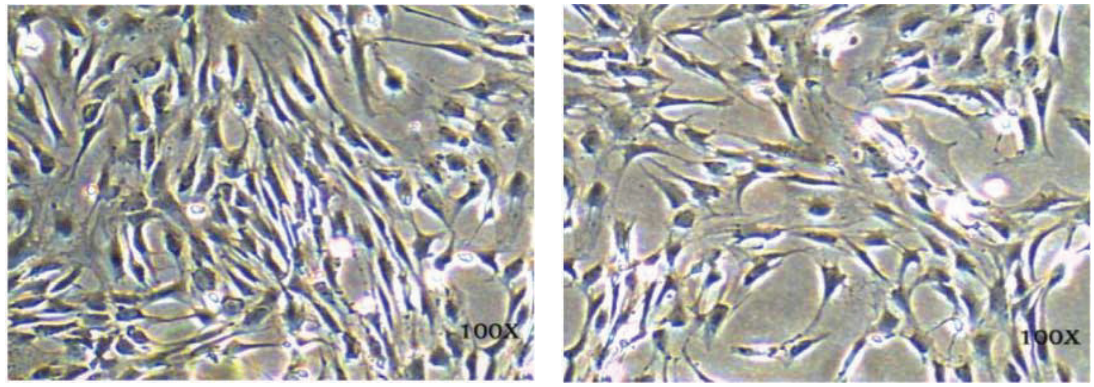

(a) (b)

Figure 1: Light microscopy images of ASCs. (a, b) Two different fields of cultured ASCs. Magnification, ×100.

marker) at MOI = 60 showed higher levels of GFP compared with cells infected at MOI = 40, but similar levels as cells infected with MOI = 80 (Figure 3(a)). Therefore, we used M OI = 60 for subsequent experiments.

3.4. Detection of miR-1 Expression. To confirm successful miR-1 expression in miR-1 lentivirus-infected ASCs, we performed qPCR. The 4th generation of ASCs infected with miR-1-expressing lentivirus (Lv-miR-1 group) and control lentivirus-infected cells (Lv-NC group) were collected and examined by qPCR. The results confirmed significantly higher miR-1 expression levels in Lv-miR-1 cells than in Lv-NC cells ($P < 0.01$), as shown in Figure 3(b).

3.5. Expressions of Notch1 and Hes1 after Treatment with DAPT. We next examined the expression of Notch and Hes1, a Notch1 target, in ASCs in response to treatment with DAPT, an antagonist of the Notch pathway. The ASCs infected with miR-1-expressing lentivirus were divided into three subgroups: Lv-miR-1-DA (DAPT treatment), Lv-miR-1-DM (DMSO treatment), and Lv-miR-1 (untreated). ASCs infected with control lentivirus were divided into two subgroups: Lv-NC-DA (DAPT treatment) and Lv-NC (untreated). Uninfected ASCs were used as negative control. The indicated groups were treated with DAPT or DMSO for 7 days. The total protein and RNA were collected, and Notch1 and Hes1 protein and gene levels were detected by Western blot and qPCR, respectively, as shown in Figure 4.

Quantification of the Western blot results showed a statistically significant increase in Notch1 expression in the Lv-miR-1 group compared with the Lv-NC group ($P < 0.01$) (Figures 4(a) and 4(b)), indicating that miR-1 expression could induce Notch1 protein levels. The Notch1 protein expression level was also significantly higher in the Lv-miR-1-DA group compared with that in the Lv-NC-DA group. We also observed significantly lower Notch1 levels in the Lv-miR-1-DA group compared with the Lv-miR-1-DM group ($P < 0.05$). The Notch1 mRNA expression level showed a similar increase in Lv-miR-1 cells compared with the Lv-NC group ($P < 0.01$) and in the Lv-miR-1-DA group compared with the Lv-NC-DA group, and Notch1 mRNA was similarly decreased in the Lv-miR-1-DA group compared with the Lv-miR-1-DM group ($P < 0.05$) (Figure 4(d)). Together, these results suggested that DAPT treatment resulted in reduced Notch1 mRNA and protein levels and miR-1 could promote Notch1 mRNA and protein expression.

The Hes1 protein expression level was lower in Lv-miR-1 cells than that in Lv-NC cells ($P < 0.05$) and lower in Lv-miR-1-DA cells compared with Lv-NC-DA cells ($P < 0.01$) (Figure 4(c)). Hes1 mRNA levels were also significantly lower in the Lv-miR-1 group than in the Lv-NC group ($P < 0.05$) and in the Lv-miR-1-DA group compared with the Lv-NC-DA group ($P < 0.01$) (Figure 4(e)). Together, these results indicated that miR-1 could reduce the expression of the Hes1 gene and protein.

3.6. Effect of miR-1 on ASCs Cocultured with CMs. The 3rd-generation miRNA-1 or control lentivirus-infected ASCs were divided into treatment groups as follows: (1) Lv-miR-1-CMs (miR-1-expressing cells cocultured with CMs), (2) Lv-miR-1 (miR-1-expressing cells), (3) Lv-NC-CMs (control infected cells cocultured with CMs), and (4) Lv-NC (control infected cells). ASCs infected with miRNA-1 or control lentivirus were cocultured with CMs for 7 days and then screened with 1.7 μg/ml of puromycin for 7 days. Two more CM groups were set as control groups: one was used as the control of puromycin screening, and the other was used as a control for myocardial marker protein expression in the experiment group. The puromycin-resistant cells were then cultured for another two generations, and the total RNA and protein were collected to evaluate the gene and protein expression levels of Hes1, Notch1, cTnI (a myocardium-specific factor), and GATA4 (a myocardium-specific transcription factor) (Figure 5).

While the miR-1-expressing cells (Lv-miR-1 group) showed mostly absent cTnI and GATA4 protein expression levels, upon coculture with CMs (Lv-miR-1-CMs group), both protein levels significantly increased ($P < 0.05$) (Figures 5(b) and 5(c)). Notably, the expression of these proteins was also significantly higher in the miR-1-expressing coculture group (Lv-miR-1-CMs group) compared with control cocultured cells (Lv-NC-CMs) ($P < 0.05$). Similarly, the Notch1 protein

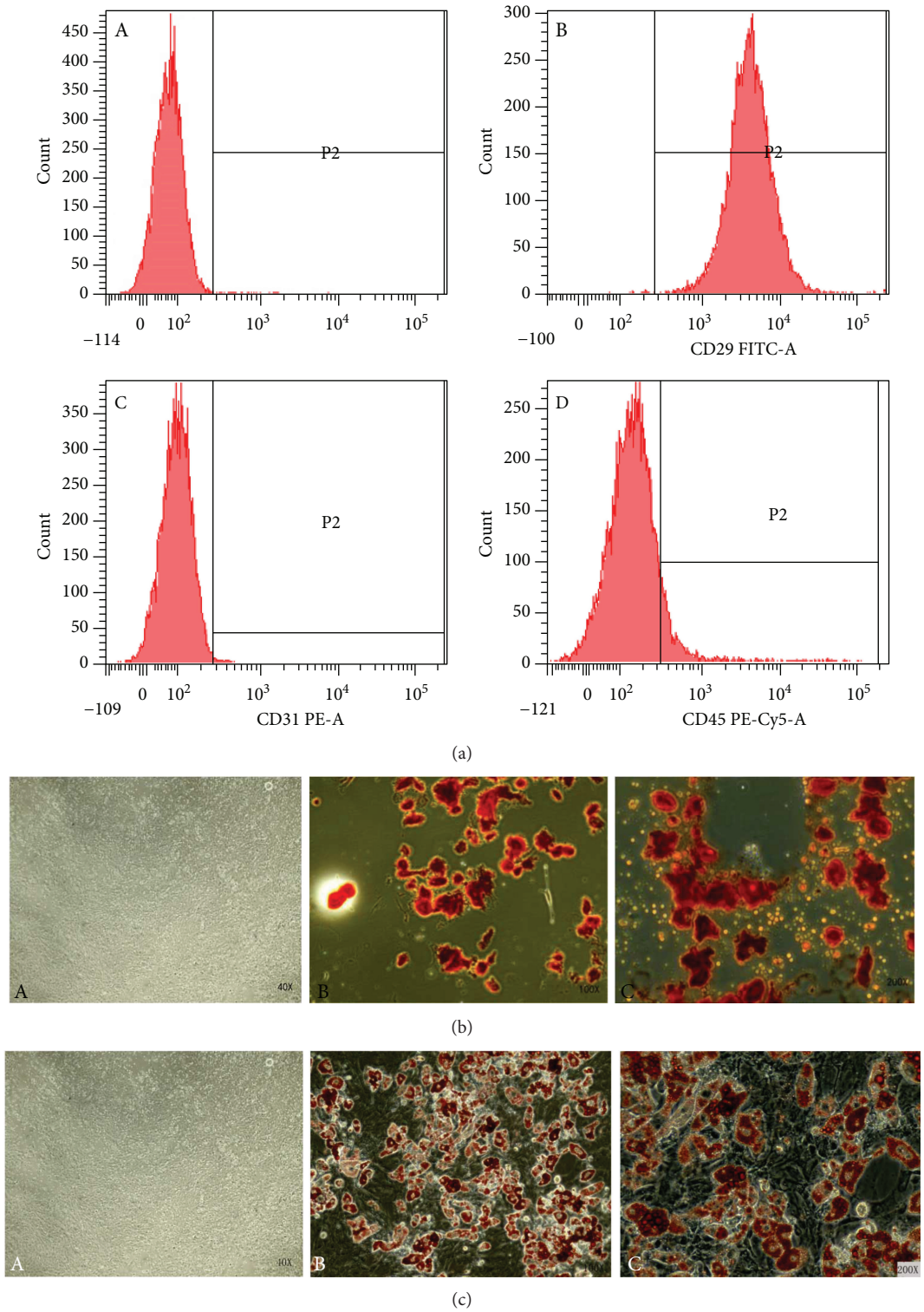

Figure 2: Identification of ASCs. (a) Cell surface antigen detection results of ASCs using flow cytometry. (A) Negative control ASCs treated with PBS. (B) CD29 FITC-labeled ASCs. The positive rate was 99.8%. (C) CD31PE-A labeled ASCs. The positive rate was 0.3%. (D) CD45 PE-CY5-A labeled ASCs. (b) Osteoblast induction and Alizarin Red staining of ASCs. (A) Control ASCs without induction, dyed with Alizarin Red. Magnification, ×40. (B and C) Differentiated ASCs dyed with Alizarin Red. Red mineralized nodules can be observed. Magnification, ×100 (B) and ×200 (C). (c) Adipogenic induction and Oil Red O staining of ASCs. (A) Control ASCs without induction, dyed with Oil Red O. Magnification, ×40. (B and C) Differentiated ASCs dyed with Oil Red O; cells showed red droplet formation. Magnification, ×100 (B) and ×200 (C).

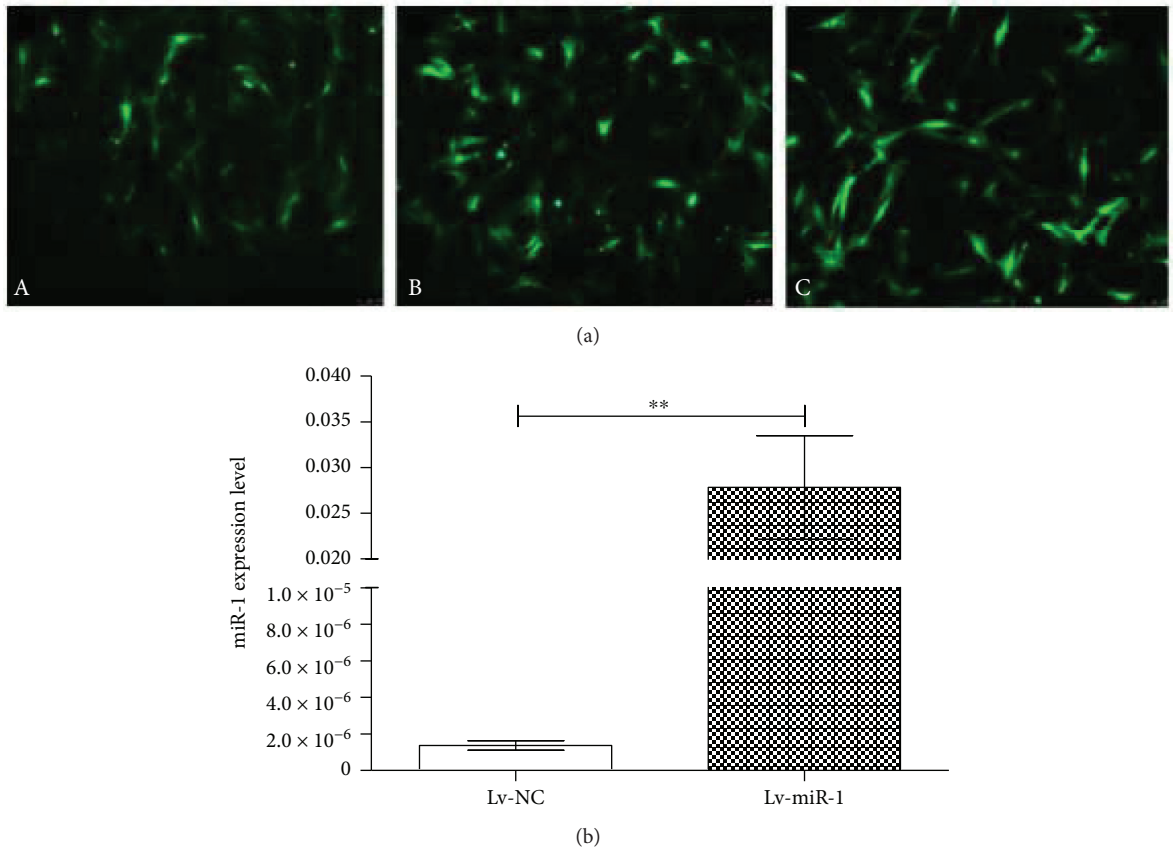

Figure 3: ASCs infected with microRNA-1 lentivirus. (a) Immunofluorescence microscopy of GFP in ASCs infected with miRNA-1 lentivirus. GFP expression in ASCs after 48 h infection with miRNA-1-expressing lentivirus at (A) MOI = 40, (B) MOI = 60, and (C) MOI = 80. (b) miR-1 expression level in miR-1-expressing ASCs. qPCR for miRNA-1 expression in 4th-generation ASCs infected with miRNA-expressing lentivirus (Lv-miR-1 group) or control lentivirus (Lv-NC group). $^{**}P < 0.01$.

expression level was also higher in the Lv-miR-1-CMs group compared with that in the Lv-miR-1 group as well as the Lv-NC-CM group ($P < 0.05$) (Figure 5(d)). Hes1 protein showed a different expression pattern; no changes were observed in miR-1-expressing cells upon coculture (Lv-miR-1-CMs and Lv-miR-1 groups), although a reduced expression level was detected in Lv-miR-1-CMs compared with the control Lv-NC-CM group ($P < 0.05$) (Figure 5(e)).

Overall, we observed similar trends in the qPCR results with the protein expression patterns. The cTnI, GATA4, and Notch 1 gene expression levels were all significantly higher in the Lv-miR-1-CM group than in Lv-miR-1 and Lv-NC-CM groups ($P < 0.05$) (Figures 5(f)–5(h)). Consistent with the protein expression results, the Hes1 gene expression level was lower in the Lv-miR-1-CM group than in the Lv-NC-CM group ($P < 0.05$) (Figure 5(i)).

These data also indicated that the expression levels of Hes1 and Notch1 in the Lv-miR-1-CM and Lv-NC-CM groups (after coculture) showed no significant difference compared with the noncocultured groups. However, GATA4 and cTnI expression levels were upregulated in miRNA-1-expressing cells after coculture (Lv-miR-1-CMs compared with Lv-miR-1 cells), which proved that miR-1 could promote the differentiation of ASCs into cardiomyocyte-like cells.

3.7. Immunofluorescent Assay Results. We next performed immunofluorescence detection of GATA4 in Lv-miR-1-CMs, Lv-NC-CMs, and Lv-miR-1 cells (Figure 6). Consistent with the results above, the miR-1-expressing cells (Lv-miR-1 group) showed low expression of GATA4 (red fluorescence) and coculture with CMs (Lv-miR-1-CMs) resulted in a higher number of cells expressing GATA4. We also found that GATA4 expression in the Lv-miR-1-CM group was higher than that in the Lv-NC-CM group.

4. Discussion

Stem cell transplantation has been widely used as a myocardial regeneration method in treating myocardial infarction and can reduce long-term mortality and mitigate heart failure after acute myocardial infarction. Multipotential stem cells can be derived from fat tissue, as it contains abundant MSCs that can rapidly proliferate and differentiate into many cell lineages *in vitro* [23]. Furthermore, small animal models have shown that transplanted stem cells can express endothelium and myocardium markers, which could improve cardiac function after myocardial infarction [24]. ASCs can differentiate into myocardial cells and vascular cells, which further increase the expression of VEGF and neovascularization [25]. ASCs are abundant and easy to obtain. The

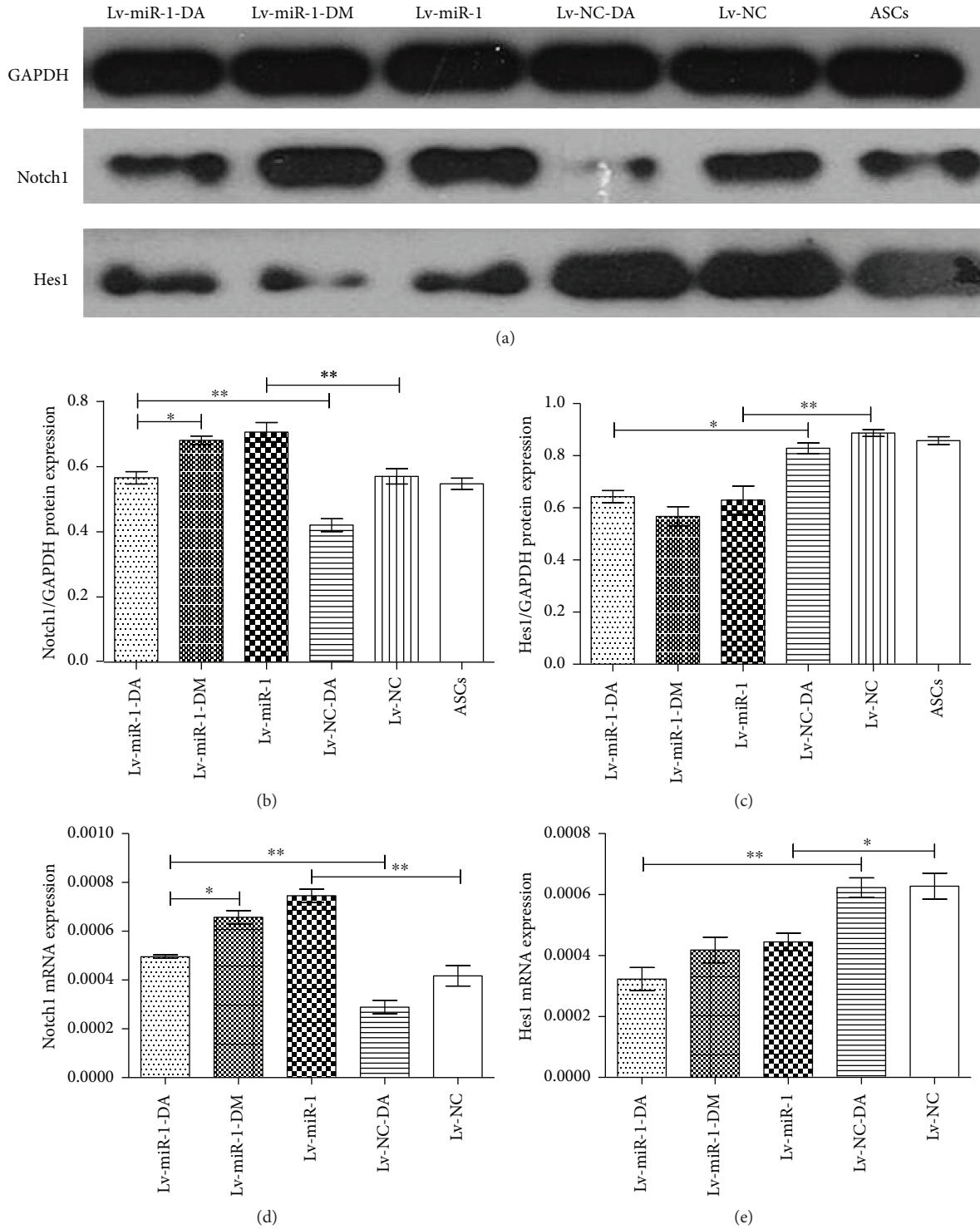

Figure 4: Notch1 and Hes1 protein and gene expression levels in miRNA-1-expressing ASCs after DAPT treatment. ASCs infected with miRNA-1-expressing lentivirus were treated for 7 days with DAPT (Lv-miR-1-DA) or DMSO (Lv-miR-1-DM) or untreated (Lv-miR-1). ASCs infected with control lentivirus were treated for 7 days with DAPT (Lv-NC-DA) or untreated (Lv-NC). Uninfected ASCs were used as negative control. (a) Western blot results of Notch1 and Hes1 protein expression. GAPDH was used as normalization control. (b and c) Quantification of the relative expression level of each protein compared with the control. * and ** as determined by one-way ANOVA. (d and e) Notch1 and Hes1 mRNA levels compared with control. * and ** as determined by one-way ANOVA.

transplantation of bone marrow stromal cells (BMSCs) and ASCs into the myocardium after myocardial infarction could optimize the anti-inflammatory cytokine level with no obvious inflammation reaction. Furthermore, ASCs can significantly improve heart function and reduce the infarction area and showed better effects than BMSC transplantation

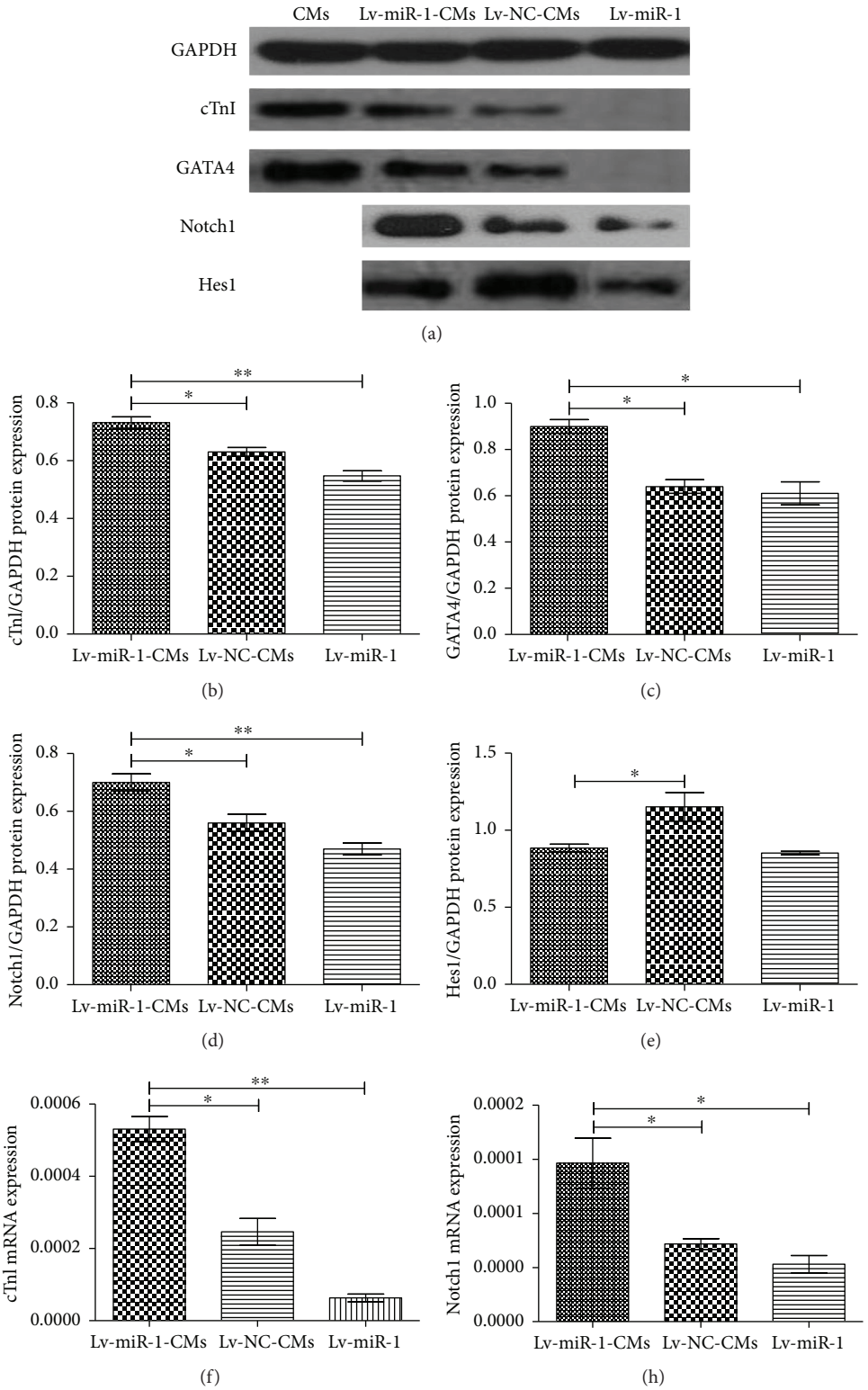

Figure 5: Continued.

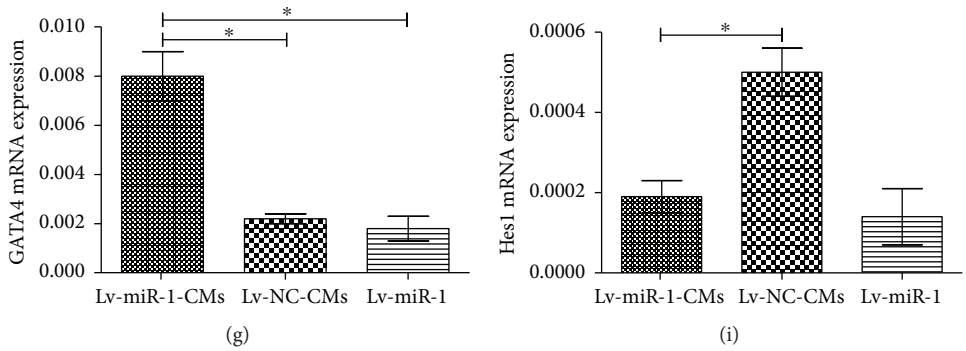

Figure 5: Expression levels of Notch1, Hes1, cTnI, and GATA4 proteins in ASCs after coculture with CMs. Three groups of 3rd-generation lentivirus (Lv)-infected ASCs were examined as follows: (1) Lv-miR-1-CMs (miRNA-1-expressing cells cocultured with CMs), (2) Lv-miR-1 (miRNA-1-expressing ASCs), and (3) Lv-NC-CMs (control infected ASCs cocultured with CMs). (a) Western blot analysis of the indicated proteins. GAPDH was used as normalization control. (b–e) Quantification of cTnI, GATA4, Notch1, and Hes1 protein levels, as indicated. (f–i) mRNA expression levels of cTnI, GATA4, Notch1, and Hes1, as indicated. $^{*}P < 0.05$ and $^{**}P < 0.01$.

can [26]. In this study, we demonstrated that ASCs can differentiate into MSCs and showed a positive expression of CD29 and a negative expression of CD31 and CD45. ASCs can also be induced into osteoblasts and adipocytes. Previous studies showed that *in vitro* transplantation of ASCs showed low efficiency in differentiation into cardiomyocyte-like cells, of which the repair effect has been greatly restricted. Thus, the promotion of the differentiation rate from ASCs into cardiomyocyte-like cells is a key point in improving the ASC treatment effect on myocardial infarction.

MiRNAs are a type of endogenous noncoding small RNA with a length of 18–22 bp. Previous studies have shown that miRNAs play important roles in various cellular processes, including proliferation, differentiation, and apoptosis, as well as cardiac differentiation [27, 28]. miRNAs regulate signal pathways via the regulation of target gene expression [29]. Previous studies showed that miR-1 can promote the differentiation of mouse and human embryonic stem cells into myocardial cells after 4 days of embryoid body differentiation. miR-1 expression was detected in the mesoblast of mice and promoted the expression of the molecular marker Bry in the early mesoderm of pluripotent stem cells. On the 6th and 10th days of embryoid body differentiation, overexpression of miR-1 increased the expression of the early cardiac marker and transcription factor Nkx2.5 [11].

The myocardium-specific gene cTnI and myocardium-specific transcription factor GATA4 show specific expression in myocardial cells, and their expression levels were higher in cardiomyocyte-like cells compared with other cell lines. GATA family proteins are zinc finger protein transcription factors that show a tissue-specific expression and play important roles in multiple tissues and processes, especially in muscular tissue differentiation and development. GATA4 plays significant roles in myocardial differentiation and development, and its expression is closely related to the cardiomyocyte markers β-myosin heavy chain, calcium and sodium, and the transcription and expression of cardiac troponin. Moreover, GATA4 is expressed during the entire mouse heart development, and its expression in cardiac muscle is sustained until birth [30]. In this study, ASCs cultured for 7 days in the myocardial microenvironment showed higher expression levels of cTnI and GATA4 compared with the control group. Importantly, we found that overexpression of miR-1 in ASCs in coculture conditions promoted ASC differentiation into cardiomyocyte-like cells to higher levels than control ASCs in coculture conditions. ASCs overexpressing miR-1 (without coculture) showed no obvious expression of cTnI and GATA4. These results indicate that miRNA-1 overexpression is closely related with the differentiation of ASCs into cardiomyocyte-like cells, but the specific underlying mechanisms have been unknown.

The Notch signal pathway is highly conserved and plays multiple roles in regulating cell differentiation, proliferation, and apoptosis. Abnormalities in the Notch pathway would lead to evolutionary changes of multicellular organisms and various human diseases. The Notch signal pathway consists of multiple ligands, receptors, and target genes, including four homologous receptors (Notch1–4) and five homologous Notch ligands (Delta like(Dll)1, Delta like(Dll)3, Delta like(Dll)4, Jaggedl, and Jagged2) in humans.

Previous studies have examined the role of the Notch signal pathway in MSC differentiation into osteoblasts, but the results have been controversial. An *in vitro* study showed that Notch plays dual roles in inducing the differentiation of MSCs into osteoblasts [31]. Notch1 showed higher expression levels in a coculture model of MSCs and myocardial cells *in vitro* compared with MSCs cultured alone. In the process of BMSCs undergoing osteogenic differentiation, an upregulated expression of Notch was detected, which indicated that activation of the Notch signal could promote osteogenesis, and Notch played important roles in regulating BMSC proliferation and differentiation. Moreover, differentiated MSCs showed significantly higher Notch1 expression levels than proliferating MSCs [32]. Our results suggest that miR-1 may promote the differentiation of BMSCs into myocardial cells by downregulation of the Notch target gene, Hes1 [21].

As our results demonstrated, miR-1 could regulate the expression of Hes1 and Notch1 in the Notch signal pathway. Overexpression of miR-1 in ASCs resulted in reduced Hes1

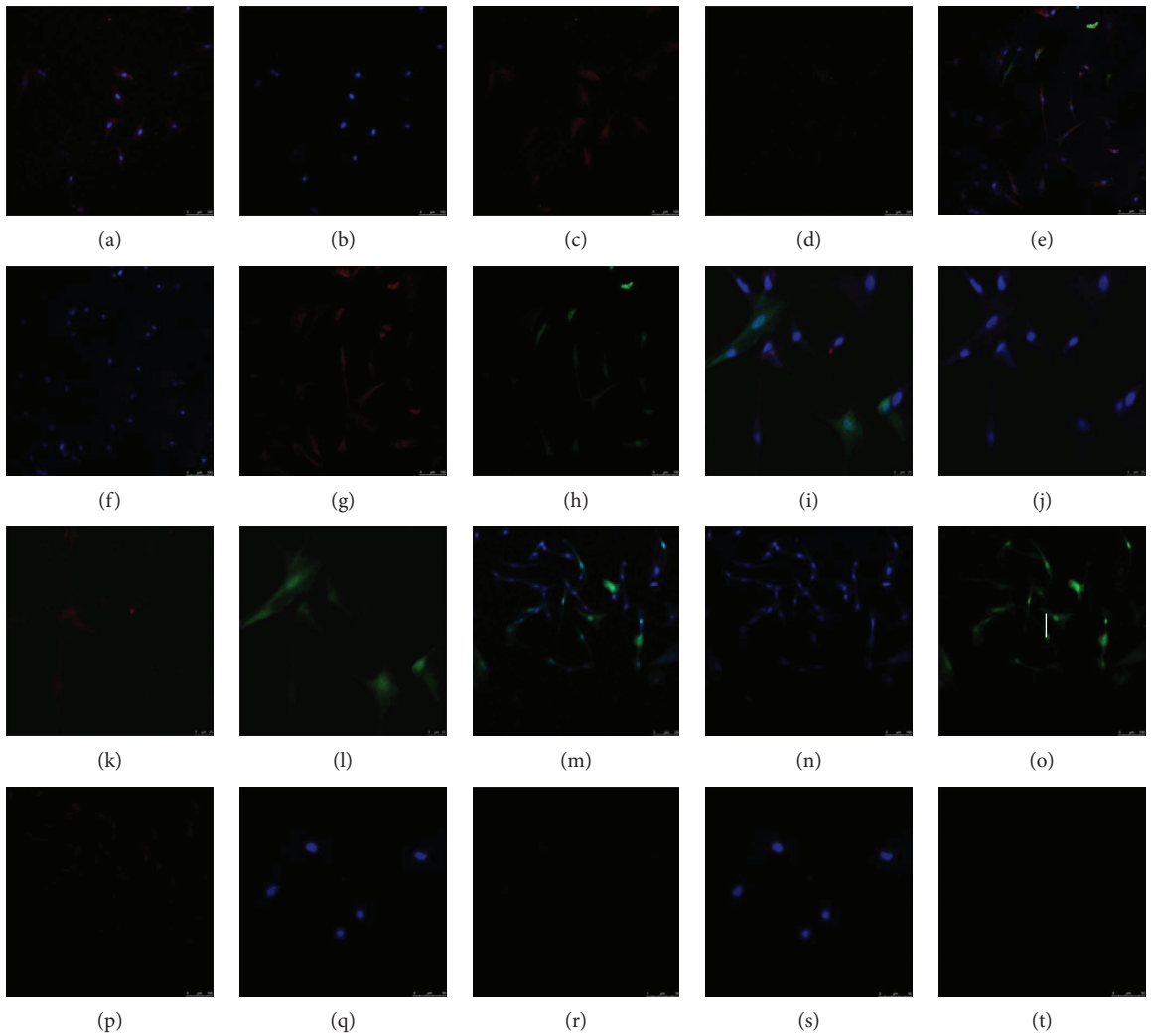

Figure 6: Immunofluorescence detection of the myocardium-specific transcription factor GATA in ASCs overexpressing miRNA-1 and cocultured with CMs. Five groups of 3rd-generation lentivirus (Lv)-infected ASCs and/or CMs were examined as follows: (a–d) CMs alone; (e–h) Lv-miR-1-CMs (miRNA-1-expressing ASCs cocultured with CMs); (i–l) Lv-NC-CMs (control infected ASCs cocultured with CMs); (m–p) Lv-miR-1 cells (miRNA-1-expressing ASCs); (q–t) ASCs alone. (a, e, i, m, and q) Merged images; (b, f, j, n, and r) DAPI fluorescence stain; (c, g, k, o, and s) GFP, indicating ASC fluorescence labeling; (d, h, l, p and t) red fluorescence, indicating GATA4.

expression and increased protein and mRNA expression of Notch1. Even after blocking of Notch1 protein expression by DAPT, miR-1 was still able to promote Notch1 expression. After transdifferentiation of ASCs, the Notch1 expression level was higher in the Lv-miR-1-CMs group than in the Lv-miR-1 group, which demonstrated that miR-1 regulated the Notch pathway-related receptors. These results demonstrated that miR-1 overexpression and coculture with myocardial cells created a microenvironment that together promoted ASC differentiation into myocardial cells.

This study investigated the mechanisms of miR-1 in regulating the differentiation of ASCs into cardiomyocyte-like cells. Our results showed that ASCs could be induced to differentiate into cardiomyocyte-like cells in the myocardial microenvironment and express cardiomyocyte-specific markers. Overexpression of miR-1 could promote the differentiation process, and the cardiomyocyte-specific markers cTnI and GATA4 showed significantly higher expression levels in miRNA-1-overexpressing cells compared with controls in coculture conditions. In noninduced ASCs, DAPT treatment resulted in downregulation of Notch1 protein expression; further, Notch1 expression levels in the miRNA-1-overexpressing group were higher than in the control group, which indicated that miRNA-1 promoted the expression of Notch1 in ASCs. DAPT treatment caused no changes in the Notch1 pathway target gene Hes1 in ASCs, but in the miR-1 overexpression group, Hes1 expression was significantly downregulated. After induction of differentiation, Notch1 and Hes1 expression levels were almost the same as those preinduction. Therefore, in the process of miR-1 promoting stem cell differentiation, miR-1 appears to activate the Notch pathway, which resulted in the increase of Notch1 receptors and the reduced expression of the Hes1 target gene, which resulted in induction of ASC differentiation. The specific mechanisms of how Notch1 and Hes1 affect ASC differentiation into myocardial cells are still

unknown, and further experiments should be carried out to investigate the underlying mechanisms.

5. Conclusions

In conclusion, our findings showed that miR-1 could promote the differentiation of ASCs in the myocardial microenvironment, and this may be regulated by mechanisms involving Notch1-Hes1. Based on the identification of this pathway in ASC differentiation, future studies could examine the use of gene overexpression or silencing to improve the differentiation rate of ASCs and increase the survival rate of ASCs *in vivo*.

Conflicts of Interest

The authors declare that there is no conflict of interests regarding the publication of the paper.

Acknowledgments

This paper was supported by the National Natural Science Foundation of China (nos. 81300035 and 81741129), Collaborative Innovation and Platform Environment Construction Projects of Guangdong Province (2015A050502049), Natural Science Foundation of Guangdong Province (2015A030313520 and 2016A020214017), Research Project of Traditional Chinese Medicine Bureau of Guangdong Province (20151259), and Stem Cell Preclinical Research Projects of the Affiliated Hospital of Guangdong Medical University (2018PSSC004).

References

[1] D. A. De Ugarte, K. Morizono, A. Elbarbary et al., "Comparison of multi-lineage cells from human adipose tissue and bone marrow," *Cells, Tissues, Organs*, vol. 174, no. 3, pp. 101–109, 2003.

[2] W. Huang, B. Dai, Z. Wen et al., "Molecular strategy to reduce *in vivo* collagen barrier promotes entry of NCX1 positive inducible pluripotent stem cells ($iPSC^{NCX1+}$) into ischemic (or injured) myocardium," *PLoS One*, vol. 8, no. 8, article e70023, 2013.

[3] D. Simpson, H. Liu, T. H. Fan, R. Nerem, and S. C. Dudley Jr., "A tissue engineering approach to progenitor cell delivery results in significant cell engraftment and improved myocardial remodeling," *Stem Cells*, vol. 25, no. 9, pp. 2350–2357, 2007.

[4] B. Dai, W. Huang, M. Xu et al., "Reduced collagen deposition in infarcted myocardium facilitates induced pluripotent stem cell engraftment and angiomyogenesis for improvement of left ventricular function," *Journal of the American College of Cardiology*, vol. 58, no. 20, pp. 2118–2127, 2011.

[5] P. A. Zuk, M. Zhu, H. Mizuno et al., "Multilineage cells from human adipose tissue: implications for cell-based therapies," *Tissue Engineering*, vol. 7, no. 2, pp. 211–228, 2001.

[6] S. Rangappa, C. Fen, E. H. Lee, A. Bongso, and E. S. K. Wei, "Transformation of adult mesenchymal stem cells isolated from the fatty tissue into cardiomyocytes," *The Annals of Thoracic Surgery*, vol. 75, no. 3, pp. 775–779, 2003.

[7] A. P. Cai, D. D. Zheng, Y. G. Dong et al., "Efficacy of atorvastatin combined with adipose-derived mesenchymal stem cell transplantation on cardiac function in rats with acute myocardial infarction," *Acta Biochimica et Biophysica Sinica*, vol. 43, no. 11, pp. 857–866, 2011.

[8] V. Planat-Bénard, C. Menard, M. André et al., "Spontaneous cardiomyocyte differentiation from adipose tissue stroma cells," *Circulation Research*, vol. 94, no. 2, pp. 223–229, 2004.

[9] C. Kwon, Z. Han, E. N. Olson, and D. Srivastava, "MicroRNA1 influences cardiac differentiation in *Drosophila* and regulates Notch signaling," *Proceedings of the National Academy of Sciences of the United States of America*, vol. 102, no. 52, pp. 18986–18991, 2005.

[10] N. S. Sokol and V. Ambros, "Mesodermally expressed *Drosophila microRNA-1* is regulated by Twist and is required in muscles during larval growth," *Genes & Development*, vol. 19, no. 19, pp. 2343–2354, 2005.

[11] K. N. Ivey, A. Muth, J. Arnold et al., "MicroRNA regulation of cell lineages in mouse and human embryonic stem cells," *Cell Stem Cell*, vol. 2, no. 3, pp. 219–229, 2008.

[12] J. P. Sluijter, A. van Mil, P. van Vliet et al., "MicroRNA-1 and -499 regulate differentiation and proliferation in human-derived cardiomyocyte progenitor cells," *Arteriosclerosis, Thrombosis, and Vascular Biology*, vol. 30, no. 4, pp. 859–868, 2010.

[13] L. P. Lim, N. C. Lau, P. Garrett-Engele et al., "Microarray analysis shows that some microRNAs downregulate large numbers of target mRNAs," *Nature*, vol. 433, no. 7027, pp. 769–773, 2005.

[14] N. Nakajima, T. Takahashi, R. Kitamura et al., "MicroRNA-1 facilitates skeletal myogenic differentiation without affecting osteoblastic and adipogenic differentiation," *Biochemical and Biophysical Research Communications*, vol. 350, no. 4, pp. 1006–1012, 2006.

[15] J. F. Chen, E. M. Mandel, J. M. Thomson et al., "The role of microRNA-1 and microRNA-133 in skeletal muscle proliferation and differentiation," *Nature Genetics*, vol. 38, no. 2, pp. 228–233, 2006.

[16] P. Xu, S. Y. Vernooy, M. Guo, and B. A. Hay, "The *Drosophila* microRNA Mir-14 suppresses cell death and is required for normal fat metabolism," *Current Biology*, vol. 13, no. 9, pp. 790–795, 2003.

[17] Y. Zhao, J. F. Ransom, A. Li et al., "Dysregulation of cardiogenesis, cardiac conduction, and cell cycle in mice lacking miRNA-1-2," *Cell*, vol. 129, no. 2, pp. 303–317, 2007.

[18] K. Niessen and A. Karsan, "Notch signaling in the developing cardiovascular system," *American Journal of Physiology Cell Physiology*, vol. 293, no. 1, pp. C1–C11, 2007.

[19] M. D. Chau, R. Tuft, K. Fogarty, and Z. Z. Bao, "Notch signaling plays a key role in cardiac cell differentiation," *Mechanisms of Development*, vol. 123, no. 8, pp. 626–640, 2006.

[20] Y. Tian, R. Guo, B. Shi, L. Chen, L. Yang, and Q. Fu, "MicroRNA-30a promotes chondrogenic differentiation of mesenchymal stem cells through inhibiting Delta-like 4 expression," *Life Sciences*, vol. 148, pp. 220–228, 2016.

[21] F. Huang, L. Tang, Z. F. Fang, X. Q. Hu, J. Y. Pan, and S. H. Zhou, "miR-1-mediated induction of cardiogenesis in mesenchymal stem cells via downregulation of Hes-1," *Biomed Research International*, vol. 2013, Article ID 216286, 9 pages, 2013.

[22] M. Sjöqvist, D. Antfolk, S. Ferraris et al., "PKCζ regulates Notch receptor routing and activity in a Notch signaling-

dependent manner," *Cell Research*, vol. 24, no. 4, pp. 433–450, 2014.

[23] X. Bai and E. Alt, "Myocardial regeneration potential of adipose tissue-derived stem cells," *Biochemical and Biophysical Research Communications*, vol. 401, no. 3, pp. 321–326, 2010.

[24] X. Bai, Y. Yan, Y. H. Song et al., "Both cultured and freshly isolated adipose tissue-derived stem cells enhance cardiac function after acute myocardial infarction," *European Heart Journal*, vol. 31, no. 4, pp. 489–501, 2010.

[25] M. Rigol, N. Solanes, S. Roura et al., "Allogeneic adipose stem cell therapy in acute myocardial infarction," *European Journal of Clinical Investigation*, vol. 44, no. 1, pp. 83–92, 2014.

[26] A. Paul, S. Srivastava, G. Chen, D. Shum-Tim, and S. Prakash, "Functional assessment of adipose stem cells for xenotransplantation using myocardial infarction immunocompetent models: comparison with bone marrow stem cells," *Cell Biochemistry and Biophysics*, vol. 67, no. 2, pp. 263–273, 2013.

[27] B. Emery, "Regulation of oligodendrocyte differentiation and myelination," *Science*, vol. 330, no. 6005, pp. 779–782, 2010.

[28] H. Hu and R. A. Gatti, "MicroRNAs: new players in the DNA damage response," *Journal of Molecular Cell Biology*, vol. 3, no. 3, pp. 151–158, 2011.

[29] G. Tiscornia and B. J. C. Izpisúa, "MicroRNAs in embryonic stem cell function and fate," *Genes & Development*, vol. 24, no. 24, pp. 2732–2741, 2010.

[30] S. M. Harlan, R. S. Reiter, C. D. Sigmund, J. L. C. Lin, and J. J. C. Lin, "Requirement of TCTG(G/C) direct repeats and overlapping GATA site for maintaining the cardiac-specific expression of *cardiac troponin T* in developing and adult mice," *The Anatomical Record: Advances in Integrative Anatomy and Evolutionary Biology*, vol. 291, no. 12, pp. 1574–1586, 2008.

[31] F. Ugarte, M. Ryser, S. Thieme et al., "Notch signaling enhances osteogenic differentiation while inhibiting adipogenesis in primary human bone marrow stromal cells," *Experimental Hematology*, vol. 37, no. 7, pp. 867–875.e1, 2009.

[32] P. Niu, Y. Q. Zhao, and X. Y. Huang, "Notch signaling system regulates the proliferation and differentiation of mesenchymal stem cells *in vitro*," *Basic & Clinical Medicine*, vol. 31, no. 11, pp. 1205–1209, 2011.

Hindawi
Stem Cells International
Volume 2017, Article ID 4252974, 8 pages
https://doi.org/10.1155/2017/4252974

Research Article

Long Noncoding RNA uc001pwg.1 Is Downregulated in Neointima in Arteriovenous Fistulas and Mediates the Function of Endothelial Cells Derived from Pluripotent Stem Cells

Lei Lv, Haozhe Qi, Xiangjiang Guo, Qihong Ni, Zezhen Yan, and Lan Zhang

Department of Vascular Surgery, Ren Ji Hospital, School of Medicine, Shanghai Jiao Tong University, Shanghai, China

Correspondence should be addressed to Lan Zhang; rjzhanglan@sjtu.edu.cn

Received 28 May 2017; Revised 19 September 2017; Accepted 2 October 2017; Published 13 December 2017

Academic Editor: Wei Lei

Recent studies indicate important roles for long noncoding RNAs (lncRNAs) as essential regulators of gene expression. However, the specific roles of lncRNAs in stenotic lesions of arteriovenous fistula (AVF) failure are still largely unknown. We first analyzed the expression profiles of lncRNAs in human stenosed and nonstenotic uremic veins using RNA-sequencing methodology. A total of 19 lncRNAs were found to be differentially expressed in stenotic lesions. Among these, uc001pwg.1 was one of the most significantly downregulated lncRNAs and enriched in both control vein segments and human umbilical vein endothelial cells (HUVECs). Further studies revealed that uc001pwg.1 overexpression could increase nitric oxide synthase (eNOS) phosphorylation and nitric oxide (NO) production in endothelial cells (ECs) derived from human-induced pluripotent stem cells (HiPSCs). Mechanistically, uc001pwg.1 improves endothelial function via mediating MCAM expression. This study represents the first effort of identifying a novel candidate lncRNA for modulating the function of iPSC-ECs, which may facilitate the improvement of stem cell-based therapies for AVF failure.

1. Introduction

Patients with end-stage renal disease rely on hemodialysis, which requires a vascular access providing high blood flow rates preferably achieved through an AVF conduit [1]. However, the problems associated with vascular access dysfunction are the most common reason for increased morbidity, mortality, and length of in-hospital stay for patients and represent major clinical, social, and financial burden even for the developed countries [2, 3]. Venous neointimal hyperplasia (NH) is the predominant cause of stenosis.

Histological investigations have confirmed that venous neointimal hyperplasia is the predominant cause of stenotic lesions of AVF failure [4]. AVF stenosis occurs at the outflow vein due to venous neointimal hyperplasia and results in the failure of 60% of AVFs within 2 years [5]. Currently, there are no prophylactic treatments to ameliorate the progression of neointimal hyperplasia in AVFs. Percutaneous transluminal angioplasty for stenosis in functioning forearm AVF has been found to significantly improve patency and decrease access-related morbidity [6]. However, the disadvantages of these procedures are that they require frequent revision as the 12-month patency rate can be as low as 26% [7]. At present, there is minimal understanding of pathological and molecular mechanisms in AVF failure. The endothelial cell (EC) monolayer is at the interface between the extravascular space and blood, playing a crucial role in the modulation of vascular homeostasis [8]. Endothelial dysfunction has been implicated as an early step in the pathogenesis of neointima [9]. Therefore, improving endothelial function is critical for the prevention and treatment of neointima.

Long noncoding RNAs (lncRNAs) represent a diverse type of long RNA molecules lacking protein-coding capacity, with a length of larger than 200 nucleotides [10, 11]. A growing body of work has proved that lncRNAs play essential roles in a variety of biological processes, such as cell growth, differentiation, and immune response. However, insufficient information is available about the effect of lncRNAs in the context of AVF failure and about the role of lncRNAs in endothelial function.

In the current study, we examined the expression profiles of lncRNAs in stenosed vein segments of primary AVFs from uremic patients via RNA-sequencing analysis. In addition, we identified an unannotated lncRNA, uc001pwg.1, which positively regulates the function of a stem cell type, ECs derived from human-induced pluripotent stem cells (HiPSCs), which is more applicable for future translational and clinical research. During this process, uc001pwg.1 regulates the expression of melanoma cell adhesion molecule (MCAM). Based on these findings, we suggest that uc001pwg.1 may offer an attractive target for improving AVF function in uremic patients.

2. Material and Methods

2.1. Patients and Tissue Samples. This study was given ethical approval by the Renji Hospital Ethical Committee, Shanghai, China. All participants provided written informed consent to participate in this study. Stenosed vein segments were harvested from the primary AVFs just distal to the anastomosis at the time of surgical revision in 4 patients. Control vein segments were harvested from 3 predialytic patients at the time of their first operation for vascular access [12]. The two groups were statistically similar in sex and age. A detailed description of the two groups is provided in Supplementary Table 1.

2.2. RNA-Sequencing Analysis and Gene Ontology Analysis. LncRNA-Seq high-throughput sequencing and subsequent bioinformatics analysis were all done by CloudSeq Biotech (Shanghai, China). Briefly, paired-end reads were harvested from Illumina HiSeq 4000 sequencer and were quality controlled by Q30. After 3′ adaptor-trimming and low quality reads removing by the cutadapt software (v1.9.3), the high-quality trimmed reads were aligned to the reference genome (UCSC HG19) guided by the Ensembl GFF gene annotation file with the hisat2 software (v2.0.4). Then, the cuffdiff software (v2.2.1, part of cufflinks) was used to get the gene level FPKM as the expression profiles of lncRNA, and fold change and q value were calculated based on FPKM, and differentially expressed LncRNAs were identified. Differentially expressed lncRNAs with statistical significance were identified through volcano plot filtering and fold-change filtering. Finally, hierarchical clustering was performed based on differentially expressed lncRNAs using Cluster Tree view software (Stanford University, Palo Alto, CA, USA). A gene ontology (GO) analysis was performed to characterize genes and gene products in terms of the biological process, cellular component, and molecular function. Fisher's exact test was used to find if there was overlap between the differentially expressed list and the GO annotation list.

2.3. Generation of iPSC-ECs. HiPSCs were generated in our laboratory previously. HiPSCs are routinely maintained on Matrigel (BD, 356234)-coated plates in TeSR-E8media (Stem Cell) and passaged mechanically. Differentiation will be induced two days after passaging colonies by replacing TeSR-E8 medium with differentiation media based on α-MEM (Gibco) and timed addition of the following factors: 25 ng/ml Activin A (PeproTech, AF-120-14E), 30 ng/ml bone morphogenetic protein (BMP) 4 (PeproTech, AF-120-05ET), 50 ng/ml VEGF 165 (R&D Systems, 293-VE), and the small molecule inhibitor CHIR99021 (Selleck, S1263). On day 3 and day 7 of differentiation, the medium will be refreshed with α-MEM containing 50 ng/ml VEGF and 10 μmol/L SB43152 (PeproTech, 1614) only. Single-cell suspensions were incubated with PE-conjugated anti-human CD31 antibody, and flow cytometry was used to purify the ECs. The purity of the HiPSC-EC was >90% by phenotype and CD31 immunostaining.

2.4. Cell Culture. Human umbilical vein endothelial cells (HUVECs), umbilical vein smooth muscle cells (HUVSMCs), and human pulmonary artery fibroblasts (HPAFs) were purchased from ScienCell (Carlsbad, CA, USA) and were cultured in fully supplemented endothelial growth medium (EGM-2, Lonza, Walkersville, MD, USA), smooth muscle cell medium (SMCM, ScienCell), and fibroblast medium (SMCM, ScienCell), respectively.

2.5. HiPSC-EC Transduction. Adenoviral vectors containing uc001pwg.1 and control adenoviruses were purchased from GeneChem Inc. (GeneChem, Shanghai). HiPSC-ECs were grown in EC growth medium (cat. number MCDB-131C, Vec Technologies) to 80% confluence and treated with adenoviruses containing uc001pwg.1 or control adenoviruses. Eighteen hours after adenoviral transduction, fresh media was added to the cells, and 3 days after transduction, transfection efficiency was confirmed by qRT-PCR.

2.6. Quantitative Real-Time PCR (qRT-PCR). Total RNA was extracted from samples using TRIzol reagent (Invitrogen) and converted into cDNA using the Fermentas RT kit according to the manufacturer's instructions. PCR was performed in a total reaction volume of 25 μL, containing 12.5 μL SYBR Premix Ex Taq (2x), 2 μL cDNA, 1 μL forward primer (10 μM), 1 μL reverse primer (10 μM), 0.5 μL ROX Reference Dye II (50x), and 8 μL double-distilled water. Amplification efficiency was evaluated via standard curve analysis. All samples were normalized to GAPDH, and the experiment was repeated three times. The following primers were used:

uc001pwg.1, forward: 5′-GCTGTGATTGTGTGCATCCT-3′, reverse: 5′-GAAGAGTGAGCAGGGAGCTG-3′; GAPDH, forward: 5′-GGCCTCCAAGGAGTAAGACC-3′, reverse: 5′-AGGGGAGATTCAGTGTGGTG-3′.

2.7. Western Blotting. The primary antibodies against MCAM (1 : 1000), eNOS (1 : 1000), phosphorylation eNOS (Ser^{1177}) (1 : 1000), and GAPDH (1 : 1000) were purchased from Cell Signaling Technology (Danvers, MA). Western blot analyses were carried out as previously reported [12].

2.8. Detection of NO. NO release was measured by using DAF-FM diacetate. Briefly, HiPSC-ECs were seeded on glass coverslips. 48 h after transduction, the cells were incubated with DMEM containing DAF-FM (5 μM) for 30 min in the dark at 37°C and then washed with PBS. Images were

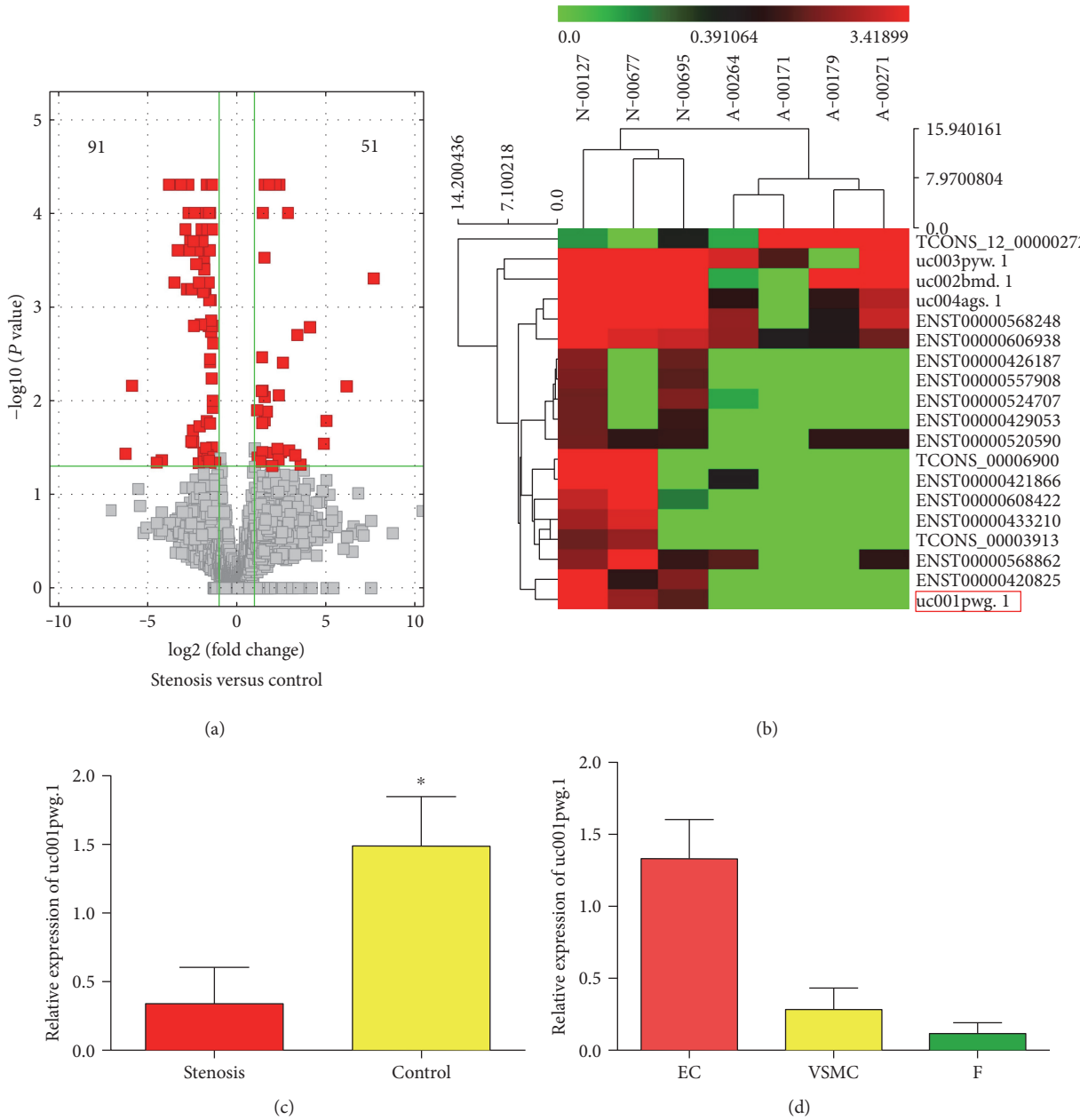

Figure 1: Long noncoding RNA (lncRNA) profiles differentiate the stenosed vein segments of arteriovenous fistulas (AVFs) from the control segments. (a) A volcano plot provided the fold change and *P* values of differentially expressed lncRNAs. The vertical lines represent a 1.5-fold change in expression (up or down), and the horizontal lines represent *P* values = 0.05. (b) Heatmap of selected aberrantly expressed lncRNAs in the stenosed vein segments of AVF and the controls. Colors indicate relative signal intensities: red and green colors indicate upregulated and downregulated lncRNAs, respectively. (c) Verification of uc001pwg.1 by quantitative reverse-transcription polymerase chain reaction (qRT-PCR) in the stenosed vein segments of AVF and the controls. (d) qRT-PCR analysis of uc001pwg.1 in different human vessel cells (VSMC: vein smooth muscle cells; EC: endothelial cells; F: fibroblasts). Triplicate assays were done for each RNA sample, and the relative amount of uc001pwg.1 was normalized to GAPDH. Values are expressed as mean ± standard deviation. $^*P < 0.05$.

obtained using fluorescence microscopy (Olympus America Inc., NY, USA).

2.9. Statistical Analysis. Results are expressed as mean ± standard deviation. The data were monitored using two-tailed *t*-test and chi-square test as appropriate. Data analyses were performed using GraphPad 5.0 software. The significance threshold was defined by a *P* value of <0.05.

3. Results

3.1. uc001pwg.1 Is Downregulated in Stenotic Veins of AVF. To explore the potential biological functions of lncRNAs in stenotic lesions of AVF failure, we examined the expression patterns of lncRNAs in stenotic veins of AVF and control veins. As shown in Figure 1(a), 142 lncRNAs were observed as differentially expressed, with 51 lncRNAs upregulated

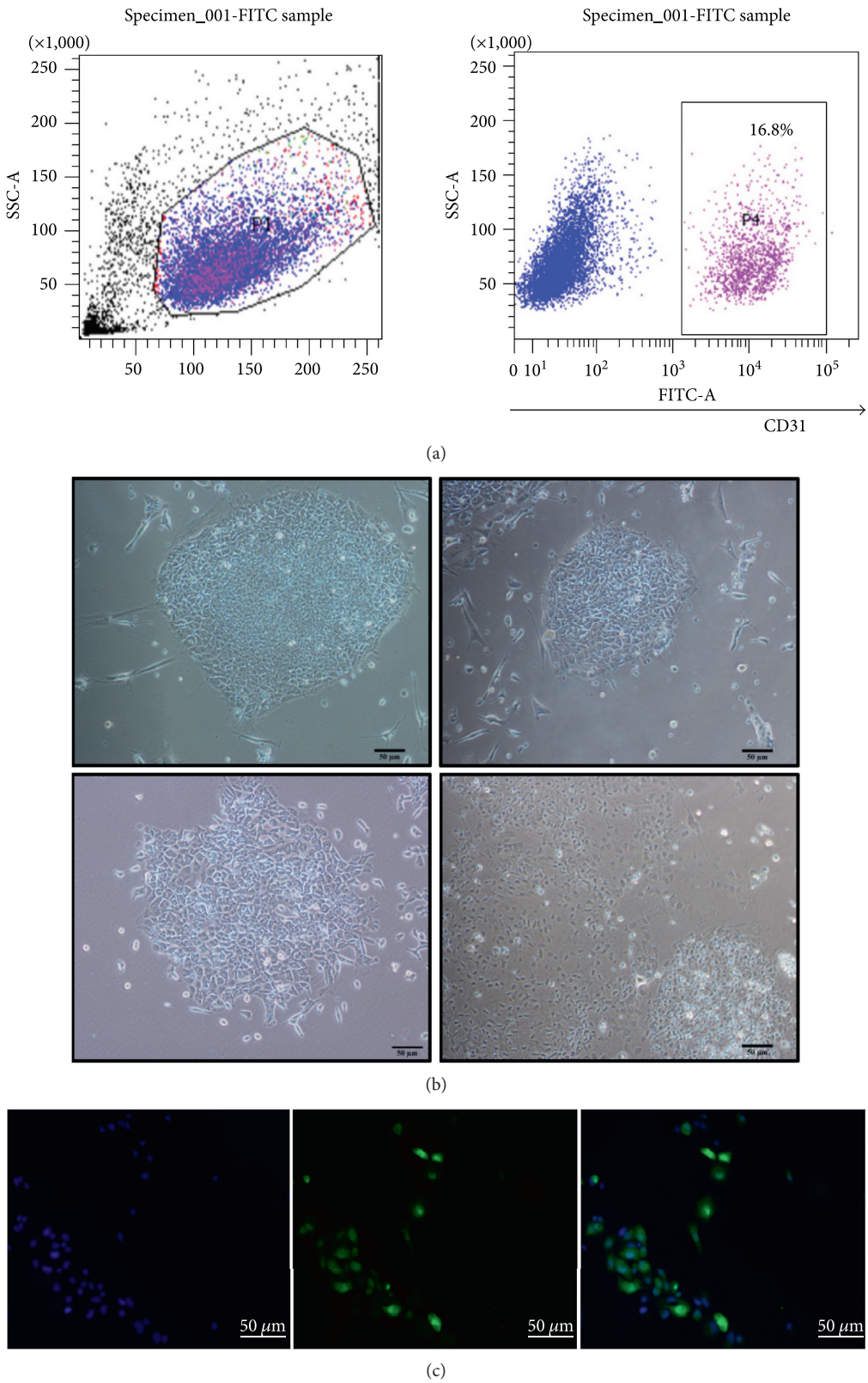

Figure 2: Characterization and differentiation of endothelial cells (ECs) derived from human induced pluripotent stem cells (HiPSCs). (a) FACS analysis showing the CD31 positive cells population upon differentiation protocol. FACS sorting by the endothelial markers CD31 at day 10. Efficiency to generate CD31-positive cells was 16.8%. (b) Differentiation of HiPS toward ECs. A phase-contrast image of cell appearance at 0 day (top left panel), 3 days (top right panel), 7 days (bottom left panel), and 10 days (bottom right panel) after differentiation. Scale bar = 50 μm. (c) Immunofluorescent images of CD 31-positive HiPSC-ECs on day 10 during EC differentiation. DAPI was used and stained the cell nucleus. Scale bar = 50 μm.

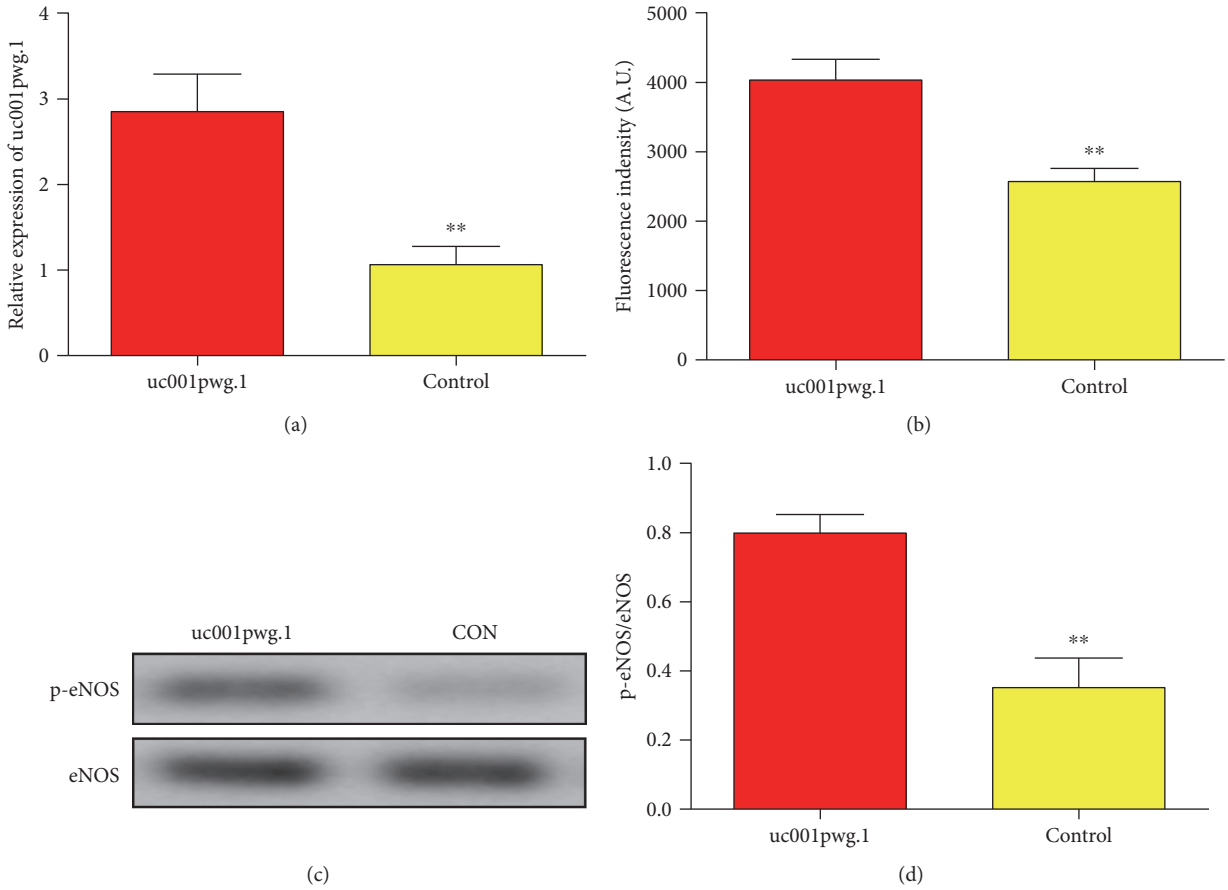

Figure 3: Functional assessment of HiPSC-ECs with or without viral transduction of uc001pwg.1. (a) qRT-PCR analysis of uc001pwg.1 in HiPSC-ECs as an indication of transduction efficiency. (b) The effect of uc001pwg.1 on nitric oxide (NO) generation in HiPSC-ECs using the cell-permeable fluorescent NO indicator DAF-FM. (c) Western blot analysis of endothelial nitric oxide synthase (eNOS) phosphorylation at Ser117 in HiPSC-ECs with overexpression of uc001pwg.1. (d) Bands were quantified by densitometric analysis, and the results are shown as relative density compared with control. Values expressed as mean ± standard deviation from three independent experiments. $^{**}P < 0.01$.

and 91 lncRNAs downregulated in the stenosis group compared to the control group. Detailed information regarding the differentially expressed lncRNAs is shown in Supplementary Table 2. The aberrantly expressed lncRNAs were further subjected to GO analysis (Supplementary Figure 1). Our data showed that some genes related to cell adhesion and junction, cell migration, membrane raft, and so forth were significantly enriched.

Afterward, we removed lncRNAs that were not expressed in the mainly same trend. We kept lncRNAs with at least a threefold change, $P < 0.05$ and FPKM > 0.1 in at least 2 samples. Finally, 19 lncRNAs which met our strict inclusion criteria were selected. Organization of the expression profiles into heatmaps better describes the expression patterns of lncRNAs (Figure 1(b)). Among the decreased lncRNAs, we identified a novel lncRNA (named uc001pwg.1), which was located on chromosome11 (119179240-119192231), enriched in both control vein segments and HUVECs (Figures 1(c) and 1(d)). Consistent with the microarray data, uc001pwg.1 is shown to be significantly suppressed in stenotic veins of AVF using qPCR (Figure 1(c)).

3.2. uc001pwg.1 Enhances the Function of HiPSC-ECs. Recent findings have indicated that HiPSC-derived cells represent an ideal tool for drug testing and might hold remarkable potential in personalized regenerative cell therapies [10]. We tried to evaluate the function of HiPSC-ECs by uc001pwg.1 overexpression. Firstly, we successfully generated ECs from HiPSCs. The HiPSC-ECs were isolated by fluorescent-activated cell sorting after 10 days of differentiation and then expanded for further characterization (Figure 2(a)). The typical yield of ECs generated from the HiPSC line ranged between 11% and 20%. The expanded HiPSC-ECs formed a "cobblestone" monolayer, and immunofluorescence staining revealed that these cells were positive for endothelial marker CD31 (Figures 2(b) and 2(c)).

HiPSC-ECs were then transfected with adenovirus-mediated uc001pwg.1 to upregulate uc001pwg.1 expression. The overexpression of uc001pwg.1 in HiPSC-ECs was confirmed by qRT-PCR (Figure 3(a)). Following adenovirus transduction with uc001pwg.1, these cells showed significantly higher NO production compared to controls (Figure 3(b)). The effect of uc001pwg.1 on eNOS phosphorylation was also

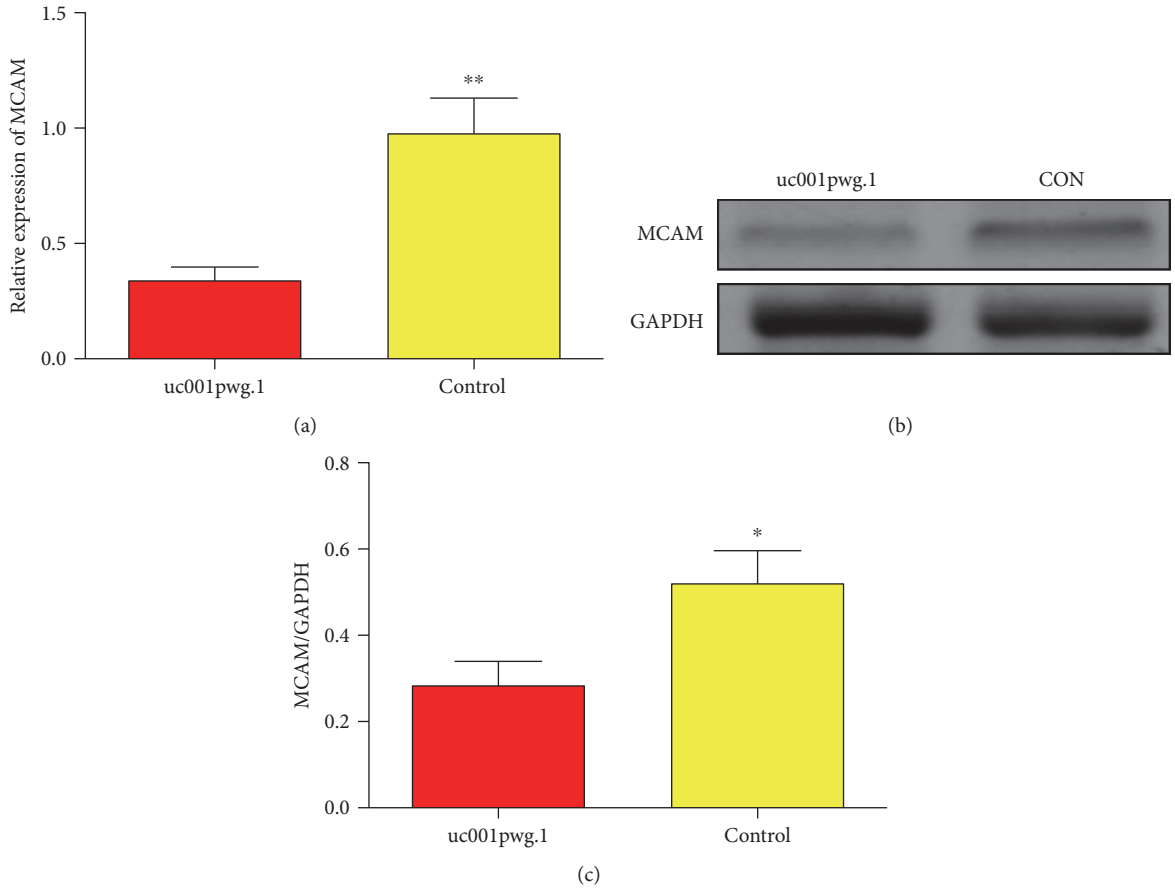

Figure 4: The regulatory effect of uc001pwg.1 on MCAM expression (a) The MCAM mRNA level in HiPSC-ECs after uc001pwg.1 upregulation by qRT-PCR analysis. (b) The MCAM protein level in HiPSC-ECs after uc001pwg.1 upregulation by Western blot analysis. (c) Bands were quantified by densitometric analysis, and the results are shown as relative density compared with control. Values expressed as mean ± standard deviation from three independent experiments. $^{*}P < 0.05$ and $^{**}P < 0.01$.

assessed by Western blotting. We found that uc001pwg.1 significantly increased eNOS-Ser^{1177} phosphorylation in HiPSC-ECs (Figures 3(c) and 3(d)). These results suggest that uc001pwg.1 is able to functionally improve ECs derived from HiPSCs.

3.3. uc001pwg.1 Negatively Regulates the Expression of MCAM. After confirming the effect of uc001pwg.1 on improving endothelial function, we further explored the underlying mechanism in this process. LncRNA can serve as one of the most vital intermediate phenotype on regulating mRNA expression. However, as a relatively novel kind of transcripts, the regulation relation between lncRNA and its putative target is barely known [13]. Thus, it attracted our attention to elucidate the effect of uc001pwg.1 on its associated gene RNA. On the basis of bioinformatics data, we found that MCAM is an mRNA neighboring uc001pwg.1 (exon sense-overlapping) in the lncRNA-mRNA network and is extensively implicated in a variety of oncogenic signaling transduction pathways [14]. After uc001pwg.1 upregulation, an obvious decrease in MCAM expression was observed at both mRNA and protein levels (Figure 4). Therefore, we postulate that uc001pwg.1 enhances the function of HiPSC-ECs by downregulating MCAM expression.

4. Discussion

Recently, a number of lncRNAs have been identified as an important controller of cellular functions via regulating RNA transcription, degradation, and translation. In the present study, the expression profiles of lncRNAs in human stenosed and nonstenotic uremic veins were examined via RNA-sequencing analysis. Long noncoding uc001pwg.1, originally discovered by UCSC_knownGene, is located on chromosome 11 with a length of 441 bps. Our current study found that lncRNA uc001pwg.1 was found enriched in both control vein segments and HUVECs and was emphasized via qRT-PCR validation as a consequence. Furthermore, HiPSC-ECs that have broader prospects in medical application were used in our research. We revealed that upregulated uc001pwg.1 enhanced the function of HiPSC-ECs. Meanwhile, our results presented that uc001pwg.1 overexpression led to the downregulation of MCAM expression, which showed a novel mechanism by which uc001pwg.1 played a vital role in endothelial function through mediating the expression of MCAM.

Our data clearly showed that effects of lncRNA uc001pwg.1 on the function of HiPSC-ECs by overexpressing the lncRNA. DAF-FM diacetate assay results indicated

that NO production was promoted in HiPSC-ECs upon uc001pwg.1 overexpression. Additionally, we found that enhanced uc001pwg.1 could increase the eNOS phosphorylation in HiPSC-ECs. Mounting evidence suggests that the hallmark of endothelial dysfunction is the reduction in the bioavailability of NO [15, 16]. Early processes involved with both expansive and constrictive vascular remodeling are usually mediated by vasomotor changes. In parallel with the importance of NO for initiating vasodilatory responses in the coronary and skeletal muscle circulations, mechanisms affecting its bioavailability are critical during vascular remodeling as crucial determinants of the final lumen size [17]. eNOS, the last of the three mammalian NOS isoforms to be isolated, was originally purified and cloned from vascular endothelium [18]. The ability of eNOS to generate NO allows for control of vascular tone along with preventing inflammation and proliferation of VSMCs in the subendothelium [19]. Alterations in eNOS activity or expression are linked to a number of cardiovascular pathologies that exhibit endothelial dysfunction. Phosphorylation/dephosphorylation of eNOS appears to be a major factor in the regulation of eNOS activity [20]. Therefore, eNOS phosphorylation and NO production of cells were detected to evaluate EC function in the present study. Our findings provide evidence that uc001pwg.1 functions as a key mediator of endothelial function. Like atherosclerosis, the neointima that develops in AVF has preferentially occurred in areas of low fluid shear stress and oscillatory flow [21]. It should be noted that hemodynamic stress plays a significant role in determining the functional phenotype of the vascular endothelium. We could extend our targeted cell delivery strategy to the use of HiPS-ECs that overexpress uc001pwg.1 for targeted cell therapy in animal AVF model in the future.

In view of the data gathered from these databases, the following investigation focused on the endothelial transmembrane protein MCAM, which is the nearby gene of the uc001pwg.1. MCAM and has been thoroughly studied and found to be physiologically expressed on different cells in the organism, as the subset of T lymphocytes Th17 and vascular cells including ECs [22, 23]. In particular, it has been identified that MCAM is a major component of the endothelial junction, controlling cell-cell cohesion, paracellular permeability, inflammatory response, and angiogenesis [24, 25]. A current study supports a role for MCAM as an essential gene for renal EC development [26]. It has been established that endothelial dysfunction (ED) occurs after coronary artery bypass grafting (CABG). A recent report shows increased concentrations of MCAM 3 months after CABG [27]. Some researchers have confirmed a role of MCAM as an endothelial cell dysfunction marker in diabetic patients [28, 29]. Thus, MCAM is considered a candidate gene involved in ED. In our study, we tried to make a clarification of lincRNA-related mechanisms underlying the functional improvement of HiPS-ECs. Interestingly, we confirmed that ectopic uc001pwg.1 expression caused a dramatic decrease of MCAM expression. These results indicate that uc001pwg.1 modulates endothelial function, at least in part, by regulating MCAM expression.

5. Conclusions

In summary, our study is the first to show that lncRNA uc001pwg.1 plays an important role in endothelial dysfunction in stenotic lesions of AVF failure. After successful generation of ECs from HiPSCs, we found that enforced uc001pwg.1 could increase eNOS phosphorylation and NO production in vitro. And the improvement of endothelial function may be related to MCAM downregulation. The strategy utilizing HiPS-ECs overexpressed uc001pwg.1 appears to be a potential for translation to the treatment of neointima formation and failed AVF in future animal studies.

Conflicts of Interest

The authors declare that there are no conflicts of interests regarding the publication of this paper.

Authors' Contributions

Lei Lv and Haozhe Qi contributed equally to this work.

Acknowledgments

This work was supported by grants from the Natural Science Foundation of China (no. 81670442).

Supplementary Materials

Supplementary 1. Clinical characteristics of two groups.
Supplementary 2. A versus N up- or downregulated transcripts.
Supplementary 3. Go analyses of the differentially expressed IncRNAs.

References

[1] M. C. Riella and P. Roy-Chaudhury, "Vascular access in haemodialysis: strengthening the Achilles' heel," *Nature Reviews Nephrology*, vol. 9, no. 6, pp. 348–357, 2013.

[2] D. McGrogan, J. Al Shakarchi, A. Khawaja et al., "Arteriovenous fistula outcomes in the elderly," *Journal of Vascular Surgery*, vol. 62, no. 6, pp. 1652–1657, 2015.

[3] P. M. Kitrou, K. Katsanos, S. Spiliopoulos, D. Karnabatidis, and D. Siablis, "Drug-eluting versus plain balloon angioplasty for the treatment of failing dialysis access: final results and cost-effectiveness analysis from a prospective randomized controlled trial (NCT01174472)," *European Journal of Radiology*, vol. 84, no. 3, pp. 418–423, 2015.

[4] P. Roy-Chaudhury, L. M. Spergel, A. Besarab, A. Asif, and P. Ravani, "Biology of arteriovenous fistula failure," *Journal of Nephrology*, vol. 20, no. 2, pp. 150–163, 2007.

[5] A. A. Al-Jaishi, M. J. Oliver, S. M. Thomas et al., "Patency rates of the arteriovenous fistula for hemodialysis: a systematic review and meta-analysis," *American Journal of Kidney Diseases*, vol. 63, no. 3, pp. 464–478, 2014.

[6] N. Tessitore, G. Mansueto, V. Bedogna et al., "A prospective controlled trial on effect of percutaneous transluminal angioplasty on functioning arteriovenous fistulae survival," *Journal of the American Society of Nephrology*, vol. 14, no. 6, pp. 1623–1627, 2003.

[7] T. W. I. Clark, D. A. Hirsch, K. J. Jindal, P. J. Veugelers, and J. LeBlanc, "Outcome and prognostic factors of restenosis after percutaneous treatment of native hemodialysis fistulas," *Journal of Vascular and Interventional Radiology*, vol. 13, no. 1, pp. 51–59, 2002.

[8] D. B. Cines, E. S. Pollak, C. A. Buck et al., "Endothelial cells in physiology and in the pathophysiology of vascular disorders," *Blood*, vol. 91, no. 10, pp. 3527–3561, 1998.

[9] Y. Wang, A. Liang, J. Luo et al., "Blocking notch in endothelial cells prevents arteriovenous fistula failure despite CKD," *Journal of the American Society of Nephrology*, vol. 25, no. 4, pp. 773–783, 2014.

[10] ENCODE Project Consortium, E. Birney, J. A. Stamatoyannopoulos et al., "Identification and analysis of functional elements in 1% of the human genome by the ENCODE pilot project," *Nature*, vol. 447, no. 7146, pp. 799–816, 2007.

[11] F. F. Costa, "Non-coding RNAs: meet thy masters," *BioEssays*, vol. 32, no. 7, pp. 599–608, 2010.

[12] L. Lv, W. Huang, J. Zhang, Y. Shi, and L. Zhang, "Altered microRNA expression in stenoses of native arteriovenous fistulas in hemodialysis patients," *Journal of Vascular Surgery*, vol. 63, no. 4, pp. 1034–1043.e3, 2016.

[13] W. Xia, X. W. Zhu, X. B. Mo et al., "Integrative multi-omics analysis revealed SNP-lncRNA-mRNA (SLM) networks in human peripheral blood mononuclear cells," *Human Genetics*, vol. 136, no. 4, pp. 451–462, 2017.

[14] N. Jouve, R. Bachelier, N. Despoix et al., "CD146 mediates VEGF-induced melanoma cell extravasation through FAK activation," *International Journal of Cancer*, vol. 137, no. 1, pp. 50–60, 2015.

[15] M. Gu, N. M. Mordwinkin, N. G. Kooreman et al., "Pravastatin reverses obesity-induced dysfunction of induced pluripotent stem cell-derived endothelial cells via a nitric oxide-dependent mechanism," *European Heart Journal*, vol. 36, no. 13, pp. 806–816, 2015.

[16] L. Y. Tanaka and F. R. M. Laurindo, "Vascular remodeling: a redox-modulated mechanism of vessel caliber regulation," *Free Radical Biology & Medicine*, vol. 109, pp. 11–21, 2017.

[17] D. Dajnowiec and B. L. Langille, "Arterial adaptations to chronic changes in haemodynamic function: coupling vasomotor tone to structural remodelling," *Clinical Science*, vol. 113, no. 1, pp. 15–23, 2007.

[18] T. Michel and O. Feron, "Nitric oxide synthases: which, where, how, and why?," *The Journal of Clinical Investigation*, vol. 100, no. 9, pp. 2146–2152, 1997.

[19] U. Forstermann and W. C. Sessa, "Nitric oxide synthases: regulation and function," *European Heart Journal*, vol. 33, no. 7, pp. 829–837, 2012.

[20] L. A. Biwer, E. P. Taddeo, B. M. Kenwood, K. L. Hoehn, A. C. Straub, and B. E. Isakson, "Two functionally distinct pools of eNOS in endothelium are facilitated by myoendothelial junction lipid composition," *Biochimica et Biophysica Acta (BBA) - Molecular and Cell Biology of Lipids*, vol. 1861, no. 7, pp. 671–679, 2016.

[21] M. Franzoni, I. Cattaneo, L. Longaretti, M. Figliuzzi, B. Ene-Iordache, and A. Remuzzi, "Endothelial cell activation by hemodynamic shear stress derived from arteriovenous fistula for hemodialysis access," *American Journal of Physiology - Heart and Circulatory Physiology*, vol. 310, no. 1, pp. H49–H59, 2016.

[22] I. M. Shih, "The role of CD146 (Mel-CAM) in biology and pathology," *The Journal of Pathology*, vol. 189, no. 1, pp. 4–11, 1999.

[23] P. K. Dagur, A. Biancotto, E. Stansky, H. N. Sen, R. B. Nussenblatt, and J. P. McCoy, "Secretion of interleukin-17 by CD8 + T cells expressing CD146 (MCAM)," *Clinical Immunology*, vol. 152, no. 1-2, pp. 36–47, 2014.

[24] F. Anfosso, N. Bardin, E. Vivier, F. Sabatier, J. Sampol, and F. Dignat-George, "Outside-in signaling pathway linked to CD146 engagement in human endothelial cells," *The Journal of Biological Chemistry*, vol. 276, no. 2, pp. 1564–1569, 2001.

[25] N. Bardin, F. Anfosso, J. M. Masse et al., "Identification of CD146 as a component of the endothelial junction involved in the control of cell-cell cohesion," *Blood*, vol. 98, no. 13, pp. 3677–3684, 2001.

[26] K. J. Halt, H. E. Parssinen, S. M. Junttila et al., "$CD146^+$ cells are essential for kidney vasculature development," *Kidney International*, vol. 90, no. 2, pp. 311–324, 2016.

[27] A. Lisowska, P. Lisowski, M. Knapp et al., "Serum adiponectin and markers of endothelial dysfunction in stable angina pectoris patients undergoing coronary artery bypass grafting (CABG)," *Advances in Medical Sciences*, vol. 59, no. 2, pp. 245–249, 2014.

[28] S. Ciftci Dogansen, A. Helvaci, M. Adas, and S. Deniz Onal, "The relationship between early atherosclerosis and endothelial dysfunction in type 1 diabetic patients as evidenced by measurement of carotid intima-media thickness and soluble CD146 levels: a cross sectional study," *Cardiovascular Diabetology*, vol. 12, no. 1, p. 153, 2013.

[29] T. Saito, O. Saito, T. Kawano et al., "Elevation of serum adiponectin and CD146 levels in diabetic nephropathy," *Diabetes Research and Clinical Practice*, vol. 78, no. 1, pp. 85–92, 2007.

Hindawi
Stem Cells International
Volume 2017, Article ID 9012152, 9 pages
https://doi.org/10.1155/2017/9012152

Research Article

Multiple Myeloma-Derived Exosomes Regulate the Functions of Mesenchymal Stem Cells Partially via Modulating miR-21 and miR-146a

Qian Cheng,[1,2] Xin Li,[1] Jingru Liu,[3] Qinmao Ye,[2] Yanfang Chen,[2] Sanqin Tan,[3] and Jing Liu[1]

[1]*Department of Hematology, The Third Xiangya Hospital of Central South University, Changsha 40013, China*
[2]*Department of Pharmacology & Toxicology, Boonshoft School of Medicine, Wright State University, Dayton, OH 45435, USA*
[3]*Department of Histology and Embryology, Medical College, Hunan Normal University, Changsha 40013, China*

Correspondence should be addressed to Jing Liu; lj0jingliu@163.com

Received 9 May 2017; Revised 5 September 2017; Accepted 12 September 2017; Published 27 November 2017

Academic Editor: Zhaohui Ye

Exosomes derived from cancer cells can affect various functions of mesenchymal stem cells (MSCs) via conveying microRNAs (miRs). miR-21 and miR-146a have been demonstrated to regulate MSC proliferation and transformation. Interleukin-6 (IL-6) secreted from transformed MSCs in turn favors the survival of multiple myeloma (MM) cells. However, the effects of MM exosomes on MSC functions remain largely unclear. In this study, we investigated the effects of OPM2 (a MM cell line) exosomes (OPM2-exo) on regulating the proliferation, cancer-associated fibroblast (CAF) transformation, and IL-6 secretion of MSCs and determined the role of miR-21 and miR-146a in these effects. We found that OPM2-exo harbored high levels of miR-21 and miR-146a and that OPM2-exo coculture significantly increased MSC proliferation with upregulation of miR-21 and miR-146a. Moreover, OPM2-exo induced CAF transformation of MSCs, which was evidenced by increased fibroblast-activated protein (FAP), α-smooth muscle actin (α-SMA), and stromal-derived factor 1 (SDF-1) expressions and IL-6 secretion. Inhibition of miR-21 or miR-146a reduced these effects of OPM2-exo on MSCs. In conclusion, MM could promote the proliferation, CAF transformation, and IL-6 secretion of MSCs partially through regulating miR21 and miR146a.

1. Introduction

Multiple myeloma (MM) is the second most common hematological malignancy and characterized by clonal proliferation of malignant plasma cells in the bone marrow (BM) [1]. Accumulating evidence indicates that MM cells can affect the function and phenotype of mesenchymal stem cells (MSCs), osteoclasts, and endothelial cells by releasing soluble factors such as cytokines/proteins [2] and extracellular particles [3], which in turn favor the progression of MM cells [4, 5]. For instance, MM cells can educate MSCs to acquire a tumor-like phenotype with the ability to secrete interleukin-6 (IL-6), IL-8, and TNF-β, which further promote MM survival [6, 7]. It has also been shown that cancer cells can affect the function and phenotype of MSCs through secreting soluble factors [8, 9].

Exosomes, through delivering biological molecules such as proteins and microRNAs (miRs), represent a novel component of tumor microenvironment and play an important role in the communication between cancer cells and MSCs [10]. Previous studies have demonstrated that exosomes released by cancer cells could be incorporated by MSCs and result in the cancer-associated fibroblast (CAF) transformation of MSCs [11–16]. These studies have shown that CAFs transformed from MSCs express fibroblast-activated protein (FAP), α-smooth muscle actin (α-SMA), and stromal-derived factor 1 (SDF-1) and display enhanced proliferation and secretion of cytokines including IL-6 and TGF-β which could contribute to a tumor-supportive microenvironment. Exosomes released by acute myeloid leukemia cells have been shown to promote MSC proliferation [12]. It has also been suggested that chronic lymphocytic leukemia-derived

exosomes could induce CAF transformation and IL-6 secretion of MSCs through transferring exosomal miR-150 and miR-146a [14]. However, whether MM exosomes can regulate MSC transformation remains unclear.

Emerging evidence indicates that miRs could be responsible for the proliferation, CAF transformation, and cytokine secretion of MSCs [13, 15]. miR-21 is a well-known oncogenic miRNA during MM proliferation and invasion and also a critical regulator in CAF transformation of breast cancer [17, 18]. It has been reported that exosomes of leukemia cells carry high levels of miR-21 and regulate MSC functions [12]. miR-146a expression has been demonstrated to be associated with levels of IL-6 secretion in breast cancer [19]. Moreover, MSC overexpressing miR-146a resulted in an increased secretion of IL-6, which further supports MM survival [20]. However, the role of miR-21 and miR-146a in regulating MSC proliferation and transformation has not fully been understood.

In this study, we examined the effects of MM-derived exosomes on MSC proliferation, CAF transformation, and IL-6 secretion, as well as the role of miR-21 and miR-146a in these effects.

2. Methods

2.1. Cell Culture. Primary human bone marrow-derived MSCs from healthy individuals were purchased from Lonza (Basel, Switzerland). All the experiments were performed with cells maintained in culture until passage 6. MSCs were maintained in MSC Growth BulletKit™ Medium (Lonza) and supplemented with 10% FBS, 2 mM L-glutamine, and penicillin/streptomycin (final concentration: 100 units/ml penicillin and 100 μg/ml streptomycin). MSCs were positive for CD105, CD166, CD29, and CD44 and negative for CD14, CD34, and CD45. Human MM cell lines OPM-2, RPMI 8226, and U266 were cultured in RPMI 1640 medium (Hyclone, USA), supplemented with 10% fetal bovine serum (Hyclone, USA), 2 mM L-glutamine, and antibiotics (Hyclone, USA).

2.2. Exosome Extraction and Purification. The extraction and purification procedures were performed according to the previous study with some modifications [21]. Briefly, OPM2 cells were conditioned in RPMI 1640 medium without FBS. When the OPM2 cells reached 80%–90% confluence, the supernatants containing exosomes were harvested. The exosomes were purified by the procedure of differential centrifugation and purification. In brief, the supernatants were centrifuged for 20 min at 2000g to remove cellular debris. The cell-free culture medium was centrifuged at 20,000g for 70 min and ultracentrifuged at 170,000g for 1.5 h to pellet exosomes. Exosome pellets were collected and diluted in filtered PBS. The collected exosomes were stored at −80°C and used for following experiments. The size and concentration of exosomes were analyzed by using Nano Tracking System Analysis (NTA) 300 (UK).

2.3. PKH26 Stain of OPM2 Exosomes. For exosome-uptaking experiment, purified exosomes derived from OPM2 (OPM2-exo) were stained using PKH26 membrane dye (Sigma, USA). Stained exosomes were washed in 2 ml of PBS, collected by ultracentrifugation as demonstrated above, and resuspended in filtered PBS. 10 μg of the PKH26-stained exosomes or the same volume of the PKH26-PBS control was added and incubated for 24 h. The binding of OPM2-exo to the MSCs was observed with a fluorescence microscope (Germany). OPM2 cells were washed twice with PBS, stained with Hoechst 33342 for 5 min, and washed twice with PBS before being photographed.

2.4. Cell Proliferation Assay. Proliferation of MSCs was determined by various methods including MTT assay (Sigma, USA), Cell Counting Kit-8 (CCK-8, Dojindo, Japan) assay, and direct cell counting. For the MTT assay, MSCs were seeded at 1×10^3 cells/plate in a 96-well plate and cocultured with 0 (PBS, vehicle control), 5, 10, 20, 40, or 80 μg/ml OPM2-exo. After day 4, the cells were incubated with 20 μl of 5 mg/ml MTT solution for 4 h at 37°C. After removing the medium containing MTT, 150 μl dimethyl sulfoxide (DMSO) was added to each well to dissolve the formazan. The optical density (OD) was measured at 490 nm by using a microplate reader (BioTek, USA). We also conducted a more sensitive assay to evaluate MSC proliferation since it has been shown that the detection sensitivity of CCK-8 is higher than that of any other tetrazolium salts such as MTT, XTT, or MTS. Briefly, cells (1×10^3 per well) were plated in 96-well plates in triplicate for culture (37°C and 5% CO_2). In the following day, the cells were cocultured with the same concentrations of OPM2-exo in a final volume of 90 μl for 4 days. After incubation, 10 μl CCK-8 solution was added to each well and incubated for 2 h. Then, the absorbance at 450 nm was measured by the microplate reader (BioTek, USA). To directly count the cell number, MSCs were seeded at low density in 6-well plates (5×10^3 cells/plate). After 24 h, OPM2 cells were washed 3 times with PBS and switched to serum-free media, and OPM2-exo (80 μg/ml) was added. The medium was changed every 3 days and added with fresh OPM2-exo. The cell number was counted at days 1, 4, and 10 with the automated cell counter (Beckman, USA) after trypan blue staining.

2.5. CAF Transformation Assay. MSCs were seeded at 5×10^3 cells/plate in 6-well plates. 12 h after seeding, MSCs were treated with OPM2-exo (80 μg/ml) to trigger the CAF transformation. The medium was changed every 3 days and added with fresh OPM2-exo. After 10 days, cells and conditioned medium were then collected and prepared for the following analysis.

2.6. Quantitative Real-Time PCR Analysis (qRT-PCR). RNA was treated with TRIzol (Invitrogen, USA). One microgram of RNA was transcribed to cDNA using TranScript cDNA Synthesis Kit (Takara, Japan), and qRT-PCR was performed using a Bio-Rad 96 System (Bio-Rad, USA) with SYBR Green II qPCR Premix (Takara, Japan). The primers were listed at Supplementary Material Table S1. The PCR was conducted at 95°C for 10 minutes, 50 cycles

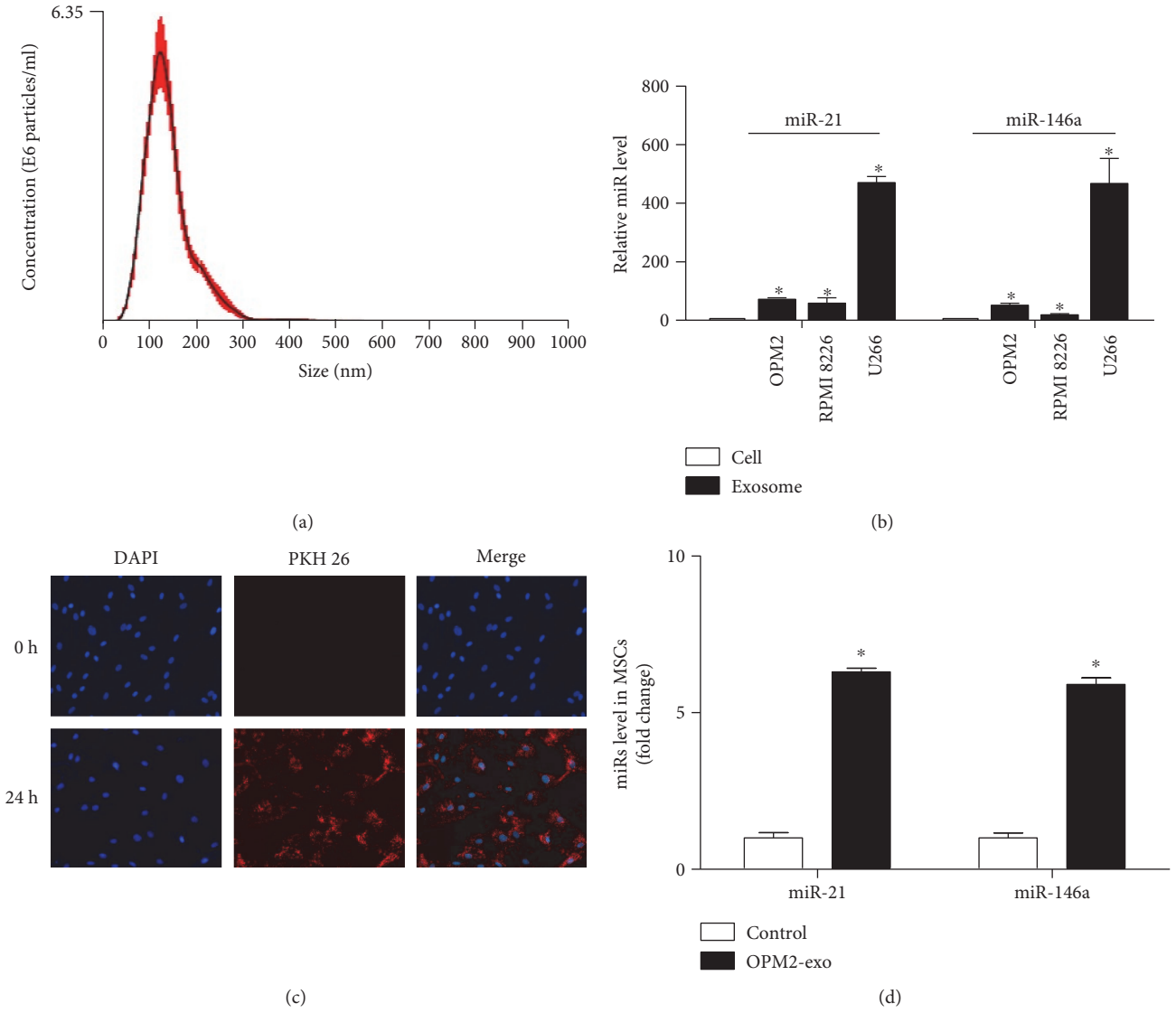

Figure 1: MM exosomes increased miR-21 and miR-146a levels in MSCs. (a) A representative picture of exosomes purified from OPM2 cells, examined by NTS300. (b) The expressions of miRs (miR-21, miR-146a) in parent MM cells (OPM2, RPMI-8226, and U266) and exosomes were measured by qPCR. (c) Fluorescence images of MSCs following the uptaking of OPM2-exo labeled with PKH26 (red) for 24 hours. (d) MSCs were cultured with OPM2-exo and the normalized expressions of miRs (miR-21, miR-146a) in MSCs were detected by qPCR. Results were shown as mean ± S.E.M. (*$p < 0.05$, compared to untreated MSCs, $N = 3$/group).

at 95°C for 30 seconds, 60°C for 30 seconds, and 72°C for 1 minute. We used GAPDH (FAP, α-SMA, and SDF-1) and U6 (miR-21, miR-146a) as the internal control for normalization and calculated the relative expression by the $2^{-\Delta\Delta Ct}$ method.

2.7. IL-6 ELISA Assay. The MSC-conditioned medium was centrifuged to remove cellular debris, and then, IL-6 protein concentrations were quantified by using the ELISA kit (Invitrogen, USA) according to the manufacturer's protocol. In brief, the conditioned medium of MSCs was harvested, and standard and sample extracts were added to the microplate precoated with an antibody specific for IL-6. HRP substrate was added to each well. The level of IL-6 was measured at 450 nm.

2.8. miR-21 and miR-146a Inhibition. 2×10^5 cell suspensions were seeded in 6-well plates and transfected with RNase-free water (vehicle (veh)), miR control (miRCtrl, 100 nM), miR-21 inhibitor, or miR-146a inhibitor by using DharmaFECT 1 Transfection Reagent (Dharmacon, USA) at days 1 and 6, separately. The transfection procedure was performed according to the manufacturer's instructions. Transfection efficacy was examined by qRT-PCR at day 10.

2.9. Statistical Analysis. Data were expressed as means ± SEM of three independent experiments. Statistical analysis was performed by using one- or two-way analysis of variance (ANOVA) (SPSS version 17.0, SPSS, USA). Differences were considered to be significant when p values were smaller than 0.05.

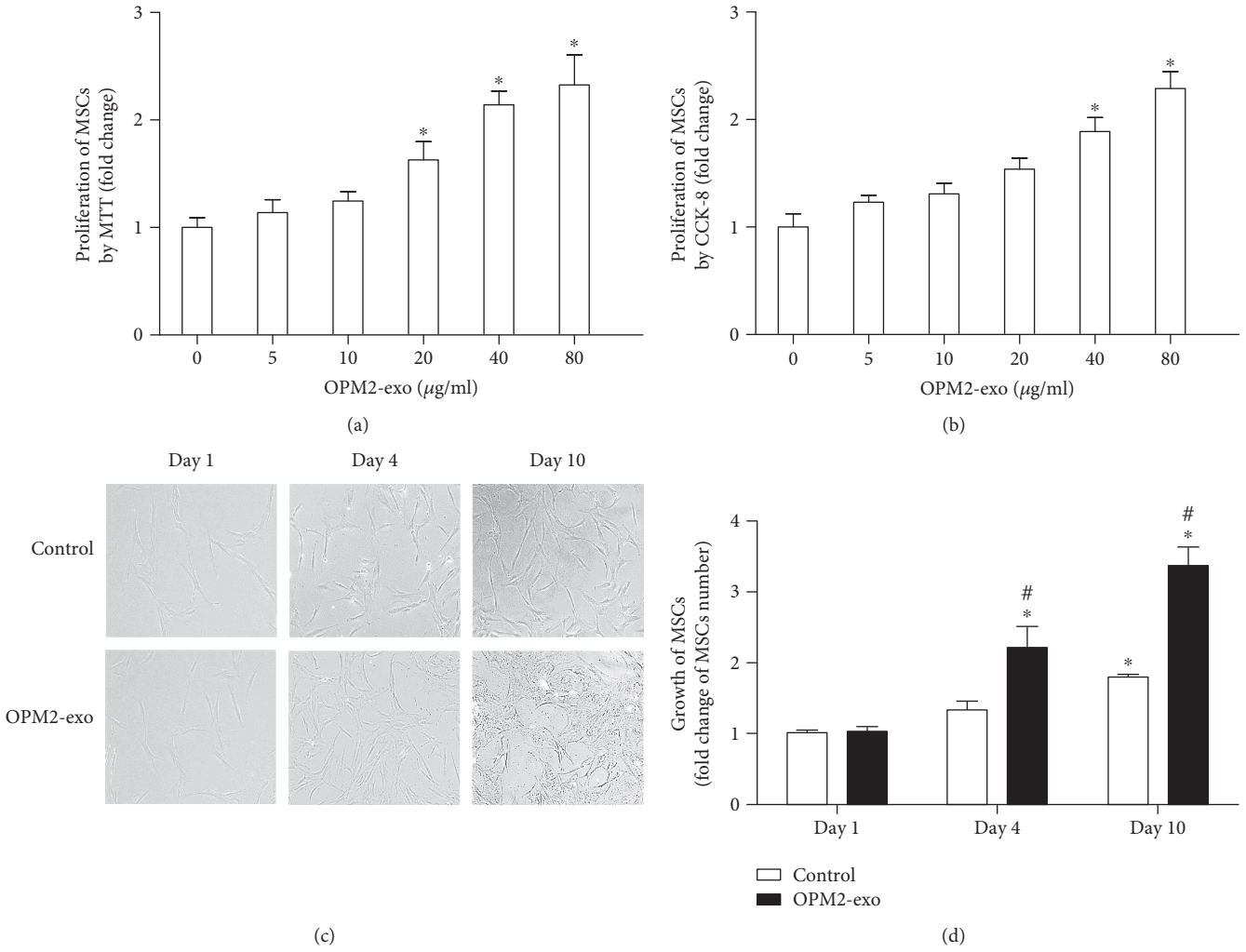

Figure 2: The effect of OPM2-exo on the proliferation of MSCs. (a) MSCs were treated with different concentrations of OPM2-exo for 4 days and proliferation was evaluated by using MTT assay. (b) MSCs were treated with different concentrations of OPM2-exo for 4 days and proliferation was evaluated by using CCK-8 assay. (c) Representative microscopy images of MSCs treated for 10 days with OPM2-exo (80 μg/ml). 10x magnification in microscopy. Representative images of three independent experiments were reported at day 1, day 4, and day 10. (d) MSCs were treated with OPM2-exo (80 μg/ml) and the cell number was counted by automated counter after day 1, day 4, and day 10, respectively. Results were shown as mean ± S.E.M. ($^{*}p < 0.05$, compared to untreated MSCs; $^{\#}p < 0.05$, compared to day 1; $N = 3$/group).

3. Results

3.1. miR-21 and miR-146a Were Rich in MM-Derived Exosomes and Their Levels in MSCs Were Increased after Coculture with OPM2-exo. As shown in Figure 1(a), NTA showed that the diameter of the isolated OPM2-exo was around 100 nm. qRT-PCR results demonstrated that exosomes derived from three MM cell lines (OPM2, RPMI 8226, and U266) contained higher levels of miR-21 and miR-146a when compared with those derived from parent MM cells (Figure 1(b)). OPM2-exo could be uptaken by MSCs after incubation for 24 hours analyzed by PKH26 stain (Figure 1(c)). With the treatment of OPM2-exo, we also observed the increased expressions of miR-21 and miR-146a in MSCs (Figure 1(d)).

3.2. OPM2-exo Promoted the Proliferation of MSCs in Dose- and Time-Dependent Manners. We performed the proliferation assay by using different concentrations of OPM2-exo (0, 5, 10, 20, 40, and 80 μg/ml) in coculture with MSCs. Both MTT (Figure 2(a)) and CCK-8 (Figure 2(b)) results showed that OPM2-exo promoted the proliferation in a dose-dependent manner. The optimal concentration for the OPM2-exo effect was considered to be 80 μg/ml. Microscopy pictures showed that MSC displayed a clear increase in cell density in a time-dependent manner which is further enhanced with the coculture of OPM2-exo (Figure 2(c)). We next examined the effect of OPM2-exo on the growth of MSCs following treatment of OPM2-exo (80 μg/ml) by directly counting the cell number. According to the cell count analysis, MSCs' number increased about 2 times after incubation with OPM2-exo at day 4 and over 2 times at day 10 (Figure 2(d)).

3.3. OPM2-exo Induced the Transformation of MSCs into CAFs with Increased IL-6 Secretion. As noted in Figure 2(c),

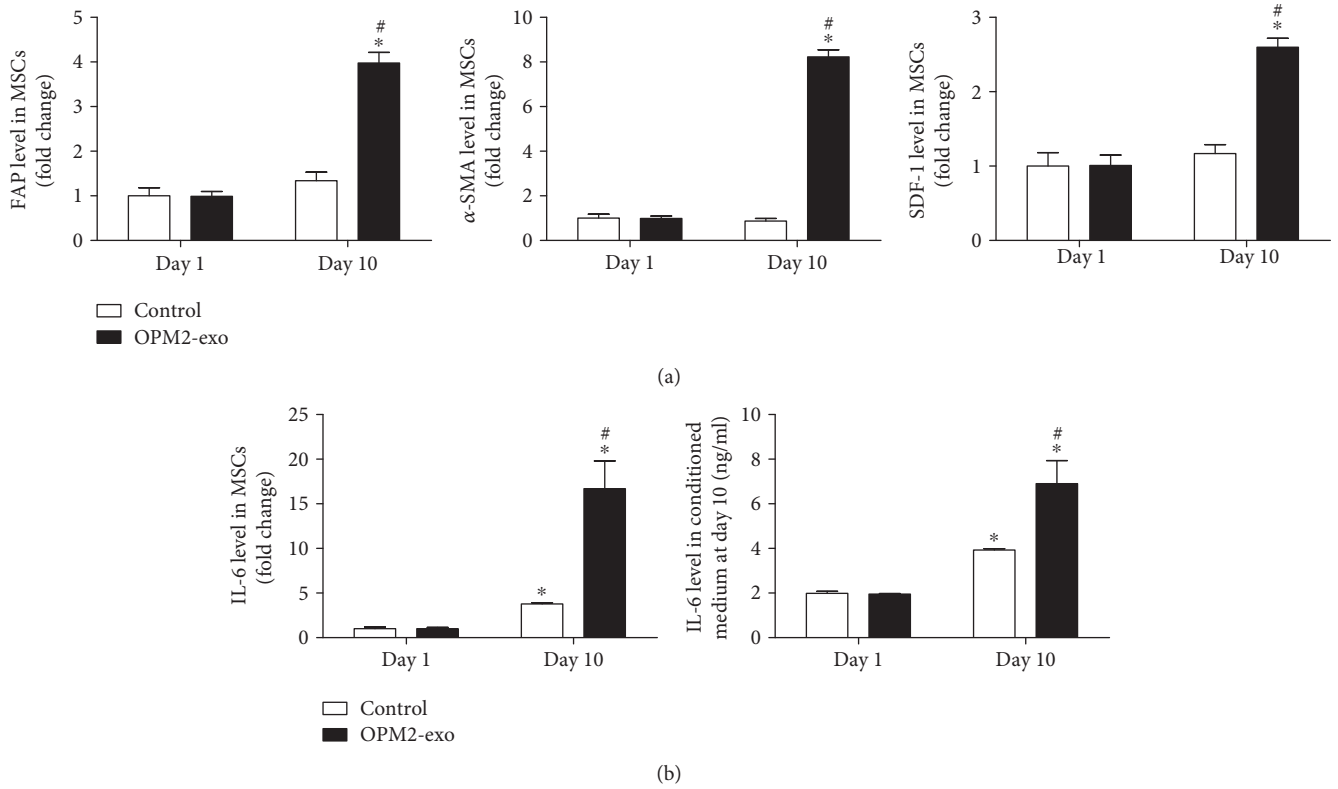

Figure 3: The effects of OPM2-exo on the CAF transformation and IL-6 secretion of MSCs. (a) Effect of OPM2-exo (80 μg/ml) on the expressions of CAF transformation markers (FAP, α-SMA, and SDF-1) in MSCs at day 10. Data were expressed as normalized to GAPDH. Statistical analysis was performed by t-test. (b) Effect of OPM2-exo (80 μg/ml) on IL-6 mRNA expression and IL-6 secretion of MSCs at day 10. Results were shown as mean ± S.E.M. ($^*p < 0.05$, compared to untreated MSCs; $^\#p < 0.05$, compared to day 1; $N = 3$/group).

MSCs displayed a different phenotype cultured with OPM2-exo for 10 days, implicating the MSC transformation. We also examined the mRNA expressions of CAF transformation markers including FAP, α-SMA, and SDF-1. Results showed that OPM2-exo (80 μg/ml) significantly induced the expressions of CAF transformation markers after being cocultured with OPM2-exo (Figure 3(a)). As shown in Figure 3(b), IL-6 mRNA was examined by using qRT-PCR and its level in the conditioned medium was measured by using ELISA after coculture with OPM2-exo (80 μg/ml) for 10 days to observe the changes. The results showed that there was an increase in IL-6 mRNA expression as well as in its secretion of MSCs at day 10, which is significantly enhanced by the treatment of OPM2-exo (80 μg/ml). Collectively, these results indicated that MSCs undergo CAF transformation in response to tumor exosome exposure.

3.4. Inhibition of miR-21 in MSCs Was Able to Inhibit the OPM2-exo-Induced MSC Proliferation and CAF Transformation. To elucidate the role of miR-21 in the proliferation and CAF transformation of MSCs, MSCs were transfected with miR-21 inhibitor and incubated with OPM2-exo (80 μg/ml) for 10 days. The transfection efficiency of miR-21 inhibitor in MSCs was evaluated by qRT-PCR (Figure 4(a)). As expected, the level of miR-21 in MSCs was significantly decreased about 60% compared with that of veh or miRCtrl after transfection. Results showed that MSCs transfected with miR-21 inhibitor could significantly decrease the proliferation of MSCs when cultured with OPM2-exo for 4 days (Figure 4(b)). Additionally, inhibition of miR-21 decreased expressions of CAF markers including FAP, α-SMA, and SDF-1 in OPM2-treated MSCs at day 10 (Figure 4(c)).

3.5. Inhibition of miR-146a Could Reduce the IL-6 Expression and Secretion of OPM2-exo-Treated MSCs. To further elucidate the role of miR-146a in the IL-6 expression and secretion of transformed MSCs, MSCs were transfected with miR-146a inhibitor and cultured with OPM2-exo for 10 days. The transfection efficiency of miR-146a inhibitor was evaluated by qPCR (Figure 5(a)), and the results showed that the miR-146a expression was significantly inhibited about 60%. Inhibition of miR-146a was able to decrease the IL-6 expression and secretion of OPM2-exo-treated MSCs (Figures 5(b) and 5(c)).

4. Discussion

In the present study, we identified the effects of MM-derived exosomes on the proliferation, CAF transformation, and IL-6 secretion of MSCs, as well as defining the role of miR-21 and miR-146a in these effects.

Increasing evidence indicates that cancer exosomes could regulate the functions of MSCs probably through delivering their carried miRs [12, 14]. It has been reported that miR-

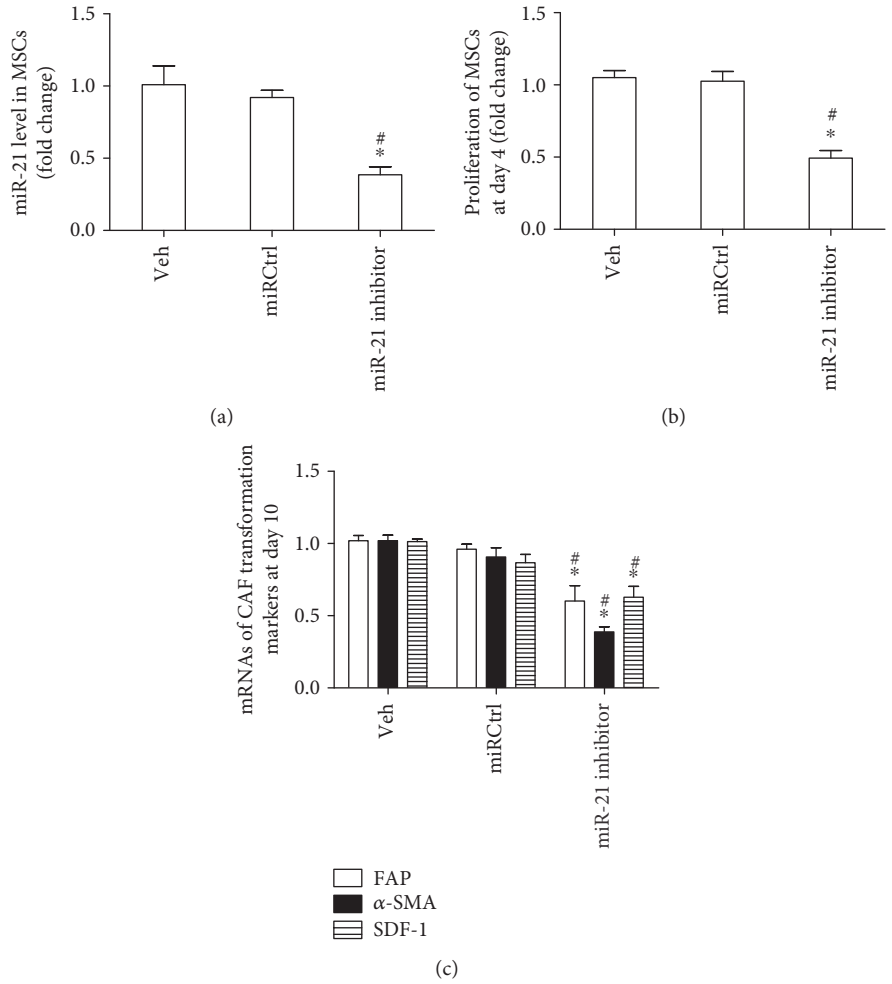

Figure 4: Inhibition of miR-21 decreased the proliferation and CAF transformation of MSCs. (a) MSCs were subjected to vehicle (veh) treatment and transfected with miRCtrl or miR-21 as indicated, and 10 days later, the miR-21 level was measured by qRT-PCR. (b) Effect of downregulating miR-21 on the proliferation of MSCs at day 4. (c) Effect of downregulating miR-21 on the expressions of CAF transformation markers in MSCs at day 10. Results were shown as mean ± S.E.M. ($^{*}p < 0.05$ versus veh; $^{\#}p < 0.05$ versus miRCtrl, $N = 3$/group).

21 and miR-146a play an important role in regulating MSC transformation and cytokine secretion [22, 23]. In this study, we analyzed that the levels of miR-21 and miR-146a in OPM2-exo and in MSCs after being coincubated with OPM2-exo. We found that miR-21 and miR-146a were enriched in OPM2-exo which enhanced the levels of these two miRs in coincubated MSCs. We also performed the qPCR analysis and found that miR-21 and miR-146a were significantly increased in exosomes from two other human MM cell lines (RPMI-8226 and U266). Our findings are consistent with previous reports showing that cancer exosomes can selectively package miRs which are able to be delivered into target cells for functioning [14, 24, 25]. For instance, exosomes of chronic lymphocytic leukemia have been shown to selectively deliver miR-21, miR-146a, miR-155, miR-148a, and let7-g to MSCs [14]. Our data suggest that miR-21 and miR-146a might be involved in regulating the functions of OPM2-exo on MSCs.

Previous studies have reported that exosomes derived from cancer cells could promote MSC proliferation [11, 12]. For instance, exosomes of T-cell leukemia/lymphoma cells are able to induce MSC proliferation, which is associated with the miR-21 expression [12]. Since miR-21 is selectively packaged in OPM2-exo, we further determined the effect of OPM2-exo on MSC proliferation and clarified whether miR-21 was the underlying mechanism. We found that MM exosomes were able to promote MSC proliferation in time- and dose-dependent manners. Moreover, we applied miR-21 inhibitor to further explore the role of miR-21 in OPM2-exo-induced MSC proliferation. Our results showed that miR-21 inhibitor significantly reduced the proliferation of MSCs induced by OPM2-exo. These data indicate that MM exosomes promote the proliferation of MSCs at least partly via miR-21, although the detail downstream pathway remains to be determined.

Exosomes derived from colorectal cancer, lung tumor, and leukemia have been shown to induce CAF transformation of MSCs [11–15]. CAFs are characterized by the expression of several markers including FAP, α-SMA, and SDF-1, as well as increasing secretion of cytokines [16, 26, 27]. The

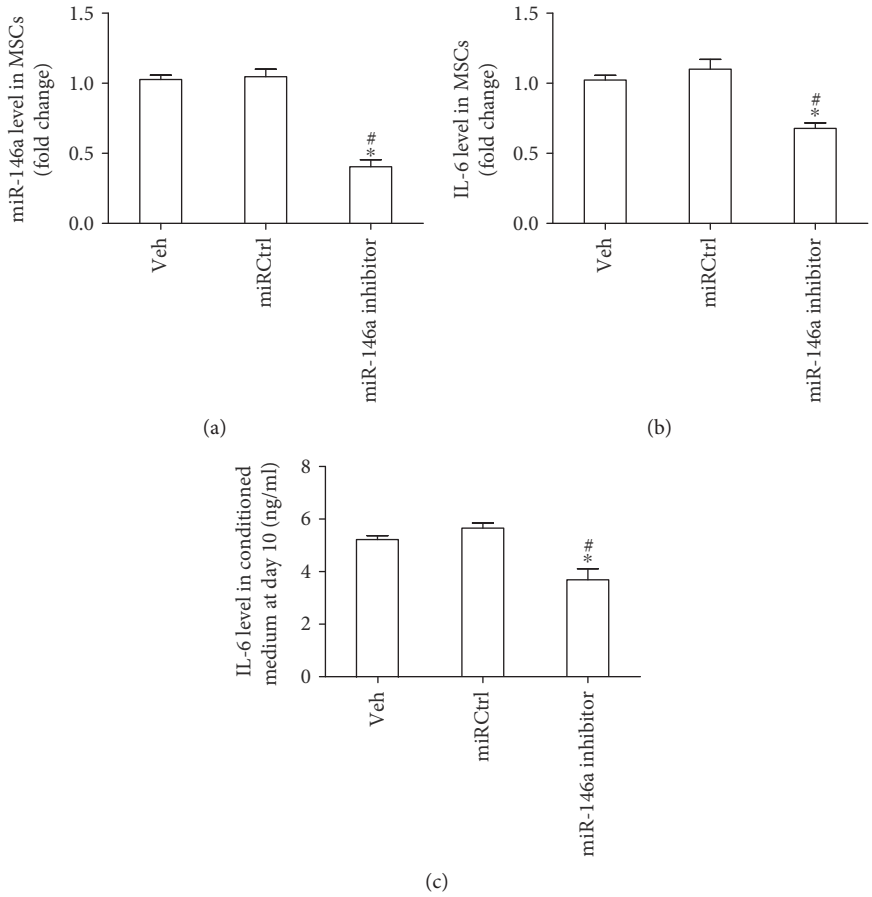

Figure 5: Inhibition of miR-146a decreased IL-6 secretion of MSCs. (a) MSCs were subjected to veh treatment and transfected with miRCtrl or miR-146a as indicated and 10 days later the miR-146a level was measured by qRT-PCR. (b) Effect of downregulating miR-146a on the IL-6 mRNA expression of MSCs at day 10. (c) Effect of downregulating miR-146a on the IL-6 secretion of MSCs at day 10. Results were shown as mean ± S.E.M. ($^{*}p < 0.05$ versus veh; $^{\#}p < 0.05$ versus miRCtrl, $N = 3$/group).

precise cellular origins of CAFs remain largely unclear; CAFs are reported to originate from various cell types such as resident fibroblasts [27], epithelial cells [28], and MSCs [8]. However, the role of MM exosome on CAF transformation of MSCs has not been determined yet. Our results showed that MSCs could be transformed to CAFs by OPM2-exos partially through the delivery of miR21 and miR146a and the activation of their downstream genes including IL-6, SDF-1, FAP, and α-SMA. It has been illustrated that miR-21 is highly associated with CAFs in breast and ovarian cancer [29, 30]. In this study, we also detected the association of elevated level of miR-21 with CAF transformation in OPM2-exo-treated MSCs. To confirm the role of miR-21 in CAF transformation of MSCs induced by OPM2-exo, we downregulated the level of miR-21 in MSCs by miR-21 inhibitor. Interestingly, we found that miR-21 inhibitor significantly decreased the effect of OPM2-exo on the expression of CAF markers, suggesting the involvement of miR-21 in CAF transformation of MSCs. Previous studies indicate that several genes including PTEN and PDCD4 are the downstreams of miR-21 in MSC. By inhibiting the expressions of PTEN, miR-21 could increase the levels of α-SMA, FAP, and SDF-1 in breast cancer. In this study, we found that miR-21 upregulated the expressions of α-SMA, FAP, and SDF-1 in the transformed MSC. Based on these, we tentatively attribute SDF-1, FAP, and α-SMA to be the target genes of miR-21. However, this hypothesis needs to be verified in the future.

Another important characteristic of transformed CAFs is their ability to secrete proinflammatory cytokines [13]. Frassanito et al. have reported that the CAFs of MM express high levels of TGF-β and IL-6 [16]. The cytokines secreted by CAFs, especially for IL-6, are believed to participate in the growth, angiogenesis, and metastases of MM [26]. Moreover, it is reported that IL-6 secretion of MSCs is regulated by miR-146a [20]. Since we detected that miR-146a was enriched in OPM2-exo and that the level of miR-146a in MSCs was increased after OPM2-exo coculture, we focused on IL-6 and miR-146a in this study. As expected, we found that IL-6 secretion was increased in transformed CAFs induced by OPM2-exo. Our data is supported by previous studies in gastric and lung cancer showing that cancer cell exosomes are able to elevate IL-6 secretion of transformed CAFs from MSCs [13, 15]. Moreover, we found that miR-146a inhibitor could significantly reduce the IL-6 expression as well as the IL-6 protein in the conditioned medium of OPM2-exo-treated MSCs. Our findings indicate that miR-146a is responsible for the increased IL-6 secretion of CAFs transformed from MSCs by MM exosomes. Previous studies have

confirmed that miR-146a upregulates the expression of the Notch/IL-6 proinflammatory pathway; we postulate that IL-6 is the downstream gene of miR-146a in MSCs. Nevertheless, our deductions remain to be further elucidated.

5. Conclusions

In conclusion, our data have demonstrated that MM exosomes are able to promote the proliferation, CAF transformation, and IL-6 secretion of MSCs. Our results also suggest that miR-21 and miR-146a are involved in regulating the functions of MSCs. Our study highlights the important roles of MM exosomes and miRs in regulating the MSC functions and MM survival, which may be potential targets for MM therapies in the future.

Conflicts of Interest

The authors declare that none of them have any kind of conflict of interests related to the present work.

Authors' Contributions

Qian Cheng and Xin Li contributed to this manuscript equally.

Acknowledgments

This work was supported by the New Xiangya Talent Projects of the Third Xiangya Hospital of Central South University to Jing Liu (no. JY20170307).

Supplementary Materials

The RT and qPCR primers used in this study (*Supplementary files).*

References

[1] S. W. Andrews, S. Kabrah, J. E. May, C. Donaldson, and H. R. Morse, "Multiple myeloma: the bone marrow microenvironment and its relation to treatment," *British Journal of Biomedical Science*, vol. 70, no. 3, pp. 110–120, 2013.

[2] M. Abe, "Cytokines and myeloma bone disease," *Clinical Calcium*, vol. 24, no. 6, pp. 871–878, 2014.

[3] J. Wang, S. Faict, K. Maes et al., "Extracellular vesicle cross-talk in the bone marrow microenvironment: implications in multiple myeloma," *Oncotarget*, vol. 7, no. 25, pp. 38927–38945, 2016.

[4] J. Wang, A. Hendrix, S. Hernot et al., "Bone marrow stromal cell-derived exosomes as communicators in drug resistance in multiple myeloma cells," *Blood*, vol. 124, no. 4, pp. 555–566, 2014.

[5] A. M. Roccaro, A. Sacco, P. Maiso et al., "BM mesenchymal stromal cell-derived exosomes facilitate multiple myeloma progression," *The Journal of Clinical Investigation*, vol. 123, no. 4, pp. 1542–1555, 2013.

[6] M. R. Reagan and I. M. Ghobrial, "Multiple myeloma mesenchymal stem cells: characterization, origin, and tumor-promoting effects," *Clinical Cancer Research*, vol. 18, no. 2, pp. 342–349, 2012.

[7] J. E. Noll, S. A. Williams, C. M. Tong et al., "Myeloma plasma cells alter the bone marrow microenvironment by stimulating the proliferation of mesenchymal stromal cells," *Haematologica*, vol. 99, no. 1, pp. 163–171, 2014.

[8] P. Barcellos-de-Souza, G. Comito, C. Pons-Segura et al., "Mesenchymal stem cells are recruited and activated into carcinoma-associated fibroblasts by prostate cancer microenvironment-derived TGF-β1," *Stem Cells*, vol. 34, no. 10, pp. 2536–2547, 2016.

[9] P. J. Mishra, P. J. Mishra, R. Humeniuk et al., "Carcinoma-associated fibroblast-like differentiation of human mesenchymal stem cells," *Cancer Research*, vol. 68, no. 11, pp. 4331–4339, 2008.

[10] H. Valadi, K. Ekström, A. Bossios, M. Sjöstrand, J. J. Lee, and J. O. Lötvall, "Exosome-mediated transfer of mRNAs and microRNAs is a novel mechanism of genetic exchange between cells," *Nature Cell Biology*, vol. 9, no. 6, pp. 654–659, 2007.

[11] L. Lugini, M. Valtieri, C. Federici et al., "Exosomes from human colorectal cancer induce a tumor-like behavior in colonic mesenchymal stromal cells," *Oncotarget*, vol. 7, no. 31, pp. 50086–50098, 2016.

[12] J. El-Saghir, F. Nassar, N. Tawil, and M. El-Sabban, "ATL-derived exosomes modulate mesenchymal stem cells: potential role in leukemia progression," *Retrovirology*, vol. 13, no. 1, p. 73, 2016.

[13] X. Li, S. Wang, R. Zhu, H. Li, Q. Han, and R. C. Zhao, "Lung tumor exosomes induce a pro-inflammatory phenotype in mesenchymal stem cells via NFκB-TLR signaling pathway," *Journal of Hematology & Oncology*, vol. 9, no. 1, p. 42, 2016.

[14] J. Paggetti, F. Haderk, M. Seiffert et al., "Exosomes released by chronic lymphocytic leukemia cells induce the transition of stromal cells into cancer-associated fibroblasts," *Blood*, vol. 126, no. 9, pp. 1106–1117, 2015.

[15] J. Gu, H. Qian, L. Shen et al., "Gastric cancer exosomes trigger differentiation of umbilical cord derived mesenchymal stem cells to carcinoma-associated fibroblasts through TGF-β/Smad pathway," *PLoS One*, vol. 7, no. 12, article e52465, 2012.

[16] M. A. Frassanito, L. Rao, M. Moschetta et al., "Bone marrow fibroblasts parallel multiple myeloma progression in patients and mice: in vitro and in vivo studies," *Leukemia*, vol. 28, no. 4, pp. 904–916, 2014.

[17] Q. Li, D. Zhang, Y. Wang et al., "MiR-21/Smad 7 signaling determines TGF-β1-induced CAF formation," *Scientific Reports*, vol. 3, p. 2038, 2013.

[18] E. Leone, E. Morelli, M. T. Di Martino et al., "Targeting miR-21 inhibits *in vitro* and *in vivo* multiple myeloma cell growth," *Clinical Cancer Research*, vol. 19, no. 8, pp. 2096–2106, 2013.

[19] D. Bhaumik, G. K. Scott, S. Schokrpur, C. K. Patil, J. Campisi, and C. C. Benz, "Expression of microRNA-146 suppresses NF-κB activity with reduction of metastatic potential in breast cancer cells," *Oncogene*, vol. 27, no. 42, pp. 5643–5647, 2008.

[20] K. De Veirman, J. Wang, S. Xu et al., "Induction of miR-146a by multiple myeloma cells in mesenchymal stromal cells stimulates their pro-tumoral activity," *Cancer Letters*, vol. 377, no. 1, pp. 17–24, 2016.

[21] J. Wang, R. Guo, Y. Yang et al., "The novel methods for analysis of exosomes released from endothelial cells and

endothelial progenitor cells," *Stem Cells International*, vol. 2016, Article ID 2639728, 12 pages, 2016.

[22] T. Wu, Y. Liu, Z. Fan et al., "miR-21 modulates the immunoregulatory function of bone marrow mesenchymal stem cells through the PTEN/Akt/TGF-β1 pathway," *Stem Cells*, vol. 33, no. 11, pp. 3281–3290, 2015.

[23] J. Xu, W. Wu, L. Zhang et al., "The role of microRNA-146a in the pathogenesis of the diabetic wound-healing impairment: correction with mesenchymal stem cell treatment," *Diabetes*, vol. 61, no. 11, pp. 2906–2912, 2012.

[24] W. X. Chen, X. M. Liu, M. M. Lv et al., "Exosomes from drug-resistant breast cancer cells transmit chemoresistance by a horizontal transfer of microRNAs," *PLoS One*, vol. 9, no. 4, article e95240, 2014.

[25] D. Q. Feng, B. Huang, J. Li et al., "Selective miRNA expression profile in chronic myeloid leukemia K562 cell-derived exosomes," *Asian Pacific Journal of Cancer Prevention*, vol. 14, no. 12, pp. 7501–7508, 2013.

[26] K. De Veirman, L. Rao, E. De Bruyne et al., "Cancer associated fibroblasts and tumor growth: focus on multiple myeloma," *Cancers*, vol. 6, no. 3, pp. 1363–1381, 2014.

[27] Y. Kojima, A. Acar, E. N. Eaton et al., "Autocrine TGF-β and stromal cell-derived factor-1 (SDF-1) signaling drives the evolution of tumor-promoting mammary stromal myofibroblasts," *Proceedings of the National Academy of Sciences of the United States of America*, vol. 107, no. 46, pp. 20009–20014, 2010.

[28] X. Wu, P. Tao, Q. Zhou et al., "IL-6 secreted by cancer-associated fibroblasts promotes epithelial-mesenchymal transition and metastasis of gastric cancer via JAK2/STAT3 signaling pathway," *Oncotarget*, vol. 8, no. 13, pp. 20741–20750, 2017.

[29] L. Rask, E. Balslev, S. Jørgensen et al., "High expression of miR-21 in tumor stroma correlates with increased cancer cell proliferation in human breast cancer," *APMIS*, vol. 119, no. 10, pp. 663–673, 2011.

[30] C. L. Au Yeung, N. N. Co, T. Tsuruga et al., "Exosomal transfer of stroma-derived miR21 confers paclitaxel resistance in ovarian cancer cells through targeting APAF1," *Nature Communications*, vol. 7, article 11150, 2016.

Hindawi
Stem Cells International
Volume 2017, Article ID 1096980, 12 pages
https://doi.org/10.1155/2017/1096980

Research Article

Hepatoma-Derived Growth Factor Secreted from Mesenchymal Stem Cells Reduces Myocardial Ischemia-Reperfusion Injury

Yu Zhou,[1,2] Panpan Chen,[1,2] Qingnian Liu,[1,2] Yingchao Wang,[1,2] Ling Zhang,[1,2] Rongrong Wu,[1,2] Jinghai Chen,[1,2] Hong Yu,[1,2] Wei Zhu,[1,2] Xinyang Hu,[1,2] and Jian-An Wang[1,2]

[1]*Department of Cardiology, Second Affiliated Hospital of Zhejiang University School of Medicine, 88 Jiefang Rd, Hangzhou 310009, China*
[2]*Cardiovascular Key Laboratory of Zhejiang Province, 88 Jiefang Rd, Hangzhou 310009, China*

Correspondence should be addressed to Jian-An Wang; jian_an_wang@yahoo.com

Received 25 May 2017; Accepted 4 October 2017; Published 14 November 2017

Academic Editor: Yanfang Chen

Objectives. The present study aimed to explore the major factors that account for the beneficial effects of mesenchymal stem cells (MSCs). *Methods*. Using isobaric tags for relative and absolute quantitation method, hepatoma-derived growth factor (HDGF) was identified as an important factor secreted by MSCs, but not by cardiac fibroblasts (CFs). The protective effects of conditioned medium (CdM) from MSCs or CFs were tested by using either H9C2 cells that were exposed by hypoxia-reoxygenation (H/R) insult or an *in vivo* mouse model of myocardial ischemia-reperfusion. *Results*. Compared to CF-CdM, MSC-CdM conferred protection against reperfusion injury. CdM obtained from MSCs that were treated with HDGF-targeted shRNA failed to offer any protection *in vitro*. In addition, administration of recombinant HDGF alone recapitulated the beneficial effects of MSC-CdM, which was associated with increased protein kinase C epsilon (PKCε) phosphorylation, enhanced mitochondria aldehyde dehydrogenase family 2 activity, and decreased 4-hydroxy-2-nonenal accumulation. A significant decrease in infarct size and ameliorated cardiac dysfunction was achieved by administration of HDGF in wild-type mice, which was absent in PKCε dominant negative mice, indicating the essential roles of PKCε in HDGF-mediated protection. *Conclusions*. HDGF secreted from MSCs plays a key role in the protection against reperfusion injury through PKCε activation.

1. Introduction

Ischemic heart diseases, such as myocardial infarction, continue to be one of the leading causes of mortality and morbidity worldwide [1]. Although the application of thrombolysis and vascular intervention salvages myocardium and significantly improves clinical outcomes, reperfusion results in myocardial injury. On reperfusion, the generation of reactive oxygen species (ROS), rapid reintroduction of adenosine triphosphate in the presence of elevated $[Ca^{2+}]_i$, and induction of the mitochondrial permeability transition lead to hypercontracture as well as apoptotic and oncotic cell death [2]. In addition, reperfusion induces accumulation of 4-hydroxy-2-nonenal (4-HNE) [3], a production of lipid peroxidation [4] that contributes to myocyte injury [5]. However, therapeutic agents to prevent these injuries remain unavailable so far. Therefore, effective cell protection after reperfusion is still an unmet clinical need.

Bone marrow-derived mesenchymal stem cells (MSCs) are one of the most rigorously studied stem cell populations [6], which are now undergoing phase II clinical trials for treating ischemic heart diseases. The low cardiac differential and retention rate of MSCs suggests that the secretion of paracrine factors [7], rather than regenerating the functional myocytes, confers cardioprotection by MSCs. Our previous work [8–11] on rodent and primate models demonstrated

that MSC therapy enhanced the survival of cardiomyocytes, reduced myocardial fibrosis, and improved angiogenesis through paracrine effects, in which the factors secreted from MSCs, including leptin [12], miR-211 [8], and heparinase [9], played an important role in cardiac protection. Of note, evidence has been put forward showing that treatment using MSC secretions is sufficient to reduce reperfusion-induced myocardial apoptosis and oxidative stress in both rodent and large animal models [13, 14]. However, the factors that contribute to the beneficial effects of MSCs have not been defined.

In the present study, by isobaric tags for relative and absolute quantitation (iTRAQ) secretomic analysis of either MSCs or cardiac fibroblasts (CFs), we have identified that hepatoma-derived growth factor (HDGF) was one of those factors secreted by MSCs and can confer protection against reperfusion-induced cardiomyocyte death. Treatment of HDGF recombinant protein reduces apoptosis and oxidative stress *in vitro* which in turn can decrease myocardial infarct size in an *in vivo* mouse model in a protein kinase C epsilon-(PKCε-) dependent fashion.

2. Materials and Methods

2.1. Animals. For detailed methods, please refer to the Supplementary Material available online at https://doi.org/10.1155/2017/1096980. Wild-type (WT) littermates and PKCε-dominant negative (PKCε-DN) mice were kindly provided from Professor Peipei Ping [15]. All animal studies were performed with the approval of the Institutional Animal Care and Use Committee, Zhejiang University and according to the Chinese Guideline for Laboratory Animal Care and Use.

2.2. Conditioned Medium Preparation. Mice MSCs isolated from 4- to 5-week-old wild-type (WT) mouse bone marrow were examined for the characteristic surface antigen profile by flow cytometry and cultured as described previously [12]. Cardiac fibroblasts were isolated from WT mice as described previously [11]. MSCs or fibroblasts of 80% confluence were washed with PBS and cultured in serum-free medium for 24 h. The conditioned medium was then centrifugated and concentrated 25-fold less of the original volume using 3 kDa molecular weight cutoff ultrafiltration membranes (Millipore, MA, USA). The concentrated medium was desalted and diluted to 0.5 mg/mL for tail vein injection.

2.3. Ischemia-Reperfusion Models and Hemodynamic Measurement. Mice were anesthetized with intraperitoneal injection of pentobarbital sodium (60 mg/kg) and then subjected to the left anterior descending (LAD) coronary artery ligation including silicon tubing on top of the coronary artery with an 8-0 Prolene suture. Fifteen minutes before occlusion, 0.2 mL of vehicle or conditioned medium derived from MSCs (MSC-CdM) or CFs (CF-CdM) was injected via tail vein. After 45 min of ischemia, the silicon tubing was removed to achieve reperfusion. The Evan's blue and 2,3,5-triphenyltetrazolium chloride staining were performed on cardiac tissue sections to identify the area at risk and the infarct area. Hemodynamic assessment was taken at 24 h reperfusion by a 1.4 F pressure catheter inserted through the right carotid artery into the left ventricle (LV). The transducer was connected to the PowerLab system (AD Instruments, Castle Hill, Australia). LV pressure and LV maximum ± dp/dt were recorded and averaged from 15 beats.

2.4. Western Blot Analysis. Culture media were precipitated with trichloroacetic acid (1 : 100, vol/vol, overnight incubation at −20°C). The precipitates were rinsed with acetone, prior to be resuspended into lysis buffer. Proteins extracted from cells or heart tissues (40 μg protein for each sample) were electrophoresed on a SDS-PAGE and transferred onto a PVDF membranes (Bio-Rad) and incubated with primary antibodies against phosphorylated PKCε (1 : 500, Santa Cruz, CA, USA), PKCε, cleaved caspase-3, β-actin (1 : 1000, all from Cell Signaling Technology, Danvers, MA, USA), or 4-HNE (1 : 500) (both from Abcam, Cambridge, MA, USA). Then, membranes were incubated with HRP-conjugated secondary antibodies and exposed with the Chemiluminescence Detection Kit (Millipore).

2.5. Mitochondrial Aldehyde Dehydrogenase Family 2 (ALDH2) Activity Assay. Mitochondria were isolated using a mitochondrial protein extraction kit (Keygentec, Nanjing, China) according to the instruction supplied by the manufacturer. The ALDH2 activity of mitochondria from cardiomyocytes was measured using a mito-ALDH2 activity kit (Abcam) by a SpectraMax 340PC384 Microplate Reader (Molecular Devices, LLC., CA, USA).

2.6. Transferase dUTP Nick End Labeling (TUNEL) Assay and Immunofluorescence Staining. Frozen heart tissue sections were fixed and permeabilized before incubated with primary antibodies and respective secondary antibodies. The apoptosis of cells was detected in situ with TUNEL (Roche Applied Science, IN, USA). cTnI antibody (1 : 200 Abcam) was applied as a cardiomyocyte marker with DAPI counterstaining.

2.7. Flow Cytometry Analysis of Cell Apoptosis. The Annexin V-FITC/PI Apoptosis Detection Kit was used to evaluate apoptosis of cells. After rinsed with cold PBS, cells were resuspended in 200 μl of binding buffer. Annexin V solution was added to the cells and incubated for 30 min at 4°C. The cells were then incubated with 5 ml propidium iodide (PI) and immediately analyzed with a FACScan. Ten thousand events were acquired on a FACSC-LSR (Becton-Dickinson, San Jose, CA) and analyzed with CellQuest (Becton-Dickinson) software.

2.8. Lentivirus Construction and Infection. Construction of the recombinant lentivirus with HDGF was performed by the Genechem Company. For MSC infection, cells were seeded at a density of 1×10^5 cells in a six-well plate and infected with lentiviral vectors with 10 mg/ml polybrene (Millipore, Boston, MA, USA). At 12 hour postinfection, the medium was replaced. Forty-eight hours later, the transfected cells were cultured in a 5% CO_2-humidified incubator at 37°C.

2.9. Quantitative Polymerase Chain Reaction (qPCR) Analysis. Primers for amplification of mouse HDGF genes were used to determine the expression of HDGF in fibroblasts and MSCs. The amplification program consisted of initial denaturation at 95°C for 10 min followed by 40 cycles from 92°C for 15 s, annealing at 60°C for 30 s and extension at 72°C for 15 s. The relative expression levels of each gene were normalized to β-actin using the 2-ΔΔCt method.

2.10. Protein Digestion and iTRAQ Labeling. For each sample, protein was digested and the peptide mixture was labeled using chemicals from the iTRAQ reagent kit (Applied Biosystems, California, USA). Disulfide bonds were reduced in 5 mM Tris-(2-carboxyethy) phosphine (TCEP) followed by blocking cysteine residues in 10 mM methyl methanethiosulfonate (MMTS), before digestion with sequence-grade modified trypsin (Promega, Madison, WI, USA). For labeling, each iTRAQ reagent was dissolved in isopropanol and added to the respective peptide mixture. The labeled samples were combined and dried.

2.11. High pH Reverse Phase Separation. The peptide mixture was fractionated by high pH separation using the AQUITY UPLC system (Waters Corporation, Milford, MA, USA) connected to a reverse phase column(ACQUITY UPLC Peptide C18 column, 2.1 mm × 150 mm, 1.7 μm, 130 Å, Waters Corporation, Milford, MA, USA). High pH separation was performed using a linear gradient. The column was reequilibrated at initial conditions and the column flow rate was maintained at 600 μL/min. Collected fractions were dried in a vacuum concentrator for the next step.

2.12. Low pH Nano-HPLC-MS/MS Analysis. The mixed peptides were separated by nano-HPLC (Eksigent Technologies, Dublin, CA, USA) on the secondary RP analytical column (Eksigent, C18, 3 μm, 150 mm × 75 μm). Peptides were subsequently eluted using the following gradient conditions with phase B (98% ACN with 0.1% formic acid) from 5 to 45% B (5–70 min), and total flow rate was maintained at 300 nL/min. Electrospray voltage of 2.3 kV versus the inlet of the mass spectrometer was used.

Triple TOF 4600 mass spectrometer was operated in the data-dependent mode to switch automatically between MS and MS/MS acquisition. MS spectra were acquired across the mass range of 350–1250 m/z in high resolution mode using 250 ms accumulation time per spectrum. Tandem mass spectral scanned from 100–1250 m/z in high sensitivity mode with rolling collision energy. The 20 most intense precursors were selected for fragmentation per cycle with dynamic exclusion time of 9 s.

2.13. Statistical Analysis. All data are expressed as mean ± SEM and analyzed by SPSS 17 using two-tailed Student's *t*-test between two groups or one-way analysis of variance (ANOVA) when three or more groups were compared. *P* value less than 0.05 was considered as statistical significance.

3. Results

3.1. MSC-CdM but Not CF-CdM Induced Myocardial Protection against Reperfusion Injury. To compare the effects of MSC-CdM and CF-CdM on cardiac reperfusion injury, mice were intravenously treated with vehicle, MSC-CdM, or CF-CdM 15 min before occlusion of the LAD coronary artery. These mice were then subjected to 45 min of myocardial ischemia followed by 24 h of reperfusion. The area at risk was not different among the 3 experimental groups, but systemic delivery of MSC-CdM significantly reduced the infarct area/area at risk (I/AAR) and infarct area/left ventricular (I/LV) ratio by 24.6% and 25.6% ($P < 0.05$), respectively, compared with infarcted mice injected with vehicle (Figure 1(a)). In contrast, CF-CdM did not significantly affect the infarct size, showing a similar I/AAR to that in the control mice.

The decreased infarct size in the MSC-CdM group was accompanied by improved functional recovery. Compared with the vehicle group, values for maximal left-ventricular pressure ($+dp/dt_{max}$) and minimal left-ventricular pressure ($-dp/dt_{max}$) measured at 24 h reperfusion were both significantly improved ($P < 0.05$) in MSC-CdM treated mice, which were, however, not observed ($P > 0.05$) in CF-CdM-treated mice (Figure 1(b)). In parallel, LV end-diastolic pressure (LVEDP) was not affected by MSC-CdM, indicating that the increase of $+dp/dt_{max}$ is not due to altered preload (Supplementary Table 1). As Tau, an index of globe left-ventricular relaxation, was not changed by MSC-CdM, the improvement of $-dp/dt_{max}$ may have reflected the higher $+dp/dt_{max}$ in this group.

The extent of apoptosis at 24 h reperfusion was assessed by TUNEL staining (Figure 1(c)). MSC-CdM-treated mice had significantly decreased TUNEL positive myocytes ($P < 0.05$) in the peri-infarct area of the heart compared with controls. However, CF-CdM did not decrease the percentage of apoptotic cells after reperfusion. Similarly, isolated myocytes treated with MSC-CdM exhibited enhanced contractile performance (Supplementary Fig. 1A) and upregulated calcium transient amplitude (Supplementary Fig. 1B) at 2 h reoxygenation following 4 h of hypoxia, all of which were absent in CF-CdM treated cardiomyocytes.

3.2. Proteomic Profiles of Secreted Protein in MSC-CdM and CF-CdM and Highly Secreted HDGF from MSCs. To identify the specific paracrine factors that were responsible for the beneficial effects of MSC-CdM, the iTRAQ-labeled conditioned media protein samples of MSCs and CFs were analyzed. A total of 1787 proteins with at least 95% confidence were identified in the conditioned medium, among which 1595 proteins had quantification information (Supplementary Table S3). The subcellular localization information of all the identified proteins was annotated by Gene Ontology. As a result, a total of 861 proteins were assigned as extracellular (Figure 2(a)), of which 55 proteins were secreted selectively at higher level in MSC-CdM (>2-fold), while other 53 proteins were found highly secreted in CF-CdM (>2-fold). Functional classification and an enrichment analysis based on molecular functions

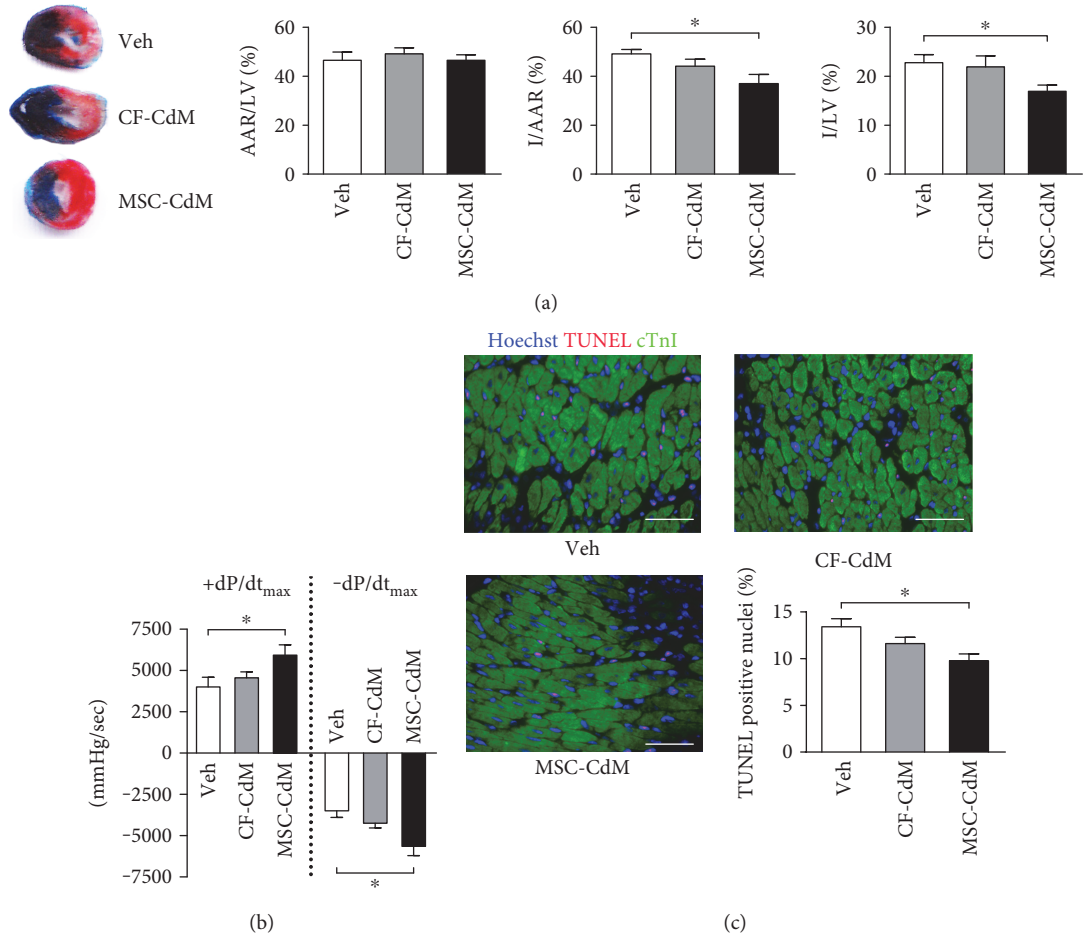

Figure 1: MSC-CdM reduce cardiac reperfusion injury. Wild-type mice were given 5 mg/kg CF-CdM, 5 mg/kg MSC-CdM, or vehicle i.v. 15 min before 45 min of ischemia. MSC-CdM: conditioned medium derived from MSC; CF-CdM: conditioned medium derived from cardiac fibroblasts. (a) Ratio of area at risk (AAR) to left ventricular (LV) area, ratio of infarct size (I) to AAR, and ratio of infarct size to LV after 24 h of reperfusion. Data represent mean ± standard error of mean (SEM) of values from five mice. (b) The maximum rates of rise and decline of left-ventricular pressure ($+dp/dt_{max}$ and $-dp/dt_{max}$) assessed at 24 h reperfusion. Data are mean ± SEM of values from six mice. (c) TUNEL staining at 24 h reperfusion; apoptotic nuclei were stained (red), and cardiomyocytes were detected by cardiac troponin I staining (green). Bar = 50 μM. Data are mean ± SEM of values from three hearts per group, with at least 3000 nuclei examined per heart. $^*P < 0.05$.

and biological processes revealed that these 108 differentially secreted proteins fell into many functional categories. We found that the number of proteins varied greatly for the different categories (Supplementary Fig. S2). Compared to CFs, MSCs secreted more proteins that were involved in the categories of "cellular process," "metabolic process," and "developmental process." In addition, MSC-CdM contained more secreted proteins that were related to catalytic activity.

Among the list of 55 proteins specifically highly secreted by MSCs (Table 1), HDGF was selected for further study because this candidate could relay paracrine communication between MSCs and myocytes, as well as exhibit antiapoptosis and proliferation effects [16–19]. To validate that HDGF was secreted by MSCs, RT-qPCR was performed to detect the expression level of HDGF in MSCs and fibroblasts. The mRNA abundance of HDGF in MSCs was significantly higher compared with that in fibroblasts ($P < 0.05$) (Figure 2(b)). These data were consistent with immunoblotting results which showed that HDGF was highly selectively expressed in MSC-CdM with high density (Figure 2(c)). Thus, our data provided strong evidence that HDGF was highly secreted by MSCs.

3.3. HDGF Contributed to the Protective Effects of MSC-CdM. To test whether HDGF was involved in protective effects of MSC-CdM, we first used lentiviral shRNA to knockdown HDGF in MSCs and investigated apoptosis in heart-derived H9C2 cells subjected to 4 h of reoxygenation following 9 h of hypoxia. PI-Annexin V double staining was used to identify the prevention effects of MSC-CdM (Figure 3(a)). Conditioned medium derived from MSCs that transfected with empty vector (MSC^{null}) reduced population of PI-Annexin V double positive cells

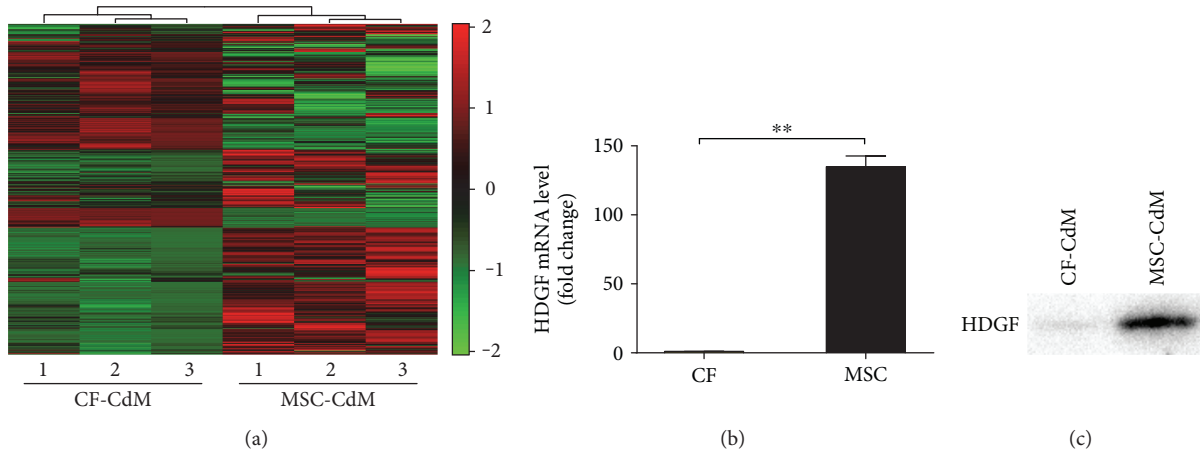

Figure 2: Secretome patterns and different HDGF expression between MSCs and fibroblasts. (a) iTRAQ analysis was applied and 1596 proteins were identified. Hierarchical clustering displayed as a heatmap. Red indicates an increase in expression, and green indicates decreases in expression compared with fibroblasts. (b) HDGF mRNA levels of MSCs and fibroblasts were assessed by RT-qPCR. Data represent mean ± SEM of values from three determinations. (c) Western blot assays on proteins precipitated from the MSC-CdM and CF-CdM. Representative of three independent experiments. $^{**}P < 0.01$.

by 45.7% after reoxygenation injury, which was absent when treated with the conditioned medium derived from MSCs that transfected shRNA lentivirus targeting HDGF. Being consistent with PI-Annexin V double staining, MSC^{null}-CdM significantly attenuated ($P < 0.05$) reoxygenation-induced activation of caspase-3 in H9C2 cells (Figure 3(b)). In contrast, knockdown of HDGF in MSCs impaired ($P < 0.05$) the MSC-CdM-mediated inhibitive effects on caspase-3 activation.

3.4. HDGF Reduced Apoptosis and Activated PKCε Pathway. To further validate the direct protective effects of HDGF on reperfusion injury, we applied mouse HDGF recombinant protein (100 nmol/L, Novoprotein Scientific, NJ, USA) or PBS as vehicle (Veh) to H9C2 cells that were subjected to H/R injury. PI-Annexin V double positive population was reduced by 29.2% when treated with HDGF recombinant protein (Figure 4(a)). In addition, a decrease in percentage of Annexin V positive and low PI cell population (in Q4 quadrant) was observed, suggesting that HDGF protected against reperfusion-induced early stage apoptosis. We also performed immunoblotting assay to detect the activation of caspase-3 and found that cleaved caspase-3 was significantly reduced in the HDGF group, compared to the control (Figure 4(b)).

To explore the intracellular mechanisms underlying the protective effects of HDGF, we examined PKCε activity as this pathway has been proved to play essential roles in myocardial preconditioning and cytoprotection [20–23]. Our data showed that HDGF induced PKCε phosphorylation (Figure 4(c)).Phosphorylated PKCε has been shown to translocate into mitochondria and interacts with ALDH2 contributing to 4-HNE detoxification during reperfusion injury [24]. Therefore, we assessed ALDH2 activity in myocardial mitochondria and 4-HNE which could reflect whether PKCε has been activated by HDGF. Our data showed that the delivery of recombinant HDGF significantly enhanced the activity of ALDH2 in mitochondria ($P < 0.05$) (Figure 4(d)) and prevented 4-HNE accumulation (Figure 4(e)), compared with the control group. Thus, these data support the notion that HDGF reduced reoxygenation-induced oxidative stress through PKCε activation.

3.5. PKCε Played a Key Role in HDGF-Mediated Protection against Reperfusion Injury. To further determine the role of PKCε in HDGF-mediated protection *in vivo*, recombinant mouse HDGF (50 μg/kg) or PBS (as vehicle) was administered intramyocardially to both PKCε-DN mice and WT littermate (as controls). Administration of recombinant HDGF reduced I/AAR to 33.8 ± 3.1% ($P < 0.05$), compared to 44.9 ± 2.6% in the control group (Figure 5(a)). However, this reduction in infarct size by HDGF delivery was absent in PKCε-DN mice that had similar I/AAR to those without HDGF intervention, although the I/AAR was similar between PKCε-DN and WT mice, and AAR/LV in all groups had no significant difference. In addition, recombinant HDGF markedly increased $+dp/dt_{max}$ and $-dp/dt_{max}$ at 24 h reperfusion in WT mice ($P < 0.05$) (Figure 5(b) and Supplementary Table 2). Although the mean value of $+dp/dt_{max}$ and $-dp/dt_{max}$ in PKCε-DN mice was increased by HDGF treatment, the HDGF-mediated improvement of hemodynamic performance was significantly limited compared to that in WT ($P < 0.05$).

Being consistent with the infarct size quantification, administration of recombinant HDGF significantly decreased TUNEL positive myocytes ($P < 0.05$) in the peri-infarct area in WT mice, which was not observed in PKCε-DN mice (Figure 5(c)). Meanwhile, we detected an enhanced mitochondrial ALDH2 activity (Figure 5(d)) and a significant reduction in 4-HNE accumulation (Figure 5(e)) in reperfusion-injured myocardium of WT mice, but not in that of PKCε-DN mice.

Moreover, HDGF enhanced contractile performance (Supplementary Fig. S3A, B) and upregulated calcium

Table 1: Functional classification of the highly secreted protein identified in MSC-CdM.

GO classification	Gene	Protein
ADP catabolic process	NUDT9	ADP-ribose pyrophosphatase, mitochondrial
Apoptotic process	HINT1	Histidine triad nucleotide-binding protein 1
	NME1	Nucleoside diphosphate kinase A
	NME2	Nucleoside diphosphate kinase B
Biological process	OAF	Out at first protein homolog
Biosynthetic process	HRT1	Hypoxanthine-guanine phosphoribosyltransferase
	ADA	Adenosine deaminase
	EEF1A1	Elongation factor 1-alpha 1
	TPI1	Triosephosphate isomerase
	PGAM1	Phosphoglycerate mutase 1
	EIF2S3X	Eukaryotic translation initiation factor 2 subunit 3, X-linked
Catabolic process	GSTO1	Glutathione S-transferase omega-1
Cell adhesion	SPP1	Osteopontin
Cell cycle	PIN4	Peptidyl-prolyl cis-trans isomerase NIMA-interacting 4
Cell differentiation	TPT1	Translationally controlled tumor protein
	STMN1	Stathmin
Cell growth	MTPN	Myotrophin
Cell morphogenesis	SMARCA4	Transcription activator BRG1
Cell motility	BRK1	Protein BRICK1
Cell-cell signaling	HDGF	Hepatoma-derived growth factor
Cellular component morphogenesis	CFL1	Cofilin-1
	TUBA4A	Tubulin alpha-4A chain
	SAA3	Serum amyloid A-3 protein
Cellular process	SOD3	Extracellular superoxide dismutase [Cu-Zn]
	LCN2	Neutrophil gelatinase-associated lipocalin
	NAMPT	Nicotinamide phosphoribosyltransferase
	UCHL3	Ubiquitin carboxyl-terminal hydrolase isozyme L3
DNA replication	PCNA	Proliferating cell nuclear antigen
Endothelial cell proliferation	HMGB1	High mobility group protein B1
Fatty acid catabolic process	ACOT7	Cytosolic acyl coenzyme A thioester hydrolase
Glycolysis	LDHA	L-lactate dehydrogenase A chain
	PGK1	Phosphoglycerate kinase 1
	GAPDH	Glyceraldehyde-3-phosphate dehydrogenase
	ENO1	Alpha-enolase
G-protein coupled receptor signaling pathway	CXCL5	C-X-C motif chemokine 5
	CCL8	C-C motif chemokine 8
Immune system process	HMGB2	High mobility group protein B2
	MIF	Macrophage migration inhibitory factor
	PSMA1	Proteasome subunit alpha type-1
Metabolic process	PKM	Pyruvate kinase PKM
Monosaccharide metabolic process	GALM	Aldose 1-epimerase
Oxidation-reduction process	AKR1B1	Aldose reductase
	AKR1B8	Aldose reductase-related protein 2
Pentose phosphate shunt	PGLS	6-phosphogluconolactonase
Protein folding	HSP90AA1	Heat shock protein HSP 90-alpha
	HSP90AB1	Heat shock protein HSP 90-beta
	ST13	Hsc70-interacting protein

Table 1: Continued.

GO classification	Gene	Protein
Protein metabolic process	LAP3	Cytosol aminopeptidase
Regulation of biological process	IGFBP6	Insulin-like growth factor-binding protein 6
Response to oxidative stress	PRDX5	Peroxiredoxin-5, mitochondrial
RNA splicing	PTBP1	Polypyrimidine tract-binding protein 1
	PCBP1	Poly(rC)-binding protein 1
	SFPQ	Splicing factor, proline- and glutamine-rich
Translation	RPS20	40S ribosomal protein S20
Carbohydrate metabolic process	GLO1	Lactoylglutathione lyase

GO: Gene Ontology.

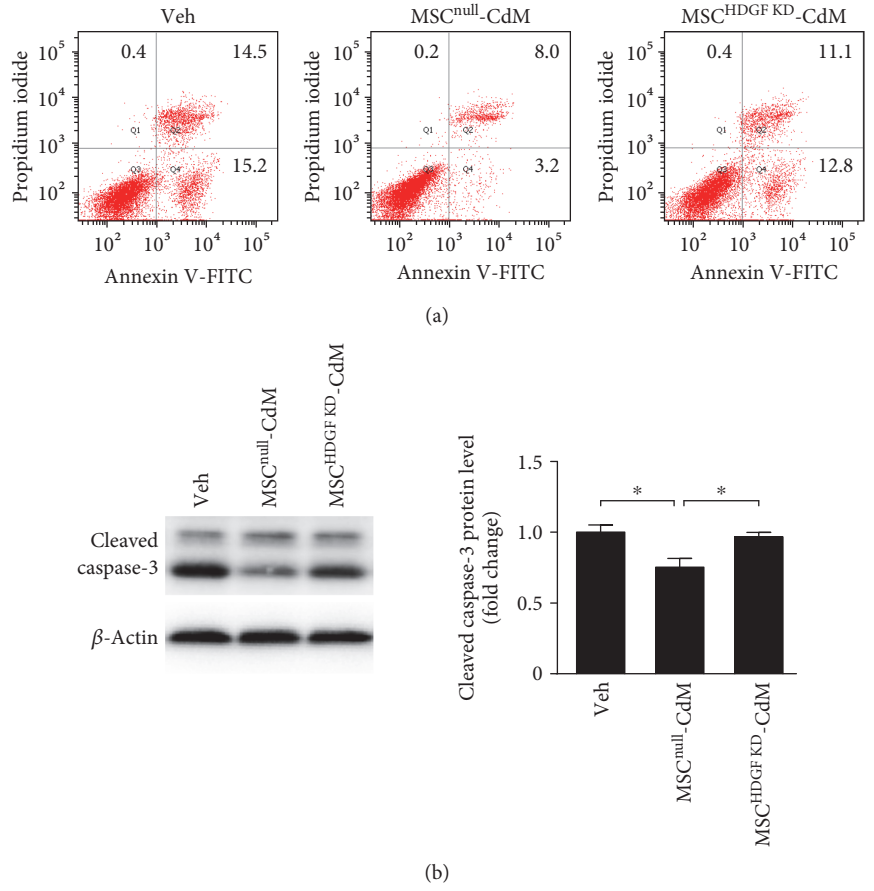

Figure 3: HDGF contributed to the protective effects of MSC-CdM. Conditioned medium that collected from MSCs transfected with vector (MSC^{null}-CdM) or HDGF shRNA lentivirus ($MSC^{HDGF\ KD}$-CdM) were treated to H9C2 cells subjected to 9 h of hypoxia followed by 4 h of reoxygenation. (a) Cell death was evaluated with flow cytometry analysis. Annexin V−/PI−: viable cells; Annexin V+/PI−: early apoptotic cells; Annexin V+/PI+: late apoptotic or necrotic cells; Annexin V−/PI+: necrotic cells. (b) Cleaved caspases-3 as detected by Western blotting. Data represent mean ± SEM of values from three determinations. $^*P < 0.05$.

transient amplitude (Supplementary Fig. S3C, D) in myocytes isolated from both WT and PKCε-DN mice. This set of data could account for the improved hemodynamic performance in HDGF-treated PKCε-DN mice but also imply that additional mechanisms might be involved in HDGF-induced function recovery.

4. Discussion

In the present study, we have demonstrated that the conditioned medium derived from MSCs could exert cardioprotection. Through an iTRAQ-based proteomic analysis of the secretion from MSCs and CFs, we identified

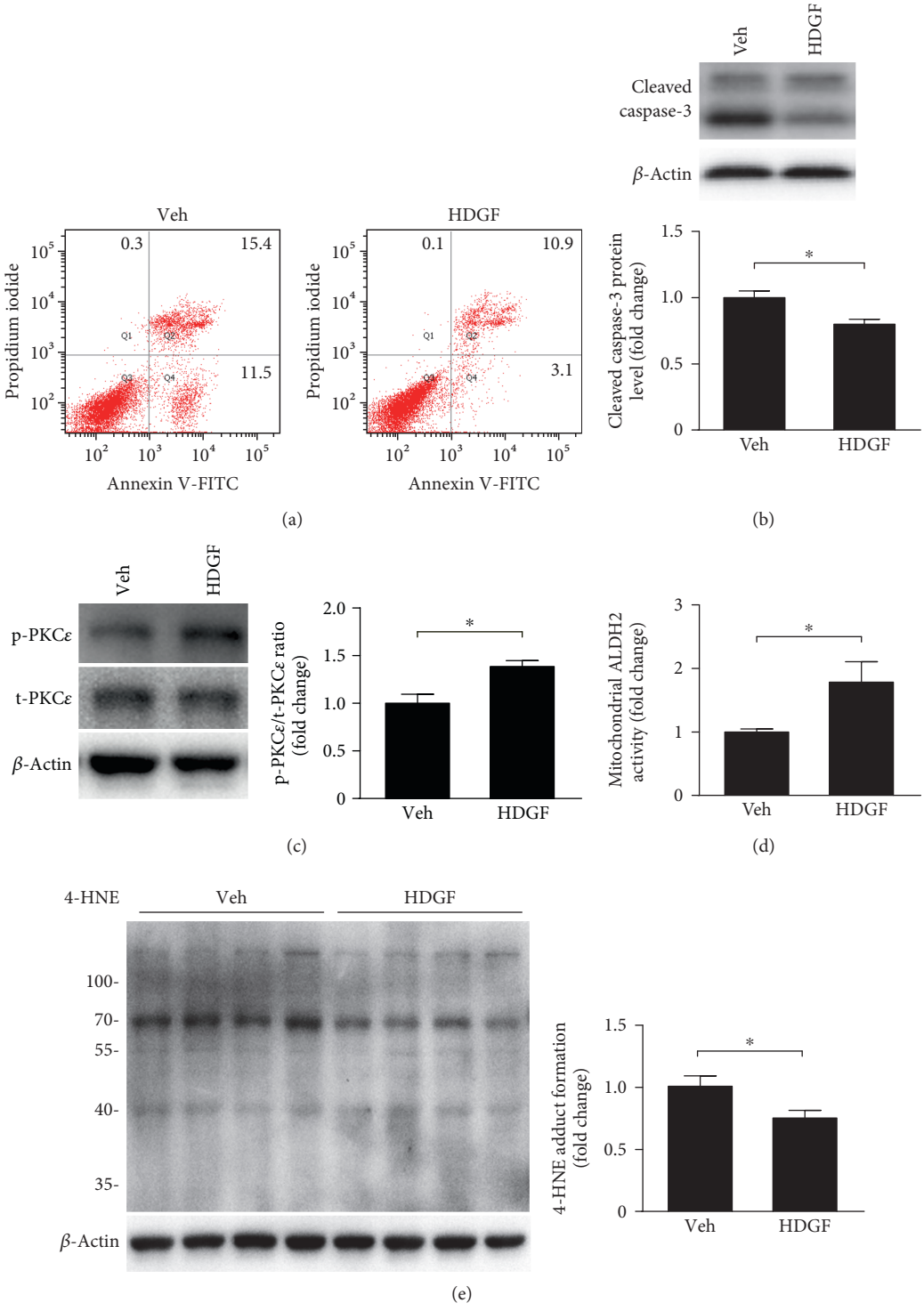

Figure 4: HDGF reduced apoptosis and activated PKCε pathway. H9C2 cells treated by recombinant mouse HDGF (100 nmol/L) or vehicle control were subjected to 9 h of hypoxia followed by 4 h of reoxygenation. (a) Cell death was evaluated with flow cytometry analysis. (b) Cleaved caspases-3 as detected by Western blotting. Data represent mean ± SEM of values from three determinations. (c) Phosphorylation of PKCε as detected by Western blotting. Data represent mean ± SEM of values from three determinations. (d) Mitochondria were isolated from H9C2 cells and activity of ALDH2 in mitochondria was measured. Data represent mean ± SEM of values from three mice. (e) 4-HNE protein adducts in H9C2 cells were assessed. Data represent mean ± SEM of values from four determinations. $^*P < 0.05$.

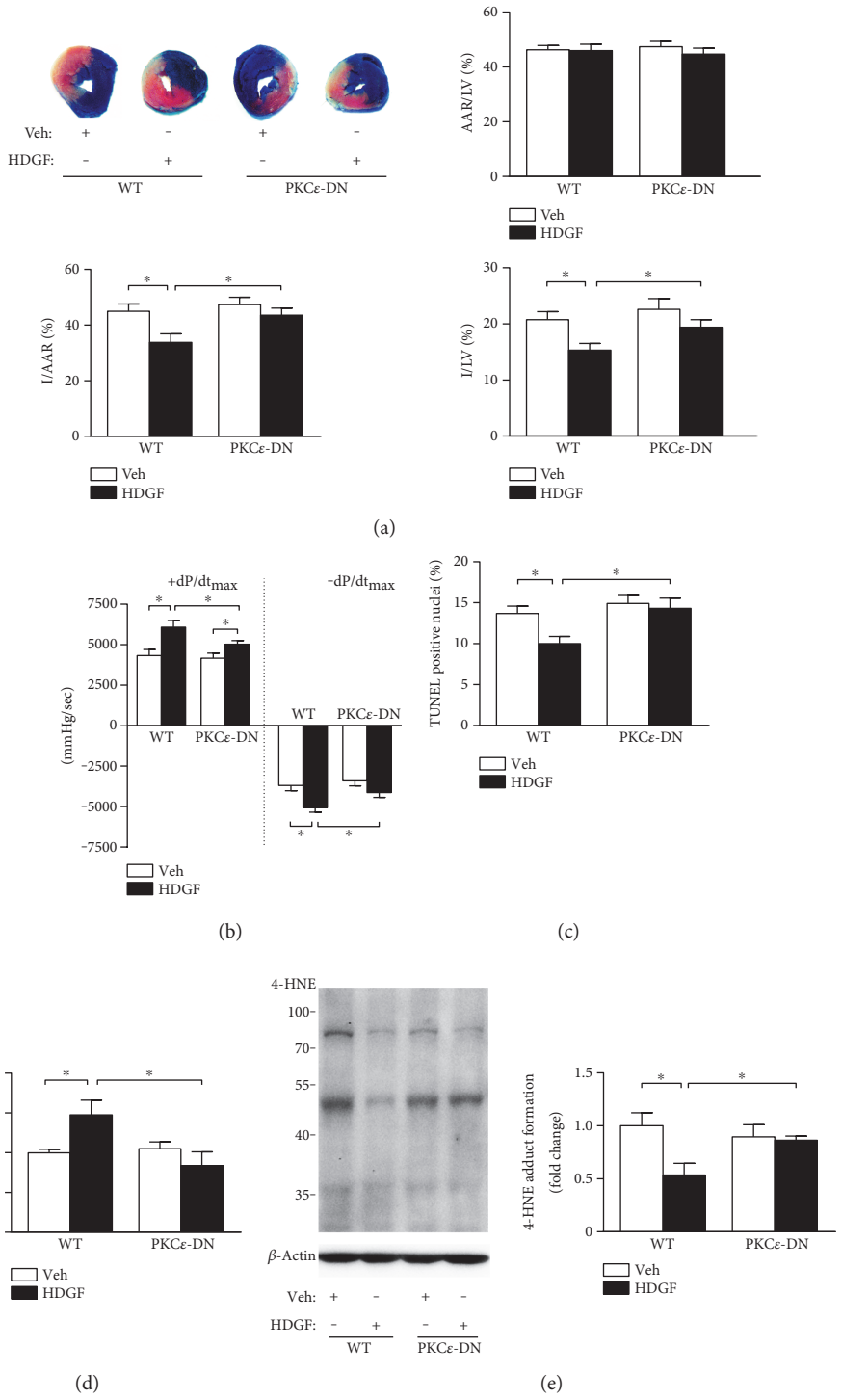

Figure 5: PKCε contributed to HDGF-induced reduction of reperfusion injury. PKCε dominant negative mice (PKCε-DN) and wild-type (WT) littermates with or without 50 μg/kg recombinant mouse HDGF treatment intramyocardially were subjected to 45 min of cardiac ischemia followed by 24 h reperfusion. (a) Ratio of area at risk to left ventricle area (AAR/LV), ratio infarct size to AAR ratio (I/AAR), and ratio of infarct size to LV area (I/LV) of hearts were assessed. Data represent mean ± SEM of values from five mice. (b) The maximum rates of rise and decline of left-ventricular pressure ($+dp/dt_{max}$ and $-dp/dt_{max}$) assessed at 24 h reperfusion. Data are mean ± SEM of values from six mice. (c) Quantitative analysis of TUNEL positive cells at 24 h reperfusion. Data are mean ± SEM of values from three hearts per group, with at least 3000 nuclei examined per heart. (d) Mitochondria were isolated from heart tissue after reperfusion injury and the activity of ALDH2 in mitochondria was measured. Data represent mean ± SEM of values from three mice. (e) 4-HNE protein adducts in heart tissues was assessed. Data represent mean ± SEM of values from three mice. $^*P < 0.05$.

HDGF as an important component that played an essential role in the prosurvival effects offered by MSC therapy. Administration of recombinant HDGF alone recapitulated MSC-mediated protection, resulting in a reduction in infarct size, decreased apoptosis, and improved cardiac function through PKCε pathway.

Although CFs secrete paracrine factors such as FGF-1, FGF-2, IL-33, and tissue inhibitory metalloproteinases (TIMPs) that are beneficial to cardioprotection [25, 26], limited effects of CF-CdM were observed in our study. MSCs have been reported to secrete some distinct cytokines compared to dermal fibroblasts, which allow MSC therapy to exhibit superiority over fibroblasts therapy in the wound healing process [27, 28]. As MSCs hold great promise for cell-based therapy, the identification of secreted factors along with the related underlying mechanisms is of great biological and therapeutic importance. We, for the first time, applied iTRAQ-based proteomics analysis to compare the secretion from MSCs and CFs. A list of secreted factors specifically highly expressed by MSCs was defined, among which HDGF was further investigated and proved to induce myocardial protection. Thus, we provided a feasible approach to identify protective factors in the secretions from MSCs. Of note, hypoxia can improve the paracrine effects of different types of cells. The conditioned medium from hypoxia-preconditioned CFs was reported to be able to induce protection for reperfusion-injured myocardium [29], which was not observed in our study when the conditioned medium was collected under normoxic condition. Our previous studies demonstrated that hypoxia preconditioning enhanced biological function and cardioprotective effects of MSCs in rodent and primate models of permanent myocardial ischemia [10, 11]. Therefore, it remains to be further investigated whether hypoxic preconditioning enhances MSC protection against reperfusion injury and triggers MSC secretome alterations.

PKCε is one of the central players in protection induced by ischemic preconditioning [20, 21], which is considered as the most efficient way to prevent reperfusion injury [30]. Activation of PKCε induces its translocation to the mitochondria and triggers a variety of mechanisms to induce antiapoptotic and antinecrotic effects, including enhancement of ALDH2 activity which detoxifies ROS-generated 4-HNE [20, 24], interaction with cytochrome *c* oxidase subunit IV [31], inhibition of mitochondrial permeability transition pore (mPTP) opening [32], and stabilization of mitochondrial membrane potential ($\Delta\psi$m). PKCε is known to be activated during reperfusion injury. However, the extent of PKCε activation by reperfusion may be insufficient to induce significant cardioprotection, since there is no difference in cardiac function and infarct sizes between WT and PKCε knockout mice [33, 34]. Further deterioration was neither observed in PKCε-DN mice in our study. On the other hand, deletion of PKCε can abolish ischemic preconditioning-mediated protection [34, 35], indicating that PKCε is indispensable and might be further enhanced to take part in the protection against reperfusion injury. In this regard, identifying agents, such as HDGF that stimulates the PKCε pathway, will be of therapeutic benefit. Our data indicates that HDGF activates PKCε and induces a PKCε-dependent protection, including suppression of apoptosis, limitation of reperfusion-induced oxidative stress, and reduction in infarct size.

It has to be born in mind though that PKCε may not be the sole pathway involved in HDGF-mediated protection, since HDGF-induced effects on myocyte contractility and calcium handling were not impaired when PKCε was disrupted. In addition, we utilized isolated adult cardiomyocytes to detect myocyte calcium cycling and contractility in the present study. The H9C2 cell line was also used, due to the ease of handling as well as the ethical issues of laboratory animal use without significantly compromising the mechanistic molecular experiment. However, it is a cloned embryonic cardiac myoblast cell line obtained from embryonic rat heart, which does not truly possess morphological characteristics of matured cardiomyocytes.

HDGF was originally isolated from the conditioned medium of hepatoma-derived cells as a heparin-binding growth factor, and its role in the development of cardiovascular tissues was proved afterwards [36]. Over the last two decades, HDGF has been reported to be involved in many biological processes, such as wound repair [37], angiogenesis [38], and antiapoptosis [39]. Downregulation of HDGF impairs activation of certain survival pathways, leading to the cellular apoptosis under stress [18, 39]. Therefore, HDGF may function as an antiapoptotic factor underlying the protection of MSCs. In this study, knockdown of HDGF impaired the effects of MSCs, indicating that HDGF plays an important role in MSC protection. HDGF also can improve proliferation [16] and migration [40], both of which are important processes in cardiac repair and regeneration. Administration of recombinant HDGF has been shown to induce a reduction in infarct size and improved cardiac function, suggesting that HDGF can be of great clinical benefit in the prevention of reperfusion injury.

Abbreviations

HDGF: Hepatoma-derived growth factor
MSC: Mesenchymal stem cell
CF: Cardiac fibroblast
CdM: Conditioned medium
PKCε: Protein kinase C epsilon
WT: Wild type
PKCε-DN: PKCε dominant negative
4-HNE: 4-hydroxy-2-nonenal
ALDH2: Aldehyde dehydrogenase family 2
KD: Knockdown.

Conflicts of Interest

None of the authors has any conflicts of interest to disclose relevant to this work.

Acknowledgments

The authors thank Professor Peipei Ping for the kind gift of PKC epsilon-dominant negative transgenic mice, and

Dr. Hong Lu and Professor Keith A. Webster for their critical input on this manuscript. This work was supported by the National High-tech R&D 863 Program (no. 2013AA020101), the National Basic Research Program of China (973 Program nos. 2014CB965100 and 2014CB965103), grants from the National Natural Science Foundation of China (nos. 31171418, 81320108003 and 31371498 for Jian-An Wang; nos. 81170308 and 81370247 for Xinyang Hu; no. 81573641 for Ling Zhang; no. 31271585 for Hong Yu; and no. 81370346 for Wei Zhu), the Science and Technology Department of Zhejiang Province public welfare projects (no. 2013C37054 for Xinyang Hu and no. 2014C33190 for Rongrong Wu), and the Zhejiang Provincial Natural Science Foundation (no. LY16H280003 for Ling Zhang and no. 2013C24009 for Hong Yu).

References

[1] V. L. Roger, A. S. Go, D. M. Lloyd-Jones et al., "Heart disease and stroke statistics—2012 update: a report from the American Heart Association," *Circulation*, vol. 125, pp. e2–e220, 2012.

[2] L. Wu, J. L. Tan, Z. H. Wang et al., "ROS generated during early reperfusion contribute to intermittent hypobaric hypoxia-afforded cardioprotection against postischemia-induced Ca^{2+} overload and contractile dysfunction via the JAK2/STAT3 pathway," *Journal of Molecular and Cellular Cardiology*, vol. 81, pp. 150–161, 2015.

[3] E. Lopez-Bernardo, A. Anedda, P. Sanchez-Perez, B. Acosta-Iborra, and S. Cadenas, "4-Hydroxynonenal induces Nrf2-mediated UCP3 upregulation in mouse cardiomyocytes," *Free Radical Biology & Medicine*, vol. 88, pp. 427–438, 2015.

[4] Y. C. Awasthi, K. V. Ramana, P. Chaudhary, S. K. Srivastava, and S. Awasthi, "Regulatory roles of glutathione-S-transferases and 4-hydroxynonenal in stress-mediated signaling and toxicity," *Free Radical Biology & Medicine*, vol. 111, pp. 235–243, 2017.

[5] P. Eaton, J. M. Li, D. J. Hearse, and M. J. Shattock, "Formation of 4-hydroxy-2-nonenal-modified proteins in ischemic rat heart," *The American Journal of Physiology*, vol. 276, pp. H935–H943, 1999.

[6] S. T. Ji, H. Kim, J. Yun, J. S. Chung, and S. M. Kwon, "Promising therapeutic strategies for mesenchymal stem cell-based cardiovascular regeneration: from cell priming to tissue engineering," *Stem Cells International*, vol. 2017, Article ID 3945403, 13 pages, 2017.

[7] K. Tamama and D. J. Barbeau, "Early growth response genes signaling supports strong paracrine capability of mesenchymal stem cells," *Stem Cells International*, vol. 2012, Article ID 428403, 7 pages, 2012.

[8] X. Hu, P. Chen, Y. Wu et al., "MiR-211/STAT5A signaling modulates migration of mesenchymal stem cells to improve its therapeutic efficacy," *Stem Cells*, vol. 34, pp. 1846–1858, 2016.

[9] X. Hu, L. Zhang, J. Jin et al., "Heparanase released from mesenchymal stem cells activates integrin beta1/HIF-2alpha/Flk-1 signaling and promotes endothelial cell migration and angiogenesis," *Stem Cells*, vol. 33, pp. 1850–1862, 2015.

[10] X. Hu, Y. Xu, Z. Zhong et al., "A large-scale investigation of hypoxia-preconditioned allogeneic mesenchymal stem cells for myocardial repair in nonhuman primates: paracrine activity without remuscularization," *Circulation Research*, vol. 118, pp. 970–983, 2016.

[11] P. Chen, R. Wu, W. Zhu et al., "Hypoxia preconditioned mesenchymal stem cells prevent cardiac fibroblast activation and collagen production via leptin," *PLoS One*, vol. 9, article e103587, 2014.

[12] X. Hu, R. Wu, Z. Jiang et al., "Leptin signaling is required for augmented therapeutic properties of mesenchymal stem cells conferred by hypoxia preconditioning," *Stem Cells*, vol. 32, no. 10, pp. 2702–2713, 2014.

[13] L. Timmers, S. K. Lim, I. E. Hoefer et al., "Human mesenchymal stem cell-conditioned medium improves cardiac function following myocardial infarction," *Stem Cell Research*, vol. 6, pp. 206–214, 2011.

[14] L. Timmers, S. K. Lim, F. Arslan et al., "Reduction of myocardial infarct size by human mesenchymal stem cell conditioned medium," *Stem Cell Research*, vol. 1, pp. 129–137, 2007.

[15] C. P. Baines, J. Zhang, G.-W. Wang et al., "Mitochondrial PKCε and MAPK form signaling modules in the murine heart: enhanced mitochondrial PKCε-MAPK interactions and differential MAPK activation in PKCε-induced cardioprotection," *Circulation Research*, vol. 90, pp. 390–397, 2002.

[16] M. Li, J. Shen, X. Wu et al., "Downregulated expression of hepatoma-derived growth factor (HDGF) reduces gallbladder cancer cell proliferation and invasion," *Medical Oncology*, vol. 30, p. 587, 2013.

[17] Y. Kishima, K. Yoshida, H. Enomoto et al., "Antisense oligonucleotides of hepatoma-derived growth factor (HDGF) suppress the proliferation of hepatoma cells," *Hepato-Gastroenterology*, vol. 49, pp. 1639–1644, 2002.

[18] S. S. Hsu, C. H. Chen, G. S. Liu et al., "Tumorigenesis and prognostic role of hepatoma-derived growth factor in human gliomas," *Journal of Neuro-Oncology*, vol. 107, pp. 101–109, 2012.

[19] Y. Yu, H. Shen, H. Yu et al., "Systematic proteomic analysis of human hepotacellular carcinoma cells reveals molecular pathways and networks involved in metastasis," *Molecular BioSystems*, vol. 7, pp. 1908–1916, 2011.

[20] G. R. Budas, E. N. Churchill, and D. Mochly-Rosen, "Cardioprotective mechanisms of PKC isozyme-selective activators and inhibitors in the treatment of ischemia-reperfusion injury," *Pharmacological Research*, vol. 55, pp. 523–536, 2007.

[21] H. Tong, W. Chen, C. Steenbergen, and E. Murphy, "Ischemic preconditioning activates phosphatidylinositol-3-kinase upstream of protein kinase C," *Circulation Research*, vol. 87, pp. 309–315, 2000.

[22] M. O. Gray, J. S. Karliner, and D. Mochly-Rosen, "A selective ε-protein kinase C antagonist inhibits protection of cardiac myocytes from hypoxia-induced cell death," *Journal of Biological Chemistry*, vol. 272, pp. 30945–30951, 1997.

[23] G. S. Liu, M. V. Cohen, D. Mochly-Rosen, and J. M. Downey, "Protein kinase C- ξ is responsible for the protection of preconditioning in rabbit cardiomyocytes," *Journal of Molecular and Cellular Cardiology*, vol. 31, pp. 1937–1948, 1999.

[24] G. R. Budas, E. N. Churchill, M.-H. Disatnik, L. Sun, and D. Mochly-Rosen, "Mitochondrial import of PKCε is mediated by HSP90: a role in cardioprotection from ischaemia and reperfusion injury," *Cardiovascular Research*, vol. 88, pp. 83–92, 2010.

[25] K. Seki, S. Sanada, A. Y. Kudinova et al., "Interleukin-33 prevents apoptosis and improves survival after experimental myocardial infarction through ST2 signaling," *Circulation Heart Failure*, vol. 2, pp. 684–691, 2009.

[26] Z. S. Jiang, G. B. Wen, Z. H. Tang, W. Srisakuldee, R. R. Fandrich, and E. Kardami, "High molecular weight FGF-2 promotes postconditioning-like cardioprotection linked to activation of protein kinase C isoforms, as well as Akt and p70 S6 kinases," *Canadian Journal of Physiology and Pharmacology*, vol. 87, pp. 798–804, 2009.

[27] L. Chen, E. E. Tredget, W. PY, and Y. Wu, "Paracrine factors of mesenchymal stem cells recruit macrophages and endothelial lineage cells and enhance wound healing," *PLoS One*, vol. 3, article e1886, 2008.

[28] S. Wang, H. Yang, Z. Tang, G. Long, and W. Huang, "Wound dressing model of human umbilical cord mesenchymal stem cells-alginates complex promotes skin wound healing by paracrine signaling," *Stem Cells International*, vol. 2016, Article ID 3269267, 8 pages, 2016.

[29] M. Abrial, C. C. Da Silva, B. Pillot et al., "Cardiac fibroblasts protect cardiomyocytes against lethal ischemia-reperfusion injury," *Journal of Molecular and Cellular Cardiology*, vol. 68, pp. 56–65, 2014.

[30] C. E. Murry, R. B. Jennings, and K. A. Reimer, "Preconditioning with ischemia: a delay of lethal cell injury in ischemic myocardium," *Circulation*, vol. 74, pp. 1124–1136, 1986.

[31] M. Ogbi and J. A. Johnson, "Protein kinase Cε interacts with cytochrome c oxidase subunit IV and enhances cytochrome *c* oxidase activity in neonatal cardiac myocyte preconditioning," *The Biochemical Journal*, vol. 393, pp. 191–199, 2006.

[32] C. P. Baines, C. X. Song, Y. T. Zheng et al., "Protein kinase Cε interacts with and inhibits the permeability transition pore in cardiac mitochondria," *Circulation Research*, vol. 92, pp. 873–880, 2003.

[33] M. O. Gray, H. Z. Zhou, I. Schafhalter-Zoppoth, P. Zhu, D. Mochly-Rosen, and R. O. Messing, "Preservation of base-line hemodynamic function and loss of inducible cardioprotection in adult mice lacking protein kinase Cε," *The Journal of Biological Chemistry*, vol. 279, pp. 3596–3604, 2004.

[34] A. T. Saurin, D. J. Pennington, N. J. Raat, D. S. Latchman, M. J. Owen, and M. S. Marber, "Targeted disruption of the protein kinase C epsilon gene abolishes the infarct size reduction that follows ischaemic preconditioning of isolated buffer-perfused mouse hearts," *Cardiovascular Research*, vol. 55, pp. 672–680, 2002.

[35] P. Ping, H. Takano, J. Zhang et al., "Isoform-selective activation of protein kinase C by nitric oxide in the heart of conscious rabbits: a signaling mechanism for both nitric oxide-induced and ischemia-induced preconditioning," *Circulation Research*, vol. 84, pp. 587–604, 1999.

[36] A. D. Everett, "Identification, cloning, and developmental expression of hepatoma-derived growth factor in the developing rat heart," *Developmental Dynamics*, vol. 222, pp. 450–458, 2001.

[37] A. D. Everett, D. R. Lobe, M. E. Matsumura, H. Nakamura, and C. A. McNamara, "Hepatoma-derived growth factor stimulates smooth muscle cell growth and is expressed in vascular development," *Journal of Clinical Investigation*, vol. 105, pp. 567–575, 2000.

[38] A. D. Everett, J. V. Narron, T. Stoops, H. Nakamura, and A. Tucker, "Hepatoma-derived growth factor is a pulmonary endothelial cell-expressed angiogenic factor," *American Journal of Physiology Lung Cellular and Molecular Physiology*, vol. 286, pp. L1194–L1201, 2004.

[39] T. Y. Tsang, W. Y. Tang, W. P. Tsang, N. N. Co, S. K. Kong, and T. T. Kwok, "Downregulation of hepatoma-derived growth factor activates the Bad-mediated apoptotic pathway in human cancer cells," *Apoptosis*, vol. 13, pp. 1135–1147, 2008.

[40] C. H. Wang, F. Davamani, S. C. Sue et al., "Cell surface heparan sulfates mediate internalization of the PWWP/HATH domain of HDGF via macropinocytosis to fine-tune cell signalling processes involved in fibroblast cell migration," *Biochemical Journal*, vol. 433, pp. 127–138, 2011.

Hindawi
Stem Cells International
Volume 2017, Article ID 6825427, 6 pages
https://doi.org/10.1155/2017/6825427

Review Article

Noncoding RNA and Cardiomyocyte Proliferation

Shuang Qu, Chunyu Zeng, and Wei Eric Wang

Department of Cardiology, Chongqing Institute of Cardiology & Chongqing Cardiovascular Clinical Research Center, Daping Hospital, Third Military Medical University, Chongqing 400042, China

Correspondence should be addressed to Chunyu Zeng; chunyuzeng01@163.com and Wei Eric Wang; weiericwang@163.com

Received 30 June 2017; Accepted 20 August 2017; Published 31 October 2017

Academic Editor: Yaoliang Tang

It is acknowledged that postnatal mammalian cardiomyocytes (CMs) turn over with a very limited efficacy in both physiological and pathological conditions. Recent studies showed that those newly formed CMs are derived from preexisting CMs. Thus, stimulating CM proliferation becomes a promising strategy for inducing cardiac regeneration. Noncoding RNAs were found differently expressed in CMs with different proliferation potential. Moreover, manipulation of noncoding RNAs, in particular microRNAs, was proved to promote or suppress CM proliferation, indicating that noncoding RNAs are involved in the underlying mechanism of CM proliferation. This review mainly summarizes the roles of noncoding RNAs, as a class of influential factors, in the regulation of CM proliferation.

1. Introduction

Cardiovascular diseases are the leading causes of morbidity and mortality all over the world. Particularly, myocardial infarction (MI) and heart failure following myocardial ischemia can lead to a large number of CM death [1]. In the past, the adult mammalian CMs are regarded as terminally differentiated cells without the ability to proliferate. Fetal CMs proliferate during development but lose this ability quickly after birth, and myocardium goes through a hyperplastic to hypertrophic transition. After this transition, the predominant form of growth is an increase in cell size and myofibril density rather than the number of CMs [2].

It is now recognized that a low level of postnatal CM proliferation was demonstrated in both normal and injured hearts. Taking advantage of integration of ^{14}C into DNA to establish the age of CMs in human, a seminal study carried by Bergmann and his colleagues indicated that about 0.5–1% of CMs renews every year, so nearly 50% of CMs is replenished over a life span [3]. Recently, a combination of genetic fate mapping with stable isotope labeling and multi-isotope imaging mass spectrometry shows the renewal of CMs is predominantly from the division of preexisting CMs, rather than the differentiation from the stem cells or progenitors [4]. Our previous study showed that mature adult CMs can reenter the cell cycle and form new CMs through a three-step process, dedifferentiation, proliferation, and redifferentiation [5]. However, the proliferation is not enough to replenish the lost CMs and repair the injured myocardium, and the underlying mechanism regulating CM proliferation is still unclear. To decipher the molecular mechanism controlling CM proliferation is of great importance for stimulating the endogenous cardiac regeneration, which might be a new therapeutic approach to those patients suffering from heart diseases.

Noncoding RNAs are those RNAs which cannot code proteins, such as microRNAs (miRNAs), long noncoding RNAs (lncRNAs), and circular RNAs, and were found to play important roles in the regulation of multiple cellular activities including proliferation [6]. This review mainly summarizes the roles of noncoding RNAs in the regulation of mammalian CM proliferation.

2. The Role of miRNAs in CM Proliferation

MicroRNA is a small noncoding RNA molecule containing 20 ~ 24 nucleotides. Each miRNA can have multiple target genes, and it can have various spatial and temporal expression patterns which express differently in diverse tissues and developmental stages [7]. An miRNA array showed that,

among the over 1000 miRNAs analyzed, 204 miRNAs increased and 311 miRNAs decreased during neonatal rat CM proliferation [8]. miRNAs were demonstrated to influence CM proliferation in neonatal and adult stages, which were summarized in Table 1.

3. miRNAs Regulate Neonatal CM Proliferation

The proliferation capacity of mammalian CM is robust in fetal period and is switched off early after birth. In mouse, the 1-day-old neonatal hearts can regenerate after partial surgical resection, but this capacity is lost by 7 days of age [9].

MiR-499 is a miRNA which is abundantly found in CMs and almost does not express in human cardiac stem cells or human embryonic stem cells [10]. By transfecting with pre-miR-499, EdU incorporation indicated CM proliferation was increased by 50% [11]. MiR-499 displayed a highlighted ability to promote neonatal CM proliferation via its function on Sox6 and cyclin D1 [12]. Sox6 played a role in cell viability, inhibited cell proliferation, and promoted cell apoptosis [13]. MiR-410 and miR-495 both belong to Gtl2-Dio3 miRNAs and were reported to promote CM proliferation. Overexpressing miR-410 and miR-495 in NRVMs induced about a 2.5-fold increase of proliferation analyzed with EdU incorporation assay. Meanwhile, Ki-67 immunostaining showed a threefold increase of proliferation [14]. The target gene of miR-410 and miR-495 is Cited2, a coactivator required for proper cardiac development. Cited2 knockdown reduced the expression of cell cycle inhibitor Cdkn1c/p57/Kip2 in neonatal CMs [14]. In the ischemic injury model, miR-222-overexpressing mice showed a twofold phosphohistone 3 (PH3) CMs compared with controls. Inhibition of miR-222 *in vivo* blocked CM proliferation in response to exercise. Cell cycle inhibitor P27, HIPK-1, and HIPK-2 as well as HMBOX1 were found to be involved in miR-222-induced CM proliferation [15].

MiR-133a knockdown mice hearts showed excessive CM proliferation, while miR-133a overexpression transgenic mice showed a diminished CM proliferation, indicating that miR-133 could be an inhibitor of CM proliferation [16, 17]. Similarly, miR-29a also suppressed CM proliferation, while inhibiting miR-29a promoted CM division [18]. Inhibiting miR-29a in neonatal CMs promoted CM proliferation by threefold analyzed by Ki-67 and PH3 staining and decreased the number of CMs in G0/G1 phases, while increased proportion of CMs in S and G2/M phases, indicating that inhibition of miR-29a facilitates the transition of G1/S and G2/M in CMs [19].

4. miRNAs Regulate Adult CM Proliferation

Hsa-miR-590-3p and hsa-miR-199a-3p are found to induce the proliferation of not only neonatal CMs but adult CMs. By injecting synthetic miRNAs directly into the heart of neonatal mice, EdU incorporation analysis revealed a marked increase of CM proliferation. Injection of AAV9 vector-expressing hsa-miR-590 or hsa-miR-199a precursor miRNAs increased CM proliferation in both neonatal and adult mice [8]. These two miRNAs can also stimulate CM proliferation in post-MI heart, which contributes to the preserved cardiac function [8].

Overexpressing miR-204 improved CM proliferation in neonatal and adult mice CMs *in vitro*. Knockdown of its target gene Jarid2 had a similar effect as miR-204 overexpression. Transgenic mice with cardiac-specific overexpression of miR-204 showed an increase of CM proliferation throughout the embryonic and adult stages, which was associated with upregulated cell cycle regulators Cyclin A, Cyclin B, Cyclin D2, Cyclin E, CDC2, and PCNA [20].

MiR-17-92, an oncogenic miRNA cluster, proved to be essential for CM proliferation and participated in the regulation of CM proliferation in embryonic, postnatal, and adult hearts. CM proliferation decreased by about 50% in postnatal hearts of miR-17–92 cKO mice, while it was significantly increased in cardiac-specific miR-17-92 overexpressed transgenic mice analyzed with PH3 and Aurora B immunostaining [21]. Overexpression of MiR-17-3p, a member of miR-17-92 cluster, has been shown to promote CM proliferation in neonatal CMs. Furthermore, inhibition of miR-17-3p attenuated exercise-induced cardiac growth and CM proliferation in adult mouse heart [22].

Loss of miR302-367 led to decreased CM proliferation during development, while increased miR302-367 expression led to a profound increase in CM proliferation. Reexpression of miR302-367 by using miRNA mimic-based treatment promoted adult CM proliferation and reduced scar formation in the post-MI heart. The CM proliferation was evaluated with Ki-67, PH3, and Aurora B kinase staining, as well as CM number counting [23]. Besides, miR-302-367 can not only have an effect on cell cycle activity but also the nucleation of CMs evidenced by an increase of the proportion of mononucleated/binucleated CMs versus multinucleated CMs in miR302-367 gain of function mice. With the method of high-throughput sequencing of RNA isolated by cross-linking immunoprecipitation (HITS-CLIP), the miR302-307 target genes Mst1, Lats2, and Mob1b are found to be components of Hippo signaling pathway, indicating the effect of miR302-367 on CM proliferation might be through repression of the Hippo signal transduction pathway [24].

MiR-34a expressed at a low level in fetal and early postnatal hearts; it soon expressed relatively higher after the first week after birth and sustained during adulthood [25]. Cardiac injury further upregulated the expression of miR-34a [26]. In the early postnatal mice, overexpression of miR-34a can decrease the CM proliferation. In contrary, antagonism of miR-34a promoted the CM proliferation through targeting on Bcl2, Cyclin D1, and Sirt 1 in the adult mice with MI injury [25]. Overexpression of miR-195, a member of the miR-15 family, during development caused premature CM cell cycle arrest, leading to congenital heart hypoplasia [27]. MiR-195 was found to be upregulated by sixfold at postnatal day 10 compared to postnatal day 1 [28]; miR-195 overexpression prevented cardiac regeneration of postnatal day 1 hearts suffering from MI injury [27]. Overexpressing miR-195 increased the proportion of NRVMs in G2/M phase [28]. In adult MI model, inhibition of miR-15 family by using administrating-locked nucleic acid- (LNA-) modified anti-miRNAs resulted in an increase

Table 1: A summary of the effect of miRNAs on neonatal and adult cardiomyocyte proliferation analyzed with different methodologies.

MicroRNAs	miR-499	miR-410/ mi-R495	miR-590/ miR-199a	miR-204	miR-195 (miR15 family)	miR-34a	miR17-92 cluster	miR-17-3p	miR-222	miR302-367	miR-29a	miR-133	miR-1
Species	Mice	Mice	Mice	Mice	Mice	Mice	Mice	Mice	Mice	Mice	Mice	Mice and zebrafish	Mice
Experiment	*In vitro*: neonatal CMs Mouse P19CL6 cells	*In vitro*: neonatal cms	*In vivo*: neonatal adult	*In vitro*: neonatal cms and adult cms *In vivo*: adult miRNA-204 transgenic mice	*In vivo*: transgenic mice	*In vitro*: neonatal cms *In vivo*: neonatal mi and adult mi	*In vivo*: transgenic mice	*In vitro*: NRVMs *In vivo*: adult myocardial ischemia-reperfusion injury	*In vitro*: NRVMs *In vivo*: exercise model	*In vitro*: transgenic mice and adult mice treated with miRNA mimics for mir302-367	*In vitro*: neonatal cms	*In vivo*: transgenic mice	*In vivo*: transgenic mice
Methods and fold changes	EdU (~1.5-fold)	EdU (~2.5-fold) Ki-67 (~3 fold)	EdU (~3-fold)	EdU (NRVMs) ~8-fold Aurora B (NRWMs) ~2-fold NRVMs numbers: ~1.2-fold ARVM numbers: ~1.2-fold PH3 (transgenic mice): ~3-fold	PH3: ~2-fold	PH3: neonatal MI ~3-fold Adult MI ~8-fold EdU: NRVMs ~3-fold	Adult: CM numbers ~3-fold PH3 ~3-fold	EdU: ~ 1.5-fold K-i67: ~ 2.3-fold Cell number: ~1.2-fold	EdU: ~4-fold Ki-67:~ 3-fold Cell number: ~1.2-fold	Adult: CM number ~1.6-fold Neonatal: pH 3 ~6-fold Embryonic: pH 3 ~4-fold	Ki-67(~3-fold) PH3 (~3-fold)	PH3: ~ 2-fold	PH3: ~4-fold CM numbers: ~1.2-fold
Effect	Promote	Promote	Promote	Promote	Suppress	Suppress	Promote	Promote	Promote	Promote	Suppress	Suppress	Suppress
Target genes	Sox6 and Cyclin D1	Cited2	HOMER1, HOPX, and CLIC5	Jarid2	Check1	PNUTs, SRT1, Bcl2, Cyclin D1, and Sirt1	PTEN	TIMP-3 PTEN	P27, HMBOX1, HIPK-1, and HIK-2	Mst1, Lats2, and Mob1b	Cyclin D2, Akt3, and CDK2	CRF and Cyclin D2	Hand2 and SRF
Stage	Neonatal	Neonatal	Neonatal and adult	Neonatal and adult	Neonatal and adult	Neonatal and adult	Embryonic and neonatal adult	Neonatal	Neonatal	Embryonic and neonatal Adult	Neonatal	Neonatal	Adult
Reference	[11, 12]	[14]	[8]	[20]	[27, 28]	[26]	[21]	[22]	[15]	[23, 24]	[19]	[16, 17]	[29]

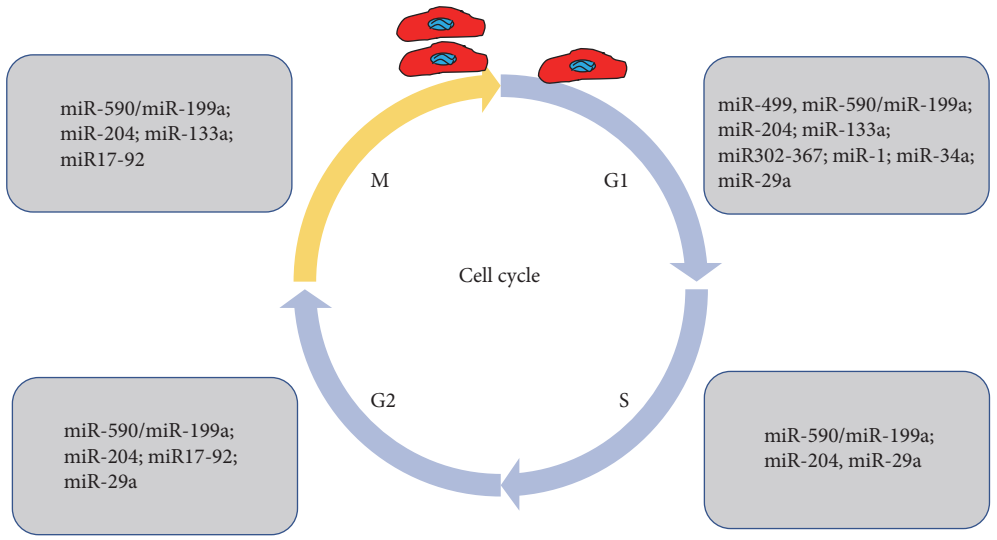

Figure 1: A summary of miRNAs in regulating cardiomyocyte proliferation at different phases of cell cycle.

in CM proliferation, with a fivefold increase of PH3-positive CMs [27]. Consistently, a chemically modified RNA oligonucleotide blocking the seed sequence of the miR-15 family members promoted adult CM proliferation and preserved cardiac function after injury [18]. In mice with miR-1-2 deletion, CM proliferation was increased, supported by 20% increased CM numbers and threefold more PH3 positive CMs [29].

5. Cell Cycle and Methodology for Evaluating CM Proliferation

Cell cycle can be divided into four phases: G1 phase, S phase (synthesis), G2 phase (collectively known as interphase), and mitotic (M) phase. Mitosis (division of the nucleus) and cytokinesis (division of cytoplasm, organelles, and cell membrane) together define the M phase of CM cell cycle [30]. The process of mitosis is divided into five stages: prophase, prometaphase, metaphase, anaphase, and telophase. It leads to multinucleated CMs if there is karyokinesis without cytokinesis during M-stage, and it leads to polyploid if there is DNA replication without karyokinesis and cytokinesis [31]. When considering the intrinsic proliferative capacity of adult mammalian CMs, it is important to reiterate that DNA synthesis does not necessarily result in genome duplication, that genome duplication does not necessarily result in mitosis, and that mitosis does not necessarily result in cytokinesis [32]. miRNAs regulate CM proliferation at different phases of cell cycle, which were summarized in Figure 1.

In most studies, the methods used for quantifying CM proliferation were based on immunostaining for DNA synthesis and cell cycle activation (BrdU/EdU incorporation, Ki-67, PH3, Aurora B, and alinin). BrdU/EdU can be incorporated into newly synthesized DNA at S phase of cell cycle. Ki-67 is detected in all active stages of cell cycle, including G1, S, G2, and M phases and is not active in the resting G0-phase cells and terminally differentiated cells [33]. K-i67 could not clearly distinguish multinucleated cells and polyploid with proliferating cells. Aurora B kinase is a protein that functions in the attachment of the mitotic spindle to the centromere, which is expressed during metaphase, anaphase and, cytokinesis in CMs [34]. In metaphase, Aurora B is associated to the chromosomes, whereas in anaphase and telophase it is localized to the midzone and midbody, respectively [34]. PH3 expresses during mitosis since chromosome condensation at mitosis is accompanied not only with phosphorylation of histone H3. Actually, all these markers could not identify a CM completing the whole cell cycle process and giving rise to two/multiple daughter cells. CMs especially adult ones are able to reenter into cell cycle but difficult to pass cytokinesis phase. However, none of these markers directly examine CM proliferation with cytokinesis. On the other hand, these methods could be complicated by DNA repair, polyploidy, and multinucleation in CMs. One must keep the interpretive restrictions in mind when comparing the results from different laboratories particularly when different assays are utilized.

Therefore, rigorous confirmation with nonambiguous molecular genetic markers or method should be requisite for any studies assessing de novo cardiomyogenesis. Time-lapse imaging observation combined with nuclei staining is a direct way to assess the CMs' proliferation and visualize the mitosis and cytokinesis processes [5]. This method could be an appropriate *in vitro* experiment, but new techniques are needed to quantify the CM proliferation *in vivo*.

6. Discussion

Understanding the underlying mechanism regulating CM proliferation could be of great clinical significance for treating MI, heart failure, and other cardiac diseases in which reduced CM numbers are the principal reason for deranged cardiac function. Noncoding RNAs especially miRNAs were demonstrated to play essential roles in CM proliferation in fetal and neonatal as well as adult stages. Manipulating the key miRNAs could be a promising strategy for stimulating

cardiac regeneration in injured hearts. Other noncoding RNAs such as lncRNAs (with more than 200 nucleotides in length) may also play a role in CM proliferation. LncRNA expressions significantly changed in cardiac hyperplastic to hypertrophic growth transition [35]. Manipulation of lncRNA-Gas5 and Sghrt in adult heart reduced the expression of cell cycle regulating genes including Ccng1 and Ccnd2 in CMs [36]. The effect of these noncoding RNAs including lncRNAs and circular RNAs on CM proliferation requires further study.

Conflicts of Interest

The authors declare that they have no conflicts of interest.

Acknowledgments

This study was supported by research grants from the National Natural Science Foundation of China (31730043 and 81670277).

References

[1] N. J. Pagidipati and T. A. Gaziano, "Estimating deaths from cardiovascular disease: a review of global methodologies of mortality measurement," *Circulation*, vol. 127, no. 6, pp. 749–756, 2013.

[2] E. R. Porrello, A. I. Mahmoud, E. Simpson et al., "Transient regenerative potential of the neonatal mouse heart," *Science*, vol. 331, no. 6020, pp. 1078–1080, 2011.

[3] O. Bergmann, R. D. Bhardwaj, S. Bernard et al., "Evidence for cardiomyocyte renewal in humans," *Science*, vol. 324, no. 5923, pp. 98–102, 2009.

[4] S. E. Senyo, M. L. Steinhauser, C. L. Pizzimenti et al., "Mammalian heart renewal by pre-existing cardiomyocytes," *Nature*, vol. 493, no. 7432, pp. 433–436, 2013.

[5] W. E. Wang, L. Li, X. Xia et al., "Dedifferentiation, proliferation, and redifferentiation of adult mammalian cardiomyocytes after ischemic injury," *Circulation*, vol. 136, 2017.

[6] L. Tao, Y. Bei, Y. Zhou, J. Xiao, and X. Li, "Non-coding RNAs in cardiac regeneration," *Oncotarget*, vol. 6, no. 40, pp. 42613–42622, 2015.

[7] G. Ruvkun, "Molecular biology: glimpses of a tiny RNA world," *Science*, vol. 294, no. 5543, pp. 797–799, 2001.

[8] A. Eulalio, M. Mano, M. Dal Ferro et al., "Functional screening identifies miRNAs inducing cardiac regeneration," *Nature*, vol. 492, no. 7429, pp. 376–381, 2012.

[9] Y. Nakada, D. C. Canseco, S. Thet et al., "Hypoxia induces heart regeneration in adult mice," *Nature*, vol. 541, no. 7636, pp. 222–227, 2017.

[10] J. D. Fu, S. N. Rushing, D. K. Lieu et al., "Distinct roles of microRNA-1 and -499 in ventricular specification and functional maturation of human embryonic stem cell-derived cardiomyocytes," *PLoS One*, vol. 6, no. 11, article e27417, 2011.

[11] M. L. Bell, M. Buvoli, and L. A. Leinwand, "Uncoupling of expression of an intronic microRNA and its myosin host gene by exon skipping," *Molecular and Cellular Biology*, vol. 30, no. 8, pp. 1937–1945, 2010.

[12] X. Li, J. Wang, Z. Jia et al., "MiR-499 regulates cell proliferation and apoptosis during late-stage cardiac differentiation via Sox6 and cyclin D1," *PLoS One*, vol. 8, no. 9, article e74504, 2013.

[13] B. Dumitriu, M. R. Patrick, J. P. Petschek et al., "Sox6 cell-autonomously stimulates erythroid cell survival, proliferation, and terminal maturation and is thereby an important enhancer of definitive erythropoiesis during mouse development," *Blood*, vol. 108, no. 4, pp. 1198–1207, 2006.

[14] A. L. Clark and F. J. Naya, "MicroRNAs in the myocyte enhancer factor 2 (MEF2)-regulated *Gtl2-Dio3* noncoding RNA locus promote cardiomyocyte proliferation by targeting the transcriptional coactivator Cited2," *Journal of Biological Chemistry*, vol. 290, no. 38, pp. 23162–23172, 2015.

[15] X. Liu, J. Xiao, H. Zhu et al., "miR-222 is necessary for exercise-induced cardiac growth and protects against pathological cardiac remodeling," *Cell Metabolism*, vol. 21, no. 4, pp. 584–595, 2015.

[16] N. Liu, S. Bezprozvannaya, A. H. Williams et al., "microRNA-133a regulates cardiomyocyte proliferation and suppresses smooth muscle gene expression in the heart," *Genes & Development*, vol. 22, no. 23, pp. 3242–3254, 2008.

[17] J. L. Morrison, S. Zhang, R. L. Tellam et al., "Regulation of microRNA during cardiomyocyte maturation in sheep," *BMC Genomics*, vol. 16, p. 541, 2015.

[18] S. Zacchigna and M. Giacca, "Extra- and intracellular factors regulating cardiomyocyte proliferation in postnatal life," *Cardiovascular Research*, vol. 102, no. 2, pp. 312–320, 2014.

[19] X. Cao, J. Wang, Z. Wang et al., "MicroRNA profiling during rat ventricular maturation: a role for miR-29a in regulating cardiomyocyte cell cycle re-entry," *FEBS Letters*, vol. 587, no. 10, pp. 1548–1555, 2013.

[20] D. Liang, J. Li, Y. Wu et al., "miRNA-204 drives cardiomyocyte proliferation via targeting *Jarid2*," *International Journal of Cardiology*, vol. 201, pp. 38–48, 2015.

[21] J. Chen, Z. P. Huang, H. Y. Seok et al., "mir-17–92 cluster is required for and sufficient to induce cardiomyocyte proliferation in postnatal and adult hearts," *Circulation Research*, vol. 112, no. 12, pp. 1557–1566, 2013.

[22] J. Shi, Y. Bei, X. Kong et al., "miR-17-3p contributes to exercise-induced cardiac growth and protects against myocardial ischemia-reperfusion injury," *Theranostics*, vol. 7, no. 3, pp. 664–676, 2017.

[23] Y. Tian, Y. Liu, T. Wang et al., "A microRNA-Hippo pathway that promotes cardiomyocyte proliferation and cardiac regeneration in mice," *Science Translational Medicine*, vol. 7, no. 279, article 279ra38, 2015.

[24] T. Heallen, M. Zhang, J. Wang et al., "Hippo pathway inhibits Wnt signaling to restrain cardiomyocyte proliferation and heart size," *Science*, vol. 332, no. 6028, pp. 458–461, 2011.

[25] Y. Yang, H. W. Cheng, Y. Qiu et al., "MicroRNA-34a plays a key role in cardiac repair and regeneration following myocardial infarction," *Circulation Research*, vol. 117, no. 5, pp. 450–459, 2015.

[26] B. C. Bernardo, X. M. Gao, C. E. Winbanks et al., "Therapeutic inhibition of the miR-34 family attenuates pathological cardiac remodeling and improves heart function," *Proceedings of the National Academy of Sciences of the United States of America*, vol. 109, no. 43, pp. 17615–17620, 2012.

[27] E. R. Porrello, A. I. Mahmoud, E. Simpson et al., "Regulation of neonatal and adult mammalian heart regeneration by the miR-15 family," *Proceedings of the National Academy of Sciences of the United States of America*, vol. 110, no. 1, pp. 187–192, 2013.

[28] E. R. Porrello, B. A. Johnson, A. B. Aurora et al., "miR-15 family regulates postnatal mitotic arrest of cardiomyocytes," *Circulation Research*, vol. 109, no. 6, pp. 670–679, 2011.

[29] Y. Zhao, J. F. Ransom, A. Li et al., "Dysregulation of cardiogenesis, cardiac conduction, and cell cycle in mice lacking miRNA-1-2," *Cell*, vol. 129, no. 2, pp. 303–317, 2007.

[30] E. Tzahor and K. D. Poss, "Cardiac regeneration strategies: staying young at heart," *Science*, vol. 356, no. 6342, pp. 1035–1039, 2017.

[31] M. Ponnusamy, P. F. Li, and K. Wang, "Understanding cardiomyocyte proliferation: an insight into cell cycle activity," *Cellular and Molecular Life Sciences*, vol. 74, no. 6, pp. 1019–1034, 2017.

[32] K. B. Pasumarthi and L. J. Field, "Cardiomyocyte cell cycle regulation," *Circulation Research*, vol. 90, no. 10, pp. 1044–1054, 2002.

[33] T. Scholzen and J. Gerdes, "The Ki-67 protein: from the known and the unknown," *Journal of Cellular Physiology*, vol. 182, no. 3, pp. 311–322, 2000.

[34] F. Beigi, J. Schmeckpeper, P. Pow-Anpongkul et al., "*C3orf58*, a novel paracrine protein, stimulates cardiomyocyte cell-cycle progression through the PI3K–AKT–CDK7 pathway," *Circulation Research*, vol. 113, no. 4, pp. 372–380, 2013.

[35] X. Sun, Q. Han, H. Luo et al., "Profiling analysis of long noncoding RNAs in early postnatal mouse hearts," *Scientific Reports*, vol. 7, article 43485, 2017.

[36] K. See, W. L. W. Tan, E. H. Lim et al., "Single cardiomyocyte nuclear transcriptomes reveal a lincRNA-regulated de-differentiation and cell cycle stress-response in vivo," *Nature Communications*, vol. 8, no. 1, p. 225, 2017.

Hindawi
Stem Cells International
Volume 2017, Article ID 9495739, 11 pages
https://doi.org/10.1155/2017/9495739

Research Article

Microarray Analysis Reveals a Potential Role of lncRNA Expression in 3,4-Benzopyrene/Angiotensin II-Activated Macrophage in Abdominal Aortic Aneurysm

Yingying Zhou,[1] Jiaoni Wang,[2] Yangjing Xue,[2] Aili Fang,[2] Shaoze Wu,[2] Kaiyu Huang,[2] Luyuan Tao,[2] Jie Wang,[2] Yigen Shen,[2] Jinsheng Wang,[2] Lulu Pan,[3] Lei Li,[2] and Kangting Ji[2]

[1]*Department of Endocrinology, The Second Affiliated Hospital and Yuying Children's Hospital of Wenzhou Medical University, Wenzhou, Zhejiang, China*
[2]*Department of Cardiology, The Second Affiliated Hospital and Yuying Children's Hospital of Wenzhou Medical University, Wenzhou, Zhejiang, China*
[3]*Children's Heart Center, The Second Affiliated Hospital and Yuying Children's Hospital, Institute of Cardiovascular Development and Translational Medicine, Wenzhou Medical University, Wenzhou, Zhejiang, China*

Correspondence should be addressed to Lei Li; leilii@uw.edu and Kangting Ji; jikt@wzmc.edu.cn

Received 15 May 2017; Revised 5 July 2017; Accepted 14 August 2017; Published 18 October 2017

Academic Editor: Yaoliang Tang

Abdominal aortic aneurysm (AAA) is a fatal disease, and exposure to 3,4-benzopyrene (Bap) is closely related to the development of AAA. We have found that Bap could impair the biological function of endothelial progenitor cells (EPCs), which are associated with the occurrence of AAA. We have also demonstrated that macrophage activation plays a key role in Bap-induced AAA, but the mechanism is unknown. Here, we used a mouse lncRNA array to investigate the expression signatures of lncRNAs and mRNAs in Bap-activated macrophage. A total of 457 lncRNAs and 219 mRNAs were found to be differentially expressed. The function of differential mRNAs was determined by pathway and Gene Ontology analysis. Eight pathways associated with inflammation were upregulated, and seven pathways including cell apoptosis were downregulated. It was worth noting that AGE-RAGE pathway, which was involved in Bap-induced EPC dysfunction, was significantly upregulated in Bap-activated macrophage and may contribute to AAA formation. Thus, lncRNAs may exert a key role in activated macrophages and intervene the core lncRNAs and may inhibit the occurrence of a series of cascade reactions in the macrophages, which may provide potential targets for AAA caused by smoking.

1. Introduction

Abdominal aortic aneurysm, generally defined as the remodeling and expansion of abdominal aorta with an arterial diameter ≥ 30 mm or a 50% increased arterial diameter, is the most common aortic disease on clinic. Because of the high pressure within the aorta, any rupture can quickly lead to death. As reported, an estimated 1% to 3% of men aged 65 to 85 years died of AAA in developed countries [1]. The pathologic mechanism of AAA is still unclear. Increasing evidence has indicated that 3,4-benzopyrene (Bap), an important component of cigarette smoke and automobile exhaust, is one of the leading risk factors of AAA [1, 2]. Our previous study has demonstrated the detrimental effects of Bap on the function of endothelial progenitor cells (EPCs), which are a population of circulating stem cells and closely correlated to endothelial damage and vascular injury [3]. It has been reported that endothelial injury is associated with the occurrence of AAA and the recovery of endothelial integrity correlates with the progression of AAA. Circulating EPCs are reduced, and the function of late EPCs is impaired in AAA patients [4, 5]. Thus, we hypothesize that Bap may play a key role in the development of AAA. Further, we constructed an Angiotensin II- (Ang II-) induced murine AAA model and discovered that Bap could cause pathological change of artery wall similar to AAA and promote the

development of AAA [6]. Recently, some studies revealed that macrophage activation and infiltration played a key role in AAA formation [7, 8]. Both the tissue samples of the patients with AAA and the biopsies from AAA model mice clearly exhibited that the infiltration and accumulation of macrophage in the artery wall participate in the whole process of AAA development, from the beginning to expansion and to eventually rupture [9, 10]. We have also confirmed the increment of macrophage infiltration, activation of NF-κB, and expression of MMP-2, MMP-9, and MMP-12 in Ang II/Bap-induced AAA model previously [6]. However, the underlying molecular regulatory mechanism in Bap-induced macrophage activation in AAA, and how to alleviate them, remains to be fully elucidated.

Long noncoding RNA (lncRNA) is defined as transcript noncoding RNA with more than 200 nucleotides. With the wide application of whole length cDNA cloning sequence analysis and genome chip technology, tens or even hundreds of thousands of lncRNAs have been counted. Though once considered as "junk" transcripts of the genome, lncRNA now has been proven to be important in the gene expression and function regulation and actively participates in many pathological processes. Efforts have been made to study the relationship between the lncRNA expression and AAA. Holdt et al. have demonstrated a close association of lncRNA CDKN2BAS (or ANRIL) in chr19q13 with atherosclerosis [11]. Wang et al. indicated that lncRNA-HIF 1 alpha-antisense RNA could interact with mRNA BRG1 in vascular smooth muscle cells in vitro, which may contribute to the pathogenesis of thoracic aortic aneurysms [12]. Recently, Yang et al. identified 3688 lncRNAs and 3007 mRNAs differently expressed between AAA and normal abdominal aortic tissues by microarray. And the lncRNA-mRNA targeting relationships were further identified using computational analysis [13]. However, the functional role of lncRNAs in activated macrophages in AAA is largely unknown.

To systematically study the role of lncRNAs in activated macrophages in AAA, we built gene expression profiles of Bap-activated macrophages and the normal control macrophages using lncRNA and mRNA gene expression microarrays. Nine differentially expressed lncRNAs identified were further confirmed via qRT-PCR. Gene Ontology (GO) and the Kyoto Encyclopedia of Genes and Genomes (KEGG) databases were used to clarify their biological functions.

2. Materials and Method

2.1. Experimental Animals. Male C57/B6J mice, weighing 35 to 40 g and aging 8 to 10 months (Weitong Lihua Experimental Animal Technology Co. Ltd., Beijing, China), were fed in a specific pathogen-free environment. Mice were divided into four groups, with 12 mice in each. Mice in the control group received a weekly intraperitoneal injection of medium-chain triglycerides (Aabrafaclipophilewl 1349; Gattefosse Co., Lyon, France). Mice in the Ang II group received a daily Ang II (Sigma-Aldrich Co., St. Louis, MO) infusion (0.72 mg/kg) via a subcutaneous osmotic minipump (Alzet Osmotic Pump, Model 2004), in addition to medium-chain triglycerides. Mice in the Bap group received a weekly intraperitoneal Bap (Sigma-Aldrich Co.) injection (10 mg/kg). Mice in the Ang II/Bap group received Ang II (0.72 mg/kg) and Bap (10 mg/kg). Bap was dissolved in medium-chain triglycerides (2 mg/ml). After 6 weeks, mice were euthanized using urethane intraperitoneally.

2.2. Aortic Tissue Collection and IF and IHC Staining. After the mice were euthanized, the abdominal and thoracic cavities were exposed, and the aorta was washed with PBS and 4% paraformaldehyde through the left ventricle in turn. The abdominal aorta tissue was carefully separated and fixed in 4% paraformaldehyde for immunohistochemistry. The primary antibodies used in IF and IHC staining were CD68 (ab53444), MMP-9 (ab38898), and TNF-α (ab6671). The nuclei were stained with DAPI or DAB. Visualization was performed with a fluorescent microscope.

2.3. Macrophage Function

2.3.1. Isolation of Murine Peritoneal Macrophage. Three days before the experiment, 3% sodium thioglycolate was injected intraperitoneally. The mice were sacrificed and placed in 75% ethanol solution 2-3 minutes. After injecting 5 ml HANKS into the abdominal cavity, the abdominal wall was gently squeezed with a hand for more than 20 times and then sucked out the lavage fluid. The suspension was washed with HANKS for 3 times before being resuspended and then was cultured in 37°C, 5% CO_2 incubator for 3-4 hours. After removal of nonadherent cells with PBS, the adherent cells were then used for the experiment. The mouse macrophage cell line RAW264.7 was purchased from American Type Culture Collection. Cells were cultured in Dulbecco's Modified Eagle's Medium containing 10% fetal bovine serum. When the cells were grown to 90% confluence, subcultivation was performed. DMSO as a solvent for Bap and Ang II, its final concentration in the culture medium did not exceed 0.1% (v/v). Cells were randomly divided into 5 groups. In the control group, cells were untreated. In other 4 groups, cells were treated with DMSO or 10 μmol/l Ang II or 20 μmol/l Bap or Ang II plus Bap. Cells were cultured for 2 h and 24 h and then collected for RNA and protein extraction, respectively.

2.4. RNA Extraction and Quality Control. Total RNA was extracted from macrophage cells with Trizol reagent (Invitrogen Life Technologies, Carlsbad, CA, USA). After being quantified and qualified, the isolated RNA of high purity was subjected to microarray and quantitative real-time polymerase chain reaction.

2.5. Microarray Analysis. An arraystar mouse lncRNA microarray v3.0, which could detect 35,923 lncRNAs and 24,881 protein-coding transcripts, was used to analyze the RNA samples. RNA labeling and array hybridization were conducted as described [14]. The expression levels of lncRNAs and mRNAs were compared between the Bap sample and the DMSO sample. Genes having a fold change > 2 and an adjusted $p < 0.05$ were considered as differentially expressed.

Table 1: Primer sequences for lncRNAs.

Sequence name	Gene symbol	Forward (5′-3′)	Reverse (5′-3′)
NR_045727	B230209E15Rik	TCCACTGAACCACCAACCAAA	CCATCTCCGCAAACTGCCTAT
NR_045799	1700123O21Rik	CCTCACTTTAGAGTCCTGGGTA	TTGAAGATTTGCTGTCTGCTG
NR_040734	4930429F24Rik	AGAAGAGGCGTAGGCGTCATA	AGACTTCTGGAGCCGTCAGGT
NR_045865	9230009I02Rik	GGGTTAAGAATCGCATGAGTA	CCAAGAAAACAAGGCAAGAGT
AK089739	AK089739	GGGTCTAACATTTACCAAGATGAAG	TGGAATATCCCCAGAGTCCTA
NR_027827	Chd3os	TCTTTTCCCCAGTATTGCTAC	GTTGACTCCCTGCTTATGATTG
NR_015506	4833418N02Rik	GCACTCAGGATGCTTGGTCTT	CCACTTGCTGCTACTTTATTTTGG
NR_015547	1700009J07Rik	AGGGCATTTTAGTTGGTTCTTACAG	GCAAGCATGGATTCTAGCGTT
NR_045314	9830166K06Rik	TCCCACAGGGTTCAGTTCTCA	GGTCTACATTATTACATCTGGCTCA

2.6. GO and KEGG Pathway Analyses. GO and KEGG pathway analyses were performed by KangChen Bio-tech Co. Ltd. (Shanghai, China), in order to analyze the differentially expressed genes systematically and enrich significant GO terms and KEGG pathways ($p < 0.05$) [15]. The significance of the p value was evaluated by the false discovery rate (FDR), and an FDR < 0.05 was recommended.

2.7. qRT-PCR Validation Assay. The reliability of the microarray data was validated by comparing the results of microarray and qPCR. Nine randomly selected lncRNAs and their expression levels were further evaluated using the SYBR Green method in a fluorescence real-time PCR (Biosystems, C1000, USA) in triplicate. Primers were designed and synthesized (Table 1). The gene expression levels were normalized to the housekeeping gene β-actin. The relative expression of the target genes was calculated as $2^{-\Delta\Delta Ct}$.

2.8. Statistical Analysis. Data represented the means ± SD. Student's t-test was used for a single comparison of 2 groups. One-way analysis of variance followed by the Bonferroni t-test was conducted for a comparison of multiple groups. Differences were considered statistically significant at $^{*}p < 0.05$ and $^{**}p < 0.01$.

3. Results

3.1. Bap Exacerbates Macrophage Infiltration, MMP-9, and TNF-α Expression in the Aortic Wall of Ang II-Infused Mice. Immunofluorescence showed prominent macrophage infiltration in abdominal aortic tissues in the Ang II group, which was further promoted by Bap (Figure 1(a)). Because Bap may regulate MMP activity and proinflammatory cytokines, we examined MMP-9 and TNF-α expression in abdominal aortic tissue by immunostaining. Ang II infusion increased MMP-9 and TNF-α expression when compared with the control group, which was further increased by Bap (Figures 1(b), 1(c), 1(d), and 1(e) for quantitative analysis of the result).

3.2. Bap Promotes MMP-9 and TNF-α Secretion in Macrophages In Vitro. Chronic inflammation and extracellular matrix degradation have been considered instigating mechanisms underlying AAA. TNF-α and MMP-9 are particularly important in this process. Hence, we examined the effect of Bap on the secretion of TNF-α and on the expression and activity of MMP-9 in macrophages. As shown in Figure 2, Bap treatment caused significant increment in the amount of MMP-9 and TNF-α protein, in both peritoneal macrophages and RAW264.7 cells ($p < 0.05$). Consistently, gelatin zymography demonstrated higher MMP-9 activity in the Ang II group, which was further promoted by Bap (Figure 2(e)).

3.3. Microarray Hybridization Data. Arraystar mouse lncRNA microarray v3.0 is designed for the global profiling of mouse lncRNAs and protein-coding transcripts. The heat map of the hierarchical clustering results was performed to show the distinguishable lncRNA and mRNA expression profiling between the two groups (Figures 3(a) and 3(b)). The results of scatterplot showed that the distribution and expression variation of the log 2 ratios of lncRNAs and mRNAs between the two groups were nearly the same (Figures 3(c) and 3(d)).

3.4. Differentially Expressed lncRNAs and mRNAs. We found that 457 detected lncRNAs demonstrated >2-fold differential expression in Bap-activated macrophage when compared to the control group (macrophage cultured with DMSO), with 249 lncRNAs showing upregulation and 208 lncRNAs showing downregulation (Table 2). At the same time, 219 mRNAs displayed beyond a 2-fold differential expression in Bap-induced macrophage, and 119 mRNAs were upregulated while 100 mRNAs were downregulated. The top ten upregulated and top ten downregulated lncRNAs and mRNAs are listed in Table 3.

3.5. GO and KEGG Analyses of Differentially Expressed mRNAs. GO analysis, including 3 structured networks: biological processes, cellular components, and molecular function, was applied to analyze the main function of the closest coding genes according to the GO database which provided the key functional classifications for the National Center for Biotechnology Information (NCBI). In our survey, GO analysis revealed the functions of differentially expressed (both upregulated and downregulated) mRNA in abnormally activated macrophages induced by Bap. The most enriched GO terms (top ten) are shown in Figure 4. Pathway analysis showed that the upregulated mRNAs participated in TNF-α

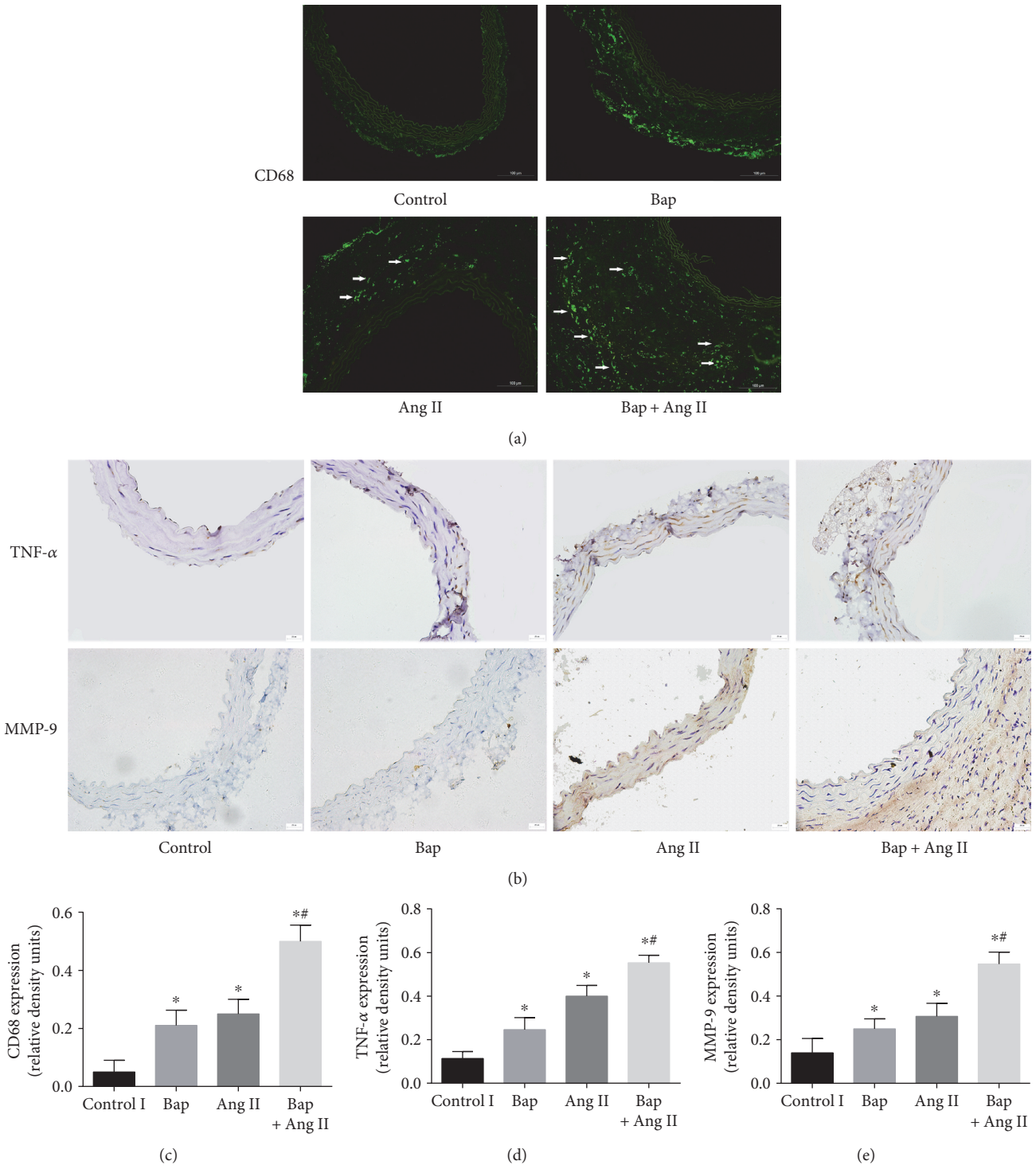

Figure 1: Ang II-induced macrophage infiltration and expression of MMP-9 and TNF-α were prominently increased in mice receiving coadministration of Bap. Abdominal aortic tissues were harvested, and transversal sections were prepared. (a) Representative photomicrographs of $CD68^+$ cell staining in suprarenal aortic sections: immunoreactivity was visualized using an Alexa Fluor 488 secondary antibody (green). (b) Representative immunohistochemistry staining of TNF-α and MMP-9 in the abdominal aorta from control animals and animals treated with Ang II, Bap, or Ang II/Bap. (c–e) For quantitative analysis of the result. $^*p < 0.05$ versus control; $^\#p < 0.05$ versus Bap or Ang II group.

signal pathway, AGE-RAGE signaling pathway, and so forth. On the other hand, the involved downregulated mRNAs refer to p53 signaling pathway, tryptophan metabolism, and so forth (Figure 5).

3.6. Validation of the Expression Levels of the lncRNAs Using qRT-PCR. Nine lncRNAs (NR_045727, NR_045799, NR_040734, NR_045865, AK089739, NR_027827, NR_015506, NR_015547, and NR_045314) were selected to validate the

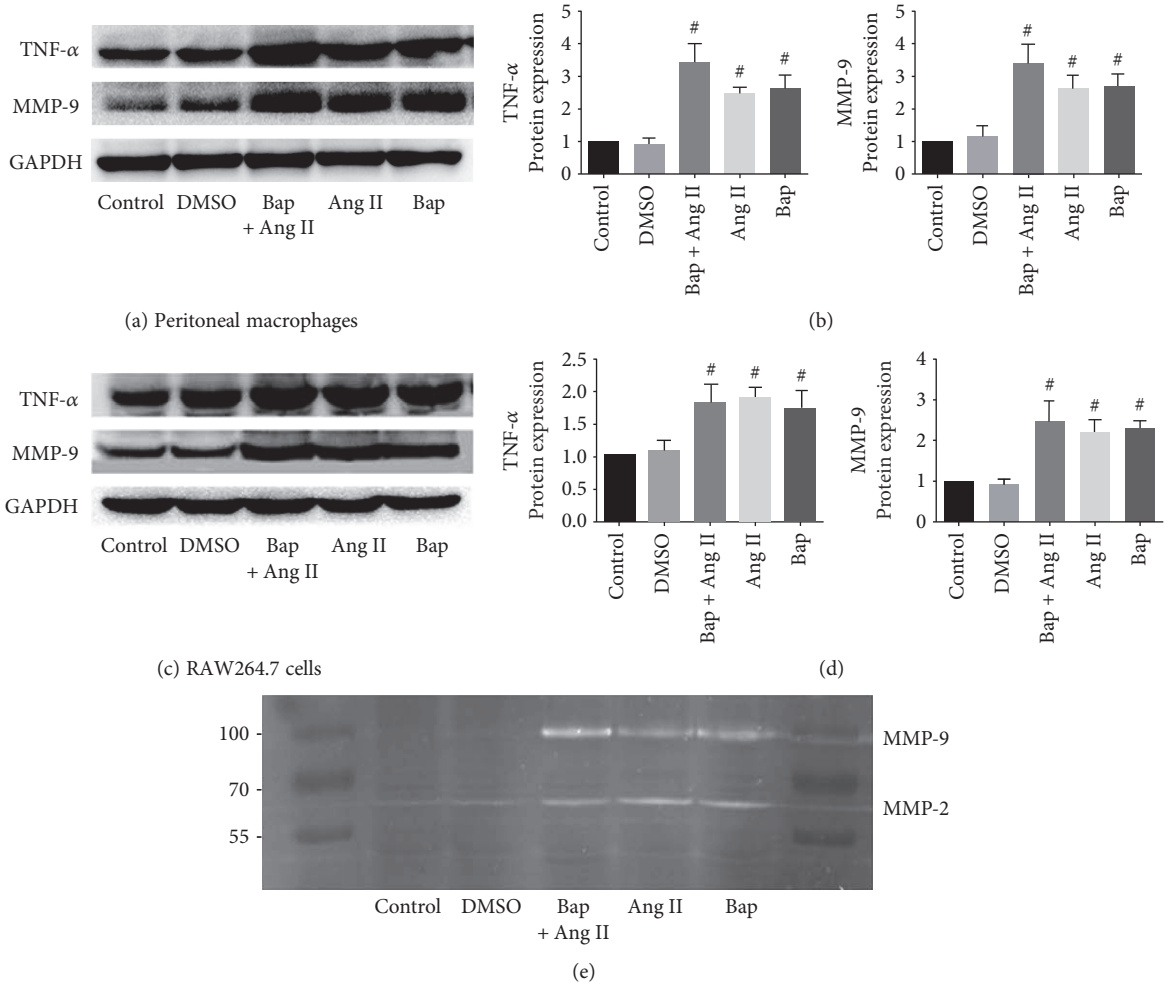

Figure 2: Bap promotes the secretion of TNF-α and increases the expression and activity of MMP-9 in macrophages in vitro. (a, b) Representative Western blot analysis of TNF-α and MMP-9 in peritoneal macrophages (a) and the quantitative analysis of the result (b). (c, d) Representative Western blot analysis of TNF-α and MMP-9 in RAW264.7 cells (c) and the quantitative analysis of the result (d). $^{\#}p < 0.05$ versus DMSO group. (e) Gelatin zymography of MMP-9 in RAW264.7 cells.

microarray consistency by using qPCR. The results demonstrated that NR_045727, NR_045799, NR_040734, and NR_045865 were significantly upregulated in both gene chip and the qRT-PCR (Figure 6).

4. Discussion

AAA is a chronic but often fatal vascular disease that is primarily associated with several risk factors including advanced age and smoking [1]. There is lack of effective therapeutic drugs to slow down the development of AAA since the molecular mechanism of AAA is still unclear. Basic research on this disease is urgently needed. Macrophage infiltration into the aortic wall is a hallmark of AAA pathology; thus, targeting vascular inflammation mediated by macrophages may be a potential therapeutic approach for aneurysm pathologies. Our previous study demonstrated that Bap contributed to the pathogenesis of AAA, and indeed, it promoted the formation of AAA in Ang II-treated mice [6]. In the current study, we confirmed that Bap promoted the infiltration of macrophages in the arterial wall of AAA mice in vivo and activates peritoneal macrophages and RAW264.7 cells in vitro. However, how Bap activates macrophages and ultimately promotes the development of AAA is unknown. In order to figure out the probable mechanism, we further carried out a mouse lncRNA profile and identified the potential role of lncRNA expression in activated macrophage in abdominal aortic aneurysm.

lncRNA is a type of noncoding RNAs (ncRNAs). According to the human genome project, the number of total protein-encoding genes in human accounts for <2% of the entire human genome sequence, and 90% of the rest noncoding sequences are transcribed, producing a huge number of ncRNAs [16]. Due to the rapid development of high-throughput RNA sequencing technology, a vast number of new ncRNAs have been discovered. The most well-known ncRNAs are microRNAs (miRNAs), which are ~21–23 nt long and have been proven to play a key role in a variety of biological and pathological processes [17, 18]. Numerous studies have already shown the involvement of microRNAs in AAA development, including miR-195, miR-21, miR-29b, and miR-24 [19–22]. lncRNAs account for 80% of

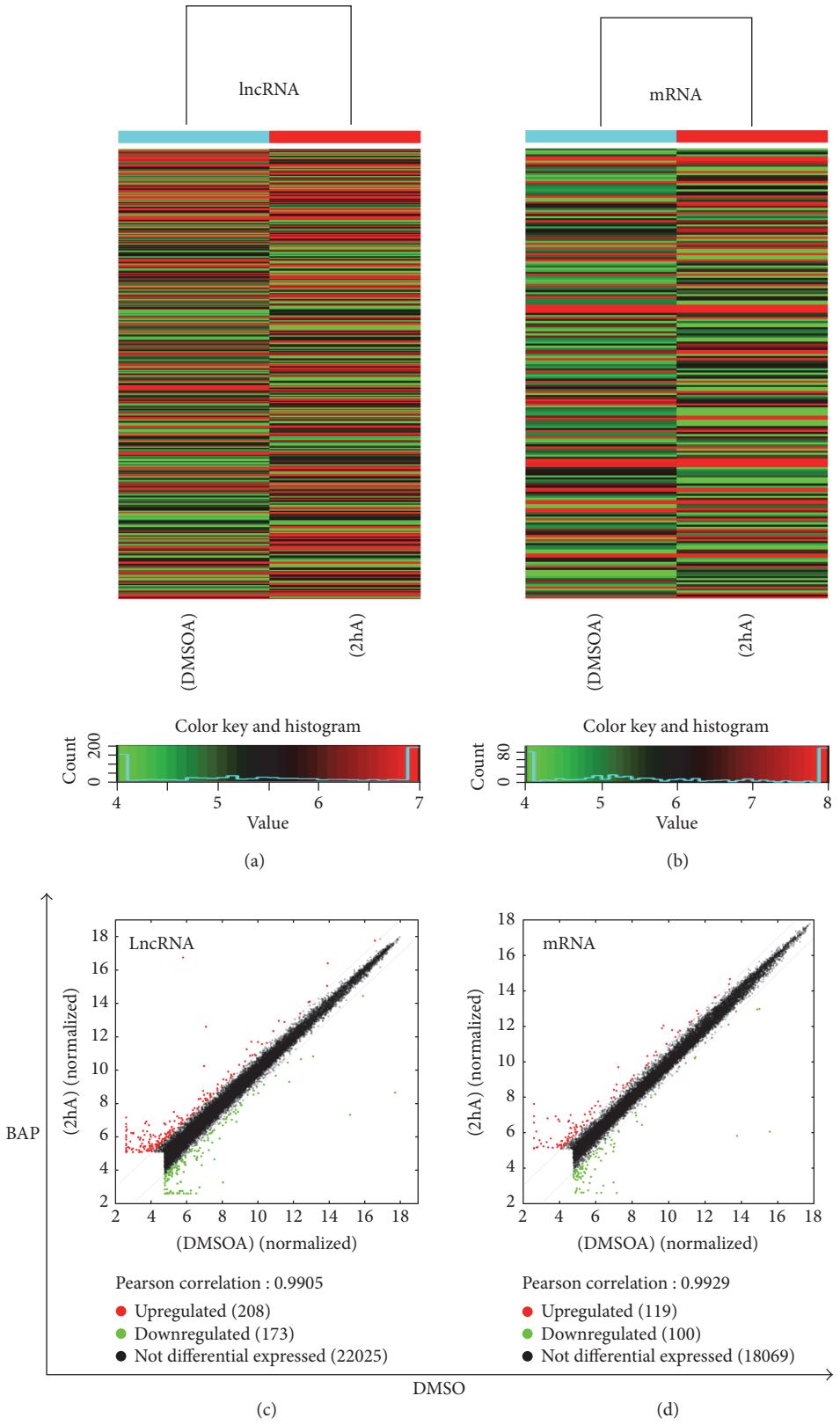

Figure 3: lncRNA and mRNA expression profile comparison between the Bap-activated macrophages and the control group. (a) The hierarchical clustering of all target value lncRNAs and (b) mRNAs. (c) The scatterplot was used for assessing the lncRNA and (d) mRNA expression variation between the Bap-activated cells and the control group. The green lines are fold change lines (the default fold change value given is 2.0). The lncRNAs above the top green line and below the bottom green line indicated >2.0-fold change in expression of lncRNAs between the 2 compared samples. "Red" denotes high relative expression levels, and "blue" denotes low relative expression levels.

Table 2: Number of differentially expressed lncRNAs.

lncRNAs	FC 2–5	FC ≥ 5	FC ≥ 10	Total
Up	211	27	11	249
Down	166	33	9	208

ncRNAs [16]. Previous studies reported that many lncRNAs were involved in cardiovascular disease. Ming et al. found that nicotinamide phosphoribosyltransferase (NAMPT) inhibited EPC senescence through a sirtuin 1 (SIRT1) antisense long noncoding RNA (AS lncRNA)/miR-22/SIRT1 pathway and promoted EPC proliferation and migration [23]. Wu et al. identified lncRNA-p21 as a key regulator of cell proliferation and apoptosis during atherosclerosis through p53 pathway [24]. Viereck and Thum proposed that lncRNAs were involved in the pathological cardiac remodeling, acting as noncoding epigenetic regulators [25]. However, the role of lncRNAs in AAA is less understood. It is a requisite to determine the lncRNA profile about AAA and find key lncRNAs that regulate the pathology of AAA. Therefore, we utilized high-throughput microarray lncRNA screening in this study and discovered differentially expressed lncRNAs in Bap-activated macrophages.

Comparing lncRNA expression in Bap-activated macrophages and the control group to explore features in inflammation of aneurysm disease is a unique approach presented here for the very first time, and the identified pathways added significantly findings to further research in the field. Several significantly changed lncRNAs in our profile were predicted to be closely related to macrophage activation. lncRNA 1700123O21Rik, a 675 nt lncRNA, is located on chromosome 16. Rbfox1 (RNA-binding protein fox-1) is the associated gene of lncRNA 1700123O21Rik. He et al. identified that rare, exonic variants in Rbfox1 had protective effects on BP traits, which could be important in searching new drugs for cardiovascular disease [26]. Hence, Rbfox1 is expressed in multiple tissues that may relate to blood pressure, and the identification of these rare coding variants will facilitate precision medicine in treating cardiovascular disease. In addition, Gao et al. revealed that Rbfox1-dependent RNA splicing, in particular, an isoform switch of MEF2 gene splice variants, was a regulatory circuit in cardiac transcriptional reprogramming, with a significant effect on the pathogenesis of heart failure [27]. We postulated that the expression of Rbfox1 may be involved in inflammation, while the mechanism underlying how this gene influence inflammation needs to be further studied. Another upregulated lncRNA NR_040734, with a FC of 2.4508004, was associated with TMEM30A, which was also known as CDC50A. CDC50A proteins are β-subunits for P4-ATPases, which upon heterodimerization form a functional phospholipid translocation complex. Emerging evidence in mouse models and men links mutations in P4-ATPase genes with human disease. Kato et al. indicated that the phospholipid flippase complex of ATP8A1 and CDC50A played a major role in cell migration and suggested that the flippase-mediated translocation of phosphatidylethanolamine at the plasma membrane is involved in the formation of membrane ruffles to promote cell migration [28]. It may be related to macrophage infiltration to the aortic wall. Generally, lncRNAs mainly affect their surrounding associated genes. lncRNA-Angptl2, of which the associated gene was angiopoietin-like 2 (Angptl2), was

Table 3: Top 10 upregulated and downregulated lncRNAs and mRNAs in activated macrophage.

Sequence name	Gene symbol	FC
Top 10 upregulated lncRNAs		
NR_040373	Asb17os	1965.641627
ENSMUST00000135495	Ccdc92	45.4580975
uc007cfx.1	AK144617	23.389015
NR_045727	B230209E15Rik	17.9220629
uc007oby.1	AK046721	15.996457
uc007oby.1	AK046721	15.996457
ENSMUST00000173219	Sox2ot	13.8832295
ENSMUST00000145380	Ckmt1	13.4032113
AK083558	AK083558	11.2153303
mouselincRNA1093	mouselincRNA1093	10.2874934
Top 10 upregulated mRNAs		
NM_015800	Crim1	32.4476525
NM_134193	Vmn1r232	20.0515965
NM_023135	Sult1e1	15.5459966
NM_146016	Eml6	11.060142
NM_001105061	Gm9268	10.1305416
NM_001001177	BC051142	8.8110002
NM_182745	1700028K03Rik	8.5059219
NM_030739	Vmn1r58	7.0052416
NM_010157	Esr2	6.3562933
NM_010104	Edn1	6.2573404
Top 10 upregulated lncRNAs		
NR_040395	D430036J16Rik	536.89308
NR_038179	1700042G15Rik	233.8747012
ENSMUST00000120698	Gm13079	27.4479976
ENSMUST00000177106	Gm20614	15.4528389
ENSMUST00000181660	2610017I09Rik	13.5374124
ENSMUST00000176851	Idi1	12.2999829
uc007gkp.1	AK054042	11.1609776
ENSMUST00000140447	1810010H24Rik	11.0132014
ENSMUST00000146208	Gm15270	10.5662387
AK033575	AK033575	9.4937891
Top 10 downregulated mRNAs		
NM_001128609	DEDD	727.5505604
NM_001276250	Cp	245.8931099
NM_001136227	Rtkn	23.4801529
NM_026100	Tctex1d1	13.7970765
NM_029751	Rpl18a	12.9072764
NM_029292	1700008F21Rik	10.9811558
NM_181682	Dsg1b	10.6274348
NM_146689	Olfr1459	7.1381074
NM_173751	Ilvbl	6.4870461
NM_177915	Igsf1	5.9488207

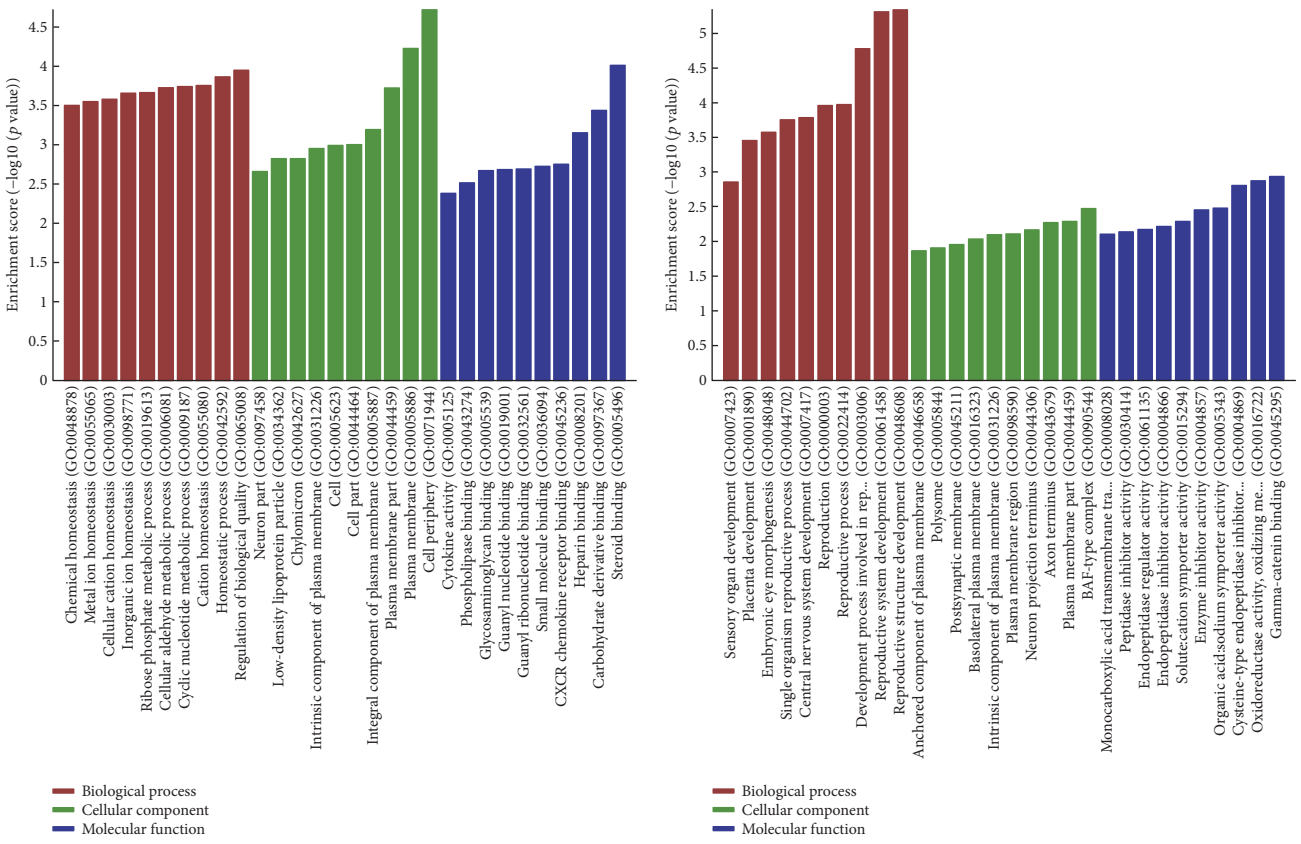

(a) Upregulated GO (b) Downregulated GO

Figure 4: Gene Ontology (GO) analysis of functional classification of the differentially expressed genes. The GO categories cover three domains: biological process, molecular function, and cellular component. (a) The upregulated GO analysis. (b) The downregulated GO analysis. The p value denotes the significance of GO term enrichment in the differentially expressed mRNA list. The lower the p value is, the more significant the GO term is (p value ≤ 0.05 is recommended).

upregulated in Bap-activated macrophage. Horio et al. found that endothelial cell-derived Angptl2 accelerates vascular inflammation by activating proinflammatory signaling and increasing macrophage infiltration, leading to endothelial dysfunction and atherosclerosis progression [29]. Richardson et al. concluded that Angptl2 positively regulates endothelial colony-forming cell (ECFC) formation in vitro through its effects on migration and in part by activating JNK and increasing MT1-MMP expression [30]. Therefore, we hypothesize that lncRNA-Angptl2 may play a key role in the formation of AAA, through acting on its associated gene Angptl2 and inducing dysfunction of EPCs and macrophages.

Simultaneously, a total of 219 mRNAs, in which119 mRNAs were upregulated and 100 mRNAs were downregulated, were identified as differentially expressed transcripts between the Bap-activated macrophages and the control group. Expression of Crim1 was the most greatly up-altered while DEDD was the most downregulated gene in abnormal activated macrophages induced by Bap. Crim1 has been reported to be necessary for coronary vascular endothelial cell development and homeostasis. Lack of Crim1 in vivo will lead to the malformation of coronary vasculature and the reduced number of endothelial cells [31]. DEDD, identified as death effector domain containing, has been reported to influence mRNA decay and promote cell apoptosis and inhibit cell proliferation [32, 33]. Besides, some of the differentially expressed mRNAs detected in this microarray were associated with the function of stem cells. Among them, IL1R1 and α-tocopherol transfer protein have been reported to affect the pathology of AAA. Farhang et al. have demonstrated that repression of TNFR1 and IL1R1 could inhibit NF-κB activation, promote extracellular matrix (ECM) deposition, and allow for maintenance of immunomodulatory properties in inflammatory conditions, which was similar to the pathology of AAA [34]. IL1R1 is a receptor for interleukin beta (IL-1β). IL-1β, an important inflammation mediator, has been shown to promote EPC proliferation, migration, and adhesion. Zhang et al. suggested that EPCs could exert self-enhancement effects by interacting with monocytes and that EPCs might also modulate inflammatory reactions by regulating IL-1β expression in monocytes. IL-1β has been reported to play a protective role in vascular repair under inflammatory environments [35]. Our chip data showed IL1R1 downregulation in Bap-activated macrophages, which may lead to a low combination of IL-1β to IL1 receptor and result in an increased inflammatory response. SEC14L2, an α-tocopherol transfer protein (Ttpa), was expressed in hepatocyte-like cells (HLCs), starting from human mesenchymal stem cells (hMSC) through induced pluripotent stem (iPS) cell reprogramming. Sa-

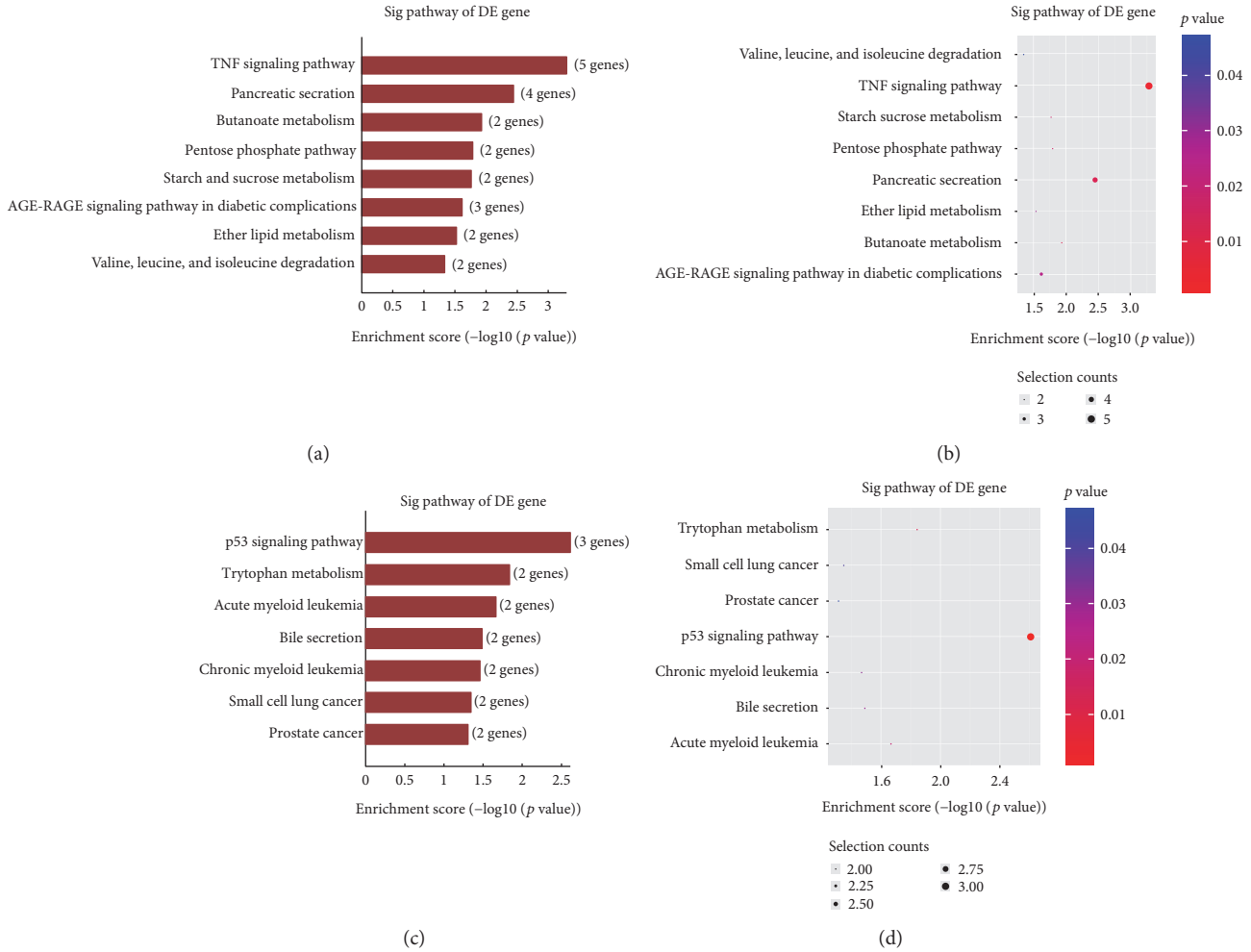

Figure 5: Pathway enrichment analysis. (a, b) The upregulated gene pathway. (c, d) The downregulated gene pathway. The figure shows the top 10 significant pathways of upregulated and downregulated genes. The p value (Fisher p value) denotes the significance of the pathway correlated to the conditions. The lower the p value, the more significant the pathway (the recommended p value cut-off is 0.05).

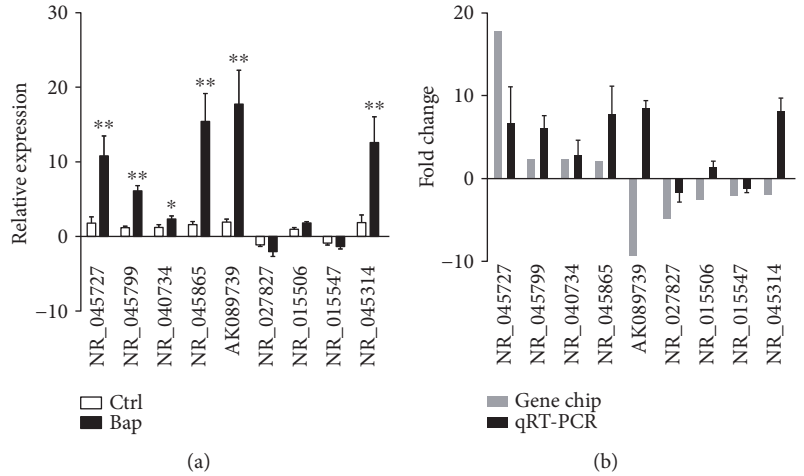

Figure 6: qRT-PCR validation of differential expressions of lncRNAs. (a) Six lncRNAs confirmed by qRT-PCR show to have significant changes between Bap-activated macrophage and the control group. Data are expressed as the mean ± standard deviation (SD) of three independent experiments ($^{*}p < 0.05$ and $^{**}p < 0.01$). (b) qRT-PCR patterns of six lncRNAs are completely consistent with those of microarray data. The y-axis represents fold change.

Ngiamsuntorn et al. indicated that, together with the expression of SEC14L2 and the addition of α-tocopherol, the expressions of inflammatory cytokines were upregulated during the infection that mimicked the inflammatory process [36].

Studies about the function of lncRNAs are difficult to carry out, for most of the lncRNAs are not determined, and there is no existing database that could be used to find their functional annotations. To solve this problem, we have tried to construct a correlation between mRNA and lncRNA. First, by GO annotation and pathway analysis, we made a systemic analysis for the functions of the differentially expressed mRNAs. TNF-α signaling pathway was mostly enriched in the upregulated genes, and p53 signaling pathway was mostly enriched in the downregulated genes in Bap-activated macrophages. Our study and previous other studies found that TNF-α signaling pathway played a key role in AAA development [37, 38]. TNF-α signaling pathway is also closely related to inflammation and oxidative stress. A recent study demonstrated that TNF-α could aggravate inflammatory reactions and oxidative damage in bone marrow-derived mesenchymal stem cells during degenerative bone disease, by upregulating miR-705 and inhibiting FoxO1 [39]. Another high-expression signal pathway involved in the activation of macrophages by Bap was AGE-RAGE signaling pathway, of which the role in the progression of AAA has been reported by Zhang et al. Blocking RAGE in a mouse aneurysm model significantly inhibited the formation of aneurysms and prevented MMP-9 expression in macrophages [40]. This suggests us that lncRNAs acting on the interaction between AGE and RAGE may ultimately lead to novel therapies to treat and prevent AAA progression. Our previous study revealed that RAGE was involved in Bap-induced EPC dysfunction. Bap significantly increased expression of RAGE protein while Astragaloside IV pretreat downregulated the expression of RAGE [6, 41]. It is well known that p53 plays an important role in the pathogenesis of apoptosis [24, 42]. Therefore, we speculate that lncRNAs regulate the activated macrophages in AAA through upregulating TNF-α signaling pathway and AGE-RAGE pathway to promote cell inflammatory progression and downregulating p53 signal pathway to inhibit cell apoptosis. Moreover, we need to establish the contact of lncRNA and mRNA in further study. Generally, there are two ways: one way is to use the physical adjacency of the mRNA and lncRNA, and the other is to use the relationship of coexpression pattern among genes.

In summary, we confirmed the function of macrophages in Bap-induced AAA in vivo and in vitro and discovered for the first time a profile of lncRNAs differentially expressed in Bap-activated macrophages in AAA. Our study on lncRNAs has greatly expanded the field of gene research in AAA. Although the mechanisms of the discovered lncRNAs in Bap-activated macrophages remain to be elucidated, we hope that our novel discovery will lead to more studies that will determine its function.

Conflicts of Interest

The authors declare that they have no competing interests.

Authors' Contributions

Yingying Zhou and Jiaoni Wang contributed equally to this work.

Acknowledgments

This work was supported by the National Natural Science Foundation of China (no. 81573185), the Scientific Research Foundation of Science and Technology Department of Zhejiang Province (no. 2014C33163), the Zhejiang Provincial and Health Science and Technology plan (2016KYB197), the Scientific Research Foundation of Wenzhou (Y20150015), and the Scientific Research Foundation of Science and Technology Department of Wenzhou City (nos. Y20130167 and H20140003).

References

[1] R. Erbel, V. Aboyans, C. Boileau et al., "Corrigendum to: 2014 ESC guidelines on the diagnosis and treatment of aortic diseases," *European Heart Journal*, vol. 36, p. 2779, 2015.

[2] M. P. Bergoeing, B. Arif, A. E. Hackmann, T. L. Ennis, R. W. Thompson, and J. A. Curci, "Cigarette smoking increases aortic dilatation without affecting matrix metalloproteinase-9 and -12 expression in a modified mouse model of aneurysm formation," *Journal of Vascular Surgery*, vol. 45, pp. 1217–1227, 2007.

[3] K. Ji, C. Xing, F. Jiang et al., "Benzo[a]pyrene induces oxidative stress and endothelial progenitor cell dysfunction via the activation of the NF-κB pathway," *International Journal of Molecular Medicine*, vol. 31, pp. 922–930, 2013.

[4] J. Dawson, J. Tooze, G. Cockerill, E. Choke, I. Loftus, and M. M. Thompson, "Endothelial progenitor cells and abdominal aortic neurysms," *Annals of the New York Academy of Sciences*, vol. 1085, pp. 327–330, 2006.

[5] S. H. Sung, T. C. Wu, J. S. Chen et al., "Reduced number and impaired function of circulating endothelial progenitor cells in patients with abdominal aortic aneurysm," *International Journal of Cardiology*, vol. 168, pp. 1070–1077, 2013.

[6] K. Ji, Y. Zhang, F. Jiang et al., "Exploration of the mechanisms by which 3,4-benzopyrene promotes angiotensin ii-induced abdominal aortic aneurysm formation in mice," *Journal of Vascular Surgery*, vol. 59, pp. 492–499, 2014.

[7] T. Saito, Y. Hasegawa, Y. Ishigaki et al., "Importance of endothelial NF-κB signalling in vascular remodelling and aortic aneurysm formation," *Cardiovascular Research*, vol. 97, pp. 106–114, 2013.

[8] M. A. Dale, M. K. Ruhlman, and B. T. Baxter, "Inflammatory cell phenotypes in AAAs: their role and potential as targets for therapy," *Arteriosclerosis, Thrombosis, and Vascular Biology*, vol. 35, pp. 1746–1755, 2015.

[9] J. Nischan, Z. Gatalica, M. Curtis, G. M. Lenk, G. Tromp, and H. Kuivaniemi, "Binding sites for ETS family of transcription factors dominate the promoter regions of differentially expressed genes in abdominal aortic aneurysms," *Circulation Cardiovascular Genetics*, vol. 2, pp. 565–572, 2009.

[10] T. Shang, Z. Liu, and C. J. Liu, "Antioxidant vitamin c attenuates experimental abdominal aortic aneurysm development in an elastase-induced rat model," *The Journal of Surgical Research*, vol. 188, pp. 316–325, 2014.

[11] L. M. Holdt, A. Stahringer, K. Sass et al., "Circular non-coding RNA ANRIL modulates ribosomal rna maturation and atherosclerosis in humans," *Nature Communications*, vol. 7, article 12429, 2016.

[12] S. Wang, X. Zhang, Y. Yuan et al., "BRG1 expression is increased in thoracic aortic aneurysms and regulates proliferation and apoptosis of vascular smooth muscle cells through the long non-coding RNA HIF1A-AS1 *in vitro*," *European Journal of Cardio-Thoracic Surgery*, vol. 47, pp. 439–446, 2015.

[13] Y. G. Yang, M. X. Li, L. Kou et al., "Long noncoding RNA expression signatures of abdominal aortic aneurysm revealed by microarray," *Biomedical and Environmental Sciences*, vol. 29, pp. 713–723, 2016.

[14] Y. Zou, C. Li, F. Shu et al., "lncRNA expression signatures in periodontitis revealed by microarray: the potential role of lncRNAs in periodontitis pathogenesis," *Journal of Cellular Biochemistry*, vol. 116, pp. 640–647, 2015.

[15] B. Zheng, H. Liu, R. Wang et al., "Expression signatures of long non-coding RNAs in early brain injury following experimental subarachnoid hemorrhage," *Molecular Medicine Reports*, vol. 12, pp. 967–973, 2015.

[16] ENCODE Project Consortium, E. Birney, J. A. Stamatoyannopoulos et al., "Identification and analysis of functional elements in 1% of the human genome by the encode pilot project," *Nature*, vol. 447, pp. 799–816, 2007.

[17] J. Krol, I. Loedige, and W. Filipowicz, "The widespread regulation of microRNA biogenesis, function and decay," *Nature Reviews Genetics*, vol. 11, pp. 597–610, 2010.

[18] L. He and G. J. Hannon, "MicroRNAs: small RNAs with a big role in gene regulation," *Nature Reviews Genetics*, vol. 5, pp. 522–531, 2004.

[19] J. M. Spin and P. S. Tsao, "Battle of the bulge: miR-195 versus miR-29b in aortic aneurysm," *Circulation Research*, vol. 115, pp. 812-813, 2014.

[20] M. Adam, U. Raaz, J. M. Spin, and P. S. Tsao, "MicroRNAs in abdominal aortic aneurysm," *Current Vascular Pharmacology*, vol. 13, pp. 280–290, 2015.

[21] L. Maegdefessel, J. M. Spin, U. Raaz et al., "miR-24 limits aortic vascular inflammation and murine abdominal aneurysm development," *Nature Communications*, vol. 5, p. 5214, 2014.

[22] L. Maegdefessel, J. Azuma, R. Toh et al., "MicroRNA-21 blocks abdominal aortic aneurysm development and nicotine-augmented expansion," *Science Translational Medicine*, vol. 4, article 122ra122, 2012.

[23] G. F. Ming, K. Wu, K. Hu, Y. Chen, and J. Xiao, "NAMPT regulates senescence, proliferation, and migration of endothelial progenitor cells through the SIRT1 AS lncRNA/miR-22/SIRT1 pathway," *Biochemical and Biophysical Research Communications*, vol. 478, pp. 1382–1388, 2016.

[24] G. Wu, J. Cai, Y. Han et al., "LincRNA-p21 regulates neointima formation, vascular smooth muscle cell proliferation, apoptosis, and atherosclerosis by enhancing p53 activity," *Circulation*, vol. 130, pp. 1452–1465, 2014.

[25] J. Viereck and T. Thum, "Long noncoding RNAs in pathological cardiac remodeling," *Circulation Research*, vol. 120, pp. 262–264, 2017.

[26] K. Y. He, H. Wang, B. E. Cade et al., "Rare variants in fox-1 homolog A (*RBFOX1*) are associated with lower blood pressure," *PLoS Genetics*, vol. 13, article e1006678, 2017.

[27] C. Gao, S. Ren, J. H. Lee et al., "RBFox1-mediated RNA splicing regulates cardiac hypertrophy and heart failure," *The Journal of Clinical Investigation*, vol. 126, pp. 195–206, 2016.

[28] U. Kato, H. Inadome, M. Yamamoto, K. Emoto, T. Kobayashi, and M. Umeda, "Role for phospholipid flippase complex of ATP8A1 and CDC50A proteins in cell migration," *The Journal of Biological Chemistry*, vol. 288, pp. 4922–4934, 2013.

[29] E. Horio, T. Kadomatsu, K. Miyata et al., "Role of endothelial cell-derived Angptl2 in vascular inflammation leading to endothelial dysfunction and atherosclerosis progression," *Arteriosclerosis, Thrombosis, and Vascular Biology*, vol. 34, pp. 790–800, 2014.

[30] M. R. Richardson, E. P. Robbins, S. Vemula et al., "Angiopoietin-like protein 2 regulates endothelial colony forming cell vasculogenesis," *Angiogenesis*, vol. 17, pp. 675–683, 2014.

[31] S. Iyer, Y. Chhabra, T. J. Harvey et al., "Crim1 is necessary for coronary vascular endothelial cell development and homeostasis," *Journal of Molecular Histology*, vol. 48, pp. 53–61, 2017.

[32] A. Ashkenazi and V. M. Dixit, "Apoptosis control by death and decoy receptors," *Current Opinion in Cell Biology*, vol. 11, pp. 255–260, 1999.

[33] G. Yu, Z. Jia, and Z. Dou, "miR-24-3p regulates bladder cancer cell proliferation, migration, invasion and autophagy by targeting DEDD," *Oncology Reports*, vol. 37, pp. 1123–1131, 2017.

[34] N. Farhang, J. M. Brunger, J. D. Stover et al., "CRISPR-based epigenome editing of cytokine receptors for the promotion of cell survival and tissue deposition in inflammatory environments," *Tissue Engineering Part A*, vol. 23, no. 15-16, pp. 738–749, 2017.

[35] Q. Zhang, I. Kandic, J. T. Barfield, and M. J. Kutryk, "Coculture with late, but not early, human endothelial progenitor cells up regulates IL-1β expression in THP-1 monocytic cells in a paracrine manner," *Stem Cells International*, vol. 2013, Article ID 859643, 2013.

[36] K. Sa-Ngiamsuntorn, A. Wongkajornsilp, P. Phanthong et al., "A robust model of natural hepatitis C infection using hepatocyte-like cells derived from human induced pluripotent stem cells as a long-term host," *Virology Journal*, vol. 13, p. 59, 2016.

[37] V. Lecureur, E. L. Ferrec, M. N'diaye et al., "ERK-dependent induction of TNFα expression by the environmental contaminant benzo(a)pyrene in primary human macrophages," *FEBS Letters*, vol. 579, pp. 1904–1910, 2005.

[38] S. Lindberg, M. Zarrouk, J. Holst, and A. Gottsäter, "Inflammatory markers associated with abdominal aortic aneurysm," *European Cytokine Network*, vol. 27, pp. 75–80, 2016.

[39] L. Liao, X. Su, X. Yang et al., "TNF-α inhibits FoxO1 by upregulating miR-705 to aggravate oxidative damage in bone marrow-derived mesenchymal stem cells during osteoporosis," *Stem Cells*, vol. 34, pp. 1054–1067, 2016.

[40] F. Zhang, K. C. Kent, D. Yamanouchi et al., "Anti-receptor for advanced glycation end products therapies as novel treatment for abdominal aortic aneurysm," *Annals of Surgery*, vol. 250, pp. 416–423, 2016.

[41] K. Ji, J. Chen, J. Hu et al., "The protective effect of astragaloside IV against benzo[a]pyrene induced endothelial progenitor cell dysfunction," *Life Sciences*, vol. 132, pp. 13–19, 2015.

[42] N. V. Guevara, H. S. Kim, E. I. Antonova, and L. Chan, "The absence of p53 accelerates atherosclerosis by increasing cell proliferation in vivo," *Nature Medicine*, vol. 5, pp. 335–339, 1999.

Hindawi
Stem Cells International
Volume 2017, Article ID 1719050, 13 pages
https://doi.org/10.1155/2017/1719050

Review Article

Astrocytes at the Hub of the Stress Response: Potential Modulation of Neurogenesis by miRNAs in Astrocyte-Derived Exosomes

Alejandro Luarte,[1,2] Pablo Cisternas,[1,3] Ariel Caviedes,[1] Luis Federico Batiz,[1] Carlos Lafourcade,[1] Ursula Wyneken,[1] and Roberto Henzi[1]

[1]*Centro de Investigaciones Biomédicas, Facultad de Medicina, Universidad de los Andes, Santiago, Chile*
[2]*Biomedical Neuroscience Institute, Universidad de Chile, Santiago, Chile*
[3]*Cells for Cells, Santiago, Chile*

Correspondence should be addressed to Roberto Henzi; rpjhenzi@gmail.com

Received 1 July 2017; Accepted 16 August 2017; Published 7 September 2017

Academic Editor: Mark W. Hamrick

Repetitive stress negatively affects several brain functions and neuronal networks. Moreover, adult neurogenesis is consistently impaired in chronic stress models and in associated human diseases such as unipolar depression and bipolar disorder, while it is restored by effective antidepressant treatments. The adult neurogenic niche contains neural progenitor cells in addition to amplifying progenitors, neuroblasts, immature and mature neurons, pericytes, astrocytes, and microglial cells. Because of their particular and crucial position, with their end feet enwrapping endothelial cells and their close communication with the cells of the niche, astrocytes might constitute a nodal point to bridge or transduce systemic stress signals from peripheral blood, such as glucocorticoids, to the cells involved in the neurogenic process. It has been proposed that communication between astrocytes and niche cells depends on direct cell-cell contacts and soluble mediators. In addition, new evidence suggests that this communication might be mediated by extracellular vesicles such as exosomes, and in particular, by their miRNA cargo. Here, we address some of the latest findings regarding the impact of stress in the biology of the neurogenic niche, and postulate how astrocytic exosomes (and miRNAs) may play a fundamental role in such phenomenon.

1. The Relevance of the Hippocampus in the Stress Response

Stressful life events are strong precipitating factors of neuropsychiatric pathologies including mood disorders such as major depression (MD) or bipolar disorder (BD) [1]. Stress can be defined as any adaptive mechanism triggered to recover the organism's homeostasis, composed of a vast array of modifications in the physiology of different organs, including the central nervous system (CNS) at different scales, that is, plastic changes which range from molecular dynamics to behavioral adaptations [2].

The proper adaptive response to stressors is known as "stress resilience" and the multiple biological processes underlying resilience are collectively termed allostasis [3]. Nevertheless, plastic changes can be deleterious to cerebral and overall body health under prolonged stress (reviewed in [4]). Furthermore, increasing evidence shows that stress impacts the induction not only of psychiatric but also systemic pathologies such as cardiovascular diseases, cancer, and inflammation-related diseases [5–7].

The mechanisms that participate in the stress response involve the CNS, where the hypothalamus-pituitary-adrenal axis (HPA) has a central role. HPA activation leads to an increase in the systemic levels of glucocorticoids (GCs) (cortisol in humans and corticosterone in rodents) in concomitance with changes in the activity of the autonomic system, with norepinephrine and epinephrine as final products [2]. GCs are key hormones of the stress response that are able to cross the blood-brain

barrier due to their lipophilic nature. Receptors in target cells include the high-affinity mineralocorticoid receptor [8] or the low-affinity glucocorticoid receptors [9]. In the brain, both receptors are mainly occupied by GCs and translocate to the nucleus after binding to their ligand, where they modify the expression of different genes that govern the stress response. The brain area profoundly affected during chronic stress is the hippocampus. The human and rodent hippocampi correspond to a CNS region where glucocorticoid receptors (GRs) are expressed in neurons, astrocytes as well as in some neural stem cells [10–12], conferring a high sensitivity of this forebrain structure to changes in glucocorticoids levels [13]. A negative feedback loop mediated by cortisol regulates the activity of the HPA by targeting structures such as the paraventricular nucleus and the hippocampus. In the latter, synaptic inputs can directly exert an overall inhibitory effect on the activity of the HPA [14]. Stress triggers molecular and structural changes in the hippocampus, including dendritic and spine atrophy that is concomitant to downregulation of specific synaptic protein [15, 16]. Many of these glucocorticoid-mediated changes can be mimicked by exogenous application of these corticosteroids (extensively reviewed by [13]).

Intriguingly, the hippocampus harbors one of the two identified brain structures in mammals that retains the capacity to generate new neurons in adulthood, that is, the neurogenic niche of the subgranular zone (SGZ) in the dentate gyrus (DG). The process by which new neurons are continuously generated in the SGZ of adults is known as adult neurogenesis and implies the self-renewal, proliferation/activation of neural stem/precursor cells, their differentiation into neurons, as well as their migration, maturation, and even their integration into the hippocampal functional circuits [17–19]. Any modification in one of these stages can influence (positively or negatively) the generation of new neurons, and diverse pathological conditions including chronic stress have been described to decrease adult hippocampal neurogenesis [20]. Conversely, antidepressant interventions show an increase in the number of neural stem/precursor cells in the DG. In fact, some antidepressant drugs depend on neurogenesis to induce recovery from depressive symptoms [21–24].

Hippocampal newborn neurons are essential for the proper endocrine and behavioral adaptation to stress [25], and SGZ neurogenesis contributes to the negative feedback on the HPA axis, as its disruption induces a larger response to a mild stressor [26]. Consistently, it has been described that altered neurogenesis leads to a slower recovery of GC levels after stress [27], suggesting a cross talk between hippocampal neurogenesis and the HPA axis. Likewise, reduced neurogenesis is associated with impaired responsiveness of the HPA axis in the dexamethasone suppression test [28]. Thus, any process that restores hippocampal neurogenic activity might contribute to better cope with stress. This could take place at the various stages involved in this process, from cell proliferation to the generation of mature DG neurons.

2. The Adult Hippocampal Neural Stem/Precursor Cells

Seri and coworkers [29] observed for the first time that neural stem cells that undergo proliferation in the SGZ display radial glia characteristics expressing the glial fibrillary acidic protein (GFAP), in addition to markers of undifferentiated cells such as vimentin, SOX2, and Nestin. SGZ stem cells are called type 1 cells (reviewed by Ming and Song [30]). These give rise, through asymmetric division, to highly proliferative intermediate progenitors known as type 2a (positive for Nestin and PSA-NCAM and negative for GFAP) and 2b cells (positive for Tbr2 and PSA-NCAM). The latter cells give rise to neuroblasts or type 3 cells (positive for doublecortin, PSA-NCAM, and NeuN) that migrate into the inner granular layer. Within days, type 3 cells will become immature neurons that, after about 4 weeks, extend dendrites towards the molecular layer and project axons through the hilus toward the CA3 (reviewed by Zhao et al., Covic et al., and Bonaguidi et al. [17, 31, 32]). In summary, both neural stem and progenitor cells coexist in the SGZ and can generate new granule neurons [33, 34]. In the present review, we will use the acronym NSPCs to describe both neural stem cells and precursor cells.

3. Magnitude of Adult Hippocampal Neurogenesis

It has been estimated that in the rat hippocampus 9000 new cells are generated every 25 hours [35]. In mice, on the other hand, the number is much lower: only 2700 new cells per day are generated [36]. After 30 days, ~30% of new cells survive and differentiate into mature neurons with complex dendritic and axonal structure. In humans, direct evidence of adult neurogenesis has been provided first by the use of the synthetic analog BrdU (bromodeoxyuridine, 5-bromo-2′-deoxyuridine) [37] and later on by an elegant publication which presented an integrated model of cell turnover dynamics in the hippocampus by measuring the concentration of nuclear bomb test-derived ^{14}C in hippocampal cells. This work shows that one-third of human hippocampal neurons are exchanged throughout life and that 700 new neurons are added per day. The authors calculated a turnover of 1.75% newborn neurons per year that decreased modestly during aging. Taken together, this data indicates that adult hippocampal neurogenesis is not a minor process and may contribute significantly to human brain function during physiology and disease [38].

4. Adult-Born Hippocampal Neurons and the Impact of Stress

After stressful experiences, the activation of the HPA axis and the elevation of systemic GC levels lead to the impairment of NSPC proliferation in the SGZ both in developmental stages as well as in adulthood [39, 40].

Consistently, adrenalectomy increases the formation of new neurons in young and aged rodents [41–43]. Furthermore, the hyporesponsive stress period in rats (from 2 days after birth to 2 weeks old), characterized by low basal levels

of GCs and a diminished response to stress [44], is associated with the maximal neurogenesis period in the SGZ [45, 46]. Likewise, adrenalectomy prevents the suppression of neurogenesis induced by stress [47, 48]. The effect of GCs on the neurogenic potential has shown to be dose-dependent in a human hippocampal progenitor cell line. Interestingly, low concentrations of cortisol stimulate proliferation and gliogenesis and decrease neurogenesis by signaling through mineralocorticoid receptors. On the other hand, high doses of cortisol decreased proliferation through glucocorticoid receptor signaling, with no effect on gliogenesis [49]. Similarly, decreased neurogenesis has been observed in different stress models, including chronic and acute stress, for example, subordination stress [50], resident-intruder stress [51], footshock [52], restraint stress [53, 54], or stress-induced by isolation [55] and predator odor [56]. It is worth remarking that stress has been shown to affect neurogenesis in a reduced window of time. Tanapat et al. observed that animals may experience a rebound in cell proliferation after the initial stress-induced suppression to compensate the alteration [47]. These results agree with several publications in which acute stressful experiences increases neurogenesis [57–60].

Despite significant advances in the field of neurogenesis and stress over the past two decades, detailed mechanisms underlying the inhibition of cell proliferation under stress conditions and its adaptations remain unknown.

5. Astrocytes Are Key Players in Adult Neurogenic Niche

Neurogenesis is regulated through its specialized microenvironment, the neurogenic niche. In adult mammals, including humans, neurogenic niches are concentrated in restricted areas; the most commonly described are the subventricular zone (SVZ) of the lateral ventricles and, mentioned above, the SGZ of hippocampal DG [61, 62]. The regulation of neurogenesis in the neurogenic niche is such that NSPCs obtained from exogenous SVZ and grafted into another SVZ host are able to generate new neurons; but NSPCs from the SVZ grafted into nonneurogenic brain regions show a scarce neurogenic potential, suggesting that here, a very particular cellular and molecular context accounts for the control of neurogenesis [63, 64].

Any cellular type within the niche can influence the neurogenic process by diffusible signals or by cell-cell interactions. In the SGZ, the main cellular components are astrocytes, endothelial cells, pericytes, oligodendrocytes, microglia, different types of neurons present in the DG, and the aforementioned NSPCs [65]. Although each cell type may have a significant contribution to the neurogenic process, in the present review, we will focus on the role of astrocytes as key elements in the control of the neurogenic process under stress.

Astrocytes subserve a myriad of functions that have been described both *in vitro* and *in vivo* (extensively reviewed by Khakh and Sofroniew [66]). In the hippocampus, protoplasmic astrocytes extend their processes radially and some of them contact blood vessels to form perivascular end feet of the blood-brain barrier (BBB), while others may contact neurons (e.g., tripartite synapse) or be coupled to oligodendrocytes through connexins [67]. In addition, astrocytes may connect with other astrocytes through connexins, generating a sort of functional syncytium able to signal by propagating calcium waves along several distant cells *in vivo* [68]. It is therefore not surprising that they are thought to have a central role in the functional output of the neurogenic process [69]. For example, astrocytes negatively influence the differentiation of NSPCs after the activation of jagged1-mediated Notch pathway by cell-cell contact [70] or by the secretion of growth factors such as insulin-like growth factor binding protein 6 (IGFBP6) and decorin [71]. On the contrary, released factors such as Wnt3a, neurogenesin-1, and different interleukins such as IL-1β and IL-6 or cell-to-cell contact mediated by ephirn-B2 signaling positively regulate neurogenesis [29, 71–74]. Thus, it is possible that, depending on the physiological and anatomical context, the astrocyte secretome has distinct effects on the neurogenic process [71]. In this line, hippocampal astrocytes are more efficient than cortical astrocytes in promoting neuronal differentiation of NSPCs [75].

The secretory activity of astrocytes in the DG mediates the synaptic and network integration of newborn neurons *in vivo*, highlighting their role as key mediators of the functional output of neurogenesis [76]. Previous data supports this view, as astrocytes promote the differentiation of progenitor cells and control the maturation and synaptic integration of newborn neurons *in vitro* [77, 78].

6. Stress, Astrocyte Plasticity, and Neurogenesis

A wide body of evidence has shown that acute and/or chronic stress can alter the morphology and functionality of different glial cell types in the brain, such as microglia [79, 80], oligodendroglia [81], and astrocytes [82].

Czéh et al. observe that tree shrews subjected to 5 weeks of psychosocial stress showed a 25% reduction in the intermediate filament protein of astrocytes GFAP, as well as a 25% reduction in the somatic volume of hippocampal astrocytes [83]. In the past few years, several publications using other stress protocols have led to similar observations [84–86]. Nevertheless, some publications using the chronic restraint model have reported an increase in GFAP positive cell number and in the protein level in the hippocampus [87, 88].

Other proteins expressed by astrocytes such as connexin 30 and 43 (gap junction proteins), the water channel aquaporin-4 (AQP4), the calcium-binding protein S100β and the amino acid transporters 1 and 2 (EAAT1, EAAT2), and glutamine synthetase have altered expression levels in both animals models of stress and in human brain samples analyzed postmortem compared with controls (reviewed in [89]). Despite the importance of some of these proteins in calcium homeostasis, there is a lack of studies showing how astrocytic calcium metabolism is regulated under stress conditions.

Moreover, a recent publication by Zhao et al. has shown that a decrease in glycogen content is associated with chronic stress, being one of the main mechanism in astrocytes

Table 1: Effect of stress over neurogenesis mediated by astrocytes.

Type of stress	Type of study	Cellular effect	Molecular mechanism	References
Acute and chronic induced by dexamethasone	*In vivo*	Growth inhibition of astrocytes	After inducing cell cycle exit by reduction of cyclin D1 and increase of p27	[128]
	In vitro	Inhibition of NSPC proliferation (cultured with CM of stressed astrocytes)	By altered expression of neurotrophic factors (*BDNF*, *NGF*) and mitogenic factors (*BFGF*, *VEGF*) and death-inducing factors (FasL, Trail, Tweak, and TNFα)	
Acute induced by dexamethasone or corticosterone	*In vitro*	Inhibition of astrocytes proliferation	By inducing reduction of GR expression	[129]
Chronic induced by administration of ACTH	*In vivo*	Inhibition of astrocytes proliferation	By inducing reduction of GR expression	
Acute and chronic	*In vivo*	Regulation of mRNAs in a cell type-dependent fashion	By glucocorticoids receptors	[130]
Acute	*In vivo*	Increase hippocampus cellular proliferation	Increase of astrocytes FGF2 expression	[131]

capable of inducing their structural and molecular alterations. This result may be of importance as it moves away from the GC-centered theory of stress [90].

On the other hand, different publications have reported that when astrocytes are exposed to high levels of GCs, GC bound to GRs translocates to the nucleus and enhances the expression of genes related with neurogenesis, one example is the Fgf2 gene [91]. FGF2, the protein encoded by Fgf2, is a potent and necessary proliferative factor in adult NSPCs [92]. Nevertheless, other different effects mediated by astrocytes over the adult neurogenesis after a stressful condition have not been fully unveiled. In Table 1, we resume the main effects described for this issue, both *in vivo* and *in vitro*.

7. Exosomes Biogenesis and the Relevance of Their Content in Controlling Cellular Function

In addition to soluble components (see Section 5), the astrocyte secretome contains extracellular vesicles (EVs) such as exosomes [93] that represent a different source of cell-cell communication [94, 95]. Exosomes are generated in the endocytic pathway after the invagination and subsequent fission of a domain in the endosomal membrane that give rise to an exosome precursor called intraluminal vesicle (ILV) of the multivesicular body (MVB). After the fusion with the plasma membrane, the ILVs are released into the extracellular space as spherical vesicles of 40–100 nm, called exosomes [96]. The biogenesis of exosomes requires different molecular components including the mechanisms dependent of the ESCRT (endosomal sorting complex required for transport) machinery [97, 98] and lipid-dependent mechanisms [99, 100]. Proteins that participate in their biogenesis are frequently used as positive markers of exosomes, as well as proteins associated with lipid rafts and tetraspanins such as Alix, flotillin, TSG101, and CD63 [101].

Exosomes contain a complex molecular cargo that include proteins, lipids, and nucleic acids that may be biologically active on recipient cells [102]. The protein composition is diverse and depends on the cellular type and the physiological context; nevertheless, as they originate in the endocytic pathway, the most common proteins independent of the cell type of origin are related to vesicular transport and fusion (Rab GTPasas, SNAREs, annexins, and flotillin), different integrins and tetraspanins (CD63, CD9, CD81, and CD82), and heat shock proteins (Hsc/Hsp 70 and 90) and proteins implicated in the biogenesis of MVB (Alix and TSG 101) [103]. Regarding their lipidic content, one characteristic of the exosomes is their enrichment in lipid rafts including cholesterol, sphingolipids (such as ceramide), and glycerophospholipids with long and saturated fatty acyl chains [101]. Finally, among the most relevant biologically active molecules present in exosomes are nucleic acids, particularly small noncoding RNAs such as miRNAs (see below).

Exosomes play a significant role in the secretome of a given cell, subserving functions in the communication between cells [104]. Furthermore, virtually all eukaryotic cells release exosomes and are capable of taking them up [105, 106]. Regarding the CNS, oligodendrocytes, neurons, astrocytes, and microglia are capable of releasing exosomes with functional consequence on neuronal physiology [107]. Actually, exosomes have been proposed to be key players in the pathogenesis of different CNS diseases, including neurodegenerative diseases, infectious diseases, neuroinflammation, and even psychiatric disorders such as depression [108, 109]. Considering the high molecular diversity and complexity of their cargo, a fundamental question to understand the biological relevance of astrocytic exosomes in neurogenesis is a critical analysis of the relevant molecular cargo that could potentially control the fate of NSPCs and the neurogenic process.

So far, the functional transfer/interaction of exosomes to target cells has been shown mostly *in vitro*, but there is increasing data being obtained *in vivo*. Analysis of *in vivo* evidence is crucial as it settles the basis to propose that astrocytes within the neurogenic niche might be able to modify

Table 2: miRNA associated with neurogenesis present in astrocytes- and astrocytes-derived exosomes.

miRNA	Expression level	Cellular process	Molecular target	References
miR-9	Overexpression	Reduces axonal branching and neurite outgrowth	MAP1b	[132]
miR-9	Upregulation/ overexpression	Promotes neuronal differentiation	Notch signaling, several targets	[133]
miR-9	Upregulation/ overexpression	Promotes neuronal differentiation and dendritic branching, inhibits migration	TLX, REST, Rap2a, and stathmin	[134]
miR-9	Upregulation/ overexpression	Suppresses astrogliogenesis	Lifr-beta, Il6st (gp130), and Jak1 (jack/stat pathway)	[135]
miR-9	Upregulation/ overexpression	Promotes neuronal differentiation and migration	TLX/Nre1, Foxg1, REST/NRSF, CoREST, Meis2, Gsh2, Islet1, Id4, and stathmin	[136]
miR-9	Overexpression	Mediates neural differentiation of ES cell	STAT3	[137]
miR-9	Overexpression	Promotes neuronal differentiation	Foxg1, Gsh2, SIRT1, and REST/NRSF	[138]
miR-9	Overexpression	Inhibits NSPC proliferation and facilitates NSPC differentiation	TLX	[118]
miR-9	Overexpression	Inhibits NSPC proliferation and facilitates NSPC differentiation	Hes1 (notch signaling)	[139]
miR-26a	Upregulation	Inhibits spine enlargement	RSK3	[140]
miR-26a	Downregulation	Prevents axonal regeneration	GSK3β	[141]
miR-26b	Upregulation	Promotes neuronal differentiation	Ctdsp2	[142]
miR-29a	Upregulation	Increase axonal branching	DCX	[143]
miR-34a	Upregulation	Promotes neural differentiation and synaptogenesis	TAp73, synaptotagmin-1, and sintaxin-1A	[144]
miR-34a	Upregulation	Inhibits neuronal differentiation, promotes proliferation	Numbl, NeuroD1, and Mash1	[134]
miR-34a	Upregulation	Promotes apoptosis, inhibits cell cycle progression and synaptic development	BCL-2, Cdk-4 Cyclin D2 synaptotagmin syntaxin-1A	[134]
miR-34a	Upregulation	Negatively regulate neurite outgrowth and dendritic branching		[134]
miR-125b	Upregulation	Promotes neuronal differentiation	BMP/TGFβ signaling	[133]
miR-125b	Upregulation	Promotes neuronal differentiation	Nestin	[145]
miR-125b	Upregulation	Inhibits NSPC proliferation and promotes differentiation	Musashi1	[146]
miR-129	Upregulation	Determination of the bipolar cell identity in retina	Xotx2, Xvsv1	[147]
miR-135b	Upregulation/ Overexpression	Promotes neuronal induction	BMP/TGFβ signaling	[148]
miR-145	Upregulation	Promotes neuronal differentiation	OCT4, SOX2, and KLF4	[149]
miR-145	Upregulation	Promotes neuronal differentiation	SOX2, Lin28/let7	[150]
miR-221	Downregulated	Neurite guidance		[151]
Let-7 family	Upregulation	Pluripotency inhibitor promoting neural lineage, promotes neuronal differentiation	Lin28	[133]
Let-7 family	Upregulation	Promotes NSPCs differentiation	c-Myc, Lin28	[136]
Let-7b	Upregulation	Inhibits proliferation and promotes the differentiation of NSPCs	TLX, Cyclin D1	[152]
miR-543	Upregulation	Promotes neural stem cell differentiation and neuronal migration	N-Cadherin, TrappC8	[153]

NSPCs' physiology through functional transfer of exosomal cargo in physiological conditions and during diseases. In this regard, an outstanding result came from the work of Zhang et al. where they found *in vivo* that tumor cells lose the expression of the tumor suppressor protein phosphatase and tensin homolog (PTEN) after incorporating astrocytic exosomes, due to the presence of a microRNA (miRNA) that targets PTEN [110].

Thus, although still speculative, we discuss a putative scenario where astrocytes in the neurogenic niche modulate the cellular behavior of NSPCs on the virtue of exosome transfer. It is important to notice that, in the literature, several of the

Table 3: miRNA associated with neurogenesis enriched in astrocytes derived exosomes.

miRNA	Expression level	Cellular process	Molecular target	Reference
miR-25b	Overexpression	Promotes proliferation and differentiation of NSPCs	IGF signaling	[154]
miR-17-92	Overexpression	Increase axonal outgrowth	PTEN	[123]
miR-92a	Upregulation/ overexpression	Inhibits the transition from radial glial cells to intermediate progenitors	Tbr2	[155]
miR-184	Upregulation	Inhibits differentiation and promotes proliferation of NSPCs	Numbl	[156]
miR-302	Upregulation	Block neural progenitor induction	BMP/TGFβ, NR2F2	[157]
miR-96	Upregulation	Block neural progenitor induction	PAX6	[158]

Table 4: miRNA associated with neurogenesis modified after different stimulus.

miRNA	Expression level	Cellular process	Molecular target	Reference
miR-181a	Upregulated by morphine	Promote astrocyte-preferential differentiation of NSPCs	Prox1/Notch2	[159]
miR-23b	Upregulated by morphine	Adult neurogenesis	Morphine receptor expression (MOR1)	[160]
miR-190	Downregulated by fentanyl	Adult neurogenesis	NeuroD	[161]
miR-143	Upregulation by IGF-1	Promotes proliferation, neural differentiation, and cell survival	PDGFRA, PRKCE, MAPK7, DSSP, DMP-1, KRAS, and BCL-2	[162]
miR-181c	Upregulation by IGF1/LIF	Enhanced self-renewal of NSPCs	PTPN11, PTPN22, PTEN, Dusp6, PBX3, ZEB2, and IRF8	[162]

functional effects described for exosomes are attributed to mRNA or miRNA transfer rather than proteins or lipids (as an example see [111]), though there is a growing interest to examine the relevance of these molecules in the exosomal cargo.

8. miRNAs in Astrocyte-Derived Exosomes as Modulators of Adult Neurogenesis and Stress Response

miRNAs are small noncoding RNAs (20–22 nucleotides) that cause deadenylation as well as translational repression of mRNAs by binding to their 3′ untranslated region (3′UTR). They have been proposed to be integral regulatory molecules in both physiological conditions and in disease states, because a single miRNA molecule can repress several hundreds (and even thousands) of mRNA molecules [112, 113]. Furthermore, the targeting of a single mRNA by a miRNA can potentially modulate the transcription of a vast array of proteins [114].

miRNAs are known to be a key element for neuronal differentiation; for example, Kawase-Koga et al. observed that NSPCs undergo cell death and affecting also the neuronal differentiation and their maturation after conditionally deleting the expression of the RNAse III enzyme DICER, an enzyme that processed miRNA precursor into mature miRNAs in specific stages of mice development [115]. Another miRNA that has also proved to modulate neuronal differentiation is miR-124, which contributes to the downregulation of Ezh2, a histone H3 Lys-27 histone methyltransferase that governs the transcription of several neuron-specific genes, diminishing the differentiation of mouse embryonic NSPCs as a final outcome [116, 117].

On the other hand, an increase in the expression of miR-9 in neurogenic regions leads to a reduction of NSPC proliferation and accelerated neural differentiation due to its modulation of TLX, a key regulator of NSPCs self-renewal, whereas the knock-in of miR-9 leads to increased proliferation of NSPCs [118]. Other miRNAs such as miR-128 and miR-137 promote differentiation of NSPCs, while their knockdown compromises their self-renewal [119].

Recently, Han et al. have shown that miRNA-19 (a member of polycistronic miRNA genes critical for brain development) is enriched in NSPCs and decreases during neuronal development. They found that this miRNA controls the maturation and positioning of newborn neurons in the granular cell layer of the DG by suppressing Rap guanine nucleotide exchange factor 2 (Rapgef2) [120]. In another study, the authors found that miR-20 downregulates the transcriptional repressor gene REST, inhibiting the differentiation of NSPCs [121]. Other miRNAs controlling both proliferation and differentiation of adult NSPCs are miR-137 [122] and rno-miR-592 [123]. Taken together, these data indicate an important participation of miRNAs in adult neurogenesis.

Multiple evidence has shown a relationship between miRNAs and stress, both in animal models of stress and in human patients with depression. Furthermore, some

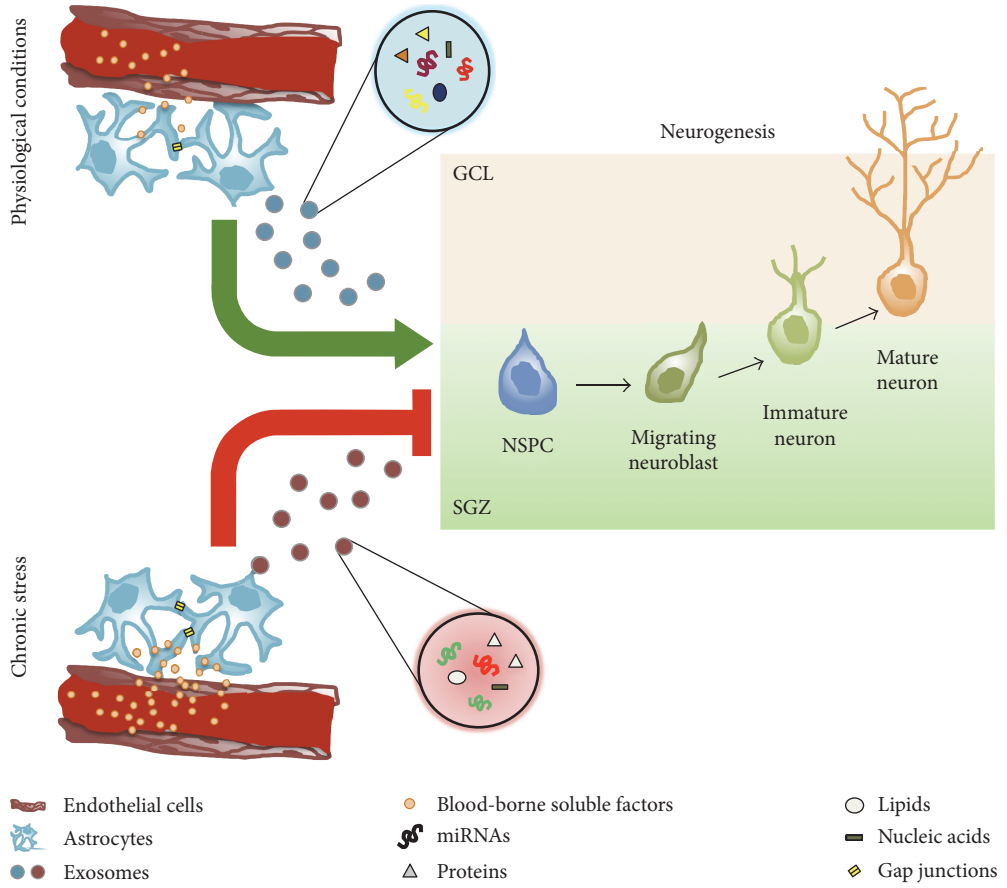

Figure 1: Blood-borne soluble factors reach astrocytes in the neurogenic niche, thus triggering the release of exosomes. In physiological conditions, the content of their cargo may exert a positive modulatory effect over one or more neurogenic stages (e.g., enhancing proliferation, and differentiation). During pathological conditions such as chronic stress, astrocytes respond to blood-borne soluble factors (e.g., corticosteroids and cytokines) by releasing exosomes with a cargo that may have a negative modulatory influence over one or more neurogenic stages. Astrocytes may in turn communicate with each other through gap junctions and/or by exosomal release. This may partly explain the decrease in differentiation and proliferation observed under such conditions. Note that the exosomal content under pathological or physiological conditions may differ in terms of the identity of the molecules (e.g., different types of miRNAs or proteins) and/or in their overall quantity. GCL: granule cell layer; SGZ: subgranular zone; NPSC: neural stem/precursor cell.

miRNAs have been postulated as potential biomarkers of stress/depression (extensively reviewed by Dwivedi and Brites and Fernandes [124, 125]). miRNAs also may play important roles in the mechanism of action of antidepressants: for example, in early-life stress models, the downregulation of miR-451 was reversed after antidepressant treatment [126].

Regarding astrocytes, although the information available about the differential cargo of astrocyte-derived exosomes after stressful conditions is scarce, it is worth pointing out that several miRNAs that are up or downregulated in stress conditions are contained in exosomes secreted by astrocytes. These miRNAs have also been described to play a role in the neurogenic process (Tables 2 and 3). Interestingly, miRNAs contained in astrocyte-derived exosomes are differentially enriched as compared to their levels in astrocytes [127], suggestive of their unique role in cellular communication. Moreover, many of the miRNAs contained in astrocytes can be modulated by different stimuli (see Table 4). All these data lead us to postulate astrocyte-derived exosomes as potential modulators of proliferation, migration, and/or differentiation of NSPCs within the neurogenic niche, and that changes in exosomal release as well as in their miRNA cargo can play a role in neurogenesis under stress conditions, in a similar fashion as it has been described for other CNS pathologies.

9. Conclusions and Future Perspectives

The production and proliferation of neural lineages (neurons, astrocytes, and oligodendrocytes) are a complex phenomenon tightly regulated by a multiplicity of factors. This regulation is susceptible to profound modifications when the homeostasis of the environment changes due to acute or chronic disorders. In the case of chronic stress, the observed modifications in the neurogenic niche (i.e., a decrease in NSPC proliferation/differentiation) lack a solid molecular explanation. Astrocytes may be key players to further understand on how and why the neurogenic niche responds the way it does in physiological and pathophysiological conditions. This is especially true in the case of the

SGZ, where, due to their proximity with the vasculature, astrocytes may respond to factors in circulation (e.g., corticosteroids) to influence the behavior of the neurogenic niche [18]. We propose that a putative mechanism by which astrocytes exert their influence is through exosomal delivery of specific miRNAs. This could provide a finely tuned regulatory system, acting through two mechanisms: the first one is related to the unique membrane protein footprint that would enable astrocyte-derived exosomes to target specifically some, but not all, cell types of the neurogenic niche, and the second one is related with the miRNA cargo that most probably is unique under certain conditions. This could provide an exquisite temporal and spatial regulation for every single cell type implicated during the whole process of neurogenesis (Figure 1).

Conflicts of Interest

The authors declare no competing interests.

Acknowledgments

This work was supported by CONICYT (FONDECYT Program 3170887 (Alejandro Luarte), FONDECYT Program 1140108 (Ursula Wyneken), and FONDECYT Program 1141015 (Luis Federico Batiz)) and by the Universidad de los Andes Fondo de Ayuda a la Investigación (FAI Carlos Lafourcade and FAI Roberto Henzi).

References

[1] C. Hammen, "Stress and depression," *Annual Review of Clinical Psychology*, vol. 1, no. 1, pp. 293–319, 2005.

[2] G. P. Chrousos, "Stress and disorders of the stress system," *Nature Reviews Endocrinology*, vol. 5, no. 7, pp. 374–381, 2009.

[3] B. S. McEwen, "Plasticity of the hippocampus: adaptation to chronic stress and allostatic load," *Annals of the New York Academy of Sciences*, vol. 933, no. 1, pp. 265–277, 2006.

[4] R. M. Sapolsky, "Stress, glucocorticoids, and damage to the nervous system: the current state of confusion," *Stress*, vol. 1, no. 1, pp. 1–19, 1996.

[5] E. M. Reiche, S. O. Nunes, and H. K. Morimoto, "Stress, depression, the immune system, and cancer," *Lancet Oncology*, vol. 5, no. 10, pp. 617–625, 2004.

[6] S. F. Sorrells, J. R. Caso, C. D. Munhoz, and R. M. Sapolsky, "The stressed CNS: when glucocorticoids aggravate inflammation," *Neuron*, vol. 64, no. 1, pp. 33–39, 2009.

[7] A. Tawakol, A. Ishai, R. A. Takx et al., "Relation between resting amygdalar activity and cardiovascular events: a longitudinal and cohort study," *Lancet*, vol. 389, no. 10071, pp. 834–845, 2017.

[8] J. Arriza, C. Weinberger, G. Cerelli et al., "Cloning of human mineralocorticoid receptor complementary DNA: structural and functional kinship with the glucocorticoid receptor," *Science*, vol. 237, no. 4812, pp. 268–275, 1987.

[9] S. Hollenberg, C. Weinberger, E. Ong et al., "Primary structure and expression of a functional human glucocorticoid receptor cDNA," *Nature*, vol. 318, no. 6047, pp. 452–457, 1985.

[10] M. Joëls, "Role of corticosteroid hormones in the dentate gyrus," *Progress in Brain Research*, vol. 163, pp. 355–370, 2007.

[11] Q. Wang, J. Van Heerikhuize, E. Aronica et al., "Glucocorticoid receptor protein expression in human hippocampus; stability with age," *Neurobiology of Aging*, vol. 34, no. 6, pp. 1662–1673, 2013.

[12] A. Garcia, B. Steiner, G. Kronenberg, A. Bick-sander, and G. Kempermann, "Age-dependent expression of glucocorticoid- and mineralocorticoid receptors on neural precursor cell populations in the adult murine hippocampus," *Aging Cell*, vol. 3, no. 6, pp. 363–371, 2004.

[13] C. D. Conrad, "Chronic stress-induced hippocampal vulnerability: the glucocorticoid vulnerability hypothesis," *Reviews in the Neurosciences*, vol. 19, no. 6, pp. 395–411, 2008.

[14] J. P. Herman, H. Figueiredo, N. K. Mueller et al., "Central mechanisms of stress integration: hierarchical circuitry controlling hypothalamo–pituitary–adrenocortical responsiveness," *Frontiers in Neuroendocrinology*, vol. 24, no. 3, pp. 151–180, 2003.

[15] M. Popoli, Z. Yan, B. S. McEwen, and G. Sanacora, "The stressed synapse: the impact of stress and glucocorticoids on glutamate transmission," *Nature Reviews Neuroscience*, vol. 13, no. 1, pp. 22–37, 2012.

[16] B. S. McEwen, N. P. Bowles, J. D. Gray et al., "Mechanisms of stress in the brain," *Nature Neuroscience*, vol. 18, no. 10, pp. 1353–1363, 2015.

[17] C. Zhao, W. Deng, and F. H. Gage, "Mechanisms and functional implications of adult neurogenesis," *Cell*, vol. 132, no. 4, pp. 645–660, 2008.

[18] G. L. Ming and H. Song, "Adult neurogenesis in the mammalian brain: significant answers and significant questions," *Neuron*, vol. 70, no. 4, pp. 687–702, 2011.

[19] J. T. GonÇalves, S. T. Schafer, and F. H. Gage, "Adult neurogenesis in the hippocampus: from stem cells to behavior," *Cell*, vol. 167, no. 4, pp. 897–914, 2016.

[20] P. J. Lucassen and C. A. Oomen, "Stress, hippocampal neurogenesis and cognition: functional correlations," *Frontiers in Biology*, vol. 11, no. 3, pp. 182–192, 2016.

[21] J. E. Malberg, A. J. Eisch, E. J. Nestler, and R. S. Duman, "Chronic antidepressant treatment increases neurogenesis in adult rat hippocampus," *The Journal of Neuroscience*, vol. 20, no. 24, pp. 9104–9110, 2000.

[22] T. M. Madsen, A. Treschow, J. Bengzon, T. G. Bolwig, O. Lindvall, and A. Tingstrom, "Increased neurogenesis in a model of electroconvulsive therapy," *Biological Psychiatry*, vol. 47, no. 12, pp. 1043–1049, 2000.

[23] M. Sairanen, "Brain-derived neurotrophic factor and antidepressant drugs have different but coordinated effects on neuronal turnover, proliferation, and survival in the adult dentate gyrus," *The Journal of Neuroscience*, vol. 25, no. 5, pp. 1089–1094, 2005.

[24] T. D. Perera, J. D. Coplan, S. H. Lisanby et al., "Antidepressant-induced neurogenesis in the hippocampus of adult nonhuman primates," *The Journal of Neuroscience*, vol. 27, no. 18, pp. 4894–4901, 2007.

[25] T. Kino, "Stress, glucocorticoid hormones, and hippocampal neural progenitor cells: implications to mood disorders," *Frontiers in Physiology*, vol. 6, p. 230, 2015.

[26] R. J. Schloesser, H. K. Manji, and K. Martinowich, "Suppression of adult neurogenesis leads to an increased

hypothalamo-pituitary-adrenal axis response," *Neuroreport*, vol. 20, no. 6, pp. 553–557, 2009.

[27] J. S. Snyder, A. Soumier, M. Brewer, J. Pickel, and H. A. Cameron, "Adult hippocampal neurogenesis buffers stress responses and depressive behaviour," *Nature*, vol. 476, no. 7361, pp. 458–461, 2011.

[28] T. J. Schoenfeld and E. Gould, "Stress, stress hormones, and adult neurogenesis," *Experimental Neurology*, vol. 233, no. 1, pp. 12–21, 2012.

[29] B. Seri, J. M. Garcı, B. S. Mcewen, and A. Alvarez-buylla, "Astrocytes give rise to new neurons in the adult mammalian hippocampus," *The Journal of Neuroscience*, vol. 21, no. 18, pp. 7153–7160, 2001.

[30] G. Ming and H. Song, "Adult neurogenesis in the mammalian brain: significant answers and significant questions," *Neuron*, vol. 70, no. 4, pp. 687–702, 2012.

[31] M. Covic, E. Karaca, and D. C. Lie, "Epigenetic regulation of neurogenesis in the adult hippocampus," *Heredity (Edinburg)*, vol. 105, no. 1, pp. 122–134, 2010.

[32] M. A. Bonaguidi, J. Song, G. Ming, and H. Song, "A unifying hypothesis on mammalian neural stem cell properties in the adult hippocampus," *Current Opinion in Neurobiology*, vol. 22, no. 5, pp. 754–761, 2012.

[33] M. A. Bonaguidi, M. A. Wheeler, J. S. Shapiro et al., "In vivo clonal analysis reveals self-renewing and multipotent adult neural stem cell characteristics," *Cell*, vol. 145, no. 7, pp. 1142–1155, 2011.

[34] S. M. G. Braun and S. Jessberger, "Adult neurogenesis: mechanisms and functional significance," *Development*, vol. 141, no. 10, pp. 1983–1986, 2014.

[35] H. A. Cameron and R. D. G. Mckay, "Adult neurogenesis produces a large pool of new granule cells in the dentate gyrus," *The Journal of Comparative Neurology*, vol. 435, no. 4, pp. 406–417, 2001.

[36] J. S. Snyder, J. S. Choe, M. A. Clifford et al., "Adult-born hippocampal neurons are more numerous, faster maturing, and more involved in behavior in rats than in mice," *The Journal of Neuroscience*, vol. 29, no. 46, pp. 14484–14495, 2009.

[37] P. S. Eriksson, E. Perfilieva, T. Björk-Eriksson et al., "Neurogenesis in the adult human hippocampus," *Nature Medicine*, vol. 4, no. 11, pp. 1313–1317, 1998.

[38] K. L. Spalding, O. Bergmann, K. Alkass et al., "Dynamics of hippocampal neurogenesis in adult humans," *Cell*, vol. 153, no. 6, pp. 1219–1227, 2013.

[39] E. Gould and H. A. Cameron, "Regulation of neuronal birth, migration and death in the rat dentate gyrus," *Developmental Neuroscience*, vol. 18, pp. 22–35, 1996.

[40] C. Mirescu and E. Gould, "Stress and adult neurogenesis," *Hippocampus*, vol. 16, no. 3, pp. 233–238, 2006.

[41] E. Gould, H. A. Cameron, D. C. Daniels, C. S. Woolley, and B. S. McEwen, "Adrenal hormones suppress cell division in the adult rat dentate gyrus," *The Journal of Neuroscience*, vol. 12, no. 9, pp. 3642–3650, 1992.

[42] H. A. Cameron and E. Gould, "Adult neurogenesis is regulated by adrenal-steroids in the dentate gyrus," *Neuroscience*, vol. 61, no. 2, pp. 203–209, 1994.

[43] H. A. Cameron and R. D. McKay, "Restoring production of hippocampal neurons in old age," *Nature Neuroscience*, vol. 2, no. 10, pp. 894–897, 1999.

[44] R. M. Sapolsky and M. Meaney, "Maturation of the adrenocortical stress response: neuroendocrine control mechanisms and the stress hyporesponsive period," *Brain Research*, vol. 396, no. 1, pp. 64–76, 1986.

[45] J. Altman and S. A. Bayer, "Migration and distribution of two populations of hippocampal granule cell precursors during the perinatal and postnatal periods," *The Journal of Comparative Neurology*, vol. 301, no. 3, pp. 365–381, 1990.

[46] P. Tanapat, L. A. Galea, and E. Gould, "Stress inhibits the proliferation of granule cell precursors in the developing dentate gyrus," *Internation of Journal Developmental Neuroscience*, vol. 16, no. 3-4, pp. 235–239, 1998.

[47] P. Tanapat, N. B. Hastings, T. A. Rydel, L. A. M. Galea, and E. Gould, "Exposure to fox odor inhibits cell proliferation in the hippocampus of adult rats via an adrenal hormone-dependent mechanism," *The Journal of Comparative Neurology*, vol. 437, no. 4, pp. 496–504, 2001.

[48] C. Mirescu, J. D. Peters, and E. Gould, "Early life experience alters response of adult neurogenesis to stress," *Nature Neuroscience*, vol. 7, no. 8, pp. 841–846, 2004.

[49] C. Anacker, A. Cattaneo, A. Luoni et al., "Glucocorticoid-related molecular signaling pathways regulating hippocampal neurogenesis," *Neuropsychopharmacology*, vol. 38, no. 5, pp. 872–883, 2013.

[50] E. Gould, B. S. S. McEwen, P. Tanapat, L. A. Galea, and E. Fuchs, "Neurogenesis in the dentate gyrus of the adult tree shrew is regulated by psychosocial stress and NMDA receptor activation," *The Journal of Neuroscience*, vol. 17, no. 7, pp. 2492–2498, 1997.

[51] E. Gould, P. Tanapat, B. S. Mcewen, G. Flgge, and E. Fuchs, "Proliferation of granule cell precursors in the dentate gyrus of adult monkeys is diminished by stress," *Neurobiology*, vol. 95, no. 6, pp. 3168–3171, 1998.

[52] J. E. Malberg and R. S. Duman, "Cell proliferation in adult hippocampus is decreased by inescapable stress: reversal by fluoxetine treatment," *Neuropsychopharmacology*, vol. 28, no. 9, pp. 1562–1571, 2003.

[53] K. Pham, J. Nacher, P. R. Hof, and B. S. McEwen, "Repeated restraint stress suppresses neurogenesis and induces biphasic PSA-NCAM expression in the adult rat dentate gyrus," *The European Journal of Neuroscience*, vol. 17, no. 4, pp. 879–886, 2003.

[54] M. J. Bain, S. M. Dwyer, and B. Rusak, "Restraint stress affects hippocampal cell proliferation differently in rats and mice," *Neuroscience Letters*, vol. 368, no. 1, pp. 7–10, 2004.

[55] V. M. Heine, S. Maslam, M. Joëls, and P. J. Lucassen, "Increased P27KIP1 protein expression in the dentate gyrus of chronically stressed rats indicates G 1 arrest involvement," *Neuroscience*, vol. 129, no. 3, pp. 593–601, 2004.

[56] E. M. Falconer and L. A. M. Galea, "Sex differences in cell proliferation, cell death and defensive behavior following acute predator odor stress in adult rats," *Brain Research*, vol. 975, no. 1-2, pp. 22–36, 2003.

[57] R. M. Thomas, J. H. Urban, and D. A. Peterson, "Acute exposure to predator odor elicits a robust increase in corticosterone and a decrease in activity without altering proliferation in the adult rat hippocampus," *Experimental Neurology*, vol. 201, no. 2, pp. 308–315, 2006.

[58] R. M. Thomas, G. Hotsenpiller, and D. A. Peterson, "Acute psychosocial stress reduces cell survival in adult hippocampal

neurogenesis without altering proliferation," *The Journal of Neuroscience*, vol. 27, no. 11, pp. 2734–2743, 2007.

[59] G. Dagyte, E. A. Van der Zee, F. Postema et al., "Chronic but not acute foot-shock stress leads to temporary suppression of cell proliferation in rat hippocampus," *Neuroscience*, vol. 162, no. 4, pp. 904–913, 2009.

[60] N. D. Hanson, M. J. Owens, K. A. Boss-Williams, J. M. Weiss, and C. B. Nemeroff, "Several stressors fail to reduce adult hippocampal neurogenesis," *Psychoneuroendocrinology*, vol. 36, no. 10, pp. 1520–1529, 2011.

[61] A. Alvarez-Buylla and D. A. Lim, "For the long run: maintaining germinal niches in the adult brain," *Neuron*, vol. 41, no. 5, pp. 683–686, 2004.

[62] M. A. Bonaguidi, C.-Y. Peng, T. McGuire et al., "Noggin expands neural stem cells in the adult hippocampus," *The Journal of Neuroscience*, vol. 28, no. 37, pp. 9194–9204, 2008.

[63] F. H. Gage, "Mammalian neural stem cells," *Science*, vol. 287, no. 5457, pp. 1433–1438, 2000.

[64] D. A. Lim, A. D. Tramontin, J. M. Trevejo, D. G. Herrera, J. M. García-Verdugo, and A. Alvarez-Buylla, "Noggin antagonizes BMP signaling to create a niche for adult neurogenesis," *Neuron*, vol. 28, no. 3, pp. 713–726, 2000.

[65] L. F. Bátiz, M. A. Castro, P. V. Burgos et al., "Exosomes as novel regulators of adult neurogenic niches," *Frontiers in Cellular Neuroscience*, vol. 9, pp. 1–28, 2016.

[66] B. S. Khakh and M. V. Sofroniew, "Diversity of astrocyte functions and phenotypes in neural circuits," *Nature Neuroscience*, vol. 18, no. 7, pp. 942–952, 2015.

[67] J. L. Orthmann-Murphy, C. K. Abrams, and S. S. Scherer, "Gap junctions couple astrocytes and oligodendrocytes," *Journal of Molecular Neuroscience*, vol. 35, no. 1, pp. 101–116, 2008.

[68] N. Kuga, T. Sasaki, Y. Takahara, N. Matsuki, and Y. Ikegaya, "Large-scale calcium waves traveling through astrocytic networks in vivo," *The Journal of Neuroscience*, vol. 31, no. 7, pp. 2607–2614, 2011.

[69] G. Kempermann, "Astrocytes, makers of new neurons," *Neuron*, vol. 88, no. 5, pp. 850-851, 2015.

[70] U. Wilhelmsson, M. Faiz, Y. De Pablo et al., "Astrocytes negatively regulate neurogenesis through the jagged1-mediated notch pathway," *Stem Cells*, vol. 30, no. 10, pp. 2320–2329, 2012.

[71] B. Z. Barkho, H. Song, J. B. Aimone et al., "Identification of astrocyte-expressed factors that modulate neural stem/progenitor cell differentiation," *Stem Cells and Development*, vol. 15, no. 3, pp. 407–421, 2006.

[72] T. Ueki, M. Tanaka, K. Yamashita et al., "A novel secretory factor, neurogenesin-1, provides neurogenic environmental cues for neural stem cells in the adult hippocampus," *The Journal of Neuroscience*, vol. 23, no. 37, pp. 11732–11740, 2003.

[73] Z. Lu and J. Kipnis, "Thrombospondin 1—a key astrocyte-derived neurogenic factor," *The FASEB Journal*, vol. 24, no. 6, pp. 1925–1934, 2010.

[74] R. S. Ashton, A. Conway, C. Pangarkar et al., "Astrocytes regulate adult hippocampal neurogenesis through ephrin-B signaling," *Nature Neuroscience*, vol. 15, no. 10, pp. 1399–1406, 2012.

[75] J. Oh, M. A. McCloskey, C. C. Blong, L. Bendickson, M. Nilsen-Hamilton, and D. S. Sakaguchi, "Astrocyte-derived interleukin-6 promotes specific neuronal differentiation of neural progenitor cells from adult hippocampus," *Journal of Neuroscience Research*, vol. 88, no. 13, pp. 2798–2809, 2010.

[76] S. Sultan, L. Li, J. Moss et al., "Synaptic integration of adult-born hippocampal neurons is locally controlled by astrocytes," *Neuron*, vol. 88, no. 5, pp. 957–972, 2015.

[77] H. Song, C. F. Stevens, and F. H. Gage, "Astroglia induce neurogenesis from adult neural stem cells," *Nature*, vol. 417, no. 6884, pp. 39–44, 2002.

[78] D. A. Lim and A. Alvarez-Buylla, "Interaction between astrocytes and adult subventricular zone precursors stimulates neurogenesis," *Proceedings of the National Academy of Sciences of the United States of America*, vol. 96, no. 13, pp. 7526–7531, 1999.

[79] F. Walker, M. Nilsson, and K. Jones, "Acute and chronic stress-induced disturbances of microglial plasticity, phenotype and function," *Current Drug Targets*, vol. 14, no. 11, pp. 1262–1276, 2013.

[80] J. C. Delpech, C. Madore, A. Nadjar, C. Joffre, E. S. Wohleb, and S. Layé, "Microglia in neuronal plasticity: influence of stress," *Neuropharmacology*, vol. 96, Part A, pp. 19–28, 2015.

[81] N. Edgar and E. Sibille, "A putative functional role for oligodendrocytes in mood regulation," *Translational Psychiatry*, vol. 2, no. 5, article e109, 2012.

[82] J. Pearson-leary, D. M. Osborne, and E. C. Mcnay, "Role of glia in stress-induced enhancement and impairment of memory," vol. 9, no. 63, pp. 1–14, 2016.

[83] B. Czéh, M. Simon, B. Schmelting, C. Hiemke, and E. Fuchs, "Astroglial plasticity in the hippocampus is affected by chronic psychosocial stress and concomitant fluoxetine treatment," *Neuropsychopharmacology*, vol. 31, no. 8, pp. 1616–1626, 2006.

[84] Y. Ye, G. Wang, H. Wang, and X. Wang, "Brain-derived neurotrophic factor (BDNF) infusion restored astrocytic plasticity in the hippocampus of a rat model of depression," *Neuroscience Letters*, vol. 503, no. 1, pp. 15–19, 2011.

[85] J.-D. Sun, Y. Liu, Y.-H. Yuan, J. Li, and N.-H. Chen, "Gap junction dysfunction in the prefrontal cortex induces depressive-like behaviors in rats," *Neuropsychopharmacology*, vol. 37, no. 5, pp. 1305–1320, 2012.

[86] R. J. Tynan, S. B. Beynon, M. Hinwood et al., "Chronic stress-induced disruption of the astrocyte network is driven by structural atrophy and not loss of astrocytes," *Acta Neuropathologica*, vol. 126, no. 1, pp. 75–91, 2013.

[87] S. Jang, S. H. Suh, H. S. Yoo, Y. M. Lee, and S. Oh, "Changes in iNOS, GFAP and NR1 expression in various brain regions and elevation of sphingosine-1-phosphate in serum after immobilized stress," *Neurochemical Research*, vol. 33, no. 5, pp. 842–851, 2008.

[88] M. S. Kwon, Y. J. Seo, J. K. Lee et al., "The repeated immobilization stress increases IL-1B immunoreactivities in only neuron, but not astrocyte or microglia in hippocampal CA1 region, striatum and paraventricular nucleus," *Neuroscience Letters*, vol. 430, no. 3, pp. 258–263, 2008.

[89] G. Rajkowska and C. A. Stockmeier, "Astrocyte pathology in major depressive disorder: insights from human postmortem brain tissue," *Current Drug Targets*, vol. 14, no. 11, pp. 1225–1236, 2013.

[90] Y. Zhao, Q. Zhang, X. Shao et al., "Decreased glycogen content might contribute to chronic stress-induced atrophy of hippocampal astrocyte volume and depression- like behavior in rats," *Scientific Reports*, vol. 7, pp. 1–14, 2017.

[91] E. M. Gubba, J. W. Fawcett, and J. Herbert, "The effects of corticosterone and dehydroepiandrosterone on neurotrophic factor mRNA expression in primary hippocampal and astrocyte cultures," *Molecular Brain Research*, vol. 127, no. 1-2, pp. 48–59, 2004.

[92] H. Chipperfield, K. S. Bedi, S. M. Cool, and V. Nurcombe, "Heparan sulfates isolated from adult neural progenitor cells can direct phenotypic maturation," *The International Journal of Developmental Biology*, vol. 46, no. 4, pp. 661–670, 2002.

[93] A. Verkhratsky, M. Matteoli, V. Parpura, J.-P. Mothet, and R. Zorec, "Astrocytes as secretory cells of the central nervous system: idiosyncrasies of vesicular secretion," *The EMBO Journal*, vol. 35, no. 3, pp. 239–257, 2016.

[94] C. Harding, J. Heuser, and P. Stahl, "Receptor-mediated endocytosis of transferrin and recycling of the transferrin receptor in rat reticulocytes," *The Journal of Cell Biology*, vol. 97, no. 2, pp. 329–339, 1983.

[95] C. Théry, "Exosomes: secreted vesicles and intercellular communications," *F1000 Biology Reports*, vol. 3, p. 15, 2011.

[96] G. van Niel, I. Porto-Carreiro, S. Simoes, and G. Raposo, "Exosomes: a common pathway for a specialized function," *Journal of Biochemistry*, vol. 140, no. 1, pp. 13–21, 2006.

[97] J. H. Hurley, "ESCRT complexes and the biogenesis of multivesicular bodies," *Current Opinion in Cell Biology*, vol. 20, no. 1, pp. 4–11, 2008.

[98] W. M. Henne, H. Stenmark, and S. D. Emr, "Molecular mechanisms of the membrane sculpting ESCRT pathway," *Cold Spring Harbor Perspectives in Medicine*, vol. 3, no. 10, pp. 1–12, 2013.

[99] K. Trajkovic, C. Hsu, S. Chiantia et al., "Ceramide triggers budding of exosome vesicles into multivesicular endosomes," *Science*, vol. 319, no. 5867, pp. 1244–1247, 2008.

[100] F. Bianco, C. Perrotta, L. Novellino et al., "Acid sphingomyelinase activity triggers microparticle release from glial cells," *The EMBO Journal*, vol. 28, no. 8, pp. 1043–1054, 2009.

[101] G. Raposo and W. Stoorvogel, "Extracellular vesicles: exosomes, microvesicles, and friends," *The Journal of Cell Biology*, vol. 200, no. 4, pp. 373–383, 2013.

[102] L. O'Driscoll, "Expanding on exosomes and ectosomes in cancer," *The New England Journal of Medicine*, vol. 372, no. 24, pp. 2359–2362, 2015.

[103] M. Simons and G. Raposo, "Exosomes – vesicular carriers for intercellular communication," *Current Opinion in Cell Biology*, vol. 21, no. 4, pp. 575–581, 2009.

[104] M. Colombo, G. Raposo, and C. Théry, "Biogenesis, secretion, and intercellular interactions of exosomes and other extracellular vesicles," *Annual Review of Cell and Developmental Biology*, vol. 30, pp. 255–289, 2014.

[105] M. A. Lopez-Verrilli and F. A. Court, "Exosomes: mediators of communication in eukaryotes," *Biological Research*, vol. 46, no. 1, pp. 5–11, 2013.

[106] A. Luarte, L. F. Bátiz, U. Wyneken, and C. Lafourcade, "Potential therapies by stem cell-derived exosomes in CNS diseases: focusing on the neurogenic niche," *Stem Cells International*, vol. 2016, Article ID 5736059, 16 pages, 2016.

[107] V. Budnik, C. Ruiz-Cañada, and F. Wendler, "Extracellular vesicles round off communication in the nervous system," *Nature Reviews Neuroscience*, vol. 17, no. 3, pp. 160–172, 2016.

[108] D. M. Pegtel, L. Peferoen, and S. Amor, "Extracellular vesicles as modulators of cell-to-cell communication in the healthy and diseased brain," *Philosophical Transactions of the Royal Society of London, Series B: Biological Sciences*, vol. 369, no. 1652, 2014.

[109] D. Brites and A. Fernandes, "Neuroinflammation and depression: microglia activation, extracellular microvesicles and microRNA dysregulation," *Frontiers in Cellular Neuroscience*, vol. 9, p. 476, 2015.

[110] L. Zhang, S. Zhang, J. Yao et al., "Microenvironment-induced PTEN loss by exosomal microRNA primes brain metastasis outgrowth," *Nature*, vol. 527, no. 7576, pp. 100–104, 2015.

[111] T. Katsuda and T. Ochiya, "Molecular signatures of mesenchymal stem cell-derived extracellular vesicle-mediated tissue repair," *Stem Cell Research & Therapy*, vol. 6, p. 212, 2015.

[112] H. Guo, N. Ignolia, J. Wiessman, and D. Bartel, "Mammalian microRNAs predominantly act to decrease target mRNA levels," *Lung*, vol. 466, no. 7308, pp. 835–840, 2011.

[113] W. Gao, X. Lu, L. Liu, J. Xu, D. Feng, and Y. Shu, "MiRNA-21: a biomarker predictive for platinum-based adjuvant chemotherapy response in patients with non-small cell lung cancer," *Cancer Biology & Therapy*, vol. 13, no. 5, pp. 330–340, 2012.

[114] J. Hausser and M. Zavolan, "Identification and consequences of miRNA-target interactions—beyond repression of gene expression," *Nature Reviews Genetics*, vol. 15, no. 9, pp. 599–612, 2014.

[115] Y. Kawase-Koga, G. Otaegi, and T. Sun, "Different timings of Dicer deletion affect neurogenesis and gliogenesis in the developing mouse central nervous system," *Developmental Dynamics*, vol. 238, no. 11, pp. 2800–2812, 2009.

[116] W. H. Neo, K. Yap, S. H. Lee et al., "MicroRNA miR-124 controls the choice between neuronal and astrocyte differentiation by fine-tuning Ezh2," *Nature Structural & Molecular Biology*, vol. 289, no. 30, pp. 20788–20801, 2014.

[117] M. Akerblom, R. Sachdeva, I. Barde et al., "MicroRNA-124 is a subventricular zone neuronal fate determinant," *The Journal of Neuroscience*, vol. 32, no. 26, pp. 8879–8889, 2012.

[118] C. Zhao, G. Sun, S. Li, Y. Shi, and D. Discovery, "A feedback regulatory loop involving microRNA-9 and nuclear receptor TLX in neural stem cell fate determination," *Nature Structural & Molecular Biology*, vol. 16, no. 4, pp. 365–371, 2009.

[119] M. C. Santos, A. N. Tegge, B. R. Correa, S. Mahesula, and L. O. Kohnke, "miR-124, −128, and −137 orchestrate neural differentiation by acting on overlapping gene sets containing a highly connected transcription factor network," *Stem Cells*, vol. 34, no. 1, pp. 220–232, 2016.

[120] J. Han, H. J. Kim, S. T. Schafer et al., "Functional implications of miR-19 in the migration of newborn neurons in the adult brain article functional implications of miR-19 in the migration of newborn neurons in the adult brain," *Neuron*, vol. 91, no. 1, pp. 79–89, 2016.

[121] Y. Cui, J. Han, Z. Xiao et al., "The miR-20-Rest-Wnt signaling axis regulates neural progenitor cell differentiation," *Scientific Reports*, vol. 6, article 23300, 2016.

[122] K. E. Szulwach, X. Li, R. D. Smrt et al., "Cross talk between microRNA and epigenetic regulation in adult neurogenesis," *The Journal of Cell Biology*, vol. 189, no. 1, pp. 127–141, 2010.

[123] Y. Zhang, Y. Ueno, X. S. Liu et al., "The MicroRNA-17-92 cluster enhances axonal outgrowth in embryonic cortical neurons," *The Journal of Neuroscience*, vol. 33, no. 16, pp. 6885–6894, 2013.

[124] Y. Dwivedi, "Emerging role of microRNAs in major depressive disorder: diagnosis and therapeutic implications," *Dialogues in Clinical Neuroscience*, vol. 16, no. 1, pp. 43–61, 2014.

[125] D. Brites and A. Fernandes, "Neuroinflammation and depression: microglia activation, extracellular microvesicles and microRNA dysregulation," *Frontiers in Cellular Neuroscience*, vol. 9, no. 476, pp. 1–20, 2015.

[126] R. M. O. Connor, S. Grenham, T. G. Dinan, and J. F. Cryan, "microRNAs as novel antidepressant targets: converging effects of ketamine and electroconvulsive shock therapy in the rat hippocampus," *The International Journal of Neuropsychopharmacology*, vol. 16, no. 8, pp. 1885–1892, 2013.

[127] A. Jovičić and A. D. Gitler, "Distinct repertoires of microRNAs present in mouse astrocytes compared to astrocyte-secreted exosomes," *PLoS One*, vol. 12, no. 2, article e0171418, 2017.

[128] S. Yu, S. Yang, F. Holsboer, N. Sousa, and O. F. X. Almeida, "Glucocorticoid regulation of astrocytic fate and function," *PLoS One*, vol. 6, no. 7, article e22419, 2011.

[129] K. Unemura, T. Kume, M. Kondo, Y. Maeda, Y. Izumi, and A. Akaike, "Glucocorticoids decrease astrocyte numbers by reducing glucocorticoid receptor expression in vitro and in vivo," *Journal of Pharmacological Sciences*, vol. 119, no. 1, pp. 30–39, 2012.

[130] B. S. Carter, D. E. Hamilton, and R. C. Thompson, "Acute and chronic glucocorticoid treatments regulate astrocyte-enriched mRNAs in multiple brain regions in vivo," *Frontiers in Neuroscience*, vol. 7, no. 7, p. 139, 2013.

[131] E. D. Kirby, S. E. Muroy, W. G. Sun et al., "Acute stress enhances adult rat hippocampal neurogenesis and activation of newborn neurons via secreted astrocytic FGF2," *eLife*, vol. 2, article e00362, 2013.

[132] F. Dajas-bailador, B. Bonev, P. Garcez, P. Stanley, F. Guillemot, and N. Papalopulu, "microRNA-9 regulates axon extension and branching by targeting Map1b in mouse cortical neurons," *Nature Neuroscience*, vol. 15, no. 5, pp. 697–699, 2012.

[133] L. Stappert, B. Roese-koerner, and O. Brüstle, "The role of microRNAs in human neural stem cells, neuronal differentiation and subtype specification," *Cell and Tissue Research*, vol. 359, no. 1, pp. 47–64, 2015.

[134] P. Bielefield, C. Mooney, D. Henshall, and C. Fitzsimons, "miRNA-mediated regulation of adult hippocampal neurogenesis; implications for epilepsy," *Brain Plasticity*, pp. 1–17, 2016.

[135] J. Zhao, Q. Lin, K. J. Kim, F. D. Dardashti, and J. Kim, "Ngn1 inhibits astrogliogenesis through induction of miR-9 during neuronal fate specification," *eLife*, vol. 4, article e06885, 2015.

[136] H. Kawahara, T. Imai, and H. Okano, "MicroRNAs in neural stem cells and neurogenesis," *Frontiers in Neuroscience*, vol. 6, no. 30, pp. 1–13, 2012.

[137] A. M. Krichevsky, K.-C. Sonntag, O. Isacson, and K. S. Kosik, "Specific microRNAs modulate embryonic stem cell-derived neurogenesis," *Stem Cells*, vol. 24, no. 4, pp. 857–864, 2006.

[138] T. Wakabayashi, R. Hidaka, and S. Fujimaki, "MicroRNAs and epigenetics in adult neurogenesis," *Advances in Genetics*, vol. 86, pp. 27–44, 2014.

[139] B. Bonev, P. Stanley, and N. Papalopulu, "MicroRNA-9 modulates *Hes1* ultradian oscillations by forming a double-negative feedback loop," *Cell Reports*, vol. 2, no. 1, pp. 10–18, 2012.

[140] Q.-H. Gu, D. Yu, Z. Hu et al., "miR-26a and miR-384-5p are required for LTP maintenance and spine enlargement," *Nature Communications*, vol. 6, p. 6789, 2015.

[141] J.-J. Jiang, C.-M. Liu, B.-Y. Zhang et al., "MicroRNA-26a supports mammalian axon regeneration *in vivo* by suppressing GSK3β expression," *Cell Death & Disease*, vol. 6, no. 8, article e1865, 2015.

[142] H. Dill, B. Linder, and A. Fehr, "Intronic miR-26b controls neuronal differentiation by repressing its host transcript, ctdsp2," *Genes & Development*, vol. 26, no. 1, pp. 25–30, 2012.

[143] H. Li, S. Mao, H. Wang, K. Zen, C. Zhang, and L. Li, "MicroRNA-29a modulates axon branching by targeting doublecortin in primary neurons," *Protein & Cell*, vol. 5, no. 2, pp. 160–169, 2014.

[144] M. Agostini, P. Tucci, R. Killick et al., "Neuronal differentiation by TAp73 is mediated by microRNA-34a regulation of synaptic protein targets," *Proceedings of the National Academy of Sciences of the United States of America*, vol. 108, no. 52, pp. 21093–21098, 2011.

[145] Y. Cui, Z. Xiao, J. Han et al., "MiR-125b orchestrates cell proliferation, differentiation and migration in neural stem/progenitor cells by targeting Nestin," *BMC Neuroscience*, vol. 13, no. 1, p. 116, 2012.

[146] U. Gioia, V. Di Carlo, P. Caramanica et al., "Mir-23a and mir-125b regulate neural stem/progenitor cell proliferation by targeting Musashi1," *RNA Biology*, vol. 11, no. 9, pp. 1105–1112, 2014.

[147] S. Decembrini, D. Bressan, R. Vignali et al., "MicroRNAs couple cell fate and developmental timing in retina," *Proceedings of the National Academy of Sciences of the United States of America*, vol. 106, no. 50, pp. 21179–21184, 2009.

[148] A. Bhinge, J. Poschmann, S. C. Namboori et al., "MiR-135b is a direct PAX6 target and specifies human neuroectoderm by inhibiting TGF- b/BMP signaling," *The EMBO Journal*, vol. 33, no. 11, pp. 1271–1283, 2014.

[149] N. Xu, T. Papagiannakopoulos, G. Pan, J. A. Thomson, and K. S. Kosik, "MicroRNA-145 regulates OCT4, SOX2, and KLF4 and represses pluripotency in human embryonic stem cells," *Cell*, vol. 137, no. 4, pp. 647–658, 2009.

[150] A. L. Morgado, M. Rodrigues, and S. Solá, "MicroRNA-145 regulates neural stem cell differentiation through the Sox2-Lin28/let-7 signaling pathway," *Stem Cells*, vol. 34, no. 5, pp. 1386–1395, 2016.

[151] H. Cheng, L. Zhou, B. Li, and M. Zhu, "Nano-topology guided neurite outgrowth in PC12 cells is mediated by miRNAs," *Nanomedicine Nanotechnology, Biology and Medicine*, vol. 10, no. 8, pp. 1871–1875, 2014.

[152] C. Zhao, G. Sun, S. Li et al., "MicroRNA let-7b regulates neural stem cell proliferation and differentiation by targeting nuclear receptor TLX signaling," *Proceedings of the National Academy of Sciences*, vol. 107, no. 5, pp. 1876–1881, 2010.

[153] L. Rago, R. Beattie, V. Taylor, and J. Winter, "miR 379 – 410 cluster miRNAs regulate neurogenesis and neuronal migration by fine-tuning N-cadherin," *The EMBO Journal*, vol. 33, no. 8, pp. 906–920, 2014.

[154] J. O. Brett, V. M. Renault, V. A. Rafalski, A. E. Webb, A. Brunet, and N. Program, "The MicroRNA cluster miR-106b ~ 25 regulates adult neural stem/progenitor cell proliferation and neuronal differentiation," *Aging (Albany NY)*, vol. 3, no. 2, pp. 108–124, 2011.

[155] T. J. Nowakowski, V. Fotaki, A. Pollock, T. Sun, T. Pratt, and D. J. Price, "MicroRNA-92b regulates the development of intermediate cortical progenitors in embryonic mouse brain,"

Proceedings of the National Academy of Sciences, vol. 110, no. 17, pp. 7056–7061, 2013.

[156] C. Liu, Z.-Q. Teng, N. J. Santistevan et al., "Epigenetic regulation of miR-184 by MBD1 governs neural stem cell proliferation and differentiation," *Cell Stem Cell*, vol. 6, no. 5, pp. 433–444, 2010.

[157] I. Lipchina, Y. Elkabetz, M. Hafner et al., "Genome-wide identification of microRNA targets in human ES cells reveals a role for miR-302 in modulating BMP response," *Genes & Development*, vol. 25, no. 20, pp. 2173–2186, 2011.

[158] Z. Du, L. Ma, C. Phillips, and S. Zhang, "miR-200 and miR-96 families repress neural induction from human embryonic stem cells," *Development*, vol. 140, no. 12, pp. 2611–2618, 2013.

[159] C. Xu, Y. Zhang, H. Zheng, H. Loh, and P. Law, "Morphine modulates mouse hippocampal progenitor cell lineages by up-regulating miR-181a level," *Stem Cells*, vol. 32, no. 11, pp. 2961–2972, 2014.

[160] Q. Wu, L. Zhang, P. Law, L. Wei, and H. H. Loh, "Long-term morphine treatment decreases the association of μ-opioid receptor (MOR1) mRNA with polysomes through miRNA23b," *Molecular Pharmacology*, vol. 75, no. 4, pp. 744–750, 2009.

[161] H. Zheng, Y. Zeng, X. Zhang, J. Chu, H. H. Loh, and P. Law, "μ-Opioid receptor agonists differentially regulate the expression of miR-190 and NeuroD," *Molecular Pharmacology*, vol. 77, no. 1, pp. 102–109, 2010.

[162] S. Pati, N. E. Supeno, S. Muthuraju et al., "MicroRNA profiling reveals unique miRNA signatures in IGF-1 treated embryonic striatal stem cell fate decisions in striatal neurogenesis *in vitro*," *BioMed Research International*, vol. 2014, Article ID 503162, 14 pages, 2014.

Hindawi
Stem Cells International
Volume 2017, Article ID 6374504, 10 pages
https://doi.org/10.1155/2017/6374504

Review Article

Human Long Noncoding RNA Regulation of Stem Cell Potency and Differentiation

Seahyoung Lee,[1] Hyang-Hee Seo,[2] Chang Youn Lee,[3] Jiyun Lee,[2] Sunhye Shin,[3] Sang Woo Kim,[1] Soyeon Lim,[1] and Ki-Chul Hwang[1]

[1]*Institute for Biomedical Convergence, College of Medicine, Catholic Kwandong University, Gangneung-si, Gangwon-do, Republic of Korea*
[2]*Brain Korea 21 PLUS Project for Medical Science, Yonsei University, Seoul, Republic of Korea*
[3]*Department of Integrated Omics for Biomedical Sciences, Yonsei University, Seoul, Republic of Korea*

Correspondence should be addressed to Soyeon Lim; slim724@cku.ac.kr and Ki-Chul Hwang; kchwang@cku.ac.kr

Received 27 April 2017; Revised 12 July 2017; Accepted 2 August 2017; Published 30 August 2017

Academic Editor: Mark W. Hamrick

Because of their capability of differentiation into lineage-specific cells, stem cells are an attractive therapeutic modality in regenerative medicine. To develop an effective stem cell-based therapeutic strategy with predictable results, deeper understanding of the underlying molecular mechanisms of stem cell differentiation and/or pluripotency maintenance is required. Thus, reviewing the key factors involved in the transcriptional and epigenetic regulation of stem cell differentiation and maintenance is important. Accumulating data indicate that long noncoding RNAs (lncRNAs) mediate numerous biological processes, including stem cell differentiation and maintenance. Here, we review recent findings on the human lncRNA regulation of stem cell potency and differentiation. Although the clinical implication of these lncRNAs is only beginning to be elucidated, it is anticipated that lncRNAs will become important therapeutic targets in the near future.

1. Introduction

Stem cells are specialized cells capable of differentiating into lineage-specific cells. Depending on their potential to differentiate and source of origin, stem cells can be broadly categorized into embryonic stem cells (ESCs), induced pluripotent stem cells (iPSCs), and adult stem cells such as bone marrow mesenchymal stem cells (BM-MSCs) and adipose-derived stem cells (ADSCs). Due to their differentiation and self-renewal abilities, stem cells have been highly regarded as an effective therapeutic modality in regenerative medicine [1]. Effective stem cell therapeutics should be based on a meticulously designed strategy, especially if the goal of stem cell-based therapy involves in situ differentiation of stem cells. In other words, to develop an effective stem cell-based therapeutic strategy with predictable results, deeper understanding of the underlying molecular mechanisms of stem cell differentiation and/or pluripotency maintenance is required. Therefore, it is worth reviewing the key factors involved in the transcriptional and epigenetic regulation of stem cell differentiation and maintenance. One of such key factors of stem cell biology is a group of noncoding RNAs (ncRNAs) [2, 3].

A large portion of the human genome is transcribed into RNAs without coding proteins. Noncoding RNAs are such RNAs that are not translated into proteins. Based on their sizes, they can be classified into the following 2 categories: small ncRNAs and long ncRNAs. Small ncRNAs refer to ncRNAs shorter than 200 nucleotides long, while long ncRNAs (lncRNAs) refer to ncRNAs composed of 200 or more nucleotides. Small ncRNAs can be further categorized into subcategories based on their length, function, and subcellular localization such as microRNAs (miRNAs), short interfering RNAs (siRNAs), Piwi-interacting RNAs (piRNAs), small nucleolar RNAs (snoRNAs), short hairpin RNAs (shRNA), and other short RNAs [4, 5]. These small ncRNAs have been implicated in stem cell biology, and many excellent articles on the role of these small ncRNAs in stem cell biology

are already available [6–8]. Therefore, only the lncRNAs with documented functions affecting human stem cell biology will be discussed in this particular review.

2. General Regulatory Mechanisms of lncRNA

LncRNAs are a class of RNAs that do not encode proteins but participate in multiple biological processes. Thanks to the advanced RNA sequencing technology, the number of sequence-verified lncRNAs is rapidly increasing [9]. The transcriptional process of lncRNAs is the same as that of protein-coding messenger RNAs (mRNAs). RNA polymerase II (PolII) transcribes lncRNAs from genomic loci, and the transcribed lncRNAs are frequently 5′ capped, spliced, and polyadenylated [10]. Except few specific characteristics of lncRNAs (lack of translated open reading frames, relatively shorter length, and poor conservation of primary sequence [11]), there is no known fundamental biochemical difference between messenger RNAs (mRNAs) and lncRNAs. A recent review authored by Quinn and Chang can provide more information on the general lifecycle of lncRNAs and known functions in depth [12]. Accumulating data indicates that lncRNAs mediate numerous regulatory processes such as imprinting genomic loci, chromosomal conformation, and allosteric regulation of enzyme activity [13, 14]. LncRNA-mediated regulatory mechanisms are diverse, and few examples of the regulatory mechanisms of lncRNAs are described in Figure 1.

In cytoplasm, lncRNAs can regulate gene expression by modulating turnover, translation, or suppression of partially complementary mRNAs [15]. It has been reported that a double-stranded structure formed by the interaction between the Alu elements of lncRNAs and the complementary Alu elements in the 3′ untranslated region of an mRNA facilitates Staufen-mediated mRNA turnover [16]. As an example of lncRNA-mediated mRNA translation, it has been reported that lncRNA containing short interspersed nuclear elements B2 (SINEB2) repeats increased ubiquitin carboxy-terminal hydrolase L1 (Uchl1) mRNA translation through association with the 5′ region [17]. LncRNAs can also block miRNA-mediated silencing of an mRNA by masking the miRNA-binding sites on a target mRNA [18]. Some lncRNAs can act as a sponge for endogenous miRNAs, neutralizing miRNA-mediated silencing of mRNAs [19, 20]. LncRNA-mediated signaling pathway modulation in cytoplasm also has been reported. According to a previous study, NF-kappaB interacting LncRNA (NKILA) inhibits NF-κB signaling by masking the IκB phosphorylation sites of NF-κB/IκB complex, stabilizing the complex [21].

Nuclear lncRNAs can act as an epigenetic regulator or a guide by recruiting chromatin modification factors to locus. For example, lncRNA PVT1 has been reported to recruit enhancer of zeste homolog 2 (EZH2, a histone modifying enzyme) to the large tumor suppressor kinase 2 (LATS2) promoter, repressing LATS2 transcription [22]. As scaffolds, nuclear lncRNAs bring together multiple proteins to form ribonucleoprotein (RNP) complexes. Such lncRNA-RNP complexes can either affect histone modifications or stabilize signaling complexes or nuclear structures [23]. Another way of nuclear lncRNA facilitating gene expression is acting as decoys. Decoy lncRNAs modulate transcription by sequestering regulatory factors such as transcription factors and catalytic proteins, rendering them less available for transcription [24]. Additionally, lncRNAs can regulate mRNA splicing process. For example, metastasis-associated lung adenocarcinoma transcript 1 (MALAT-1) regulates alternative splicing by modulating the phosphorylation of serine/arginine splicing factors [25].

3. Human lncRNA in Stem Cells

During the last few years, a number of good reviews on the role of lncRNAs in stem cell biology have been published [2, 26–28]. However, those previous reviews were not specific to the lncRNAs reported to exist in human. Although animal models (i.e., mouse) provide us a great deal of information that can be directly applied to human biology, not all the information obtained from animal studies can be applied to humans. In fact, studies have indicated that lncRNAs are less conserved than protein-coding genes [11, 29]. According to a previous study conducted a clone-based genome assembly of mouse, only a small portion of mouse lncRNAs had evidence of human expression [30]. This particular study indicated that only half of the mouse lncRNA sequences (1538 out of 3051 mouse lncRNAs documented) could be mapped to the human genome assembly, and furthermore, only 14% of the mouse lncRNA sequences (439 out of 3051 mouse lncRNAs documented) had evidence of orthologous transcription in human based on expressed sequence tag (EST) or cDNA. Of course, those lncRNAs lacking evidence of human orthologs may be simply unidentified in humans as yet. However, it is still worth summarizing lncRNAs identified in human stem cells considering that one of the major purposes of studying stem cell regulation is to develop more effective clinical strategies utilizing stem cells. Therefore, this review deals with the lncRNAs (1) whose regulatory function has been confirmed in human stem cells or (2) whose existence has been verified in human and the function of its orthologs from other species has been reported in stem cells.

3.1. Eosinophil Granule Ontogeny (EGO). In 2007, Wagner and colleagues first identified EGO as a long noncoding RNA nested within an intron of inositol triphosphate receptor type 1 (ITPR1) by demonstrating that EGO transcript was not associated with ribosomes [31]. According to their study, the transcript level of EGO increased during interleukin-5-(IL-5-) induced eosinophil differentiation of human $CD34^+$ hematopoietic stem cells from healthy donors. Silencing EGO subsequently decreased the mRNA expression of major basic protein (MBP) and eosinophil-derived neurotoxin (EDN), suggesting that EGO was required to maintain normal level of MBP and EDN during eosinophilopoiesis of umbilical cord blood $CD34^+$ cells. EGO acting as a small interfering RNA (siRNA) or protecting mRNAs from degradation by forming an RNA-protein complex has been proposed as possible mechanisms.

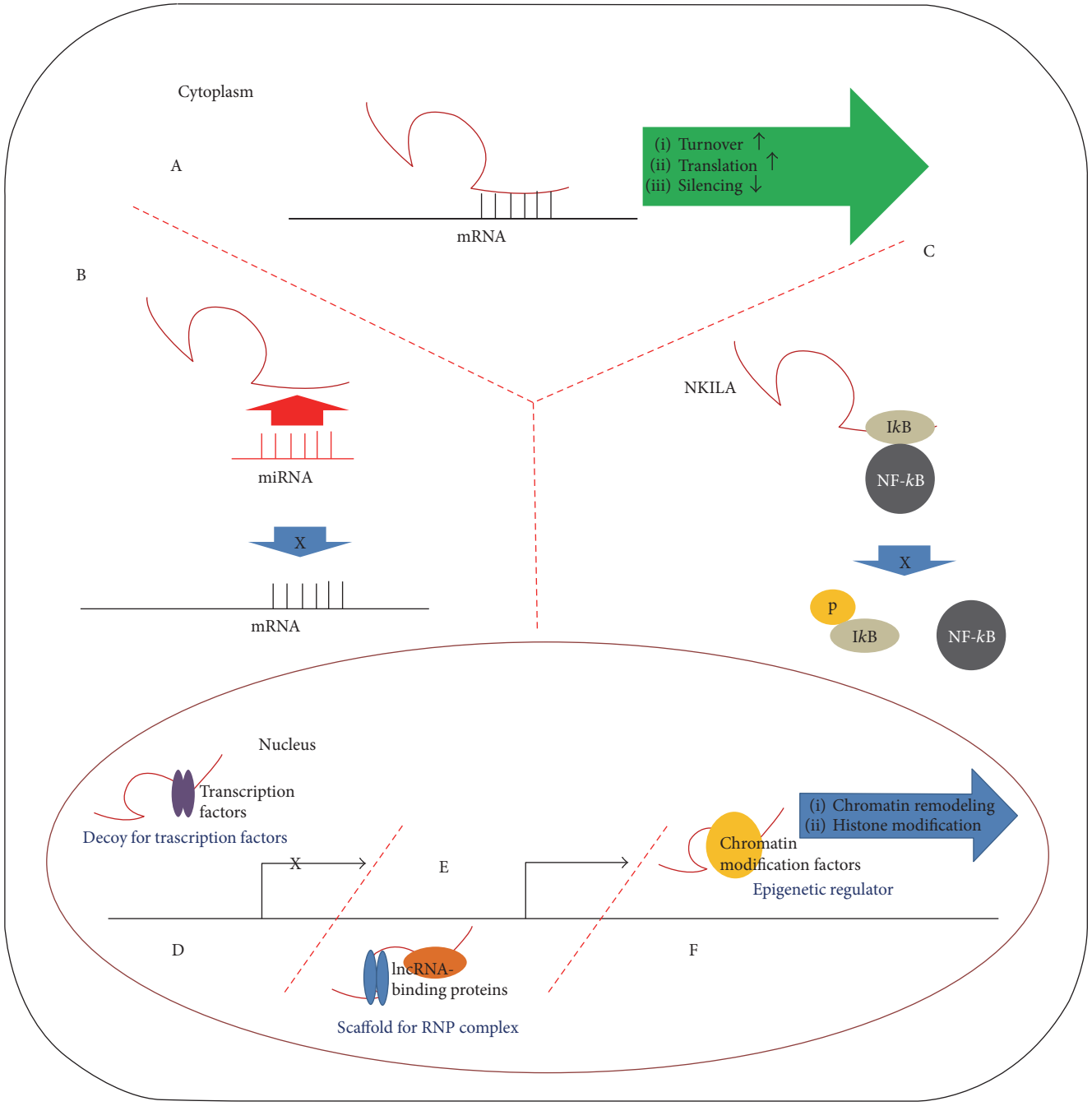

Figure 1: Schematic diagram of lncRNA-mediated regulatory mechanism. In cytoplasm, (A) lncRNAs can regulate turnover, translation, and silencing of partially complementary mRNAs. (B) lncRNAs can act as a miRNA sponge, reducing miRNA availability. (C) lncRNAs can modulate signaling pathways by interacting with signaling molecules. In nucleus, (D) nuclear lncRNAs can be decoys for regulatory proteins such as transcription factor. (E) Nuclear lncRNAs can serve as a scaffold for RNA-protein complex. RNP: ribonucleoprotein. (F) Nuclear lncRNAs can be an epigenetic regulator by recruiting chromatin modification factors.

3.2. Gomafu (Alias: MIAT or RNCR2). In 2004, retinal noncoding RNA 2 (RNCR2) was first reported in the developing retina of mouse with nuclear- or perinuclear-localized expression pattern [32]. More recent study reported that nuclear-localized RNCR2 regulates retinal cell specification acting as a suppressor of differentiation into amacrine interneurons and Müller glia cells [33]. In between those two studies mentioned above, Sone and colleagues reported a noble mRNA-like noncoding gene named Gomafu (meaning "spotted pattern" in Japanese) as a neuron-specific component of the nuclear matrix [34]. They found that Gomafu shares homologous region with RNCR2 and that human homologous sequence was located in a syntenic region of chromosome 22q12. As to the role of Gomafu in stem cell biology, it has been suggested that Gomafu and Oct4 establish an autofeedback loop to maintain pluripotency of mouse

embryonic stem cells (mESCs) [35]. RNAi-mediated downregulation of Gomafu led to downregulation of Oct4, along with decreased expression of Oct4-driven pluripotency markers, such as Sox2, Klf4, Gdf3, Fgf4, and Dppa3/Stella. On the other hand, RNAi specific to Gomafu increased the expression of trophoblast markers such as Cdx2, Hand1, Eomes, and Gata3 [36–38], suggesting a possible role of Gomafu as an endogenous inhibitor of differentiation along the trophoblast lineage.

Gomafu was also involved in neurogenesis and oligodendrocyte (OL) lineage specification of neural stem cells (NSCs) [39]. Gradient of sonic hedgehog (Shh) signaling promotes differentiation of nestin-positive NSC in the ventral forebrain into bipotent Nkx2.1-expressing bipotent neuronal-OL progenitor (N/OP) that can be further differentiated into GABAergic neurons (GABANs) and OLs [40]. During basic fibroblast growth factor (bFGF) and N-terminal active form of sonic hedgehog- (N-Shh-) induced N/OP differentiation of NSCs, Gomafu was downregulated but increased again in OL lineage specification and maturation [39]. However, the underlying mechanisms of Gomafu regulation or functional consequences have not been elucidated. Another alias of Gomafu is myocardial infarction-associated transcript (MIAT) [41]. A very recent study reported that knockdown of MIAT promoted osteogenic differentiation of human adipose-derived stem cells (hASCs), suggesting its role as an endogenous suppressor of osteogenic differentiation of stem cells [42]. Nevertheless, the underlying mechanisms remain unexplored.

3.3. Embryonic Ventral Forebrain 2 (Evf2). Evf2 is an antisense lncRNA to distal-less homeobox 6 (Dlx-6) genes of Dlx-5/6 cluster, and it forms a complex with Dlx-2 to increase the activity of Dlx-5/6 enhancer during neurogenesis [43]. Evf2 is transcribed from the Dlx-5/6 intergenic enhancer elements ei and transcripts analysis using human EST database indicated that it is conserved in human. Although no specific function of Evf2 in stem cell has been elucidated, it has been reported that its expression increased during GABAN differentiation of N/OP [39].

3.4. Metastasis-Associated Lung Adenocarcinoma Transcript 1 (MALAT-1). MALAT-1 is an oncogenic lncRNA conserved across several species including human and highly expressed in lung, pancreas, and non-small-cell lung cancer [44]. It was first reported in cancer, and accumulating data also indicate it plays significant roles in cancer stem cell biology. MALAT-1 has been reported to activate the transcription of latent-transforming growth factor beta-binding protein 3 (LTBP3), a transforming growth factor beta (TGF-β) bioactivity-regulating gene [45], by recruiting transcription factor Sp1 to the LTBP3 promoter in MSCs from myeloma patients [46]. The oncogenic role of MALAT-1 may be partially mediated by TGF-β production because TGF-β can promote tumor cell growth by triggering interleukin-6 (IL-6) and vascular endothelial growth factor (VEGF) production [47].

According to another study using human glioma stem cell line SHG139S, downregulation of MALAT-1 suppressed the expression of stemness markers such as Sox2 and Nestin, while it increased the proliferation of SHG139S by activating ERK/MAPK signaling [48]. Furthermore, MALAT-1 increased the proportion of chemotherapy-resistant pancreatic cancer stem cells with enhanced self-renewing capacity, and this was related to the increased expression of Sox2 [49]. A more recent study demonstrated that MALAT-1, with another lncRNA highly upregulated in liver cancer (HULC) [50], increased the expression of telomere repeat-binding factor 2 (TRF2) and accelerated liver cancer stem cell growth [51]. Such stemness and proliferation regulating role of MALAT-1 are reported in non-cancer stem cells such as iPSCs [52] and hematopoietic cells [53], as well.

3.5. H19. lncRNA H19 is the first lncRNA discovered, and it is paternally imprinted [54]. Human H19 is mapped to the H19-insulin-like growth factor 2 (IGF2) loci of chromosome 11p15.5. H19 transcribes a 2.3 kb lncRNA composed of 5 exons. From the first exon, H19 transcript produces the oncomir miR-675-5p and miR-675-3p [55]. MiR-675 is known to be expressed exclusively in the gestational placenta inhibiting placental growth [56]. The expression of miR-675 and H19 has been verified in human cells [57, 58]. The first evidence that H19 is involved in embryonic stem cell differentiation was reported in 1991. Poirier and colleagues demonstrated that H19 expression was activated during early murine embryogenesis [59]. Recently, the role of H19-IGF2 locus in adult hematopoietic stem cell (HSC) quiescence was reported. Maternal-imprinted H19-derived miR-675 suppresses IGF2-IGFR1 signaling pathway leading to Foxo3-mediated cell cycle arrest. This causes adult HSC quiescence which is required for long-term maintenance of HSC [60].

3.6. HOX Antisense Intergenic RNA Myeloid 1 (HOTAIRM1). HOTAIRM1 was discovered as a myeloid-specific intergenic lncRNA of human HOXA1 and HOXA2 [61]. In their study, Zhang and colleagues reported that HOTAIRM1 was upregulated during granulocyte differentiation of human HSCs in a myeloid lineage-specific manner. Furthermore, knockdown of HOTAIRM1 attenuated the expression of CD11b and CD18, well known myeloid cell markers [62], suggesting HOTAIRM1 is an important mediator of myeloid cell differentiation.

3.7. Maternally Expressed Genes 3 (MEG3). Another human-imprinted gene MEG3 is located in the delta-like homolog 1 gene and type III iodothyronine deiodinase (DLK1-DIO3) locus on human chromosome 14q [63]. MEG3 is expressed in normal tissues but downregulated by aberrant DNA methylation in human cancers implying its role as a tumor suppressor [64, 65]. Genomic imprinting of MEG3 is unstable in human ESCs [66], as well as in iPSCs [67]. According to the study conducted by Mo and colleagues, human ESCs with low MEG3 expression level (designated as MEG3-OFF) also showed significantly low expressions of DLK1-DIO3 locus-derived noncoding RNAs, including MEG8, miR-127, miR-376, miR-494, miR-495, miR-496, and miR-154, compared to its counterpart MEG3-ON [68]. Further,

they demonstrated that MEG3-OFF led to suppressed expression of neural lineage markers such as PAX6, RTN1, and Sox11, suggesting its role as a positive regulator of neuronal differentiation.

Another known function of MEG3 is to recruit polycomb repressive complex 2 (PRC2) to chromatin to maintain transcriptional repression of lineage-specific genes during development. PRC2 is responsible for the di- and trimethylation of lysine 27 in histone H3 (H3K27me2/3) [69], which is one of the important characteristics of inactive heterochromatin [70]. MEG3 recruits PRC2 to chromatin via interaction with jumonji family, ARID domain-containing protein 2 (JARID2) [71]. Chromatin-bound JARID2 further interacts with MEG3 forming a scaffold for maximum PRC2 recruitment. Subsequently, PRC2 is recruited and assembled on a specific location of chromatin, resulting in increased H3K27me3 during ESC differentiation. This suggests that MEG3 is an important factor in epigenetic regulation of lineage-specific genes during ESC differentiation.

Additionally, MEG3 has been implicated in osteogenic differentiation of stem cells, but the results have been inconsistent depending on the source of stem cells. First, MEG3 has been reported to promote osteogenic differentiation of MSCs from multiple myeloma patients by releasing sex-determining region Y box 2- (SOX2-) mediated transcriptional suppression of bone morphogenetic protein 4 (BMP4) promoter [72]. However, few years later, the antiosteogenic effect of MEG3 in bone marrow MSCs of postmenopausal osteoporosis patient by increasing the expression of miR-133a-3p was reported [73]. Although the mechanism of such discrepancy still remains unclear, disease type-dependent effect is suspected.

3.8. Nuclear-Enriched Abundant Transcript 1 (NEAT1). As the full name indicates, NEAT1 is frequently observed in nuclei, especially in the subnuclear body called paraspeckles [74]. Paraspeckles were first identified as a distinct form of nuclear structure different from the nuclear speckles that are enriched in splicing factors [75]. Paraspeckles regulate the expression of genes in differentiated cells by nuclear retention of mRNAs. The formation of paraspeckles around NEAT1 has been reported by several groups [74, 76, 77]. Paraspeckles are only observed in mammalian cells, including primary cell lines and embryonic fibroblasts [78, 79]. However, paraspeckles are not present in undifferentiated human embryonic stem cells but are induced upon differentiation [76]. Other than the role as a mediator of RNA retention, NEAT1 has been implicated in the adipogenic differentiation of ADSCs into adipocytes. Mature miR-140 interacts with NEAT1 in the nucleus, and this subsequently increases NEAT1 expression leading to adipogenesis [80]. However, they only demonstrated that miR-140-mediated NEAT1 expression is required for adipogenesis, without providing the underlying mechanism of how the increased NEAT1 contributed to adipogenesis.

3.9. LincRNA-Regulator of Reprogramming (LincRNA-RoR). LincRNA-RoR was first identified as an lncRNA enriched in human iPSCs and suspected as a modulator of chromatin complexes to regulate pluripotent cell-specific epigenetic architecture [81]. Another study demonstrated that lincRNA-RoR functioned as a miRNA sponge for the miRNAs targeting embryonic stem cell-enriched transcription factors such as Oct4, Sox2, and Nanog. Consequently, lincRNA-RoR prevented miRNA-mediated suppression of these transcription factors, enhancing the self-renewal ability of human ESCs [82].

3.10. NoRC-Associated RNA (Promoter-Associated RNA, pRNA). Promoter-associated RNAs were described *in vitro* in human [83]. Maturation of 250~300 nucleotide long pRNA is achieved by processing 2 kb long intergenic spacer rRNA (IGS-rRNA) [84]. Regarding the role of pRNA in stem cells, it has been reported that mature pRNA-mediated association between the nucleolar transcription terminator factor 1 (TTF1) and TTF1-interacting protein 5 (TIP5) was prerequisite to the generation of heterochromatic rDNA required for exit from pluripotency during ESC differentiation [85]. This indicated that mature pRNA may function as an initiator of ESC differentiation.

3.11. Antisense to Nitric Oxide Synthase 2A (Anti-NOS2A). Anti-NOS2A shares high antisense homology (approximately 80%) to the corresponding regions of NOS2A gene. It is speculated that the anti-NOS2A is a result of gene duplication followed by an internal DNA inversion [86]. The anti-NOS2A functions as a natural antisense transcript that regulates NOS gene expression. In mammalian brain, upregulation of NOS2A has been associated with neurogenesis suggesting that NOS-mediated endogenous NO production is important in neuronal differentiation [87]. In line with such findings, the expression of anti-NOS2A significantly decreased in neurospheres compared to that in undifferentiated human ESCs, while the expression of NOS2A showed an opposite pattern [86]. This indicated that anti-NOS2A may act as a neuronal differentiation suppressor in ESCs.

3.12. Small Nucleolar RNA Host Gene 3 and 1 (SNHG3 and SNHG1). Pertaining to the role of SNHG3 in stem cells, it has been reported that SNHG3 is one of the 26 lncRNAs that are required to maintain the pluripotency program of ESCs [88]. More specifically, knockdown of SNHG3 in ESCs significantly decreased the expressions of pluripotency markers including Oct4, Sox2, Nanog, Klf4, and Zfp43. Furthermore, the expression level of SNHG3 was downregulated during retinoic acid-induced differentiation of ESC, indicating that SNHG3 was one of the lncRNAs that regulate pluripotency program of ESCs. As the underlying mechanism, an ESC state controlling circuitry was proposed where ESC-specific transcription factors (e.g., Oct4, Sox2, and Nanog) derive the transcription of SNHG3, and the produced SNHG3 forms an RNA-protein complex that represses cell type-specific gene expression program. As to the role of SNHG1, it has been reported that the expression of SNHG1 significantly increased during lineage restriction of NSCs (neural stem cells) into N/OPs (bipotent neuronal/oligodendrocyte progenitors) [39]. Recent studies indicated that both SNHG1

and SNHG3 were highly correlated with poor prognosis in cancer patients [89, 90].

3.13. SOX2 Overlapping Transcript (SOX2OT). SOX2 is a HMG-box transcription factor contributes to the maintenance of pluripotency of undifferentiated ESCs [91]. In humans, approximately 700 kb long SOX2OT gene is mapped to chromosome 3q26.3 locus and the SOX2 gene is embedded in the intronic region of SOX2OT; therefore, it gets its name [92]. Concomitant upregulation of SOX2 and SOX2OT in ESCs, which decreased upon differentiation, has been reported [93], and SOX2OT functioning as an enhancer to the transcription of SOX2 was postulated as the possible underlying mechanism [94]. These reports indicate that SOX2OT modulates pluripotency of stem cells via regulation of SOX2.

3.14. VLDLR Antisense RNA1 (LincRNA-VLDLR). LincRNA-VLDLR was first identified as one of the lncRNAs significantly upregulated in human iPSCs and ESCs [81]. According to that particular study, pluripotency-regulating transcription factors such as Oct4, Sox2, and Nanog colocalized on the promoter of the lincRNA-VLDLR, suggesting pluripotency-regulating transcription factors induce the expression of lincRNA-VLDLR, and in turn, lincRNA-VLDLR regulates the maintenance of pluripotency. However, no specific target of the lincRNA-VLDLR has been identified regarding the maintenance of stem cell pluripotency [95].

3.15. Cardiac Mesoderm Enhancer-Associated Noncoding RNA (CARMEN). CARMEN was first characterized by Ounzain and colleagues as an lncRNA associated with human cardiac-specific enhancer [96]. Enhancers are an important regulatory sequences within the genome that integrates temporal, spatial, and environmental cues to regulate gene expression [97]. Enhancer-associated noncoding RNAs play important roles in heart development and disease [98]. CARMEN, as one of such enhancer-associated noncoding RNAs, is crucial for cardiac specification and differentiation of human cardiac progenitor cells (CPCs), and this was evidenced by the observation that knockdown of CARMEN inhibited cardiac specification and differentiation of human CPCs [96].

3.16. Rhabdomyosarcoma 2-Associated Transcript (RMST). RMST was first identified as an lncRNA significantly upregulated upon neuronal differentiation of human ESCs [99]. A year later, the same group elucidated the underlying mechanism of RMST in neuronal differentiation. The expression of RMST was suppressed by RE1-silencing transcription factor (REST), a master negative regulator of neuronal differentiation [100], in undifferentiated human ESCs but increased upon neuronal differentiation of human ESCs. Furthermore, nuclear localized RMST during neuronal differentiation bound to hnRNPA2/B1, a ubiquitous RNA-binding protein [101], and Sox2. Binding of RMST to Sox2 promoted Sox2 binding at the promoters of neurogenic genes, such as achaete-scute homolog 1 (ASCL1 [102]) and distal-less homeobox 1 (DLX-1 [103]), driving neuronal differentiation of human ESCs [104].

3.17. Human Endogenous Retrovirus Subfamily H (HERVH). HERVH is a transposable element preferentially expressed in human ESCs. It has been reported that the long terminal repeats of HERVH regulated the expression of neighboring pluripotency marker genes by binding to both Oct4 and coactivators such as p300 in human ESCs [105].

4. Possible Clinical Applications of the lncRNAs in Stem Cells

The research on roles of lncRNAs in stem cell biology is still in its infancy. Furthermore, only few cell therapies using stem cells have demonstrated satisfying clinical benefit to warrant their clinical use [106]. In other words, both the research on the lncRNAs in stem cells and the cell therapies using stem cells are far from being completed. Therefore, it is very difficult to discuss the clinical implications of lncRNAs in stem cells in depth. However, approximately half million single nucleotide polymorphisms (SNPs) in more than 30,000 human lncRNAs have been identified already [107], and this strongly suggests high possibility of dysregulated lncRNAs even in stem cells. It has been demonstrated that dysregulation of lncRNAs contributes to numerous human diseases, and even very simple mutations such as SNPs can have tremendous consequences in terms of lncRNA structure and function [108].

Assuming one of the major purposes of studying the stem cell biology is to design more effective cell therapy approaches, dysregulated lncRNAs in stem cells can be a selection marker for screening adequate stem cells for transplantation. Another possible application of lncRNAs in stem cells is to use lncRNAs as a therapeutic target for reinforcing stem cell function. For example, gene-editing technology can be utilized to facilitate in situ differentiation of stem cells into desired lineage of cells by editing lncRNAs that promote or suppress differentiation of stem cells. Additionally, finding and using small molecule that induces or inhibits specific lncRNAs may serve as a powerful tool to enhancing the functionality of stem cells. However, these therapeutic applications of lncRNAs in stem cells can be realized only when the regulatory mechanisms of lncRNAs in stem cells are sufficiently elucidated.

5. Conclusions and Perspectives

An increasing number of studies have provided evidence that lncRNAs are important regulators of the differentiation and pluripotency maintenance of stem cells. Studies have demonstrated that lncRNAs modulate stem cell biology by interacting with essential transcription factors responsible for maintaining pluripotency or regulating differentiation. It is clear that lncRNAs play critical roles in different types of human stem cells with diverse mechanisms. Furthermore, the existence of dysregulated lncRNAs adds a new layer of complexity to the molecular mechanisms of human disease. Despite recent progress in this field, we still have a long way to fully comprehend the roles of these important regulators in human stem cells. Therefore, further studies are strongly required, and it is expected that future study of

lncRNAs in stem cells will provide us new therapeutic targets for the prevention and treatment of human disease.

Conflicts of Interest

The authors declare that there is no conflict of interest.

Authors' Contributions

Seahyoung Lee and Hyang-Hee Seo equally contributed to this work.

Acknowledgments

This study was supported by grants funded by the Korea Ministry of Science, ICT and Future Planning (NRF-2015M3A9E6029519 and NFR-2015M3A9E6029407) and a grant from the Korea Health 21 R&D Project, Ministry of Health & Welfare, Republic of Korea (A120478).

References

[1] R. S. Mahla, "Stem cells applications in regenerative medicine and disease therapeutics," *International Journal of Cell Biology*, vol. 2016, Article ID 6940283, 24 pages, 2016.

[2] S. Hu and G. Shan, "LncRNAs in stem cells," *Stem Cells International*, vol. 2016, Article ID 2681925, 8 pages, 2016.

[3] T. Lammens, I. D'Hont, K. D'Herde, Y. Benoit, and A. Diez-Fraile, "Long non-coding RNAs in pluripotent stem cell biology," *The Veterinary Quarterly*, vol. 33, no. 4, pp. 202–206, 2013.

[4] T. Nagano and P. Fraser, "No-nonsense functions for long noncoding RNAs," *Cell*, vol. 145, no. 2, pp. 178–181, 2011.

[5] C. P. Ponting, P. L. Oliver, and W. Reik, "Evolution and functions of long noncoding RNAs," *Cell*, vol. 136, no. 4, pp. 629–641, 2009.

[6] V. K. Gangaraju and H. Lin, "MicroRNAs: key regulators of stem cells," *Nature Reviews Molecular Cell Biology*, vol. 10, no. 2, pp. 116–125, 2009.

[7] A. Shenoy and R. H. Blelloch, "Regulation of microRNA function in somatic stem cell proliferation and differentiation," *Nature Reviews Molecular Cell Biology*, vol. 15, no. 9, pp. 565–576, 2014.

[8] S. Yao, "MicroRNA biogenesis and their functions in regulating stem cell potency and differentiation," *Biological Procedures Online*, vol. 18, p. 8, 2016.

[9] M. B. Clark, T. R. Mercer, G. Bussotti et al., "Quantitative gene profiling of long noncoding RNAs with targeted RNA sequencing," *Nature Methods*, vol. 12, no. 4, pp. 339–342, 2015.

[10] M. Guttman, I. Amit, M. Garber et al., "Chromatin signature reveals over a thousand highly conserved large non-coding RNAs in mammals," *Nature*, vol. 458, no. 7235, pp. 223–227, 2009.

[11] T. Derrien, R. Johnson, G. Bussotti et al., "The GENCODE v7 catalog of human long noncoding RNAs: analysis of their gene structure, evolution, and expression," *Genome Research*, vol. 22, no. 9, pp. 1775–1789, 2012.

[12] J. J. Quinn and H. Y. Chang, "Unique features of long non-coding RNA biogenesis and function," *Nature Reviews Genetics*, vol. 17, no. 1, pp. 47–62, 2016.

[13] J. L. Rinn and H. Y. Chang, "Genome regulation by long noncoding RNAs," *Annual Review of Biochemistry*, vol. 81, pp. 145–166, 2012.

[14] T. Hung and H. Y. Chang, "Long noncoding RNA in genome regulation: prospects and mechanisms," *RNA Biology*, vol. 7, no. 5, pp. 582–5, 2010.

[15] S. Geisler and J. Coller, "RNA in unexpected places: long non-coding RNA functions in diverse cellular contexts," *Nature Reviews Molecular Cell Biology*, vol. 14, no. 11, pp. 699–712, 2013.

[16] C. Gong and L. E. Maquat, "lncRNAs transactivate STAU1-mediated mRNA decay by duplexing with 3′ UTRs via Alu elements," *Nature*, vol. 470, no. 7333, pp. 284–288, 2011.

[17] C. Carrieri, L. Cimatti, M. Biagioli et al., "Long non-coding antisense RNA controls Uchl1 translation through an embedded SINEB2 repeat," *Nature*, vol. 491, no. 7424, pp. 454–457, 2012.

[18] M. A. Faghihi, M. Zhang, J. Huang et al., "Evidence for natural antisense transcript-mediated inhibition of microRNA function," *Genome Biology*, vol. 11, no. 5, article R56, 2010.

[19] F. Morceau, S. Chateauvieux, A. Gaigneaux, M. Dicato, and M. Diederich, "Long and short non-coding RNAs as regulators of hematopoietic differentiation," *International Journal of Molecular Sciences*, vol. 14, no. 7, pp. 14744–14770, 2013.

[20] J. A. Heward and M. A. Lindsay, "Long non-coding RNAs in the regulation of the immune response," *Trends in Immunology*, vol. 35, no. 9, pp. 408–419, 2014.

[21] B. Liu, L. Sun, Q. Liu et al., "A cytoplasmic NF-kappaB interacting long noncoding RNA blocks IkappaB phosphorylation and suppresses breast cancer metastasis," *Cancer Cell*, vol. 27, no. 3, pp. 370–381, 2015.

[22] L. Wan, M. Sun, G. J. Liu et al., "Long noncoding RNA PVT1 promotes non-small cell lung cancer cell proliferation through epigenetically regulating LATS2 expression," *Molecular Cancer Therapeutics*, vol. 15, no. 5, pp. 1082–1094, 2016.

[23] K. C. Wang and H. Y. Chang, "Molecular mechanisms of long noncoding RNAs," *Molecular Cell*, vol. 43, no. 6, pp. 904–914, 2011.

[24] Y. Fang and M. J. Fullwood, "Roles, functions, and mechanisms of long non-coding RNAs in cancer," *Genomics, Proteomics & Bioinformatics*, vol. 14, no. 1, pp. 42–54, 2016.

[25] V. Tripathi, J. D. Ellis, Z. Shen et al., "The nuclear-retained noncoding RNA MALAT1 regulates alternative splicing by modulating SR splicing factor phosphorylation," *Molecular Cell*, vol. 39, no. 6, pp. 925–938, 2010.

[26] A. Rosa and M. Ballarino, "Long noncoding RNA regulation of Pluripotency," *Stem Cells International*, vol. 2016, Article ID 1797692, 9 pages, 2016.

[27] R. B. Perry and I. Ulitsky, "The functions of long noncoding RNAs in development and stem cells," *Development*, vol. 143, no. 21, pp. 3882–3894, 2016.

[28] S. J. Hafner, T. G. Talvard, and A. H. Lund, "Long noncoding RNAs in normal and pathological pluripotency," *Seminars in Cell & Developmental Biology*, vol. 65, pp. 1–10, 2017.

[29] M. N. Cabili, C. Trapnell, L. Goff et al., "Integrative annotation of human large intergenic noncoding RNAs reveals global properties and specific subclasses," *Genes & Development*, vol. 25, no. 18, pp. 1915–1927, 2011.

[30] D. M. Church, L. Goodstadt, L. W. Hillier et al., "Lineage-specific biology revealed by a finished genome assembly of the mouse," *PLoS Biology*, vol. 7, no. 5, article e1000112, 2009.

[31] L. A. Wagner, C. J. Christensen, D. M. Dunn et al., "EGO, a novel, noncoding RNA gene, regulates eosinophil granule protein transcript expression," *Blood*, vol. 109, no. 12, pp. 5191–5198, 2007.

[32] S. Blackshaw, S. Harpavat, J. Trimarchi et al., "Genomic analysis of mouse retinal development," *PLoS Biology*, vol. 2, no. 9, article E247, 2004.

[33] N. A. Rapicavoli, E. M. Poth, and S. Blackshaw, "The long noncoding RNA RNCR2 directs mouse retinal cell specification," *BMC Developmental Biology*, vol. 10, p. 49, 2010.

[34] M. Sone, T. Hayashi, H. Tarui, K. Agata, M. Takeichi, and S. Nakagawa, "The mRNA-like noncoding RNA Gomafu constitutes a novel nuclear domain in a subset of neurons," *Journal of Cell Science*, vol. 120, Part 15, pp. 2498–2506, 2007.

[35] J. Sheik Mohamed, P. M. Gaughwin, B. Lim, P. Robson, and L. Lipovich, "Conserved long noncoding RNAs transcriptionally regulated by Oct4 and Nanog modulate pluripotency in mouse embryonic stem cells," *RNA*, vol. 16, no. 2, pp. 324–337, 2010.

[36] Y. Chen, K. Wang, Y. G. Gong, S. K. Khoo, and R. Leach, "Roles of CDX2 and EOMES in human induced trophoblast progenitor cells," *Biochemical and Biophysical Research Communications*, vol. 431, no. 2, pp. 197–202, 2013.

[37] I. C. Scott, L. Anson-Cartwright, P. Riley, D. Reda, and J. C. Cross, "The HAND1 basic helix-loop-helix transcription factor regulates trophoblast differentiation via multiple mechanisms," *Molecular and Cellular Biology*, vol. 20, no. 2, pp. 530–541, 2000.

[38] A. Ralston, B. J. Cox, N. Nishioka et al., "Gata3 regulates trophoblast development downstream of Tead4 and in parallel to Cdx2," *Development*, vol. 137, no. 3, pp. 395–403, 2010.

[39] T. R. Mercer, I. A. Qureshi, S. Gokhan et al., "Long noncoding RNAs in neuronal-glial fate specification and oligodendrocyte lineage maturation," *BMC Neuroscience*, vol. 11, p. 14, 2010.

[40] W. He, C. Ingraham, L. Rising, S. Goderie, and S. Temple, "Multipotent stem cells from the mouse basal forebrain contribute GABAergic neurons and oligodendrocytes to the cerebral cortex during embryogenesis," *The Journal of Neuroscience*, vol. 21, no. 22, pp. 8854–8862, 2001.

[41] N. Ishii, K. Ozaki, H. Sato et al., "Identification of a novel non-coding RNA, MIAT, that confers risk of myocardial infarction," *Journal of Human Genetics*, vol. 51, no. 12, pp. 1087–1099, 2006.

[42] C. Jin, Y. Zheng, Y. Huang, Y. Liu, L. Jia, and Y. Zhou, "Long non-coding RNA MIAT knockdown promotes osteogenic differentiation of human adipose-derived stem cells," *Cell Biology International*, vol. 41, no. 1, pp. 33–41, 2017.

[43] J. Feng, C. Bi, B. S. Clark, R. Mady, P. Shah, and J. D. Kohtz, "The Evf-2 noncoding RNA is transcribed from the Dlx-5/6 ultraconserved region and functions as a Dlx-2 transcriptional coactivator," *Genes & Development*, vol. 20, no. 11, pp. 1470–1484, 2006.

[44] P. Ji, S. Diederichs, W. Wang et al., "MALAT-1, a novel noncoding RNA, and thymosin beta4 predict metastasis and survival in early-stage non-small cell lung cancer," *Oncogene*, vol. 22, no. 39, pp. 8031–8041, 2003.

[45] D. B. Rifkin, "Latent transforming growth factor-beta (TGF-beta) binding proteins: orchestrators of TGF-beta availability," *The Journal of Biological Chemistry*, vol. 280, no. 9, pp. 7409–7412, 2005.

[46] B. Li, P. Chen, J. Qu et al., "Activation of LTBP3 gene by a long noncoding RNA (lncRNA) MALAT1 transcript in mesenchymal stem cells from multiple myeloma," *The Journal of Biological Chemistry*, vol. 289, no. 42, pp. 29365–29375, 2014.

[47] M. Esquivel-Velazquez, P. Ostoa-Saloma, M. I. Palacios-Arreola, K. E. Nava-Castro, J. I. Castro, and J. Morales-Montor, "The role of cytokines in breast cancer development and progression," *Journal of Interferon & Cytokine Research*, vol. 35, no. 1, pp. 1–16, 2015.

[48] Y. Han, L. Zhou, T. Wu et al., "Downregulation of lncRNA-MALAT1 affects proliferation and the expression of stemness markers in glioma stem cell line SHG139S," *Cellular and Molecular Neurobiology*, vol. 36, no. 7, pp. 1097–1107, 2016.

[49] F. Jiao, H. Hu, T. Han et al., "Long noncoding RNA MALAT-1 enhances stem cell-like phenotypes in pancreatic cancer cells," *International Journal of Molecular Sciences*, vol. 16, no. 4, pp. 6677–6693, 2015.

[50] S. P. Li, H. X. Xu, Y. Yu et al., "LncRNA HULC enhances epithelial-mesenchymal transition to promote tumorigenesis and metastasis of hepatocellular carcinoma via the miR-200a-3p/ZEB1 signaling pathway," *Oncotarget*, vol. 7, no. 27, pp. 42431–42446, 2016.

[51] M. Wu, Z. Lin, X. Li et al., "HULC cooperates with MALAT1 to aggravate liver cancer stem cells growth through telomere repeat-binding factor 2," *Scientific Reports*, vol. 6, article 36045, 2016.

[52] M. Lin, E. Pedrosa, A. Shah et al., "RNA-Seq of human neurons derived from iPS cells reveals candidate long noncoding RNAs involved in neurogenesis and neuropsychiatric disorders," *PLoS One*, vol. 6, no. 9, article e23356, 2011.

[53] X. Y. Ma, J. H. Wang, J. L. Wang, C. X. Ma, X. C. Wang, and F. S. Liu, "Malat1 as an evolutionarily conserved lncRNA, plays a positive role in regulating proliferation and maintaining undifferentiated status of early-stage hematopoietic cells," *BMC Genomics*, vol. 16, p. 676, 2015.

[54] W. L. Gao, M. Liu, Y. Yang et al., "The imprinted H19 gene regulates human placental trophoblast cell proliferation via encoding miR-675 that targets nodal modulator 1 (NOMO1)," *RNA Biology*, vol. 9, no. 7, pp. 1002–1010, 2012.

[55] X. Cai and B. R. Cullen, "The imprinted H19 noncoding RNA is a primary microRNA precursor," *RNA*, vol. 13, no. 3, pp. 313–316, 2007.

[56] A. Keniry, D. Oxley, P. Monnier et al., "The H19 lincRNA is a developmental reservoir of miR-675 that suppresses growth and Igf1r," *Nature Cell Biology*, vol. 14, no. 7, pp. 659–665, 2012.

[57] P. Ohana, E. Kopf, O. Bibi et al., "The expression of the H19 gene and its function in human bladder carcinoma cell lines," *FEBS Letters*, vol. 454, no. 1-2, pp. 81–84, 1999.

[58] J. H. Yang, P. Shao, H. Zhou, Y. Q. Chen, and L. H. Qu, "deepBase: a database for deeply annotating and mining deep sequencing data," *Nucleic Acids Research*, vol. 38, Database issue, pp. D123–D130, 2010.

[59] F. Poirier, C. T. Chan, P. M. Timmons, E. J. Robertson, M. J. Evans, and P. W. Rigby, "The murine H19 gene is activated during embryonic stem cell differentiation in vitro and at the time of implantation in the developing embryo," *Development*, vol. 113, no. 4, pp. 1105–1114, 1991.

[60] A. Venkatraman, X. C. He, J. L. Thorvaldsen et al., "Maternal imprinting at the H19-Igf2 locus maintains adult haematopoietic stem cell quiescence," *Nature*, vol. 500, no. 7462, pp. 345–349, 2013.

[61] X. Zhang, Z. Lian, C. Padden et al., "A myelopoiesis-associated regulatory intergenic noncoding RNA transcript within the human HOXA cluster," *Blood*, vol. 113, no. 11, pp. 2526–2534, 2009.

[62] M. A. Arnaout, "Structure and function of the leukocyte adhesion molecules CD11/CD18," *Blood*, vol. 75, no. 5, pp. 1037–1050, 1990.

[63] N. Miyoshi, H. Wagatsuma, S. Wakana et al., "Identification of an imprinted gene, Meg3/Gtl2 and its human homologue MEG3, first mapped on mouse distal chromosome 12 and human chromosome 14q," *Genes to Cells*, vol. 5, no. 3, pp. 211–220, 2000.

[64] Y. Zhou, X. Zhang, and A. Klibanski, "MEG3 noncoding RNA: a tumor suppressor," *Journal of Molecular Endocrinology*, vol. 48, no. 3, pp. R45–R53, 2012.

[65] X. Shi, M. Sun, H. Liu, Y. Yao, and Y. Song, "Long non-coding RNAs: a new frontier in the study of human diseases," *Cancer Letters*, vol. 339, no. 2, pp. 159–166, 2013.

[66] P. J. Rugg-Gunn, A. C. Ferguson-Smith, and R. A. Pedersen, "Epigenetic status of human embryonic stem cells," *Nature Genetics*, vol. 37, no. 6, pp. 585–587, 2005.

[67] K. Nishino and A. Umezawa, "DNA methylation dynamics in human induced pluripotent stem cells," *Human Cell*, vol. 29, no. 3, pp. 97–100, 2016.

[68] C. F. Mo, F. C. Wu, K. Y. Tai et al., "Loss of non-coding RNA expression from the DLK1-DIO3 imprinted locus correlates with reduced neural differentiation potential in human embryonic stem cell lines," *Stem Cell Research & Therapy*, vol. 6, p. 1, 2015.

[69] R. Margueron and D. Reinberg, "The Polycomb complex PRC2 and its mark in life," *Nature*, vol. 469, no. 7330, pp. 343–349, 2011.

[70] P. Trojer and D. Reinberg, "Facultative heterochromatin: is there a distinctive molecular signature?," *Molecular Cell*, vol. 28, no. 1, pp. 1–13, 2007.

[71] S. Kaneko, R. Bonasio, R. Saldana-Meyer et al., "Interactions between JARID2 and noncoding RNAs regulate PRC2 recruitment to chromatin," *Molecular Cell*, vol. 53, no. 2, pp. 290–300, 2014.

[72] W. Zhuang, X. Ge, S. Yang et al., "Upregulation of lncRNA MEG3 promotes osteogenic differentiation of mesenchymal stem cells from multiple myeloma patients by targeting BMP4 transcription," *Stem Cells*, vol. 33, no. 6, pp. 1985–1997, 2015.

[73] Q. Wang, Y. Li, Y. Zhang et al., "LncRNA MEG3 inhibited osteogenic differentiation of bone marrow mesenchymal stem cells from postmenopausal osteoporosis by targeting miR-133a-3p," *Biomedicine & Pharmacotherapy*, vol. 89, pp. 1178–1186, 2017.

[74] C. M. Clemson, J. N. Hutchinson, S. A. Sara et al., "An architectural role for a nuclear noncoding RNA: NEAT1 RNA is essential for the structure of paraspeckles," *Molecular Cell*, vol. 33, no. 6, pp. 717–726, 2009.

[75] A. H. Fox, Y. W. Lam, A. K. Leung et al., "Paraspeckles: a novel nuclear domain," *Current Biology*, vol. 12, no. 1, pp. 13–25, 2002.

[76] L. L. Chen and G. G. Carmichael, "Altered nuclear retention of mRNAs containing inverted repeats in human embryonic stem cells: functional role of a nuclear noncoding RNA," *Molecular Cell*, vol. 35, no. 4, pp. 467–478, 2009.

[77] Y. T. Sasaki, T. Ideue, M. Sano, T. Mituyama, and T. Hirose, "MENepsilon/beta noncoding RNAs are essential for structural integrity of nuclear paraspeckles," *Proceedings of the National Academy of Sciences of the United States of America*, vol. 106, no. 8, pp. 2525–2530, 2009.

[78] K. V. Prasanth, S. G. Prasanth, Z. Xuan et al., "Regulating gene expression through RNA nuclear retention," *Cell*, vol. 123, no. 2, pp. 249–263, 2005.

[79] H. Sunwoo, M. E. Dinger, J. E. Wilusz, P. P. Amaral, J. S. Mattick, and D. L. Spector, "MEN epsilon/beta nuclear-retained non-coding RNAs are up-regulated upon muscle differentiation and are essential components of paraspeckles," *Genome Research*, vol. 19, no. 3, pp. 347–359, 2009.

[80] R. Gernapudi, B. Wolfson, Y. Zhang et al., "MicroRNA 140 promotes expression of long noncoding RNA NEAT1 in adipogenesis," *Molecular and Cellular Biology*, vol. 36, no. 1, pp. 30–38, 2016.

[81] S. Loewer, M. N. Cabili, M. Guttman et al., "Large intergenic non-coding RNA-RoR modulates reprogramming of human induced pluripotent stem cells," *Nature Genetics*, vol. 42, no. 12, pp. 1113–1117, 2010.

[82] Y. Wang, Z. Xu, J. Jiang et al., "Endogenous miRNA sponge lincRNA-RoR regulates Oct4, Nanog, and Sox2 in human embryonic stem cell self-renewal," *Developmental Cell*, vol. 25, no. 1, pp. 69–80, 2013.

[83] C. Mayer, M. Neubert, and I. Grummt, "The structure of NoRC-associated RNA is crucial for targeting the chromatin remodelling complex NoRC to the nucleolus," *EMBO Reports*, vol. 9, no. 8, pp. 774–780, 2008.

[84] C. Mayer, K. M. Schmitz, J. Li, I. Grummt, and R. Santoro, "Intergenic transcripts regulate the epigenetic state of rRNA genes," *Molecular Cell*, vol. 22, no. 3, pp. 351–361, 2006.

[85] N. Savic, D. Bar, S. Leone et al., "lncRNA maturation to initiate heterochromatin formation in the nucleolus is required for exit from pluripotency in ESCs," *Cell Stem Cell*, vol. 15, no. 6, pp. 720–734, 2014.

[86] S. A. Korneev, E. I. Korneeva, M. A. Lagarkova, S. L. Kiselev, G. Critchley, and M. O'Shea, "Novel noncoding antisense RNA transcribed from human anti-NOS2A locus is differentially regulated during neuronal differentiation of embryonic stem cells," *RNA*, vol. 14, no. 10, pp. 2030–2037, 2008.

[87] D. Y. Zhu, S. H. Liu, H. S. Sun, and Y. M. Lu, "Expression of inducible nitric oxide synthase after focal cerebral ischemia stimulates neurogenesis in the adult rodent dentate gyrus," *The Journal of Neuroscience*, vol. 23, no. 1, pp. 223–229, 2003.

[88] M. Guttman, J. Donaghey, B. W. Carey et al., "lincRNAs act in the circuitry controlling pluripotency and differentiation," *Nature*, vol. 477, no. 7364, pp. 295–300, 2011.

[89] T. Zhang, C. Cao, D. Wu, and L. Liu, "SNHG3 correlates with malignant status and poor prognosis in hepatocellular carcinoma," *Tumour Biology*, vol. 37, no. 2, pp. 2379–2385, 2016.

[90] D. Sahu, C. L. Hsu, C. C. Lin et al., "Co-expression analysis identifies long noncoding RNA SNHG1 as a novel predictor for event-free survival in neuroblastoma," *Oncotarget*, vol. 7, no. 36, pp. 58022–58037, 2016.

[91] H. Fong, K. A. Hohenstein, and P. J. Donovan, "Regulation of self-renewal and pluripotency by Sox2 in human embryonic stem cells," *Stem Cells*, vol. 26, no. 8, pp. 1931–8, 2008.

[92] J. Fantes, N. K. Ragge, S. A. Lynch et al., "Mutations in SOX2 cause anophthalmia," *Nature Genetics*, vol. 33, no. 4, pp. 461–463, 2003.

[93] A. Shahryari, M. S. Jazi, N. M. Samaei, and S. J. Mowla, "Long non-coding RNA SOX2OT: expression signature, splicing patterns, and emerging roles in pluripotency and tumorigenesis," *Frontiers in Genetics*, vol. 6, p. 196, 2015.

[94] P. P. Amaral, C. Neyt, S. J. Wilkins et al., "Complex architecture and regulated expression of the Sox2ot locus during vertebrate development," *RNA*, vol. 15, no. 11, pp. 2013–2027, 2009.

[95] J. H. Ng and H. H. Ng, "LincRNAs join the pluripotency alliance," *Nature Genetics*, vol. 42, no. 12, pp. 1035-1036, 2010.

[96] S. Ounzain, R. Micheletti, C. Arnan et al., "CARMEN, a human super enhancer-associated long noncoding RNA controlling cardiac specification, differentiation and homeostasis," *Journal of Molecular and Cellular Cardiology*, vol. 89, Part A, pp. 98–112, 2015.

[97] C. T. Ong and V. G. Corces, "Enhancers: emerging roles in cell fate specification," *EMBO Reports*, vol. 13, no. 5, pp. 423–430, 2012.

[98] S. Ounzain, I. Pezzuto, R. Micheletti et al., "Functional importance of cardiac enhancer-associated noncoding RNAs in heart development and disease," *Journal of Molecular and Cellular Cardiology*, vol. 76, pp. 55–70, 2014.

[99] S. Y. Ng, R. Johnson, and L. W. Stanton, "Human long non-coding RNAs promote pluripotency and neuronal differentiation by association with chromatin modifiers and transcription factors," *The EMBO Journal*, vol. 31, no. 3, pp. 522–533, 2012.

[100] Z. Gao, K. Ure, P. Ding et al., "The master negative regulator REST/NRSF controls adult neurogenesis by restraining the neurogenic program in quiescent stem cells," *The Journal of Neuroscience*, vol. 31, no. 26, pp. 9772–9786, 2011.

[101] H. Kamma, H. Horiguchi, L. Wan et al., "Molecular characterization of the hnRNP A2/B1 proteins: tissue-specific expression and novel isoforms," *Experimental Cell Research*, vol. 246, no. 2, pp. 399–411, 1999.

[102] D. S. Castro and F. Guillemot, "Old and new functions of proneural factors revealed by the genome-wide characterization of their transcriptional targets," *Cell Cycle*, vol. 10, no. 23, pp. 4026–4031, 2011.

[103] M. A. Petryniak, G. B. Potter, D. H. Rowitch, and J. L. Rubenstein, "Dlx1 and Dlx2 control neuronal versus oligodendroglial cell fate acquisition in the developing forebrain," *Neuron*, vol. 55, no. 3, pp. 417–433, 2007.

[104] S. Y. Ng, G. K. Bogu, B. S. Soh, and L. W. Stanton, "The long noncoding RNA RMST interacts with SOX2 to regulate neurogenesis," *Molecular Cell*, vol. 51, no. 3, pp. 349–359, 2013.

[105] X. Lu, F. Sachs, L. Ramsay et al., "The retrovirus HERVH is a long noncoding RNA required for human embryonic stem cell identity," *Nature Structural & Molecular Biology*, vol. 21, no. 4, pp. 423–425, 2014.

[106] A. Trounson and C. McDonald, "Stem cell therapies in clinical trials: progress and challenges," *Cell Stem Cell*, vol. 17, no. 1, pp. 11–22, 2015.

[107] J. Gong, W. Liu, J. Zhang, X. Miao, and A. Y. Guo, "lncRNASNP: a database of SNPs in lncRNAs and their potential functions in human and mouse," *Nucleic Acids Research*, vol. 43, Database issue, pp. D181–D186, 2015.

[108] O. Wapinski and H. Y. Chang, "Long noncoding RNAs and human disease," *Trends in Cell Biology*, vol. 21, no. 6, pp. 354–361, 2011.

Hindawi
Stem Cells International
Volume 2017, Article ID 1769298, 10 pages
https://doi.org/10.1155/2017/1769298

Research Article

miR-142-3p Contributes to Early Cardiac Fate Decision of Embryonic Stem Cells

Zhong-Yan Chen,[1,2] Fei Chen,[1] Nan Cao,[1] Zhi-Wen Zhou,[2] and Huang-Tian Yang[1]

[1]*Key Laboratory of Stem Cell Biology and Laboratory of Molecular Cardiology, Institute of Health Sciences, Shanghai Jiao Tong University School of Medicine (SJTUSM) and Shanghai Institutes for Biological Sciences (SIBS), Chinese Academy of Sciences (CAS), Shanghai, China*
[2]*Department of Cardiology, Shanghai Xuhui District Central Hospital, Shanghai, China*

Correspondence should be addressed to Huang-Tian Yang; htyang@sibs.ac.cn

Received 26 January 2017; Accepted 9 April 2017; Published 5 June 2017

Academic Editor: Yanfang Chen

MicroRNAs (miRNAs) play important roles in cell fate decisions. However, the miRNAs and their targets involved in the regulation of cardiac lineage specification are largely unexplored. Here, we report novel functions of miR-142-3p in the regulation of cardiomyocyte differentiation from mouse embryonic stem cells (mESCs). With a miRNA array screen, we identified a number of miRNAs significantly changed during mESC differentiation into the mesodermal and cardiac progenitor cells, and miR-142-3p was one among the markedly downregulated miRNAs. Ectopic expression and inhibition of miR-142-3p did not alter the characteristics of undifferentiated ESCs, whereas ectopic expression of miR-142-3p impaired cardiomyocyte formation. In addition, ectopic expression of miR-142-3p inhibited the expression of a cardiac mesodermal marker gene *Mesp1* and downstream cardiac transcription factors *Nkx2.5*, *Tbx5*, and *Mef2c* but not the expression of three germ layer-specific genes. We further demonstrated that miR-142-3p targeted the 3′-untranslated region of *Mef2c*. These results reveal miR-142-3p as an important regulator of early cardiomyocyte differentiation. Our findings provide new knowledge for further understanding of roles and mechanisms of miRNAs as critical regulators of cardiomyocyte differentiation.

1. Introduction

Embryonic stem cells (ESCs), derived from the inner cell mass of blastocysts, are pluripotent and self-renewing cells with the ability to give rise to all derivatives of three germ layers [1]. Differentiation of ESCs mimics the early stage of embryonic development, including the cardiomyogenic lineage commitment, thus making ESCs an ideal model to study the regulators and mechanisms of in vivo mammalian development [2, 3]. Proper differentiation requires precise regulation of signalling pathways, epigenetic modification, and transcription networks [4–6]. Accumulating evidence has shown that posttranscriptional and posttranslational regulations of lineage-specific genes by small noncoding RNAs, such as microRNAs (miRNAs), play important roles in cell fate and lineage commitment of ESCs [7]. However, the specific miRNAs that control ESC differentiation have not yet been fully clarified.

miRNAs are 22- to 25-nucleotide-long, endogenous single-stranded noncoding RNAs that regulate gene expression at the posttranscriptional level by mRNA degradation or translation repression [8]. miRNAs play important roles in embryo development and cell fate decision, proliferation, and differentiation [9–11]. ESC-derived cardiomyocyte formation involves the formation of mesodermal cells, specification of mesodermal cells to cardiac progenitor cells (CPCs), and differentiation of CPCs into immature cardiomyocytes [4]. A number of miRNAs have been identified to regulate these stages. miR-1 and miR-133 promote mesoderm formation from ESCs but have opposing functions during further differentiation into CPCs [9]. miR-499 promotes differentiation of CPCs into cardiomyocytes

[12]. We previously found that miR-125b/Lin28 axis is a critical regulator in the control of mesendodermal specification from mouse ESCs (mESCs) and subsequent cardiac differentiation [13]. However, whether there are other miRNAs that are involved in early cardiac differentiation needs to be further determined.

miR-142-3p, an evolutionally conserved miRNA of vertebrates, is a hematopoietic-specific miRNA [14] and regulates cell fate decision in the vertebrate hematopoietic system [15–17]. miR-142-3p is also a multifaceted regulator in organogenesis, homeostasis, and tumorigenesis [18]. Recently, miR-142-3p is reported to balance self-renewal and differentiation in mESCs via regulating KRAS/ERK signalling [19]. In addition, miR-142-3p is reported to regulate heart formation in zebrafish [20]. However, it is unknown whether miR-142-3p regulates mammalian cardiogenesis.

In this study, we screened miRNAs that might be involved in the differentiation of mESCs into mesoderm and CPCs by miRNA microarray and identified the changes of miR-142-3p abundance during mesodermal and early cardiac differentiation. We then examined the function of miR-142-3p on ESC self-renewal and cardiac differentiation and identified the potential targets. Our data showed that miR-142-3p is an important regulator for early cardiac differentiation of ESCs. These findings provide insights into the novel role of miR-142-3p in the regulation of cardiac lineage commitment and add information for the further development of cell therapy and drug discovery.

2. Materials and Methods

2.1. Culture and In Vitro Differentiation of ESCs. R1 and E14 mESCs carrying a Brachyury-GFP (T-GFP) were maintained on mitomycin C-inactivated mouse embryonic fibroblast cells as described previously [5, 21]. Cardiomyocyte differentiation was initiated by a hanging-drop technique [22]. In brief, ESCs were trypsinized and cultivated as embryoid bodies (EBs) in the absence of leukemia inhibitory factor (Millipore) for 2 days followed by 3 days of suspension cultured in the medium containing 10% FBS (Gibco, USA). Then, EBs were plated onto gelatin-coated tissue culture dishes. Differentiated cardiomyocytes appeared in the form of spontaneously contracting cell clusters. All cultivation medium and other reagents for cell culture were from Invitrogen (Carlsbad, CA, USA) unless indicated otherwise. E14 mESCs carrying a T-GFP were used for collecting mesodermal cells; R1 mESCs were used for other experiments.

2.2. Analysis of miRNA Expression Profiling. T-GFP$^+$ mesodermal cells were isolated from day 3 EBs of E14 mESCs carrying T-GFP by fluorescence-activated cell sorting (FACS). FLK1$^+$/CXCR4$^+$ CPCs [23] were isolated from day 5 EBs of R1 mESCs by FACS. Total RNA was isolated with TRIzol (Invitrogen, USA). miRNA expression profiling was carried out with Agilent 8x60K mouse miRNA one-color microarray (V16.0) (Agilent Technologies Inc., Santa Clara, CA, USA). miRNA hybridization and data collection were conducted following the manufacturer's instructions.

Table 1: Fold change of the miRNAs in T-GFP$^+$ versus T-GFP$^-$.

miRNA ID	Fold change	*P* value
mmu-miR-193	134.10	0.000613
mmu-miR-99b*	85.31	0.002295
mmu-miR-532-3p	44.47	0.017969
mmu-miR-99b	2.85	0.008900
mmu-miR-652	2.36	0.003940
mmu-miR-125a-5p	2.20	0.016116
mmu-miR-874	2.07	0.004076
mmu-miR-140*	−2.01	0.036421
mmu-miR-467c	−2.15	0.000925
mmu-miR-467a	−2.23	0.031586
mmu-miR-141	−2.24	0.045208
mmu-miR-297c	−2.32	0.015306
mmu-miR-135b	−2.33	0.020035
mmu-miR-497	−2.34	0.000315
mmu-miR-290-3p	−2.34	0.001229
mmu-miR-467b	−2.57	0.004658
mmu-miR-126-3p	−2.59	0.025740
mmu-miR-200a	−2.63	0.001876
mmu-miR-467e	−2.71	0.011901
mmu-miR-195	−2.73	0.006600
mmu-miR-7a	−3.04	0.012637
mmu-miR-672	−14.85	0.002030
mmu-miR-466m-5p	−76.86	0.004111
mmu-let-7f	−85.32	0.001921
mmu-miR-181c	−92.73	0.000002
mmu-miR-125b-5p	−99.27	0.000697
mmu-miR-124	−105.00	0.000622
mmu-let-7g	−115.25	0.000002
mmu-miR-142-3p	**−214.59**	**0.001338**

*The element of the miRNA names based on the miRNA nomenclature.

Table 2: Fold change of the miRNAs in FLK1$^+$/CXCR4$^+$ versus FLK1$^-$/CXCR4$^-$.

miRNA ID	Fold change	*P* value
mmu-miR-362-5p	8.73	0.0201
mmu-miR-532-3p	7.16	0.0293
mmu-miR-674*	2.48	0.0257
mmu-miR-434-5p	2.39	0.0126
mmu-miR-532-5p	2.07	0.0027
mmu-miR-181d	−2.58	0.0193
mmu-miR-293*	−5.98	0.0359
mmu-miR-466n-3p	−20.89	0.0345
mmu-miR-142-3p	**−46.98**	**0.0308**
mmu-miR-181c	−57.34	0.0454
mmu-let-7g	−83.97	0.0240

*The element of the miRNA names based on the miRNA nomenclature.

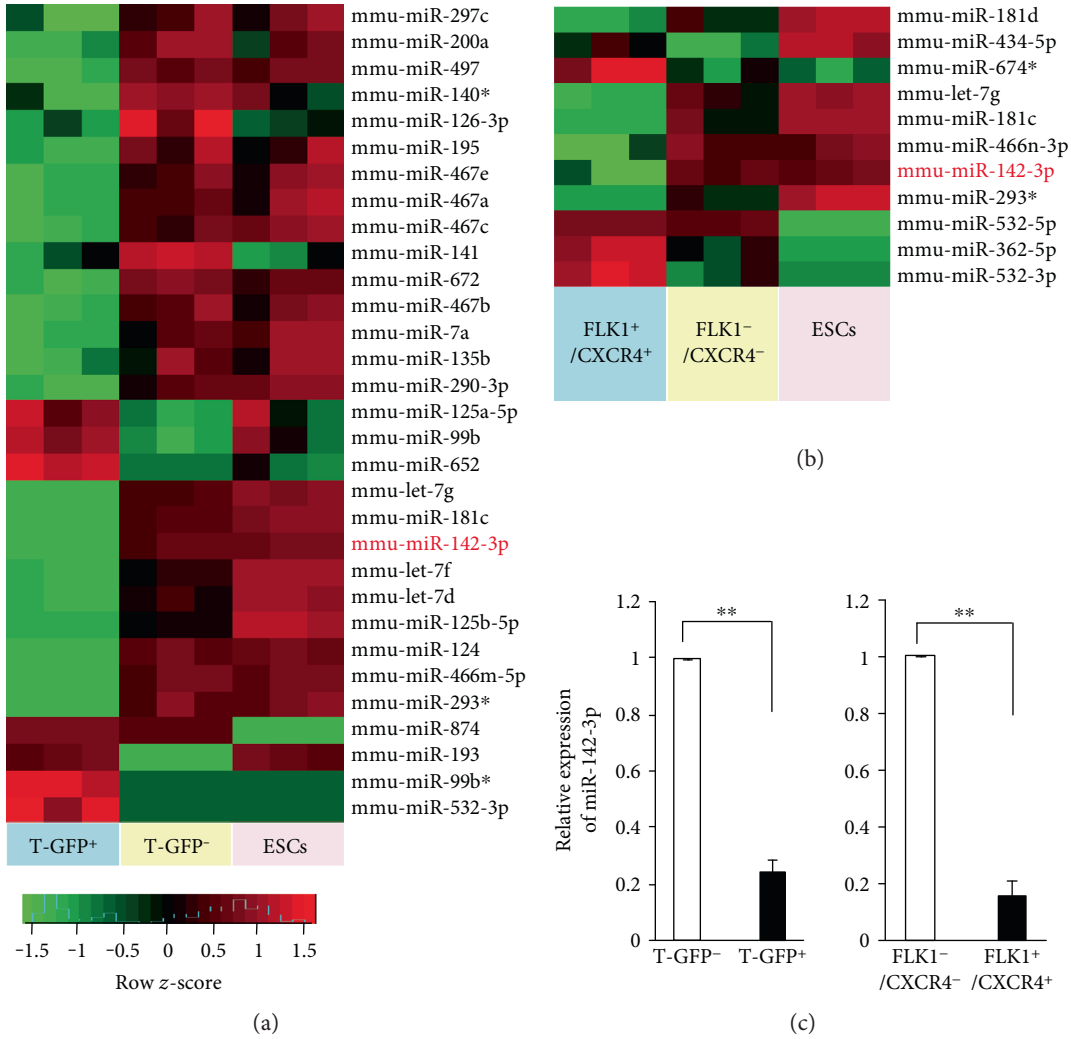

Figure 1: Microarray assay reveals miR-142-3p as the most downregulated miRNA. (a) Heat map representing hierarchical clustering of all miRNAs that displayed a 2-fold or greater difference in T-GFP$^+$ cells compared to T-GFP$^-$ cells. (b) Heat map representing hierarchical clustering of all miRNAs that displayed a 2-fold or greater difference in FLK1$^+$/CXCR4$^+$ cells compared to FLK1$^-$/CXCR4$^-$ cells. (c) Validation of miR-142-3p expression in T-GFP$^+$ mesodermal cells and FLK1$^+$/CXCR4$^+$ CPCs by qRT-PCR. $n = 3$, $^{**}P < 0.01$.

2.3. Plasmid Construction and Cell Transfection. To generate miR-142-3p-overexpressing ESC lines, the miR-142 stem-loop flanked by 170 nucleotides on each side was amplified by polymerase chain reaction (PCR) from mouse genomic DNA and inserted into pCDH-EF1-MCS-T2A-Puro lentiviral vector. Then, the vector was transfected with pMD-VSVG, pRSV-REV, and pMDLG-PRRL into HEK293FT cells to generate lentivirus. ESCs were infected with the lentivirus, and then puro-resistant clones were picked 3 days after puromycin (Gibco/BRL, USA) selection and propagated. To construct the luciferase reporter plasmid, 3′UTR regions of the gene of interest were amplified by PCR from cDNA and inserted into a luciferase reporter vector psiCHECK-2. The mutated 3′UTR were generated by PCR-based site-directed mutagenesis. For the inhibition of miR-142-3p, ESCs were transfected with the commercialized miR-142-3p inhibitors or scramble (RiboBio, China) using Lipofectamine 2000 (Invitrogen, USA) according to the manufacturer's instructions.

2.4. Reverse Transcription PCR. Cells were collected in TRIzol (Invitrogen, USA) for total RNA isolation. 1 μg of total RNA was reversed transcribed using oligo (dT) primer and Rever-Tra Ace reverse transcriptase (Toyobo, Japan). PCR was carried out using Taq PCR mix (Vazyme, China). The 28S ribosomal RNA was used for internal normalization. The primers used are listed in Supplementary Table S1 available online at https://doi.org/10.1155/2017/1769298.

2.5. Quantitative Real-Time PCR (qRT-PCR). qRT-PCR was performed on an ABI 7900HT instrument (Applied Biosystems, USA) with SYBR Green Real-time PCR Master Mix (Toyobo, Japan). For mRNA detection, glyceraldehyde 3-phosphate dehydrogenase (*Gapdh*) was used for internal

normalization. The primers used for mRNA detection are listed in Supplementary Table S1. For miRNA detection, reverse transcription and miRNA detection were carried out using the miRNA Reverse Transcription kit and TaqMan miRNA Expression Assays (Applied Biosystems, USA). Small nuclear RNA U6 was used for internal normalization.

2.6. Flow Cytometry Analysis. Undifferentiated ESCs or EBs were harvested and dissociated with trypsin. To detect SSEA1, samples were fixed with 1% paraformaldehyde, then stained for PE-conjugated SSEA1 antibody (1 : 20, eBioscience, USA) or isotype-matched negative control. To determine TNNT2$^+$ cardiomyocytes, cells were fixed and permeabilized by Cytofix/Cytoperm™ Kit (BD Biosciences, USA), blocked by 5% FBS and incubated with primary antibody of TNNT2 (1 : 200, Abcam, UK) or isotype-matched IgG control. DyLight 549-conjugated antibodies (Jackson Lab, USA) were used as the secondary antibody. Cells were then analysed and quantified by flow cytometry (FACSAria, BD Biosciences, USA). For cell sorting, live cells were harvested and double-stained with APC-conjugated FLK1 (1 : 100, BD Biosciences, USA) and PE-conjugated CXCR4 (1 : 50, BD Biosciences, USA).

2.7. Immunocytochemical Staining. Alkaline phosphatase (ALP) activity was analysed by using an ALP substrate kit III (Vector Laboratories, USA) according to the manufacturer's instructions. Immunostaining assays were performed according to the protocol described previously [24]. Briefly, cells were fixed with 4% paraformaldehyde, permeabilized in 0.3% Triton X-100, blocked in 10% normal goat serum (Vector Laboratories), and then incubated with primary antibodies against OCT4 (1 : 200, Abcam, USA), NANOG (1 : 200, Abcam, USA), and TNNT2 (1 : 500; Abcam, USA) in 4°C overnight and detected by DyLight 488- or DyLight 549-conjugated secondary antibodies. Nuclei were stained with DAPI (Sigma, USA). A Zeiss Axio Observer A1 fluorescence microscope was used for slide observing and image capture.

2.8. Luciferase Reporter Assay. HEK293FT cells were cultured to 70% confluence in 24-well plates, and then transfected with a mixture of 100 ng of 3′UTR luciferase reporter plasmid and 50 nM miRNA mimics (RiboBio, China) in each well by Lipofectamine 2000 (Invitrogen, USA). Cell lysates were harvested 24 h after transfection, and reporter activity was measured with the Dual Luciferase Assay kit (Promega, USA) according to the manufacturer's instruction.

2.9. Bioinformatics Analysis. RNAhybrid and miRanda were used to predict potential targets.

2.10. Statistical Analysis. Data were expressed as mean ± SEM. Statistical significance of differences was estimated by one-way ANOVA and two-tailed unpaired Student's *t*-test by GraphPad Prism 6.0. $P < 0.05$ was considered statistically significant.

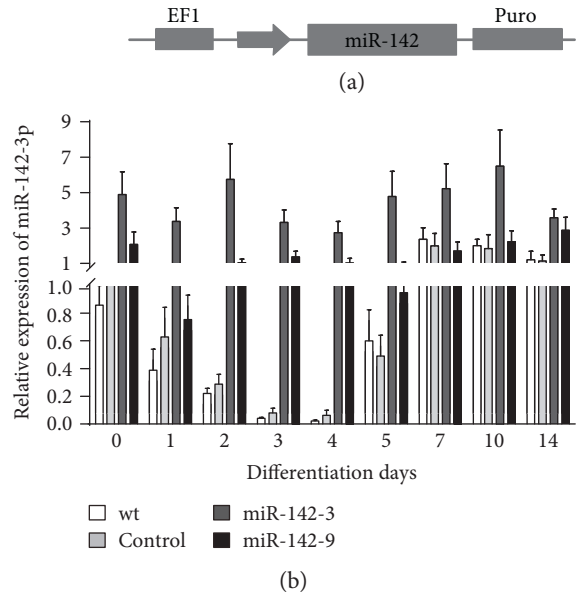

Figure 2: Establishment of miR-142-3p overexpression ESC lines. (a) Diagram depicting the construction of the miR-142-3p overexpression plasmid. (b) qRT-PCR analysis for the expression of miR-142-3p among wild-type (wt), blank vector control (control), and miR-142-3p overexpression ESC lines (miR-142-3 and miR-142-9, lower panel). $n = 5$.

3. Results

3.1. Expression Profiles of miRNAs during Early Cardiac Differentiation Stage. To identify miRNAs that might be involved in the cardiac lineage commitment, we screened miRNA expression profiles at the mesodermal and cardiac progenitor stages, which are essential for the cardiac lineage commitment [25]. mESC-derived T-GFP$^+$ mesodermal cells [26] at differentiation day 3 and FLK1$^+$/CXCR4$^+$ CPCs [23] at differentiation day 5 were isolated from corresponding T-GFP$^-$ and FLK1$^-$/CXCR4$^-$ populations by FACS (Supplemental Figure S1A–C) as previously described [27]. The enriched T-GFP$^+$ and FLK1$^+$/CXCR4$^+$ fractions were confirmed by RT-PCR analysis of mesodermal marker *T* and cardiac progenitor marker *Nkx2.5*, *Isl1*, *Tbx5*, and *Mef2c*. (Supplemental Figure S1D-E). Then, miRNA microarray was used to compare miRNA expression profiles between T-GFP$^+$ mesodermal cells and T-GFP$^-$ cells as well as between FLK1$^+$/CXCR4$^+$ cells and FLK1$^-$/CXCR4$^-$ cells. 29 miRNAs showed more than 2-fold change in T-GFP$^+$ mesoderm cells compared with the T-GFP$^-$ cells (Table 1). 11 miRNAs showed more than 2-fold change in FLK1$^+$/CXCR4$^+$ CPCs compared with FLK1$^-$/CXCR4$^-$ cells (Table 2). The heat map image of hierarchical cluster of those miRNAs revealed a distinguished grouping of miRNA expression patterns (Figures 1(a) and 1(b)). Among these miRNAs, miR-142-3p was downregulated in both T-enriched mesoderm and FLK1$^+$/CXCR4$^+$ CPCs. This was further confirmed by qRT-PCR analysis (Figure 1(c)).

3.2. Ectopic Expression of miR-142-3p Does Not Affect Self-Renewal of ESCs. To determine the role of miR-142-3p in

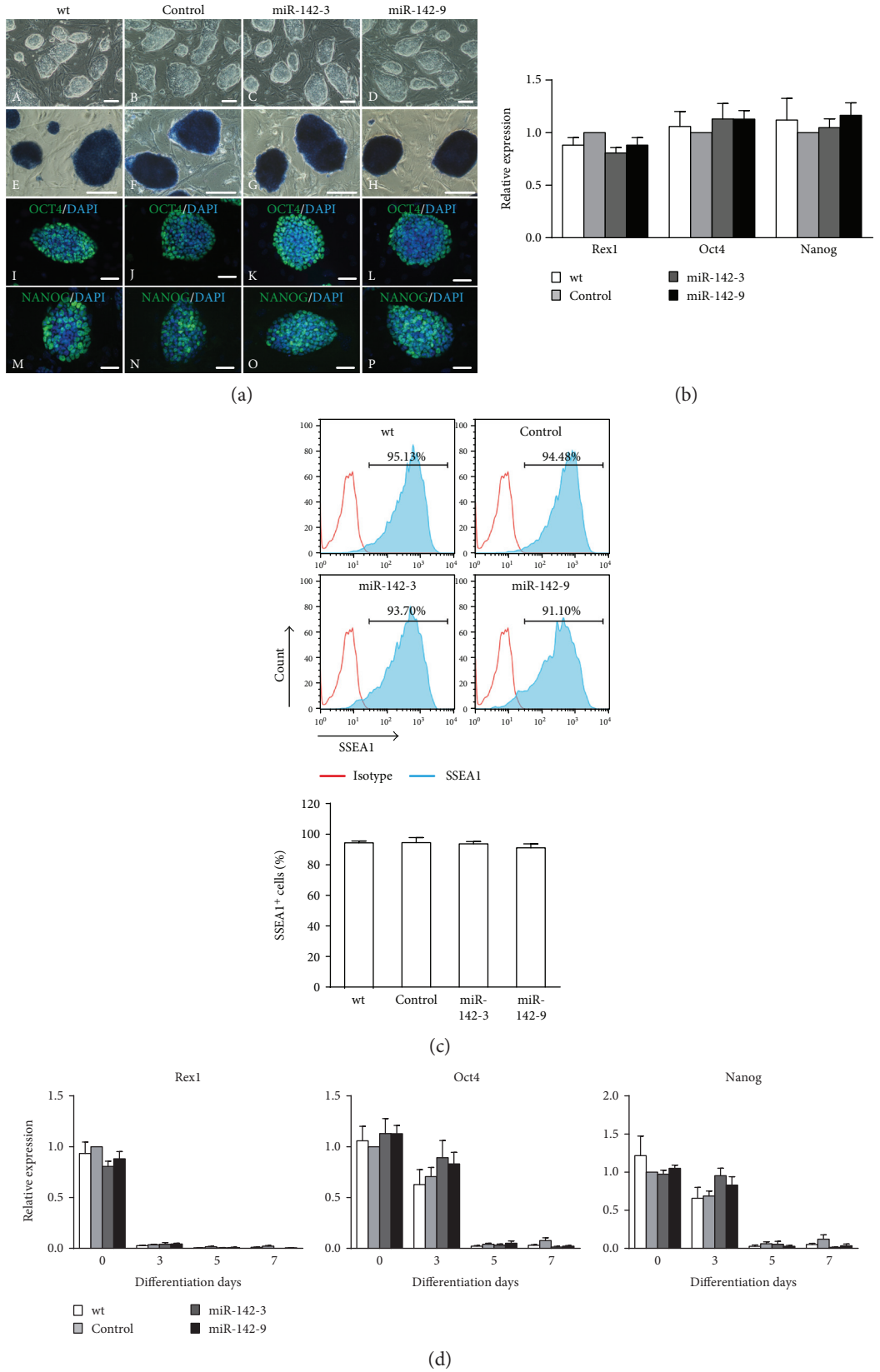

FIGURE 3: miR-142-3p overexpression does not affect the self-renewal of ESCs. (a) Morphology of the colonies of ESCs. (A–D) Phase-contrast images show undifferentiated ESC colonies. (E–H) ALP staining of ESC colonies. Immunostaining analysis of OCT4 (I–L) and NANOG (M–P). Scale bar: A–D = 100 μm, E–P = 50 μm. (b) qRT-PCR analysis for the expression of the pluripotency genes ($n = 3$). (c) Flow cytometry analysis of SSEA1 ($n = 3$). (d) qRT-PCR analysis for the expression of pluripotency genes during differentiation ($n = 3$).

self-renewal and differentiation, we established ESC lines stably expressing miR-142-3p by using lentivirus (Figure 2(a)). As shown in Figure 2(b), in wild-type (wt) cells, miR-142-3p was highly expressed in undifferentiated ESCs and declined at differentiation day 1, reaching nadir at differentiation day 4 and then gradually returned to baseline. The expression pattern of miR-142-3p in control cells transfected with the blank vector was comparable with the wt cells either in undifferentiated ESCs or in differentiating ESCs (Figure 2(b)). In undifferentiated status, the expression level of miR-142-3p in the overexpression cell lines (clones miR-142-3 and miR-142-9) was about 2- to 5-fold higher than those in wt and control cells (Figure 2(b)). During differentiation, the expression level of miR-142-3p in the overexpression cell lines remain the same as in undifferentiated status (Figure 2(b)). To confirm whether ectopic expression of miR-142-3p would affect the self-renewal property of ESCs, we compared characteristics of undifferentiated wt, control, and miR-142-3p overexpression ESCs. No significant differences in the colony morphology (Figure 3(a), A–D), ALP activity (Figure 3(a), E–H), and protein expression of pluripotency markers OCT4 and NANOG (Figure 3(a), I–P) were observed among these groups. qRT-PCR analysis also showed comparable level of *Rex1*, *Oct4*, and *Nanog* (Figure 3(b)). Flow cytometry analysis further confirmed that the number of cells expressing stage-specific embryonic antigen 1 (SSEA1) was similar among those cells (Figure 3(c)). The effect of miR-142 overexpression on the self-renewal of ESCs during differentiation was further examined, and there were no significant changes in the expression levels of pluripotency marker *Rex1*, *Oct4*, and *Nanog* in miR-142 overexpression cells compared with wt and control cells during differentiation (Figure 3(d)). To further determine the role of miR-142-3p in the self-renewal of ESCs, we suppressed the expression of miR-142-3p by using commercialized inhibitor (Supplementary Figure S2A). The cells transfected with scramble or miR-142-3p inhibitor showed similar levels of ALP activity (Supplementary Figure S2B, a-b), protein expression of pluripotency markers OCT4 and NANOG (Supplementary Figure S2B, c–f), pluripotency marker genes *Oct4*, *Nanog*, and *Rex1* (Supplementary Figure S2C), and the percentage of $SSEA1^+$ cells (Supplementary Figure S2D). Taken together, these data indicate that miR-142-3p appears to be dispensable for maintaining self-renewal of ESCs.

3.3. miR-142-3p Suppresses Cardiomyocyte Differentiation. To investigate the role of miR-142-3p during cardiac lineage commitment, ESCs were differentiated into cardiomyocytes by the EB formation. In wt and control ESCs, spontaneously contracting cardiomyocytes were visible at day 6, and the percentage of EBs containing spontaneously contracting cardiomyocytes increased gradually over time and reached over 90%, while in miR-142-3p overexpression ESCs, it dropped to 20% to 35% (Figure 4(a)). However, the number of EBs containing spontaneously contracting cardiomyocytes was indistinguishable between scramble and miR-142-3p-knockdown cells (Supplemental Figure S2E). Immunofluorescence staining confirmed that the positive area of cardiac myofilament protein TNNT2 was significantly smaller in miR-142-3p overexpression EBs than that in wt and control (Figure 4(b)). Flow cytometry analysis further confirmed that miR-142-3p overexpression decreased the percentage of $TNNT2^+$ cardiomyocytes at differentiation day 10 (Figure 4(c)). Moreover, qRT-PCR analysis showed that the expression levels of cardiac myofilament genes *Myh6*, *Myl7*, and *Tnnt2* were markedly suppressed by miR-142-3p overexpression (Figure 4(d)). These data indicate that miR-142-3p negatively regulates cardiac differentiation.

3.4. miR-142-3p Suppresses ESC Differentiation into CPCs but Not Mesoderm Formation. In vitro cardiomyocyte differentiation involves the specification of pluripotent cells to mesoderm and cardiac progenitors prior to terminal differentiation. To elucidate which differentiation stage is affected by miR-142-3p, we analysed the expression of germ layer and cardiac precursor genes by qRT-PCR. miR-142-3p overexpression did not significantly affect the expression of ectodermal (*Fgf5*, *Nestin*), endodermal (*Fox2*, *Sox17*, and *Afp*), and mesodermal (*T*, *Eomes*, and *Flk1*) marker genes (Figures 5(a), 5(b), and 5(c)). However, the expression of cardiac mesodermal gene *Mesp1* and cardiac progenitor genes *Tbx5*, *Nkx2.5*, and *Mef2c* were remarkably decreased (Figure 5(d)). Taken together, these data suggest that miR-142-3p decreases the populations of cardiac mesoderm and progenitor cells but not mesoderm formation of ESCs.

3.5. miR-142-3p Targets Mef2c in Cardiac Differentiation of ESCs. To elucidate the mechanisms by which miR-142-3p regulates cardiac differentiation, we searched for potential targets of miR-142-3p by using miRanda [28] and RNAhybrid [29]. Since *Mesp1* is the earliest marker of cardiovascular development [30], we examined whether miR-142-3p directly targets *Mesp1*. miR-142-3p was predicted to bind to the 3′UTR of *Mesp1* (Supplemental Figure S3A). However, when the 3′UTR of *Mesp1* was cloned into the luciferase reporter, miR-142-3p had no effect on the luciferase activity (Supplemental Figure S3B), indicating that miR-142-3p does not directly target *Mesp1*. Further analysis showed that the 3′UTR of *Mef2c*, a key regulator of cardiomyocyte formation [31], had a miR-142-3p binding site (Figure 6(a)). We then cloned the full length of the wt and mutant 3′ UTR of mouse *Mef2c* into the downstream of the luciferase reporter. miR-142-3p reduced the activity of the luciferase reporter bearing wt 3′UTR of *Mef2c*. By contrast, miR-142-3p did not affect the activity of the luciferase reporter bearing mutant 3′UTR of *Mef2c* (Figure 6(b)). Moreover, qRT-PCR analysis showed that the expression of *Mef2c* was decreased by miR-142-3p (Figure 4(d)). Taken together, these results suggest that *Mef2c* may be the target of miR-142-3p.

4. Discussion

Here, we showed that (i) a number of miRNAs are significantly changed during the differentiation of mesodermal and cardiac progenitor cells from ESCs; (ii) miR-142-3p is highly expressed in undifferentiated ESCs, while it is downregulated during early ESC differentiation and its expression

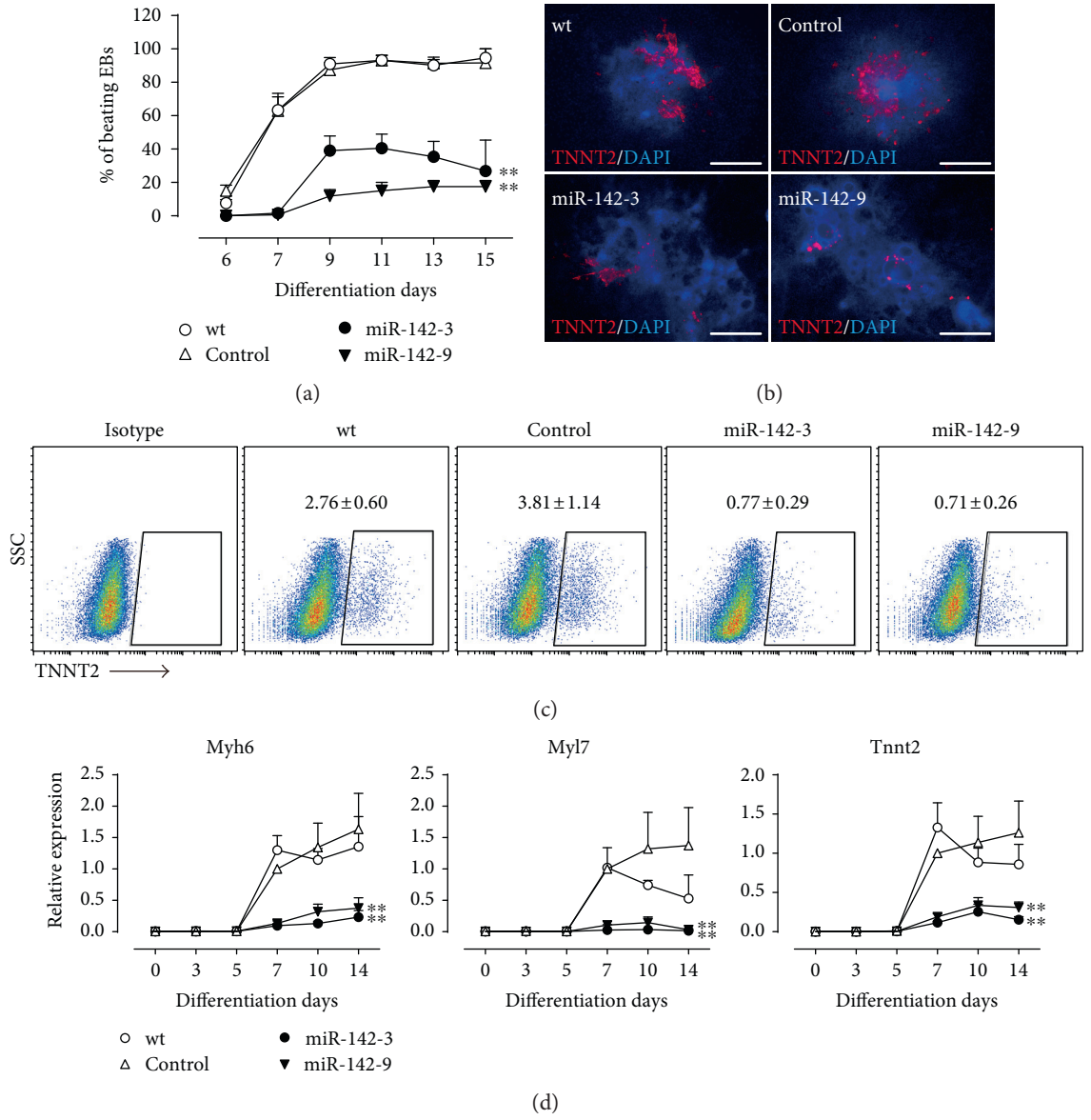

FIGURE 4: miR-142-3p overexpression suppresses cardiomyocyte differentiation of ESCs. (a) The percentage of EBs with spontaneously contracting cardiomyocytes during EB differentiation ($n = 3$). (b) Immunostaining analysis of TNNT2 in day 10 EBs. Scale bar = 500 μm. (c) Flow cytometry analysis of TNNT2 in day 10 EBs ($n = 3$). (d) qRT-PCR analysis for the expression of the cardiac myofilament genes ($n = 3$). $^{**}P < 0.01$ versus control.

is significantly lower in T-GFP$^+$ cells and FLK1$^+$/CXCR4$^+$ CPCs than in corresponding T-GFP$^-$ cells and FLK1$^-$/CXCR4$^-$ cells; (iii) ectopic expression of miR-142-3p does not affect the self-renewal and germ layer specification of ESCs, whereas it suppresses cardiomyocyte formation; (iv) this inhibition is associated with the downregulation of the expression of cardiac mesodermal marker gene *Mesp1* and the downstream cardiac progenitor marker genes *Nkx2.5*, *Tbx5*, and *Mef2c*; and (v) miR-142-3p targets the 3′ UTR of *Mef2c*. These findings reveal a novel role of miR-142-3p in the regulation of cardiac lineage fate decision and provide its potential mechanism underlying the control of cell lineage decision and cardiogenesis.

Our results show that both gain and loss of function of miR-142-3p do not affect the self-renewal of undifferentiated ESCs. This is consistent with the recent report that in undifferentiated ESCs, there are high miR-142 and low miR-142 populations, while the two populations are indistinguishable by pluripotency markers [19]. They also reported that constitutive expression of miR-142 locks ESCs in an undifferentiated state when exposed to differentiation cues [19]. However, we did not observe a significant delay of decrease of pluripotency genes upon differentiation in miR-142-3p overexpression cells. Such conflicted findings may be caused by the different overexpression levels in undifferentiated state. It may also be caused by the difference in differentiation models used. Sladitschek and Neveu [19] induced ESC differentiation by using various cytokines, while we used the EB model without addition of any cytokines.

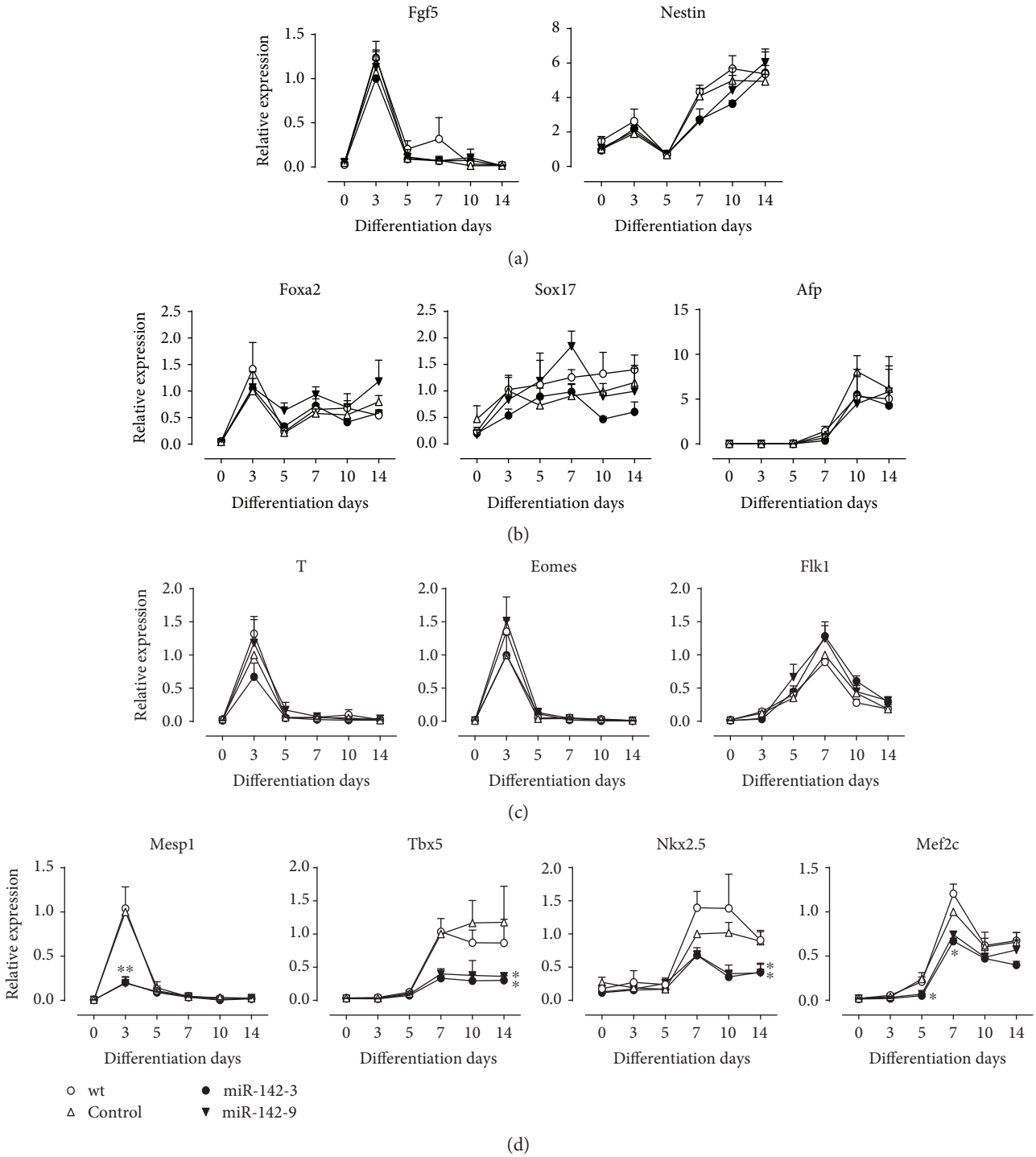

Figure 5: qRT-PCR analysis of differentiation marker genes during ESC differentiation. (a) Expression of ectodermal markers. (b) Expression of endodermal markers. (c) Expression of mesodermal markers. (d) Expression of cardiac progenitor markers ($n = 6$). $^{*}P < 0.05$ versus control, $^{**}P < 0.01$ versus control.

During the cardiomyocyte differentiation from ESCs, the cardiac mesoderm and CPC formation is critical to the cardiac lineage fate decision [25]. *Mesp1* is the master regulator of cardiac lineage commitment and is the earliest marker of cardiovascular development [30, 32]. It is transiently expressed in the nascent mesoderm, and it specifies mesodermal cells toward cardiac lineage by triggering the expression of cardiac markers [32]. Our data showed that miR-142-3p negatively regulates the formation of cardiac mesoderm and CPCs, and the subsequent cardiomyocyte differentiation. Downregulation of miR-142-3p during ESC differentiation is required for the specification of mesodermal

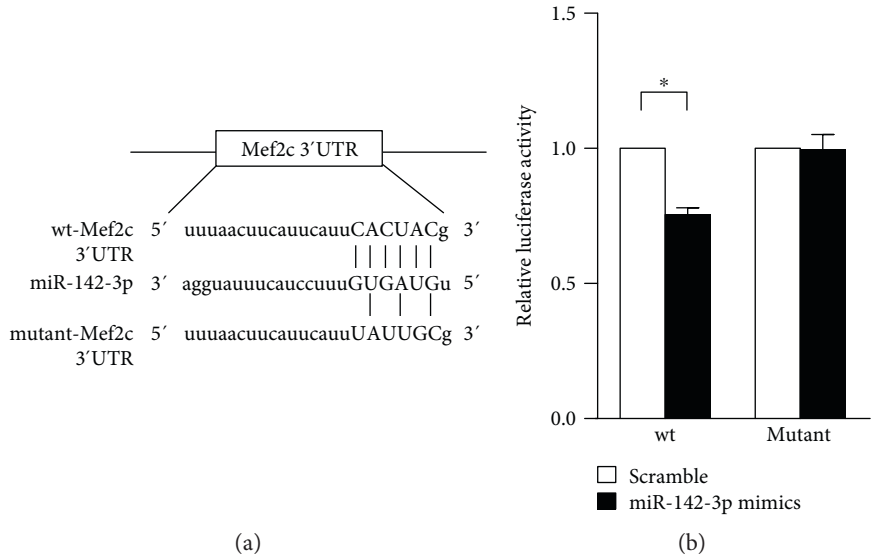

Figure 6: *Mef2c* is a downstream target of miR-142-3p. (a) The sketch construction of the wt and mutant *Mef2c* 3′UTR. (b) Relative luciferase activity of wt and mutant *Mef2c* 3′UTR vectors transfected with scramble control or miR-142-3p mimics ($n = 5$). $^*P < 0.05$.

cells to CPCs. This is supported by the findings that (i) miR-142-3p is downregulated in mesodermal and CPC populations; (ii) miR-142-3p does not affect the formation of nascent mesoderm; (iii) miR-142-3p inhibits the expression of *Mesp1* and the downstream cardiac progenitor genes; and (iv) miR-142-3p directly targets *Mef2c*, though further validation at the protein level is needed. Notably, no further increase in the cardiac differentiation is observed by knockdown of miR-142-3p, suggesting that the endogenous decline of miR-142-3p reaches the saturation level to allow sufficient CPC differentiation and subsequent cardiomyocyte formation. We found that miR-142-3p may function upstream of *Mesp1* through an indirect regulatory way. The mechanism by which miR-142-3p regulates *Mesp1* needs further investigation.

Interestingly, the role of miR-142-3p in cardiac lineage commitment seems different between zebrafish and mESCs. Knockdown of miR-142-3p during the development of zebrafish disrupts normal cardiac formation and function [20], while in the present study, miR-142-3p overexpression suppresses cardiomyocyte formation. Such difference suggests a species-dependent role of miR-142-3p. The in vivo role of miR-142-3p on cardiac development among various mammalian systems requires further investigation.

In the microarray results, some miRNAs showed similar expression pattern to that of miR-142-3p, such as miR-125b-5p, miR-124, and let-7g. We previously found that miR-125b-5p is downregulated during differentiation and controls cardiac differentiation via regulating mesendodermal specification [13]. miR-124 is a neuron-specific miRNA and known to be involved in neurogenesis [33]. Recently, it has been reported to regulate cardiomyocyte differentiation of bone marrow-derived mesenchymal stem cells [34]. However, whether miR-124 regulates cardiomyocyte differentiation remains unknown. The let-7 family member let-7c is involved in the control of cardiomyocyte differentiation by directly targeting the polycomb complex group protein *Ezh2* [35], but it is unclear whether let-7g regulates cardiomyocyte differentiation. It needs to be determined whether these miRNAs might work together with miR-142-3p in the regulation of cardiac differentiation of ESCs.

In summary, our results reveal a number of miRNAs potentially involved in ESC differentiation into mesodermal and cardiac progenitor cells. miR-142-3p negatively regulates the differentiation of cardiomyocyte through affecting the specification of cardiac mesodermal cells and CPCs.

Conflicts of Interest

The authors indicate no potential competing interests.

Acknowledgments

The study was supported by grants from the National Natural Science Foundation of China (81470422; 81520108004; 81570229), the National Basic Research Program of China (2014CB965100), and the National Key Research and Development Program of China (2016YFC1301204). The authors would like to thank Dr. Gordon Keller for kindly providing the Brachyury-GFP E14 mouse ESCs.

References

[1] M. J. Evans and M. H. Kaufman, "Establishment in culture of pluripotential cells from mouse embryos," *Nature*, vol. 292, no. 5819, pp. 154–156, 1981.

[2] G. M. Keller, "In vitro differentiation of embryonic stem cells," *Current Opinion in Cell Biology*, vol. 7, no. 6, pp. 862–869, 1995.

[3] H. Vidarsson, J. Hyllner, and P. Sartipy, "Differentiation of human embryonic stem cells to cardiomyocytes for in vitro and in vivo applications," *Stem Cell Reviews and Reports*, vol. 6, no. 1, pp. 108–120, 2010.

[4] V. Verma, K. Purnamawati, and W. Shim, "Steering signal transduction pathway towards cardiac lineage from human

pluripotent stem cells: a review," *Cellular Signalling*, vol. 25, no. 5, pp. 1096–1107, 2013.

[5] Y. Tang, Y. Z. Hong, H. J. Bai et al., "Plant homeo domain finger protein 8 regulates mesodermal and cardiac differentiation of embryonic stem cells through mediating the histone demethylation of pmaip1," *Stem Cells*, vol. 34, no. 6, pp. 1527–1540, 2016.

[6] E. N. Olson, "Gene regulatory networks in the evolution and development of the heart," *Science*, vol. 313, no. 5795, pp. 1922–1927, 2006.

[7] C. P. Hodgkinson, M. H. Kang, S. Dal-Pra, M. Mirotsou, and V. J. Dzau, "MicroRNAs and cardiac regeneration," *Circulation Research*, vol. 116, no. 10, pp. 1700–1711, 2015.

[8] T. S. Greve, R. L. Judson, and R. Blelloch, "MicroRNA control of mouse and human pluripotent stem cell behavior," *Annual Review of Cell and Developmental Biology*, vol. 29, no. 1, pp. 213–239, 2013.

[9] K. N. Ivey, A. Muth, J. Arnold et al., "MicroRNA regulation of cell lineages in mouse and human embryonic stem cells," *Cell Stem Cell*, vol. 2, no. 3, pp. 219–229, 2008.

[10] R. A. Espinoza-Lewis and D. Z. Wang, "Chapter ten - microRNAs in heart development," in *Current Topics in Developmental Biology*, G. B. Benoit, Ed., vol. 100, pp. 279–317, Academic Press, New York, 2012.

[11] J. Chen, Z. P. Huang, H. Seok et al., "mir-17-92 cluster is required for and sufficient to induce cardiomyocyte proliferation in postnatal and adult hearts," *Circulation Research*, vol. 112, no. 12, pp. 1557–1566, 2013.

[12] J. P. Sluijter, A. van Mil, P. van Vliet et al., "MicroRNA-1 and -499 regulate differentiation and proliferation in human-derived cardiomyocyte progenitor cells," *Arteriosclerosis, Thrombosis, and Vascular Biology*, vol. 30, no. 4, pp. 859–868, 2010.

[13] J. Wang, N. Cao, M. Yuan et al., "MicroRNA-125b/Lin28 pathway contributes to the mesendodermal fate decision of embryonic stem cells," *Stem Cells and Development*, vol. 21, no. 9, pp. 1524–1537, 2012.

[14] C. Z. Chen, L. Li, H. F. Lodish, and D. P. Bartel, "MicroRNAs modulate hematopoietic lineage differentiation," *Science*, vol. 303, no. 5654, pp. 83–86, 2004.

[15] R. Nimmo, A. Ciau-Uitz, C. Ruiz-Herguido et al., "miR-142-3p controls the specification of definitive hemangioblasts during ontogeny," *Developmental Cell*, vol. 26, no. 3, pp. 237–249, 2013.

[16] X. Lu, X. Li, Q. He et al., "miR-142-3p regulates the formation and differentiation of hematopoietic stem cells in vertebrates," *Cell Research*, vol. 23, no. 12, pp. 1356–1368, 2013.

[17] H. B. Fan, Y. J. Liu, L. Wang et al., "miR-142-3p acts as an essential modulator of neutrophil development in zebrafish," *Blood*, vol. 124, no. 8, pp. 1320–1330, 2014.

[18] A. Shrestha, R. T. Mukhametshina, S. Taghizadeh et al., "MicroRNA-142 is a multifaceted regulator in organogenesis, homeostasis and disease," *Developmental Dynamics*, vol. 264, no. 4, pp. 285–290, 2017.

[19] H. L. Sladitschek and P. A. Neveu, "The bimodally expressed microRNA miR-142 gates exit from pluripotency," *Molecular Systems Biology*, vol. 11, no. 12, p. 850, 2015.

[20] T. Nishiyama, R. Kaneda, T. Ono et al., "miR-142-3p is essential for hematopoiesis and affects cardiac cell fate in zebrafish," *Biochemical and Biophysical Research Communications*, vol. 425, no. 4, pp. 755–761, 2012.

[21] H. T. Yang, D. Tweedie, S. Wang et al., "The ryanodine receptor modulates the spontaneous beating rate of cardiomyocytes during development," *Proceedings of the National Academy of Sciences of the United States of America*, vol. 99, no. 14, pp. 9225–9230, 2002.

[22] K. R. Boheler, J. Czyz, D. Tweedie, H. T. Yang, S. V. Anisimov, and A. M. Wobus, "Differentiation of pluripotent embryonic stem cells into cardiomyocytes," *Circulation Research*, vol. 91, no. 3, pp. 189–201, 2002.

[23] T. J. Nelson, R. S. Faustino, A. Chiriac, R. Crespo-Diaz, A. Behfar, and A. Terzic, "CXCR4+/FLK-1+ biomarkers select a cardiopoietic lineage from embryonic stem cells," *Stem Cells*, vol. 26, no. 6, pp. 1464–1473, 2008.

[24] N. Cao, Z. Liu, Z. Chen et al., "Ascorbic acid enhances the cardiac differentiation of induced pluripotent stem cells through promoting the proliferation of cardiac progenitor cells," *Cell Research*, vol. 22, no. 1, pp. 219–236, 2012.

[25] P. W. Burridge, G. Keller, J. D. Gold, and J. C. Wu, "Production of de novo cardiomyocytes: human pluripotent stem cell differentiation and direct reprogramming," *Cell Stem Cell*, vol. 10, no. 1, pp. 16–28, 2012.

[26] H. J. Fehling, G. Lacaud, A. Kubo et al., "Tracking mesoderm induction and its specification to the hemangioblast during embryonic stem cell differentiation," *Development*, vol. 130, no. 17, pp. 4217–4227, 2003.

[27] Y. Tang, Z. Y. Chen, Y. Z. Hong et al., "Expression profiles of histone lysine demethylases during cardiomyocyte differentiation of mouse embryonic stem cells," *Acta Pharmacologica Sinica*, vol. 35, no. 7, pp. 899–906, 2014.

[28] D. Betel, A. Koppal, P. Agius, C. Sander, and C. Leslie, "Comprehensive modeling of microRNA targets predicts functional non-conserved and non-canonical sites," *Genome Biology*, vol. 11, no. 8, p. R90, 2010.

[29] M. Rehmsmeier, P. Steffen, M. Höchsmann, and R. Giegerich, "Fast and effective prediction of microRNA/target duplexes," *RNA*, vol. 10, no. 10, pp. 1507–1517, 2004.

[30] A. Bondue, G. Lapouge, C. Paulissen et al., "Mesp1 acts as a master regulator of multipotent cardiovascular progenitor specification," *Cell Stem Cell*, vol. 3, no. 1, pp. 69–84, 2008.

[31] J. Wilson-Rawls, J. D. Molkentin, B. L. Black, and E. N. Olson, "Activated notch inhibits myogenic activity of the MADS-box transcription factor myocyte enhancer factor 2C," *Molecular and Cellular Biology*, vol. 19, no. 4, pp. 2853–2862, 1999.

[32] A. Bondue and C. Blanpain, "Mesp1: a key regulator of cardiovascular lineage commitment," *Circulation Research*, vol. 107, no. 12, pp. 1414–1427, 2010.

[33] M. Åkerblom and J. Jakobsson, "MicroRNAs as neuronal fate determinants," *The Neuroscientist*, vol. 20, no. 3, pp. 235–242, 2014.

[34] B. Cai, J. Li, J. Wang et al., "microRNA-124 regulates cardiomyocyte differentiation of bone marrow-derived mesenchymal stem cells via targeting STAT3 signaling," *Stem Cells*, vol. 30, no. 8, pp. 1746–1755, 2012.

[35] A. Coppola, A. Romito, C. Borel et al., "Cardiomyogenesis is controlled by the miR-99a/let-7c cluster and epigenetic modifications," *Stem Cell Research*, vol. 12, no. 2, pp. 323–337, 2014.